



# Environmental isotopes in the hydrological cycle

Principles and applications

Edited by  
W.G. Mook

*Volume IV*

***Groundwater***

*Saturated and unsaturated zone*

by  
**Mebus Geyh**  
*Niedersächsisches Landesamt für Bodenforschung  
Hannover*

---

IHP-V | Technical Documents in Hydrology | No. 39, Vol. IV  
UNESCO, Paris, 2000



United Nations Educational,  
Scientific and Cultural Organization

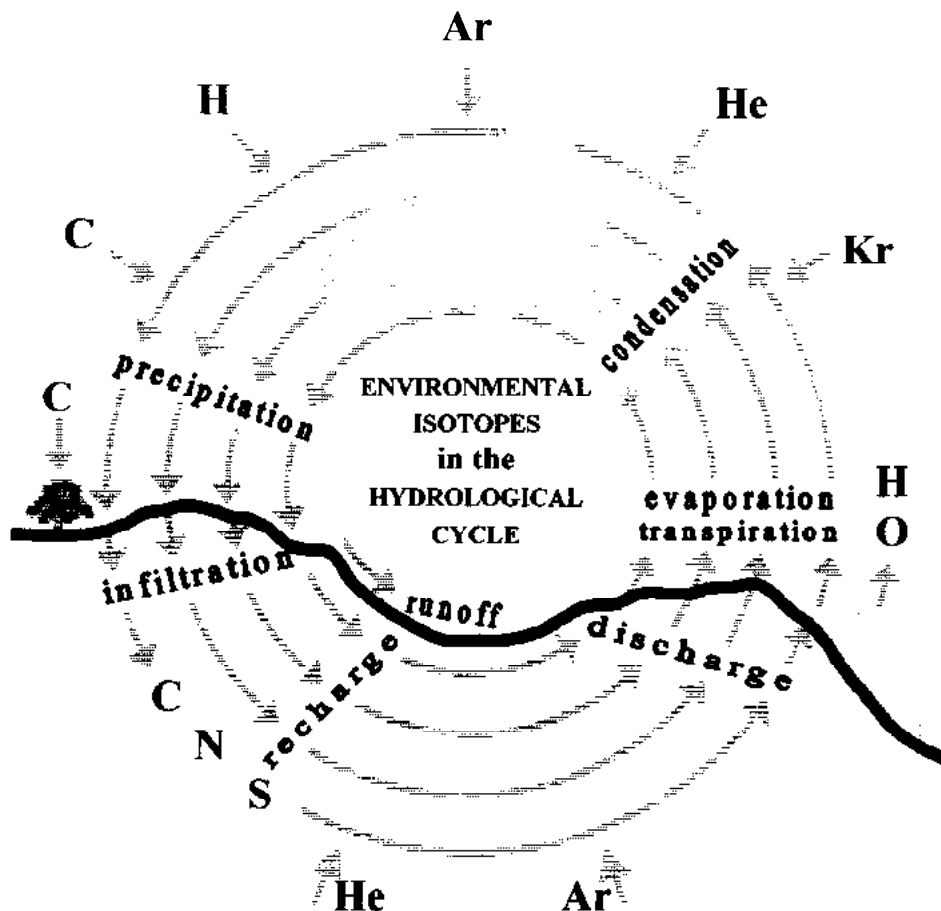


International Atomic Energy Agency

**The designations employed and the presentation of material throughout the publication do not imply the expression of any opinion whatsoever on the part of UNESCO and/or IAEA concerning the legal status of any country, territory, city or of its authorities, or concerning the delimitation of its frontiers or boundaries.**

UNESCO/IAEA Series on  
Environmental Isotopes in the Hydrological Cycle  
Principles and Applications

- ÷
- Volume I Introduction: Theory, Methods, Review
  - Volume II Atmospheric Water
  - Volume III Surface Water
  - Volume IV Groundwater: Saturated and Unsaturated Zone
  - Volume V Man's Impact on Groundwater Systems
  - Volume VI Modelling



Contributing Authors

F.D'Amore, G.Darling, T.Paces, Z.Pang, J.Šilar

# PREFACE

The availability of freshwater is one of the great issues facing mankind today - in some ways the greatest, because problems associated with it affect the lives of many millions of people. It has consequently attracted a wide scale international attention of UN Agencies and related international/regional governmental and non-governmental organisations. The rapid growth of population coupled to steady increase in water requirements for agricultural and industrial development have imposed severe stress on the available freshwater resources in terms of both the quantity and quality, requiring consistent and careful assessment and management of water resources for their sustainable development.

More and better water can not be acquired without the continuation and extension of hydrological research. In this respect has the development and practical implementation of isotope methodologies in water resources assessment and management been part of the IAEA's programme in nuclear applications over the last four decades. Isotope studies applied to a wide spectrum of hydrological problems related to both surface and groundwater resources as well as environmental studies in hydro-ecological systems are presently an established scientific discipline, often referred to as "Isotope Hydrology". The IAEA contributed to this development through direct support to research and training, and to the verification of isotope methodologies through field projects implemented in Member States.

The world-wide programme of the International Hydrological Decade (1965-1974) and the subsequent long-term International Hydrological Programme (IHP) of UNESCO have been an essential part of the well recognised international frameworks for scientific research, education and training in the field of hydrology. The International Atomic Energy Agency (IAEA) and UNESCO have established a close co-operation within the framework of both the earlier IHD and the ongoing IHP in the specific aspects of scientific and methodological developments related to water resources that are of mutual interest to the programmes of both organisations.

The first benchmark publication on isotope hydrology entitled "Guidebook on Nuclear Techniques in Hydrology" was realised in 1983 through the activity of the joint IAEA/UNESCO Working Group on Nuclear Techniques established within the framework of IHP, and it has been widely used as practical guidance material in this specific field.

In view of the fact that the IHP's objectives include also a multi-disciplinary approach to the assessment and rational management of water resources and taking note of the advances made in isotope hydrology, the IAEA and UNESCO have initiated a joint activity in preparation of

a series of six up-to-date textbooks, covering the entire field of hydrological applications of natural isotopes (environmental isotopes) to the overall domain of water resources and related environmental studies.

The main aim of this series is to provide a comprehensive review of basic theoretical concepts and principles of isotope hydrology methodologies and their practical applications with some illustrative examples. The volumes are designed to be self-sufficient reference material for scientists and engineers involved in research and/or practical applications of isotope hydrology as an integral part of the investigations related to water resources assessment, development and management. Furthermore, they are also expected to serve as "Teaching Material" or text books to be used in universities and teaching institutions for incorporating the study of "isotopes in water" in general into the curriculum of the earth sciences. Additionally the contents can fulfill the need for basic knowledge in other disciplines of the Earth Sciences dealing with water in general.

These six volumes have been prepared through efforts and contributions of a number of scientists involved in this specific field as cited in each volume, under the guidance and co-ordination of the main author/co-ordinating editor designated for each volume. W.G.Mook (Netherlands), J.Gat (Israel), K.Rozanski (Poland), W.Stichler (Germany), M.Geyh (Germany), K.P.Seiler (Germany) and Y.Yurtsever (IAEA, Vienna) were involved as the main author/co-ordinating editors in preparation of these six volumes, respectively. Final editorial work on all volumes aiming to achieve consistency in the contents and layout throughout the whole series was undertaken by W.G.Mook (Netherlands).

Mr.Y. Yurtsever, Staff Member of the Isotope Hydrology Section of the IAEA; and Ms. A. Aureli, Programme Specialist, Division of Water Sciences of UNESCO, were the Scientific Officers in charge of co-ordination and providing scientific secretariat to the various meetings and activities that were undertaken throughout the preparation of these publications.

The IAEA and UNESCO thank all those who have contributed to the preparation of these volumes and fully acknowledge the efforts and achievements of the main authors and co-ordinating editors.

It is hoped that these six volumes will contribute to wider scale applications of isotope methodologies for improved assessment and management of water resources, facilitate incorporation of isotope hydrology into the curricula of teaching and education in water sciences and also foster further developments in this specific field.

Paris / Vienna, March 2000

# PREFACE TO VOLUME IV

The interpretation of isotope hydrological data is not straightforward. Many field studies lead to a conclusion that the origin of groundwater and the chemical and isotopic processes in groundwater systems can only be studied successfully, if a composition of isotopic, chemical, geological and hydrogeological data is available for interpretation.

Following the previous volumes on isotopic principles, precipitation and surface waters, this volume is dealing with the application of isotope hydrological methods in groundwater studies. It conveys basic knowledge in geohydraulics and hydrogeology required for a consistent interpretation of isotope hydrological data.

This volume starts with a brief discussion of the characteristics and behaviour of groundwater as a medium of mass transport for gases, dissolved constituents and colloids. The geohydraulic aspects of groundwater flow under steady-state conditions are described in combination with an explanation of the most important terms related to isotope hydrology (e.g. transit time, turn-over time, mean residence time, water age). Non-steady state flow conditions caused by palaeoclimatic variations and anthropogenic activities such as over-exploitation or groundwater mining seriously affect the interpretation of isotope hydrological data. Also water-rock interactions may modify the isotope composition of a carbonate rock environment, especially in high-temperature systems.

Environmental isotope techniques are pre-eminently suitable for studying the unsaturated and saturated zone, the latter particularly concerning the stable and radioactive natural isotopes. Stable isotope data preferentially yield information on the origin of groundwater. Radioactive isotopes allow groundwater to be "dated" in support of geohydraulic investigations. In undisturbed high-temperature systems isotopic geothermometry, i.e. the study of the temperature effect of stable isotopic abundances, is applied for gaining information on water mixing as well as the origin and history of fluids. Anthropogenic changes due to steam loss, underground liquid-vapour separation and the impact of re-injection of waste water are also traced by the isotopic composition of geothermal fluids. Last but not least, a brief outline is given on the planning and performance of environmental multi-isotope studies, as well as the interpretation of the corresponding results.

Sincere thanks are due to my co-authors F. D'Amore, G. Darling, T. Paces, Z. Pang, J. Šilar, T. Paces and A. D'Amore providing draft manuscripts and figure sketches as the fundamentals of this volume. Yucel Yurtsever gently guided us to reach a uniform set of volumes. The final critical and substantial reading overtook Wim Mook which was highly appreciated.

Hannover, February 2000

Mebus A. Geyh

# CONTENTS

<b>1</b>	<b>HYDROGEOLOGY AND AQUIFER CHARACTERISTICS</b>	<b>1</b>
1.1	Definitions .....	1
1.2	Occurrence of groundwater in rocks .....	1
1.3	Geohydraulic parameters .....	2
1.3.1	Porosity.....	2
1.3.2	Storage, storage coefficient.....	4
1.3.3	Permeability and hydraulic conductivity .....	5
1.3.4	Flow nets .....	5
1.4	Hydrogeology .....	8
1.4.1	Hydrogeological properties of rocks .....	8
1.4.1.1	Igneous rocks .....	8
1.4.1.2	Metamorphic rocks .....	9
1.4.1.3	Consolidated sedimentary rocks .....	9
1.4.1.4	Unconsolidated sediments .....	10
1.4.2	Hydrogeological structures – groundwater regimes .....	10
1.4.3	Crystalline regions .....	11
1.4.3.1	Volcanic rocks .....	11
1.4.3.2	Folded sequences of sedimentary rocks .....	11
1.4.3.3	Karstified rocks.....	12
1.4.3.4	Platform sediments .....	12
1.4.3.5	Alluvial plains, fans, river deltas, glaciofluvial, sediments ..	13
<b>2</b>	<b>TRACERS AND TRANSPORT</b>	<b>15</b>
2.1	Types of tracers.....	15
2.2	Types of tracer experiments .....	16
2.3	Isotopes in groundwater .....	17
2.3.1	Stable isotopes .....	17
2.3.2	Radioactive isotopes.....	18
2.3.3	Chemicals .....	20
2.3.4	Colloids .....	21
2.3.5	Noble gases.....	22
<b>3</b>	<b>GEOHYDRAULIC ASPECTS</b>	<b>25</b>
3.1	Steady-state groundwater flow .....	26
3.1.1	Darcy velocity and tracer velocity.....	26
3.1.2	Principle groundwater flow models .....	27

3.1.3	Considerations about modelling.....	32
3.1.4	Groundwater discharge.....	32
3.1.4.1	Springs.....	33
3.1.4.2	Production wells.....	34
3.1.4.3	Well construction and sampling of water from wells.....	35
3.2	Non-steady state groundwater flow.....	36
3.2.1	Palaeoclimatic causes.....	36
3.2.2	Anthropogenic causes.....	37
<b>4</b>	<b>WATER-ROCK INTERACTIONS</b>	<b>41</b>
4.1	Anion exclusion-adsorption: physical absorption.....	42
4.2	Chemical absorption.....	42
4.3	Exchange of ions.....	43
4.4	Chemical interaction between solutes.....	43
4.4.1	Carbonate-CO <sub>2</sub> system.....	43
4.4.2	Reactions with organic matter.....	44
4.4.3	Fate of dissolved sulphur compounds.....	45
4.4.4	On the isotopic composition of strontium.....	48
<b>5</b>	<b>APPLICATIONS TO LOW-TEMPERATURE SYSTEMS</b>	<b>49</b>
5.1	Unsaturated zone.....	49
5.1.1	Principal soil parameters of the unsaturated zone.....	49
5.1.2	Geohydraulic aspects.....	50
5.1.2.1	Steady-state flow.....	50
5.1.2.2	Movement of solutes.....	51
5.1.2.2.1	Convection and advection.....	51
5.1.2.2.2	Dispersion.....	51
5.1.2.2.3	By-pass flow (dual flow).....	53
5.1.3	Solute transport.....	53
5.1.4	Application.....	54
5.1.4.1	Recharge rate determination by mass balance.....	54
5.1.4.2	Recharge rate determination by tracer peak displacement.....	55
5.1.4.3	Evaporation rate.....	59
5.1.4.4	Water loss by plant extraction.....	65
5.2	Saturated zone.....	65
5.2.1	Origin of groundwater.....	65
5.2.1.1	Oxygen ( <sup>18</sup> O/ <sup>16</sup> O) and hydrogen ( <sup>2</sup> H/ <sup>1</sup> H).....	65
5.2.1.2	Carbon ( <sup>13</sup> C/ <sup>12</sup> C).....	72
5.2.1.3	Nitrogen ( <sup>15</sup> N/ <sup>14</sup> N).....	75
5.2.1.4	Sulphur ( <sup>34</sup> S/ <sup>32</sup> S).....	79
5.2.1.5	Chlorine ( <sup>37</sup> Cl/ <sup>35</sup> Cl).....	89
5.2.1.6	Boron ( <sup>10</sup> B/ <sup>11</sup> B).....	89
5.2.1.7	Strontium ( <sup>87</sup> Sr/ <sup>86</sup> Sr).....	93
5.2.2	Groundwater dating.....	95



5.2.2.1	Tritium.....	96
5.2.2.2	<sup>3</sup> H/ <sup>3</sup> He and <sup>3</sup> He methods.....	99
5.2.2.3	Radiocarbon .....	100
5.2.2.4	Silicon-32 .....	107
5.2.2.5	Chlorine-36 .....	107
5.2.2.6	Argon-39 .....	110
5.2.2.7	Krypton-81 .....	111
5.2.2.8	Krypton-85 .....	111
5.2.2.9	Iodine-129 .....	113
5.2.2.10	Uranium/Helium and K/Ar methods .....	113
5.2.2.11	Radium/radon dating method .....	114
5.2.2.12	<sup>234</sup> U/ <sup>238</sup> U dating method .....	115
<b>6</b>	<b>APPLICATIONS TO HIGH-TEMPERATURE SYSTEMS</b>	<b>119</b>
6.1	Natural processes .....	121
6.1.1	Water-rock interaction at high temperature .....	123
6.1.2	Isotopic geothermometry .....	125
6.1.3	Tracing the origin and history of fluids .....	130
6.1.4	Mixing with geothermal fluids .....	130
6.2	Anthropogenic processes .....	134
6.2.1	Steam loss .....	134
6.2.2	Underground liquid-vapour separation processes .....	138
6.2.3	Isotope techniques in re-injection studies .....	141
6.2.4	Variability of the isotopic composition in geothermal fluid .....	143
<b>7</b>	<b>PLANNING AND PERFORMANCE OF MULTIPLE ISOTOPE STUDIES</b>	<b>151</b>
	<b>REFERENCES</b>	<b>155</b>
	<b>LITERATURE</b>	<b>175</b>
	<b>IAEA PUBLICATIONS</b>	<b>177</b>
	<b>CONSTANTS</b>	<b>180</b>
	<b>GLOSSARY</b>	<b>181</b>
	<b>SYMBOLS</b>	<b>189</b>
	<b>SUBJECT INDEX</b>	<b>191</b>

# 1 HYDROGEOLOGY AND AQUIFER CHARACTERISTICS

## 1.1 DEFINITIONS

Groundwater is one of the smallest components of the hydrosphere. Groundwater flow and the inherent hydrochemical processes belong to the hydrological cycle which depends on a) the geological-ecological structure and b) the petrological composition of the lithosphere. The latter influences the geochemical processes and the hydrochemical composition of the groundwater. Both factors explain the relative low flow velocity of groundwater, its usually long residence time and the wide range of the time scale occupied by groundwater, compared to that of surface water in the hydrological cycle (Volume II).

Most groundwater is of meteoric, i.e. atmospheric origin (Volume II). Rain water directly infiltrates into the ground or indirectly via inflow of surface water (bank storage in streams). A very small part of the groundwater (juvenile water) may have its origin from the magma in the Earth's interior.

## 1.2 OCCURRENCE OF GROUNDWATER IN ROCKS

Groundwater occurs in interstices in rocks which have various shapes, sizes and origin. The ability of rocks to transmit water through its interstices is called *permeability*. This depends on the physical properties of the rock and its genetic history (geological factors and processes). The rock interstices as pathway of groundwater flow and circulation (aquifer) may be classified as follows:

*Pores* are intergranular interstices between the grains of unconsolidated as well as of consolidated clastic sediments or of loose volcanic tuffs (Fig. 1.1a),

*Fissures* are fractures or cracks in the rocks (Fig. 1.1b), and

*Cavities* are present in carbonate rocks (Fig. 1.1c) and lava tubes in volcanic rocks.

The spatial arrangement of an aquifer controls the shape and hydrodynamic type of flow, the transit time and residence time of groundwater. In fissured zones dual-flow pathways are developed, which may substantially contribute to the groundwater recharge or may interconnect aquifers across leaky aquicludes. The petrological (lithological) composition of the aquifer and the water-rock interface control the hydrochemical reactions and behaviour of the constituents dissolved in groundwater. The most important carbonate – CO<sub>2</sub> system of

groundwater is one example which has to be taken into account for  $^{14}\text{C}$  dating of DIC in groundwater (Sect.5.2.2.3; Volume I; Clark and Fritz 1997).

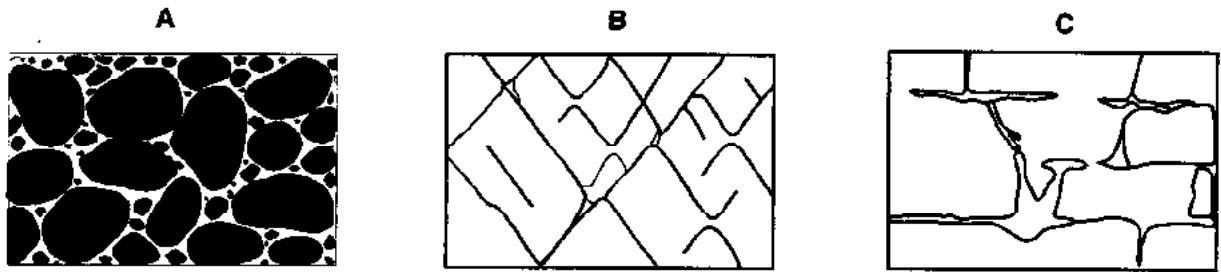


Fig.1.1 Types of rock interstices and their relation to texture and porosity. (A) Sedimentary deposits with high porosity, (B) porous rocks due to dissolved fractures, and (C) porous rocks with fissuration.

## 1.3 GEOHYDRAULIC PARAMETERS

### 1.3.1 POROSITY

A soil element has a the total volume  $V_{\text{tot}}$  and a total mass  $M_{\text{tot}}$ , a solid phase volume  $V_{\text{sol}}$  with a mass  $M_{\text{sol}}$ , a liquid phase represented by the water and dissolved salts, a volume  $V_{\text{liq}}$  and a mass  $M_{\text{liq}}$  and finally the volume of the gas phase  $V_{\text{gas}}$  (air and water vapour) with a negligible mass (Fig. 1.2).

The relative volume of pores in the rock is the total *porosity*  $n_{\text{tot}}$  defined by

$$n_{\text{tot}} = \frac{V_{\text{por}}}{V_{\text{tot}}}$$

where  $V_{\text{por}}$  is the volume of the pores, filled with gas ( $V_{\text{gas}}$ ) and with liquid ( $V_{\text{liq}}$ ):

$$V_{\text{tot}} = V_{\text{gas}} + V_{\text{liq}} + V_{\text{sol}}$$

Only part of the pore water ( $V_{\text{liq}}$ ) is free and mobile ( $V_{\text{mob}}$ ), the rest ( $V_{\text{ret}}$ ) is bound by capillary and hygroscopic forces and has a high retention time. Accordingly, free (or gravity or gravitational) water and bound (capillary and hygroscopic) water have different retention times which may be estimated by using isotope analyses.

The pore volume available for gravitational water movement ( $V_{\text{eff}}$ ) related to the total volume is the *specific yield* (also *effective porosity* or kinematic porosity):

$$n_{\text{eff}} = \frac{V_{\text{eff}}}{V_{\text{tot}}}$$

The pore volume containing water bound by capillary forces ( $V_{\text{ret}}$ ) related to the total volume

( $V_{tot}$ ) is the *specific retention* (also *capillary porosity*)

$$n_{ret} = \frac{V_{ret}}{V_{tot}}$$

The *total porosity* is the sum of the effective and capillary porosities. With increasing grain size of the clastic sediments, the total porosity  $n_{tot}$  usually decreases, the **effective porosity**  $n_{eff}$  somewhat increases and the capillary porosity  $n_{ret}$  decreases (Fig.1.3). The effective porosity is a fundamental parameter for geohydraulic calculations (mass transport modeling), while the total porosity combines the mass transport and tracer flux.

In the saturated zone, solid and liquid phases exist. In the unsaturated zone the pores in the rock are partly filled with water and partly with air (three-phase medium).

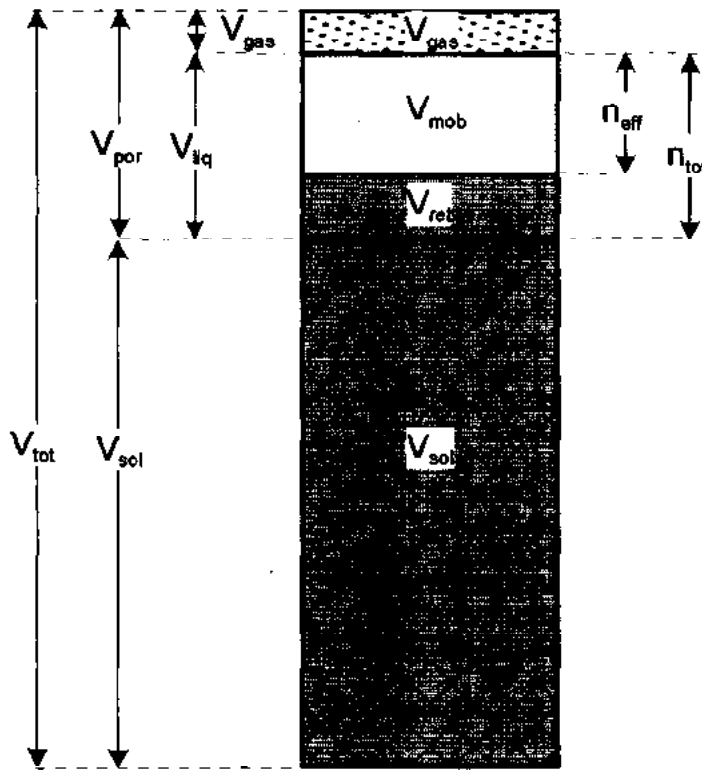


**Fig.1.2** Saturation of the pores with water.  $V_{tot}$  - bulk volume of the rock,  $V_{sol}$  - volume of the solid material (matrix),  $V_{por}$  - volume of pores,  $V_{liq}$  - volume filled with water,  $V_{gas}$  - volume filled with gas,  $V_{mob}$  - volume of pores free for gravitational flow of mobile water,  $V_{ret}$  - volume of pores filled with water which is bound by capillary and hygroscopic forces.

The *volumetric humidity* or volumetric water content is the ratio of the volume of the water to the total volume of the rock:

$$\varphi = \frac{V_{liq}}{V_{tot}}$$

The maximum volumetric humidity which can be retained against gravity is termed *field capacity*.

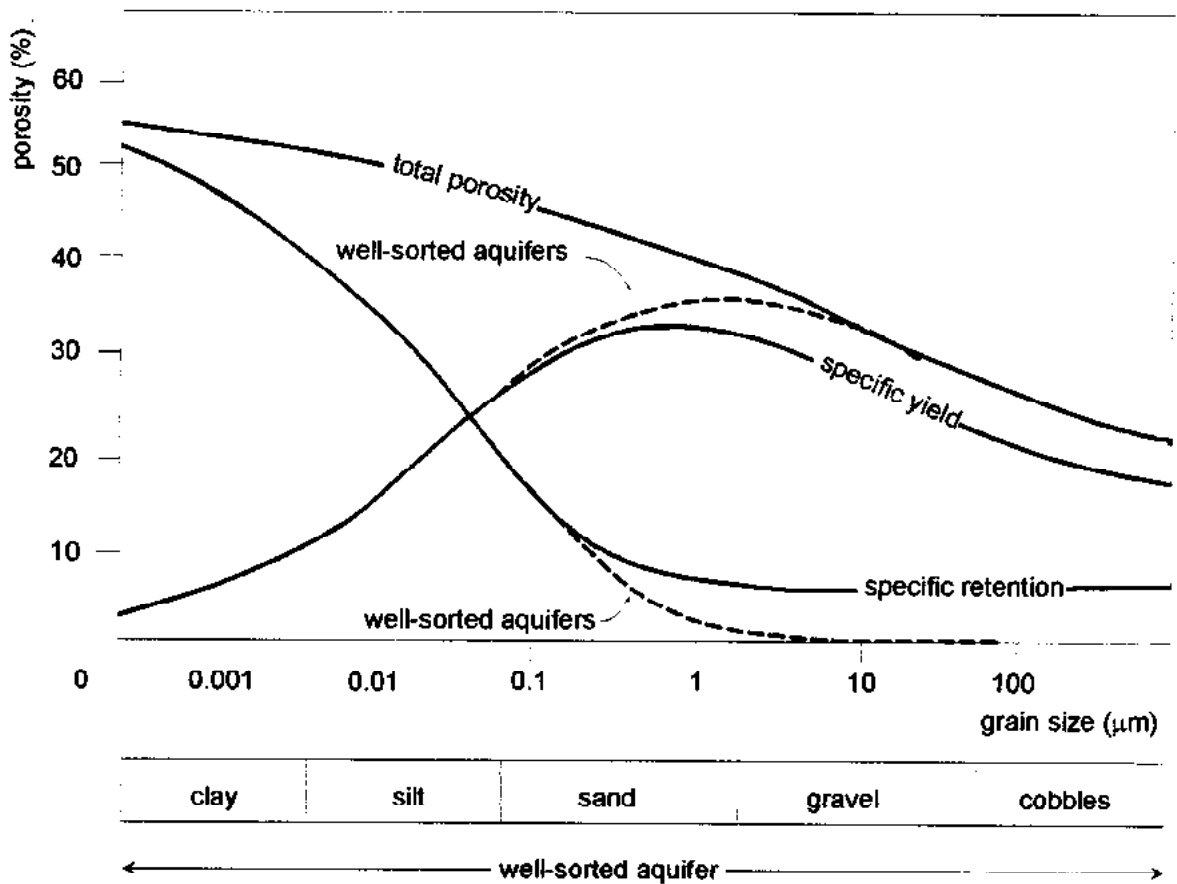


**Fig.1.3** Relation between median grain size and water-storage properties (total porosity, specific yield and specific retention) of alluvium from large valleys (after Davis and DeWiest 1966).

### 1.3.2 STORAGE, STORAGE COEFFICIENT

There are two kinds of aquifers: the *phreatic aquifer* has an open water surface, the *confined aquifer* has a confining bed. If the hydrostatic pressure of a confined aquifer is reduced, e.g. by abstraction of groundwater, the aquifer load increases and the resulting compression expels some water from the aquifer. At the same time, the lowering of the pressure causes a small expansion and subsequent release of water. The water-yielding capacity of a confined aquifer is expressed in the term of the storage coefficient.

The *storage coefficient*  $S$  is defined as the volume of water that an aquifer releases or takes into storage per unit area of aquifer per unit change of head. It equals the volume of water released from the aquifer when the piezometric surface declines by one metre. It is dimensionless and expressed as

$$S = g \cdot d (n_{eff} \cdot \beta_{liq} + \beta_{rock})$$

where  $g$  is the acceleration due to gravity,  $d$  is the thickness of the aquifer,  $n_{\text{eff}}$  is the effective porosity;  $\beta_{\text{liq}}$  and  $\beta_{\text{rock}}$  are the coefficients of compressibility of the water and rock, respectively.

In most confined aquifers, values of  $S$  are in the range of  $5 \times 10^{-5}$  to  $5 \times 10^{-3}$ . This indicates that large pressure changes over extensive areas are required to produce a substantial water yield.  $S$  is determined by pumping tests of wells. In unconfined aquifers, the storage coefficient  $S$  equals the effective porosity  $n_{\text{eff}}$  as almost all water is released by the declining, unconfined (“free”) water table due to gravitational drainage. In unconfined aquifers consisting of alluvial sediments in alluvial plains  $S$  ranges from 0.15 to 0.25, much higher than that of confined aquifers (Fig.1.3).

### 1.3.3 PERMEABILITY AND HYDRAULIC CONDUCTIVITY

*Permeability* is the property of a rock or soil to transmit water or other fluids. It determines the relation between the velocity and the hydraulic gradient, under which water flows through the rock or soil medium.

### 1.3.4 FLOW NETS

Groundwater flow in large aquifer systems can be presented as a flow net. In the three-dimensional space, the flow lines extend perpendicularly on the equipotential surface; in the two-dimensional case the flow lines are perpendicular to the equipotential lines and form a flow net of curvilinear rectangles (Fig.1.4). Equipotential lines are often called groundwater-surface contours or hydroisohypses.

The course of hydroisochrons representing the same groundwater age is usually similar to that of the piezometric contour lines. There are, however, methodical deviations which may reflect spatial peculiarities of the groundwater flow system or geohydraulic disturbances due to groundwater abstraction. Equipotential lines deviate from hydroisochrons in regions where the equipotential lines are very dense, i.e. the hydraulic gradient is high and thus the water velocity higher than elsewhere (Fig.1.5). This is also the case if the present groundwater flow is different from that of the past. For instance, an accelerated increase of the groundwater age towards the discharge area may indicate an increased groundwater recharge rate in the past.

Flow nets are meaningful only for steady-state conditions of the groundwater flow (Fig.1.5). Any change in the geohydraulic situation modifies the flow net. This fact has to be taken into account if isotope data from groundwater recharged in the past has to be related to the present flow net which might also be modified by groundwater abstraction (Sect.3.2.2).

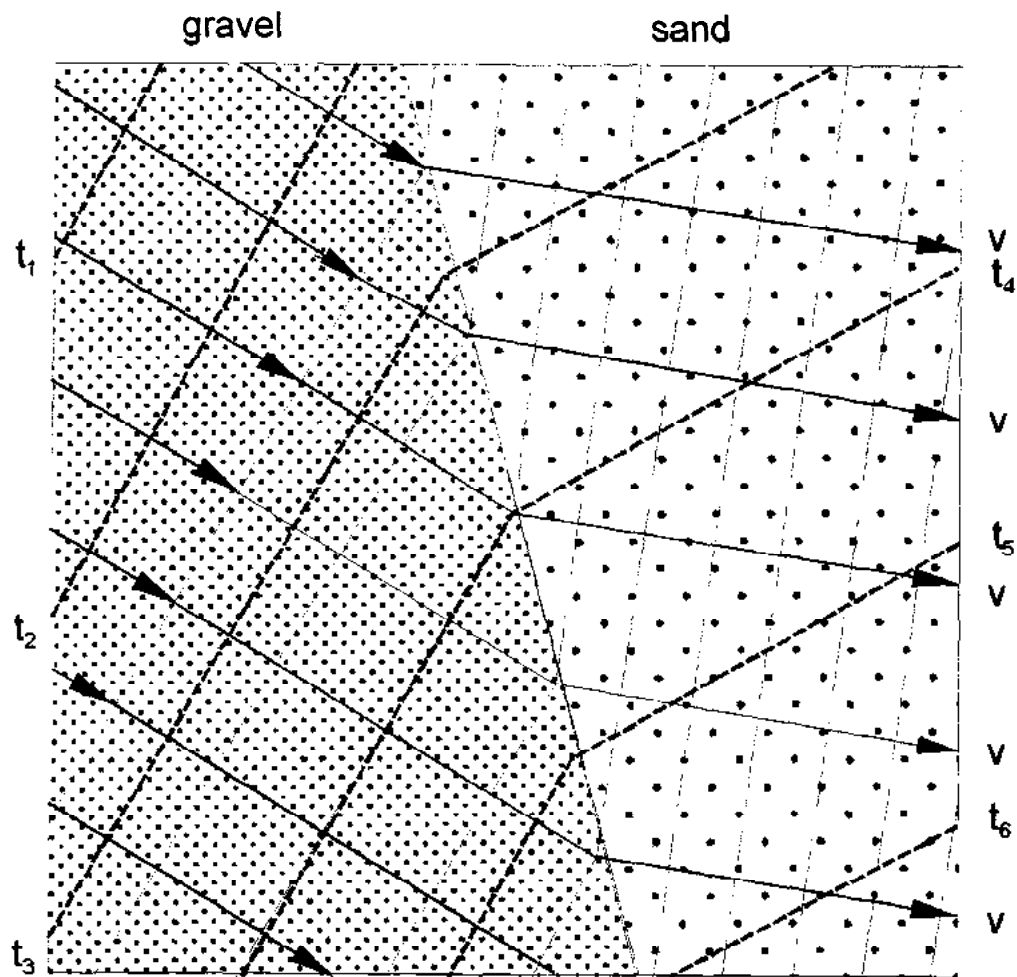


**Fig.1.4** Equipotential lines (long-dashed lines), flow lines (lines with arrows –  $v$ ) and hydroisochrons (bold short-dashed lines –  $t_1$  to  $t_6$ ) at the boundary of and within an aquifer of differing hydraulic conductivity (after Seiler and Rodriguez 1980). Equipotential lines and flow lines run perpendicularly to each other.

A flow net is usually constructed through vertical sections of the groundwater system or as a vertical projection to a horizontal plane (e.g. to illustrate the horizontal groundwater flow on a regional scale in a map). In a homogeneous and isotropic rock environment, the shape of the flow net is controlled by the groundwater level which, in humid regions with direct groundwater recharge by precipitation, usually conforms the morphology shape.

Tóth (1963) used flow nets to illustrate groundwater flow on a regional scale. Many local shallow groundwater systems may be overlain by an intermediate and a deep regional groundwater flow system. The equipotential lines for an isotropic aquifer show that the hydrological potential under surface depressions decreases in the upward direction. Therefore, such depressions discharge groundwater. In deep piezometric boreholes, the hydraulic pressure at the bottom of the borehole is larger than that at the top (artesian groundwater flow) which may not necessarily be related to a geological stratification of a system of aquifers and aquicludes.

## Aquifer Characteristics

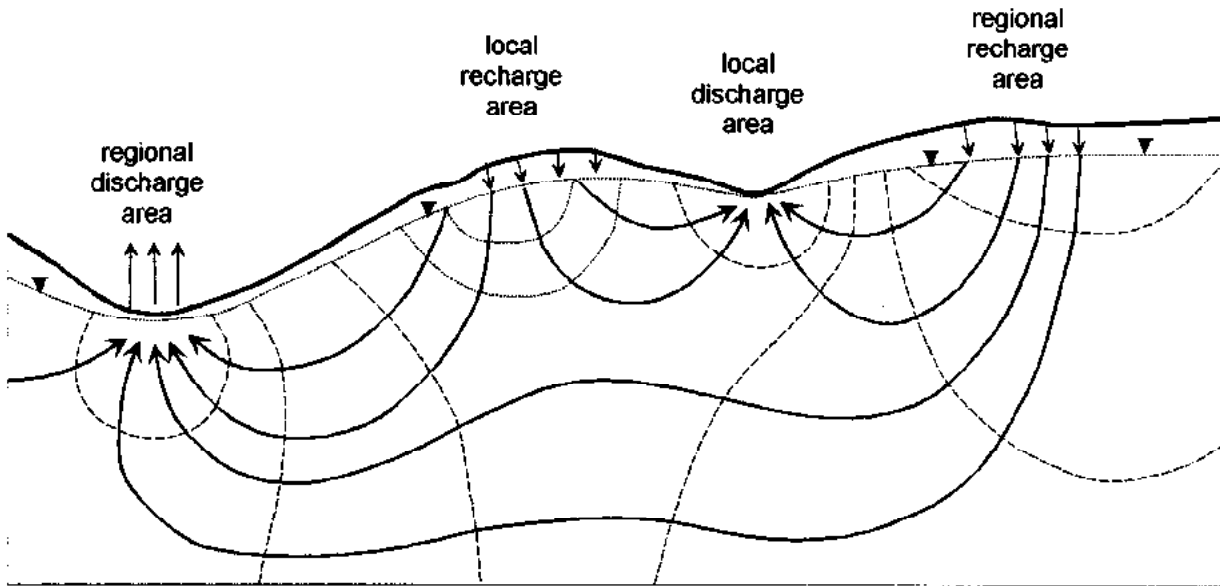


**Fig.1.5** Flow net in a vertical section through a dissected area. Full bold lines: flow lines; dashed lines: equipotential lines (after Tóth 1963).

The hydraulic conductivity of aquifers is by several orders of magnitude higher than that of the confining bed (aquitard). Thus, for a given flow rate the head loss along a flow line per unit of distance is much lower in an aquifer than in a confining bed. Consequently, lateral flow in confining beds is geohydraulically negligible while the isotope composition might become affected due to the long-lasting contribution of slow seepage to the groundwater recharge of a confined aquifer (Geyh et al. 1984). In aquifers the flow lines tend to narrow and to be parallel to the aquifer boundaries. Hence, the flow net of an anisotropic aquifer system may be very complex. As the groundwater flow net is controlled by recharge and discharge, its appearance for arid and humid regions is principally different (Fig. 1.6).

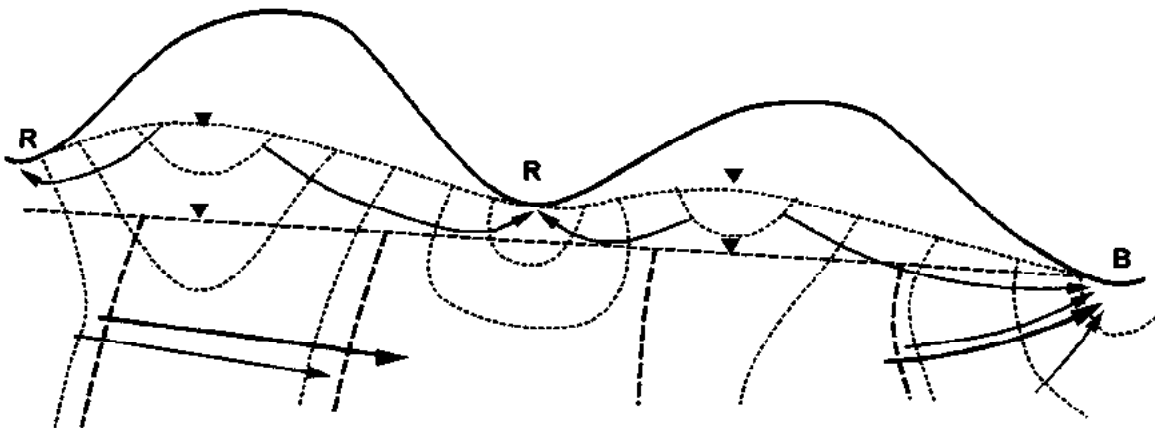


**Fig.1.6** Groundwater flow net in humid and in arid regions. Groundwater recharge in humid regions is reflected by equipotential lines (dotted lines) following the morphology. In arid regions the groundwater table is flat; R = discharge to rivers in humid regions; B discharge into basins or oasis in arid regions (after Seiler and Rodriguez 1980).



The presentation of the flow net in hydrogeological maps mirrors the groundwater flow on a regional scale and may help to solve practical problems of groundwater exploration and exploitation. It is only reliable if the hydraulic potential of a large number of piezometers in the particular aquifer was measured. Mathematical modeling can facilitate the construction of a flow net.

## 1.4 HYDROGEOLOGY

### 1.4.1 HYDROGEOLOGICAL PROPERTIES OF ROCKS

Rocks can be classified according their hydrogeological, geohydraulic (storage of water, hydraulic permeability) and pedological properties.

The Darcy equation (Sect.3.11) is only valid for laminar groundwater flow which occurs in more or less homogeneous and isotropic aquifers, e.g. in *clastic (granular) sediments* and *sedimentary rocks* (sand, gravel or sandstone). In *fissured rocks*, the spatial arrangement of fissures is usually discrete, although often a preferential spatial orientation may cause an anisotropic rock permeability. Due to this, the rock medium can only be considered homogeneous and isotropic on a very large scale. Hence, the terms porosity and hydraulic permeability cannot easily be applied to the geohydraulics of fissured rock systems.

The permeability of fissured systems reflects the geological history of the rocks, especially tectonic exposure to stress. Changes may also be due to weathering and/or other geological processes during the geological past. Younger fissure systems of late tectonic events are often more permeable than the old ones that may be sealed by secondary minerals. Uranium analyses (Sects.5.2.2.10 to 5.2.2.12) can help to distinguish young and old fissures.

In *karstified rocks* and in *lava tubes*, groundwater flow is seldom laminar; the arrangement of rock cavities is randomly distributed. Hence, the use of the Darcy law of groundwater flow may yield erratic results. Due to hydraulic interconnections of karst cavities, the results of tracer experiments are sometimes ambiguous but always yield the minimum transit time of groundwater at the time of the tracer experiment. Environmental isotope studies allow estimates of much longer mean residence times of the base flow of groundwater (Sect.5.2.2).

#### 1.4.1.1 IGNEOUS ROCKS

Igneous rocks (*plutonic* and *volcanic*) are permeable along open fissures. Usually, the width of the fissures and therefore the permeability decreases with increasing depth.

Hard *plutonic rocks* (e.g. granite) rich in quartz are prone to fissuration. By mechanical weathering they produce sandy alluvia that are permeable at the surface, while rocks poor in quartz are prone to chemical weathering, thus disintegrating to clay minerals, which are less permeable and often clog the fissures in the underlying bedrock.

*Volcanic rocks* often contain fractures that arising from the chilling of lava. In lava flows, horizontally extended permeable fractured zones occur at the surface and bottom. They often are important aquifers and occur in extensive lava flow systems of basalt plateau's.

#### 1.4.1.2 METAMORPHIC ROCKS

Metamorphic rocks are usually permeable along open fissures which are formed by weathering down to a certain depth. Acid quartz-containing gneiss as granite is prone to weathering into sandy alluvia. Metamorphic crystalline limestones are subject to karstification so that they often contain karst groundwater.

#### 1.4.1.3 CONSOLIDATED SEDIMENTARY ROCKS

According to their hydrogeological properties, there is a great variety of sedimentary rocks, but they form the most important aquifers. They can bear several types of interstices and have a wide range of permeability. The permeability may be anisotropic; that is why modeling of the regional groundwater flow and the motion of pollutants and tracers is very difficult or not impossible. *Dual-porosity* has to be taken into consideration when evaluating the groundwater flow and the movement of pollutants and tracers in such rock medium (Sect. 5.1.2.2.3). It considers fast and a slow moving components.

Groundwater flow in sedimentary rocks depends on the composition of the rock, on the lithology and facies of the entire sedimentary sequence, i.e. on the grain size and composition in horizontal (lateral) and vertical directions. Usually the permeability of sediment in the horizontal (lateral) direction is orders of magnitude higher than in the vertical direction. In consolidated sedimentary rocks the groundwater flow also depends on fissuration due tectonic disturbances and on secondary exogenous alterations (weathering, karstification, etc.). In summary:

*Sedimentary rocks* rich in carbonates and sulphates may be divided into several groups. Geochemical processes may influence the isotope composition of the groundwater (e.g.  $^{14}\text{C}$ ). Sandstones are usually important aquifers while arkose and graywacke are not.

*Claystones, marlstones and shales* have usually a very poor hydraulic permeability. This is the reason why they are often aquicludes between aquifers and determine the spatial arrangement of the flow system.

*Carbonate rocks (limestones and dolomites)* are excellent aquifers as they are usually karstified. Carbon dioxide in water dissolves the rock, widens fissures and creates karst cavities with often very large cross sections. As the filtration capacity is low, groundwater is often polluted and its flow very fast.

*Easily soluble sedimentary rocks (evaporites)* include gypsum, anhydrite, sodium chloride (halite), and other salts. In contact with groundwater large karst cavities are rapidly formed, causing subsidence of the surface and creating serious problems such as bursts of water into

salt mines. Stable isotope analyses allow to identify the origin of groundwater as well as of brines, and to support measures against such catastrophic events.

*Organic sediments of biolite type* (coal, lignite, peat, coal argillites) form insignificant aquifers, but are important for influencing the chemical and isotope composition of groundwater in supplying organic carbon components. The application of  $^{14}\text{C}$  for groundwater dating might be disturbed (Sect.5.2.2.3).

#### 1.4.1.4 UNCONSOLIDATED SEDIMENTS

Unconsolidated sediments consist of various kinds of gravel, sand and clay, sometimes with admixed organic matter. They occur as alluvia in river valleys, lacustrine sediments in lake basins, or shelf sediments along the coast. They are also found as delta sediments, sediments of alluvial cones of intermountain depressions, and glaciofluvial sediments washed out from moraines. Usually, unconsolidated sediments are excellent and the most efficient aquifers. Their porosity and permeability are usually high, unless clay is admixed, and depend on the grain-size distribution (Fig.1.3) rather than the absolute size of the grains. The decisive factor is the presence of the very fine clay particles. With increasing effective porosity the permeability increases. Thick deposits may subside considerably if the hydraulic pressure decreases due to intensive groundwater abstraction.

In humid regions, wind-blown fine and well-sorted dune sands form significant aquifers with excellent filtration properties.

#### 1.4.2 HYDROGEOLOGICAL STRUCTURES - GROUNDWATER REGIMES

The *hydrogeological structure* describes the configuration of aquifers and aquicludes within the geological environment. It determines the groundwater circulation from the *recharge area*, along the percolation and circulation pathways (*groundwater reservoir*) to the *drainage area*. *Water divides*, determined by the orography or the geology of the region, separate groundwater recharge areas of neighbouring hydrogeological systems. Thus, a hydrogeological structure has fixed limits set by both the geomorphology and the geological structure.

The drainage rate in a hydrogeological system depends on the hydraulic gradient or the slope of the piezometric surface. The latter usually changes due to the seasonally variable groundwater recharge (as the fluctuation of groundwater level is controlled by precipitation) or due to anthropogenic influences (e.g. due to pumping of water from the aquifer; Sect.3.2.2).

Under favourable conditions, a hydrogeological structure contains a usable *resource of groundwater*. The economic value depends on the *yield* (discharge rate of usable groundwater) and the storage volume (*water reserve* or *storage*).

The complex of conditions which govern the change of the quantitative and qualitative factors

of groundwater flow in time and space is called the *groundwater regime*. Such groundwater regime may be studied by analyses of environmental isotopes, supplementing classical hydrological approaches such as:

Radionuclide dating (Sect.5.2.2) in combination with analyses of stable isotopes (Sect.5.2.1) may clarify the period and climatic conditions during groundwater recharge (*groundwater dating* and *palaeohydrology*; Sect.3.2.1). In particular, isotope studies help to determine the origin of the groundwater, to clarify ecological problems related to the hydrological cycle, and to provide information needed for sustainable groundwater management and protection. For the interpretation of isotopic data the actual hydrogeological structure and the groundwater flow system have to be simplified in order to develop a model that may describe the hydrodynamic behaviour (Sect.3.1.2; Volume VI). For this task, basic knowledge on the main types of hydrogeological structures is necessary.

### **1.4.3 CRYSTALLINE REGIONS**

Hydrogeological structures in crystalline regions (in plutonic and metamorphic rocks) are characterised by shallow groundwater circulation in the zone of weathering and fissuration, which only reaches a depth of some tens of metres. These shallow groundwater flow systems may be considered as completely mixed reservoirs. In the discharge area numerous small springs and wet spots are present at the surface along faults or tectonic lines. Their spatial distribution reflect the geological structure and morphology as tectonic zones and faults act as regional groundwater drainage systems. Any deep-reaching groundwater circulation, separated from the shallow local flow system, is characterised by long residence times (e.g. thermal groundwater).

#### **1.4.3.1 VOLCANIC ROCKS**

Abundant and significant groundwater resources (e.g. in the Columbia Basin in the NW of the USA, and in some parts of the Dekkan Plateau in India) may exist in basin-like structures, which are sometimes developed in volcanic regions with extended basalt-lava flows. Particular bodies of volcanic effusions provide usually only small groundwater resources. In deeper parts piston-like lateral groundwater flow may occur. High groundwater abstraction from deep artesian aquifers may lower their piezometric level resulting in an admixture of shallow groundwater. In morphologically dissected terrains, such local shallow groundwater flow prevails in the upper parts of the aquifers.

#### **1.4.3.2 FOLDED SEQUENCES OF SEDIMENTARY ROCKS**

In folded sequences of sedimentary rocks (e.g. limestone, sandstone), the groundwater flow depends upon the type, thickness and extension of the aquifers and aquicludes. In tectonic structures deep-reaching, extended circulation systems may exist beside shallow ones (Fig.1.7) indicated by temperature anomalies in spring waters and a high concentrations of

dissolved solids. Groundwater often consists of components of different residence times complicating the evaluation of isotope data (Maloszewski and Zuber 1993, 1996, 1998; Zuber 1986; Volume VI). Each system has to be considered individually.

#### **1.4.3.3 KARSTIFIED ROCKS**

In karstified rocks, the spatial arrangement of the groundwater flow systems differs from locality to locality and is controlled by the continuously changing geological and morphological evolution. Groundwater flow occurs as large underground streams and springs, on the one hand providing excellent conditions for the exploitation of groundwater. On the other hand, the high permeability of the cavities bears the risk of groundwater contamination from the surface. In hydraulic engineering, karst systems often cause problems of reservoir leakage (Dreybroth 1984). The geochemical processes affecting the karstification have to be taken into account when evaluating isotope results.

Groundwater flow responds quickly to precipitation. The flow velocity of the short-term component is high (in the range of hundreds of metres per day), and consequently the residence time of this karst groundwater is usually short. The base flow, however, may have mean residence times of years or even decades. For the interpretation of isotope data, the reservoirs are assumed to be completely mixed (exponential model) (Volume VI). In shallow groundwater systems, the fluctuation of the recharge by precipitation is propagated through the system, while it is equalised in large and deep systems.

The geological and morphological evolution of the rock environment in the past determine the stage and depth of karstification of the present flow system. Karstification of carbonate rocks started usually from the surface and continued into the depth. A deep drainage network might had become developed similar to a surface river network.

In basin-shaped structures, under thick volcanic flows or along deep-reaching faults, karstified carbonate rocks may be confined.

#### **1.4.3.4 PLATFORM SEDIMENTS**

In platform sediments (sediments deposited on the flat surface of the previously folded and consolidated bedrock), extended basin-shaped structures might be developed which pass over to tablelands and escarpments on their margins. According to the lithological development and geological structure, often large and rich groundwater resources exist (Fig.1.7). Examples are the Dakota Basin, the Great Artesian Basin in Australia, the Nubian Sandstone Basin in North Africa, the Siberian Basin and the Paris Basin. The quality of groundwater depends on the lithological composition of the rocks and on geochemical processes. In zones of moderate, humid climate, the groundwater is usually of good quality and continuously recharged. In confined aquifers, the groundwater is protected against contamination. In deep aquifers of arid regions, also highly mineralised old groundwater is present which was recharged in the

geological past under more humid climatic conditions. Such non-renewable groundwater resources are mined when they are abstracted. Isotope hydrological methods allow identifying such old resources (Sect.5.2.1). Under such non-steady state recharge-discharge conditions, groundwater dating or estimating the groundwater flow velocity is no longer possible (Sect.3.1.2).

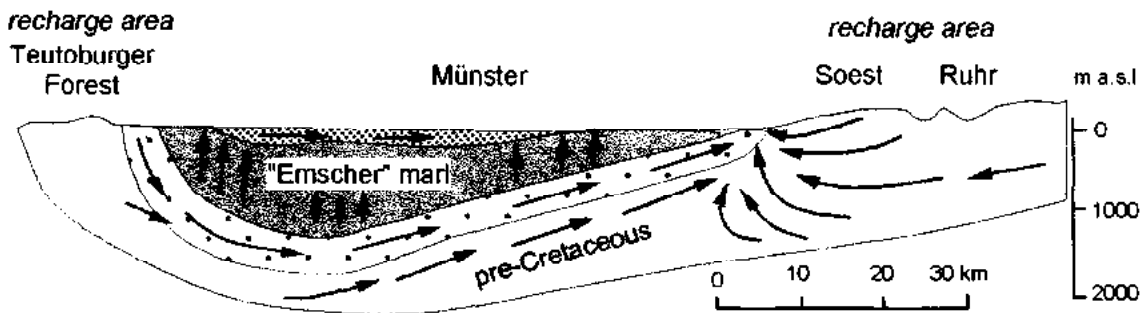


**Fig.1.7** Schematic hydrogeological cross-section through the confined Basin of Münster (after Michel and Struckmeier 1985), an example of a deep-seated basin. The pre-Cretaceous rock and the "Emscher" marl are aquitards. The arrows mark the groundwater flow.

#### 1.4.3.5 ALLUVIAL PLAINS AND FANS, RIVER DELTAS, GLACIOFLUVIAL SEDIMENTS

Alluvial plains and fans, river deltas, and glaciofluvial deposits usually of Quaternary age consist of unconsolidated sediments and often contain large groundwater resources. Gravel and sand dominate with intercalations of silt, mud and clay. The grain size composition depends upon the evolution of the riverbed and of the sedimentation basin. In humid regions such aquifers are often covered by flood loam which prevents pollution. Extended Quaternary alluvia, often several hundreds of metres thick, are located in areas of tectonic subsidence as e.g. in the alluvial plains of the rivers Amazon, Ganges and Danube.

Alluvia usually offer excellent conditions for groundwater development. During rainy periods the river level is high and water indirectly recharges the groundwater reservoir. If the river level is low, the river is replenished from groundwater (Fig.1.8). The response of the groundwater table to precipitation is fast, and the residence time of the groundwater is short. On a large scale, alluvial plains are considered as open reservoirs.

In arid regions, occasionally floods occur in channels filled with sediments (wadi, oued) which are often unsorted, sometimes of low permeability, due to the admixture of muddy material. Permeable zones develop where stream flow persists long enough to sort the coarser debris in the stream channel. They extend only over small parts of the channel, are difficult to locate and are responsible for run-off recharge, which is the dominant recharge process in arid regions.

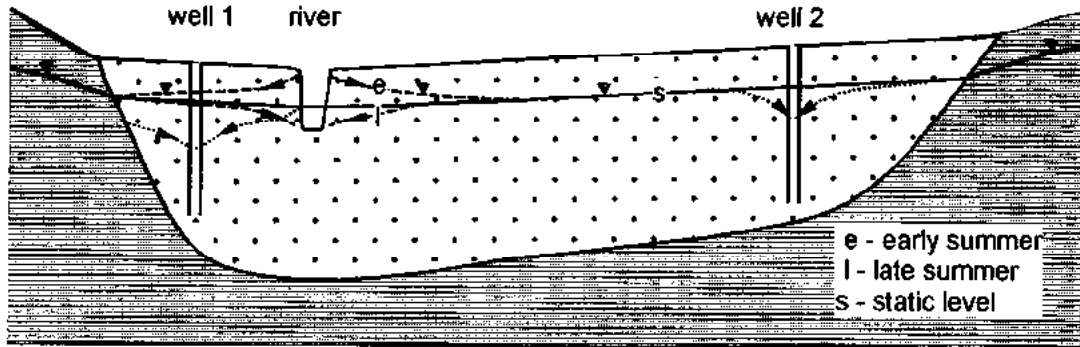


**Fig.1.8** The geohydraulic interrelation between the groundwater in alluvial sediments and the water in a stream. The static water level reflects the mean geohydraulic situation without abstraction during the year. Well 2 pumps groundwater of the alluvial sediments and lowers the static level (dotted lines). Bank infiltration may be induced from the river after the snow melt and high river level (early summer). In autumn the river is low and groundwater feeds the river. Well 1 pumped groundwater and river water (dotted lines).

## 2 TRACERS AND TRANSPORT

Groundwater contains a larger or smaller amount of inorganic and organic substances, mainly in *solution* but also in *colloidal* or even *suspended* form. Suspended matter is not a usual feature of groundwater, because such particles are effectively filtered out due to the generally slow rate of movement through the interstices in aquifers. It may be, however, a noticeable component in fast-flow systems such as those typically developed in karstic terrain.

Dissolved and to some extent colloidal contents of groundwaters have been studied extensively. The subject of groundwater chemistry in relation to water quality prediction is far from being simple - adsorption, desorption and dispersion can change concentrations during transport (Chapter 4; Clark and Fritz 1997).

The dissolved and colloidal tracers may be of *natural* or *anthropogenic origin*. These two origins tend to provide information on different aspects of groundwater movement.

### 2.1 TYPES OF TRACERS

There are general attributes for any tracer. Tracers need to be *mobile, soluble* and should not be strongly retarded by the soil or aquifer matrix. That means, the tracer should be *non-reactive (conservative)* and, of course, needs to be *easily measurable*.

We distinguish *historical tracers* and *environmental tracers*.

A historical tracer is one for which high concentrations resulted from some historical event. It has long time to move and is used to determine the rate of movement or to estimate the recharge rate. The historical events could be anything from a change of farming practice to factory pollution. The most important historical tracers for isotope hydrological studies are those that are commonly used are bomb tracers ( $^3\text{H}$ ,  $^{14}\text{C}$ ,  $^{36}\text{Cl}$ ,  $^{137}\text{Cs}$ ); for these the peak injection occurred in 1963/1964 (Fig. 2.1).

An environmental tracer exists naturally; its spatial pattern or overall mass balance is used to infer recharge and discharge rates. The major drawback is that it is usually difficult to define their exact input function (time and amplitude). Furthermore, the spatial distribution of the tracer input is not well defined. Examples are the cosmogenic radionuclides  $^{14}\text{C}$ ,  $^3\text{H}$ , and  $^{36}\text{Cl}$  (Volume I; Geyh and Schleicher 1990), but also the stable isotope abundance ratios of oxygen and hydrogen, which vary over the year (Volume I; Gat and Gonfiantini 1981).



## 2.2 TYPES OF TRACER EXPERIMENTS

The specific choice of application of environmental isotopes depends on the geometric and time scale.

*Field parameter techniques* are dealing with small areas as e.g. lysimeters. With these the effects of precipitation recharge and evapotranspiration can be determined under natural conditions. A limitation is that refilled lysimeters may not reconstitute the real structure of the soil. Usually the stable isotope composition is monitored.

On a *regional scale* the natural variation of the environmental isotope composition has a high potential for hydrogeological studies. Elevated tritium levels resulting from thermonuclear bomb tests are used to understand young groundwater systems (Sect.5.2.2.1 and 5.2.2.2). Studies with stable isotopes (Sect.5.2.1) are based on regionally different flowpaths or circulation patterns of storms and their differing stable isotope compositions (Volume II). Monitoring the natural tracer concentration in the water of rivers, springs, wells and the unsaturated zones allows to estimate the contribution of different recharge processes to the groundwater recharge (Behrens et al. 1979).

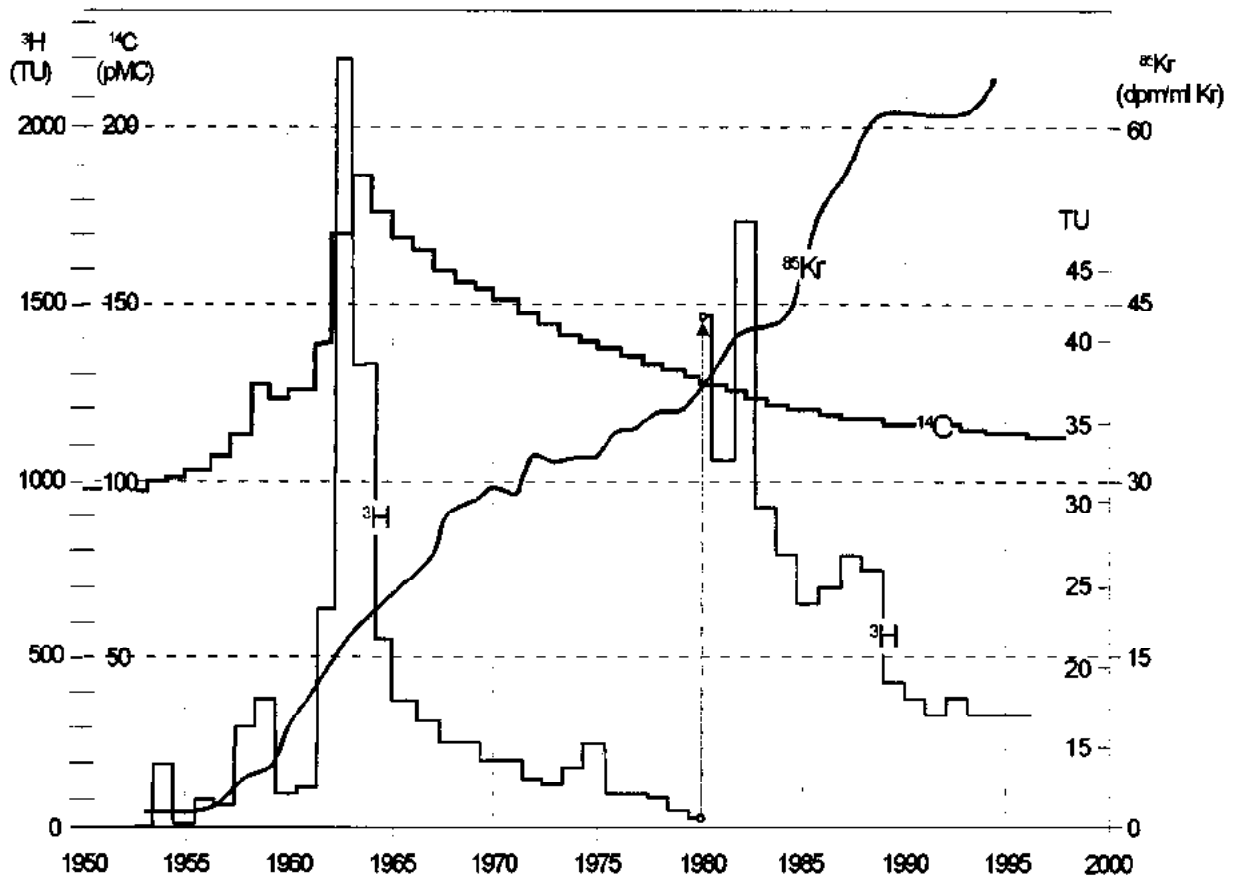


**Fig.2.1** Input curves of the radioactive tracers ( $^{14}\text{C}$ ,  $^3\text{H}$ ) from nuclear weapon tests with a peak injection at 1963/1964 and from the continuous emissions of the nuclear industry ( $^{85}\text{Kr}$ ).

## 2.3 ISOTOPES IN GROUNDWATER

Tracing groundwater by means of environmental isotopes offers unique and supplementary information on the origin and movement of groundwater and its dissolved constituents, as well as allows a quantitative evaluation of mixing (Sect.3.2.1; Volume VI) and other physical processes such as evaporation and isotopic exchange in geothermal systems (Chapter 6). Often secondary water-rock interactions can be studied (Chapter 4; Volume I), of which the occurrence is decisive for whether or not isotopes act as conservative or non-conservative tracers. Under suitable geochemical and hydrochemical conditions dating of the groundwater is possible (e.g. by the  $^{14}\text{C}$  method, Sect.5.2.2.3).

A comprehensive introduction in the physics, chemistry and measurement techniques of isotopes and the applied standard substances is given in Volume I. Various textbooks are recommended for reading (e.g. Moser and Rauert 1980, IAEA 1983 Mazor 1991, Clark and Fritz 1997).

### 2.3.1 STABLE ISOTOPES

Isotopes of the same chemical element have almost identical physical and chemical properties. However, because of their small mass differences, they have different reaction rates and different abundances in two chemical compounds or phases that are in isotopic exchange. Also physical processes such as diffusion, evaporation, condensation, melting, etc. produce isotopic differentiation. All these variations in the isotopic composition, produced by chemical or physical processes, in compounds or phases, present in the same system, are called *isotopic fractionation* (Volume I).

The atomic ratio  $R$  of the less frequent to the abundant isotope changes of a sample (spl) is usually determined by mass spectrometer and expressed as delta value referring to a certain reference material (standard, std):

$$\delta = \frac{R_{\text{spl}}}{R_{\text{std}}} - 1 \quad (\times 1000\text{‰}) \quad (2.1)$$

The most important atomic constituents of the water molecule are  $^{16}\text{O}$  and  $^{18}\text{O}$  ( $\Rightarrow \delta^{18}\text{O}$ ) and  $^1\text{H}$  and  $^2\text{H}$  ( $\Rightarrow \delta^2\text{H}$ ). These have the widest field of application in groundwater studies, for instance, tracing the origin of the water, the mode of recharge of groundwater, determining the age (short-term due to the seasonal variation and long-term due to the distinction between Holocene and Pleistocene groundwater (Sect.5.2.1.1.; Volume I).

One has to keep in mind that the  $\delta^{18}\text{O}$  value is very small and ‰ is no unit. ‰ means 1 over 1000. Hence, the delta value are always smaller than 1, although numbers in connection with per mill, e.g. 25‰, are large: 25‰ is equivalent to 0.025.

The carbon isotopes  $^{13}\text{C}$  and  $^{12}\text{C}$  ( $\Rightarrow \delta^{13}\text{C}$ ) play an important role in quantifying water-rock

interactions in the case of  $^{14}\text{C}$  age determination of groundwater (Sect.5.2.2.3). Their ratio also allows to identify the proportion of biogenic and carbonate  $\text{CO}_2$  in water and to determine initial geological settings of the groundwater recharge (Sect.5.2.1.2)

The nitrogen isotopes  $^{15}\text{N}$  and  $^{14}\text{N}$  ( $\Rightarrow \delta^{15}\text{N}$ ) are useful anthropogenic tracers. The biogenic isotopic fractionations are complex, but often allow to determine the source of organic pollution in groundwater (e.g. Heaton 1984, 1986; Sect.5.2.1.3).

The stable isotopic ratio of the sulphur isotopes  $^{32}\text{S}$  and  $^{34}\text{S}$  ( $\Rightarrow \delta^{34}\text{S}$ ) allows to differentiate between marine, evaporitic and volcanic sources of dissolved sulphate in groundwater (Krouse 1980). Biochemical processes change the isotopic composition and may thus be recovered (Sect.5.2.1.4).

Recently, the isotopic ratios  $^{37}\text{Cl}/^{35}\text{Cl}$  (Sect.5.2.1.5) and  $^{10}\text{B}/^{11}\text{B}$  (Sect.5.2.1.6) have been used in pollution studies of groundwater (Eggenkamp 1994; Frappe et al. 1995). The strontium isotopic ratio ( $^{87}\text{Sr}/^{86}\text{Sr}$ ; Sect.5.2.1.7) is a valuable tracer for mixing and source studies of mineralised groundwater.

### 2.3.2 RADIOACTIVE ISOTOPES

The other important group of isotope hydrological methods is related to radioactive environmental isotopes (Sect.5.2.2). Their main field of application is isotopic dating. The clocks begin ticking as soon as the radionuclide enters the groundwater i.e. at the time of recharge. The time unit is given by the half-life  $T_{1/2}$  during which any activity of a specific isotope decays by 50%. After 10 half-lives the activity has decreased to only 1‰ of the original activity. The range of half-lives for the various environmental isotopes is large: from 300 000 yr ( $^{36}\text{Cl}$ ), to 5730 yr ( $^{14}\text{C}$ ) and 12.43 yr ( $^3\text{H}$ ).

There are two main principles of groundwater dating: in the case of cosmogenic radionuclides the initial specific activity  $A_{\text{init}}$  of any given radionuclide in the infiltrating groundwater is known or can be estimated. It then declines according to the radioactive decay law, from which the age of the sample  $t$  follows as

$$t = \frac{\ln 2}{T_{1/2}} \cdot \ln \left( \frac{A_{\text{init}}}{A_{\text{spl}}} \right) \quad (2.2)$$

where  $T_{1/2}$  is the half-life of the given radionuclide (Fig.2.2).

The most important representative of this class of tracer applications is the  $^{14}\text{C}$  method. It provides an age of old groundwater by dating the dissolved inorganic carbon content (DIC; Sect.5.2.2.3). The application often comes to complex recherches on the water-rock interactions of the carbon isotopes (Volume I; Sect.4.4). Much older groundwater in very extended basins may be dated by  $^{36}\text{Cl}$  (Sect.5.2.2.5),  $^{81}\text{Kr}$  (Sect.5.2.2.7) and  $^{129}\text{I}$  (Sect.5.2.2.9) (see also Volume I). Groundwater ages up to 1000 yr are determined by the  $^{39}\text{Ar}$  method (Sect.5.2.2.6), if the geological setting of the aquifers excludes underground production of

this isotope. Uranium isotopes are useful for mixing studies and are also promising for groundwater dating (Sections 5.2.2). Still in an experimental stage is the groundwater by means of  $^{32}\text{Si}$  (Sect. 5.2.2.4). Multi-isotope studies together with hydrochemical analyses are recommended in any case study.

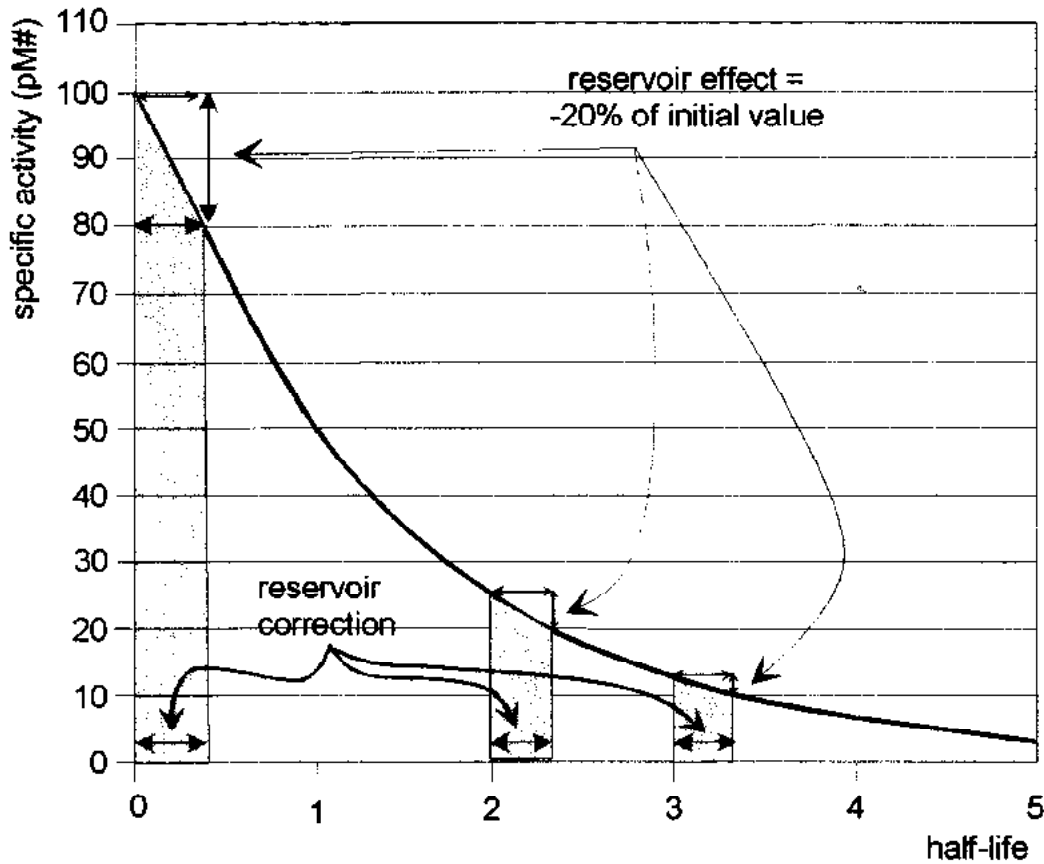


**Fig.2.2** Decrease of the specific activity  $A_{\text{spl}}$  of a sample by radioactive decay in units of the half life and for two materials with deviating initial activities  $A_{\text{init}}$ : 100 pMX and 80 pMX. It is obvious that the apparent age for the material with the lower  $A_{\text{init}}$  is higher. The relative differences of the activities of both materials (reservoir effect) just as the age difference (reservoir correction) remains constant and independent of the age.

The most important representative of this class of tracer applications is the  $^{14}\text{C}$  method. It provides an age of old groundwater by dating the dissolved inorganic carbon content (DIC; Sect.5.2.2.3). The application often comes to complex recherches on the water-rock interactions of the carbon isotopes (Volume I; Sect.4.4). Much older groundwater in very extended basins may be dated by  $^{36}\text{Cl}$  (Sect.5.2.2.5),  $^{81}\text{Kr}$  (Sect.5.2.2.7) and  $^{129}\text{I}$  (Sect.5.2.2.9). Groundwater ages up to 1000 yr are determined by the  $^{39}\text{Ar}$  method (Sect.5.2.2.6), if the geological setting of the aquifers excludes underground production of this isotope. Uranium isotopes are useful for mixing studies and are also promising for groundwater dating (Sections 5.2.2). Still in an experimental stage is the groundwater by means of  $^{32}\text{Si}$  (Sect.5.2.2.4). Multi-isotope studies together with hydrochemical analyses are recommended in any case study.

The second principle of dating groundwater is based on tracing of groundwater with isotopes with variable input functions in time. There are suitable anthropogenic radionuclides produced by nuclear weapons tests (Fig.2.1) such as  $^3\text{H}$  (Sections 5.2.2.1),  $^3\text{H}/^3\text{He}$  (5.2.2.2),  $^{14}\text{C}$  (Sect.5.2.2.3), and  $^{36}\text{Cl}$  (Sect.5.2.2.5). Some others are produced by the nuclear energy industry ( $^{85}\text{Kr}$ ; Sect.5.2.2.8).

As in tracer experiments, for this kind of groundwater dating the so-called *input function* must be known or determined, i.e. the change of the specific activity of a certain radionuclide in precipitation or the atmosphere at the moment of groundwater recharge. Depending on the atmospheric medium from which the given radionuclide is derived, the input function is related to precipitation (for  $^3\text{H}$ ), atmospheric carbon dioxide (for  $^{14}\text{C}$ ), and air (for  $^{85}\text{Kr}$ ; Fig.2.1). Through the use of appropriate geohydraulic models (Volume VI; Sect.3.1.2) it may be possible to estimate the age or mean residence time of a groundwater sample from its isotopic composition. The precision of the results depends significantly on the reliability of the input function and the validity of the applied model.

When evaluating isotope data by mathematical models, besides radioactive decay, there may be other processes, which affect the spatial and temporal change of the radionuclide content in groundwater. These processes are mainly *hydraulically controlled mixtures* (Volume VI; Sect.3.2.1). When only two components are involved, the measured values of several samples will fall on a mixing line, from which the properties of the original components (end-members) can be determined (Fig.2.3) *Hydrochemically controlled changes* occur of isotopes as radiocarbon are bound in dissolved compounds (in the case of carbon mainly as bicarbonate and carbon dioxide) which may react with the aquifer rock. Such a process affecting  $^{14}\text{C}$  would be precipitation or re-dissolution of aquifer carbonates proceeding under stationary equilibrium (Clark and Fritz 1997).

### 2.3.3 CHEMICALS

Chemical compounds have to be shortly discussed as they are often needed for an unambiguous interpretation of isotope results. The simplest natural chemical tracing of groundwater movement tends to rely on measuring the chloride concentration.  $\text{Cl}^-$  is a conservative tracer, which is subject, neither to adsorption or desorption during transport. Hence, the relation between chloride concentration and  $\delta^{18}\text{O}$  or  $\delta^2\text{H}$  values illustrates the effect of various processes such as groundwater mixing (Fig.2.3), the dissolution of halite or the admixture of saline water, seawater or brine (Sect.3.2.1.1; Fig.5.16).

During hydrochemical evolution the concentration of individual ionic species either increases, remains constant or decreases. For example, in the case of water-rock interaction a  $\text{Na}^-$  increase along the aquifer flowpath, associated with a decrease in  $\text{Ca}^{2+}$  and  $\text{Mg}^{2+}$ , is attributed to ion exchange with clay minerals (e.g. Clark and Fritz 1997); changes in  $\text{Ca}^{2+}$ ,  $\text{Mg}^{2+}$  and  $\text{SO}_4^{2-}$  are due to anhydrite dissolution and dedolomitisation (e.g. Plummer et al. 1994). The process of incongruent dissolution can have quite different effects on groundwater chemistry

depending on the rock type involved (e.g. Gislason and Eugster 1987). In other cases bacterially-mediated redox reactions may occur, commonly resulting in an increase in dissolved  $\text{Fe}^{2+}$  and  $\text{Mn}^{2+}$  along the flowpath, and not especially sensitive to the aquifer lithology (e.g. Edmunds et al. 1987; Mariotti et al. 1988). The identification of the processes is essential for  $^{14}\text{C}$  groundwater dating. These reactions also modify the  $\delta^{13}\text{C}$ ,  $\delta^{34}\text{S}$  and  $\delta^{15}\text{N}$  values.

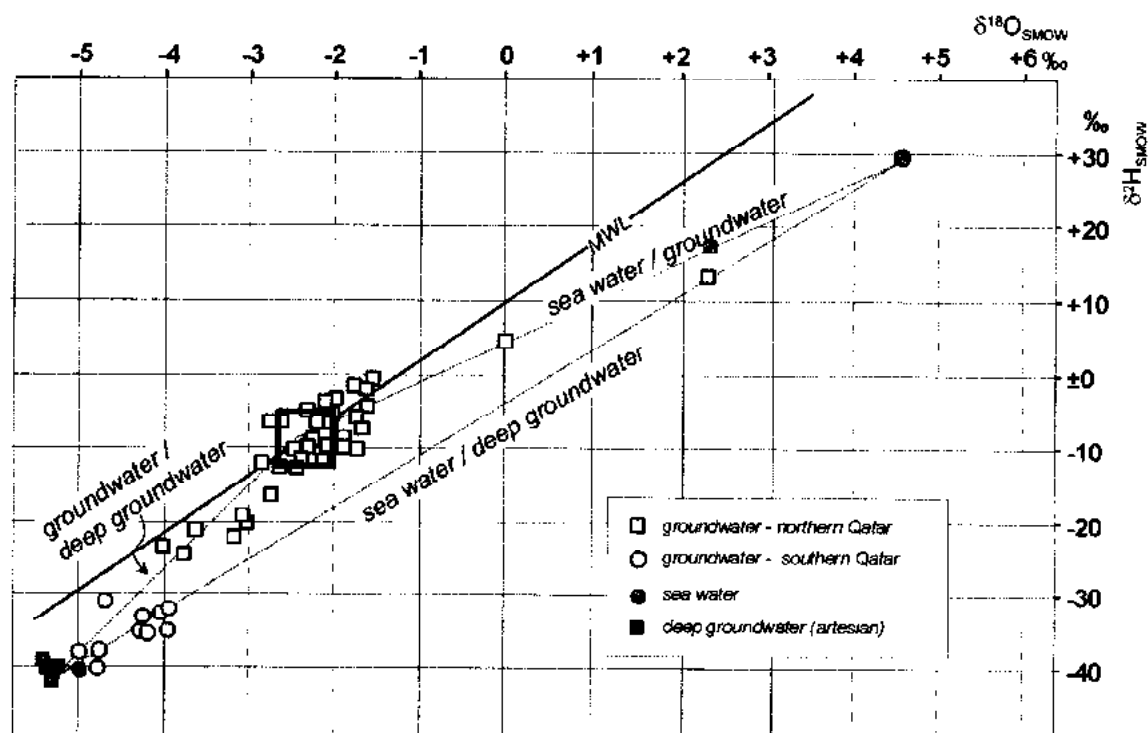


**Fig.2.3** Three-component mixing triangle: three mixing lines of two-components each between sea water/deep groundwater, sea water/groundwater and deep ground/groundwater for Qatar (Yurtsever and Payne 1979). The concept of three-component mixing is confirmed as most of the data point fall into the triangle.

### 2.3.4 COLLOIDS

Colloidal particles have diameters of less than  $10\ \mu\text{m}$  and may have an organic or mineral origin. They may result from breakdown of larger particles or, more commonly, from the aggregation of smaller particles. Owing to their relatively large and reactive surface area, they are able to absorb heavy metals, radionuclides and organic compounds. In addition they may be hydrophobic or hydrophilic, and tend to flocculate as ionic strength increases (Drever 1997). Colloids may influence the isotope compositions of various isotopes by adsorption, though no studies of this are known. In groundwater of crystalline rocks and some sandstones, colloidal complexation of the heavier metals results from silica and clay minerals, affecting also the uranium isotope composition.

Colloids are more abundant near sources of recharge, and also in karstic systems where they

may reflect storm-driven changes in chemistry or flow rates.

While many investigations have centred around the impact of colloids on radionuclide migration in low-permeability formations (e.g. Grindrod 1993; Degueldre et al. 1996), much less is known about colloids in aquifers containing potable water (Stagg et al. 1997).

The extent to which colloids are present in groundwaters varies, but concentrations are unlikely to exceed  $100 \text{ ng L}^{-1}$  except under extreme conditions (Degueldre et al. 1996). This implies that their presence is only of concern if we are dealing with highly toxic contaminant species, in principal certain radionuclides and possibly some organic compounds.

### 2.3.5 NOBLE GASES

Noble gases have attracted attention in hydrogeological studies, particularly where older groundwaters are involved. The noble gases are chemically inert. They are used for hydrogeological investigations in two quite different ways:

**Assessment of *recharge temperature*:** the aqueous solubilities of Ar, Kr and Xe change individually with temperature with the result that any particular ratio of Ar/Kr/Xe can be interpreted to give the absolute recharge temperature with a precision of about  $\pm 1.5^\circ\text{C}$  (Andrews 1991, 1992; Volume I, Sect.2.3.5). Excess Ar produced by radioactive decay of  $^{40}\text{K}$  and the presence of atmospheric Ar can be corrected for by the  $^{40}\text{Ar}/^{36}\text{Ar}$  ratio.

The noble gas temperature of groundwater reflects the climatic conditions under which a particular groundwater was recharged and gives a rough estimate of the age (Fig.2.4). Some knowledge of groundwater mineralisation is necessary, because high salinities have a significant 'salting out' effect on the gases (e.g. Suckow and Sonntag 1993). The noble-gas recharge temperature and the  $\delta^{18}\text{O}$  and  $\delta^2\text{H}$  values of the groundwater are linearly correlated (Deak et al. 1987).

Sampling for noble gas analyses is relatively simple but only few laboratories have the specialised mass spectrometers required to make precise measurements.

Estimation of *residence time* depends on the decay of short-lived isotopes like cosmogenic  $^{39}\text{Ar}$  (Sect.5.2.2.6) or the long-lived  $^{81}\text{Kr}$  (Sect.5.2.2.7), and on the production of a long-lived isotope such as  $^4\text{He}$  (Sect.5.2.2.10). The radioactive noble gas radon ( $^{222}\text{Rn}$ ) with a half-life of only 3.8 days is used to study short-term mixing of surface and groundwater (Sect.5.2.2.11).

The main disadvantage of applying these gaseous isotopes is that sampling is laborious (Lehmann et al. 1991; Cook and Solomon 1997), measurement facilities are limited, and the *in situ* production rates are not yet well characterised.

Chlorofluorocarbons like CFC-11, CFC-12 ( $\text{CCl}_3\text{F}$  and  $\text{CCl}_2\text{F}_2$ ) and  $\text{SF}_6$  have been the most widely used gases in the refrigeration and air-conditioning industries. Although their use started as far back as 1931, the major build-up has occurred in the post-war period. They are well mixed in the atmosphere (their effect on ozone in the upper atmosphere are well

documented) and therefore have a significant tracer potential instead of  $^3\text{H}$  (Busenberg and Plummer 1992; Cook and Solomon 1997).

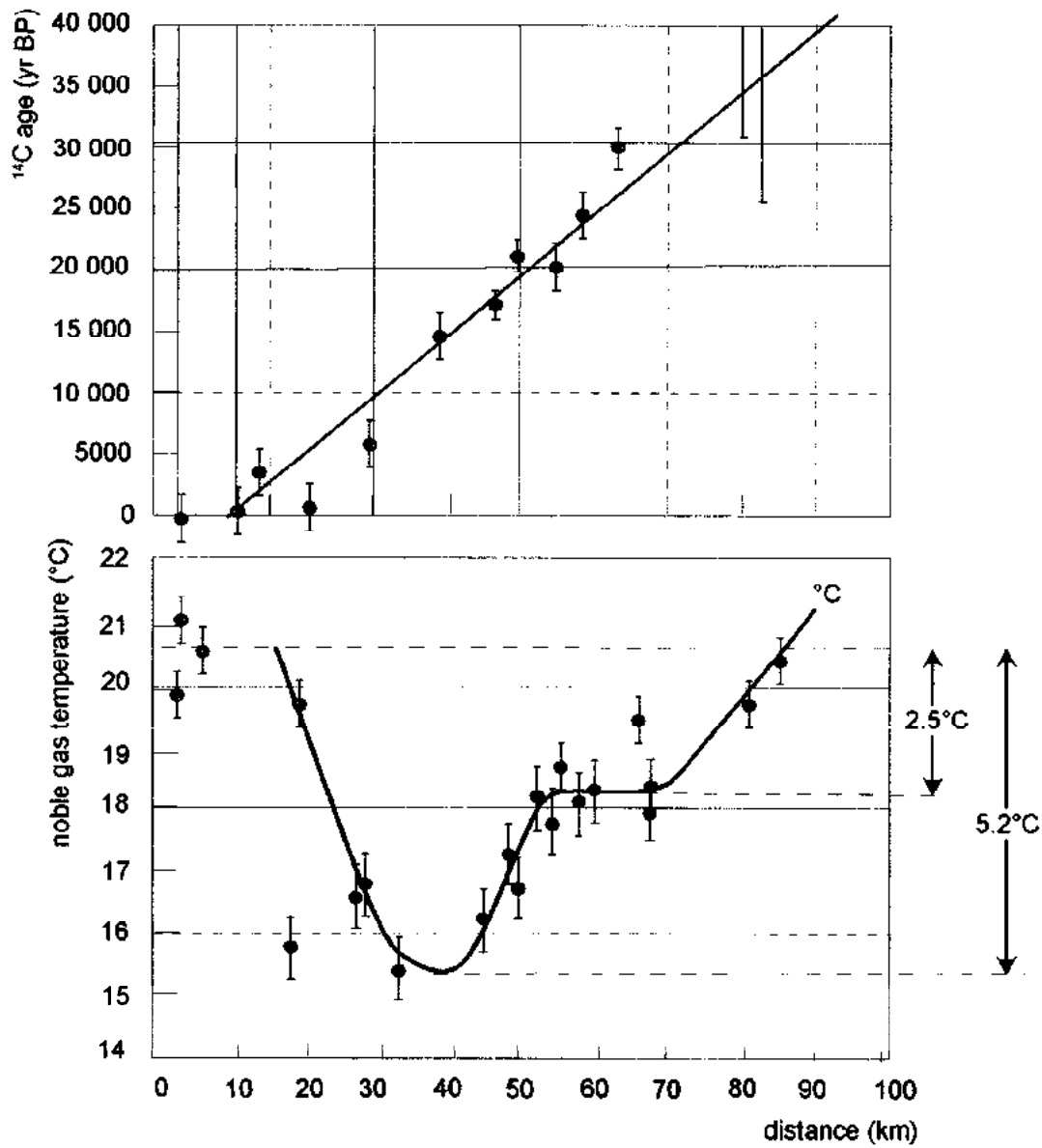


**Fig.2.4** Absolute recharge temperature of groundwater in the Budapest Basin during the last 30,000 yr determined by analyses of the noble gases dissolved in groundwater (Stute and Deak 1989).



### 3 GEOHYDRAULIC ASPECTS

Gravitation is the most important from the external forces which controls groundwater flow in the interstices of rocks. The flow may be laminar or turbulent. *Laminar flow* has distinct streamlines, while the flow direction at every point remains unchanged in time. In *turbulent flow*, the flow lines are confused and heterogeneously mixed.

Under natural conditions laminar flow prevails in unconsolidated sediments which are considered to be a homogeneous and permeable medium, though partly anisotropic. Laminar and/or turbulent flow occurs in fissured rocks, karst cavities and lava tubes. There are three principal geohydraulic conditions of groundwater flow schematically shown in Fig.3.1.

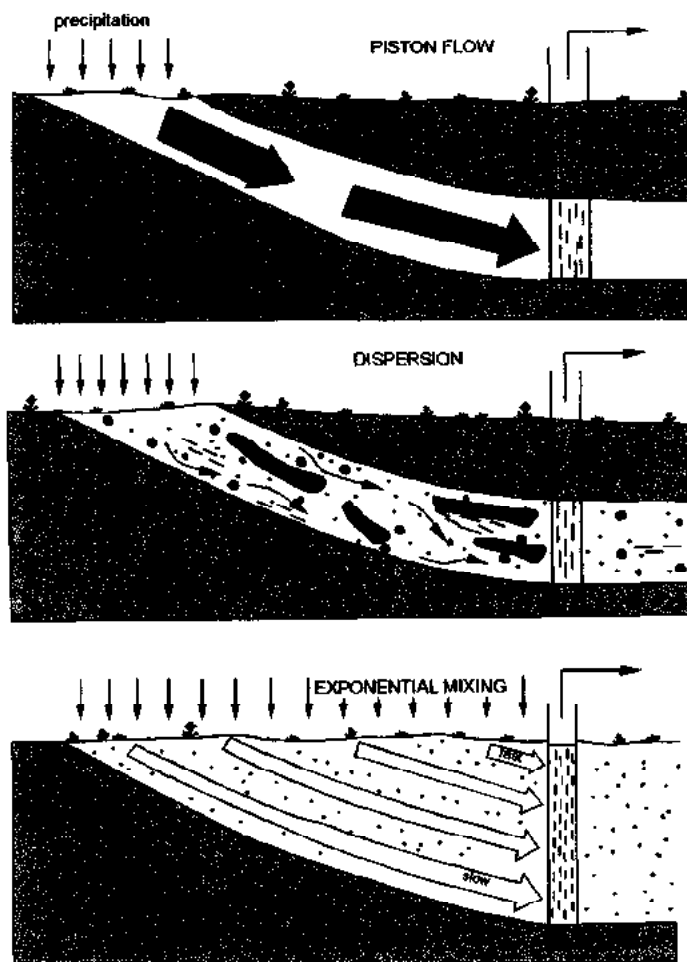


**Fig.3.1** Three cases of groundwater movement by piston-flow without and with dispersion in confined aquifer and flow in an open aquifers where different fast flowing water is mixed in the well or spring.

### 3.1 STEADY-STATE GROUNDWATER FLOW

#### 3.1.1 DARCY VELOCITY AND TRACER VELOCITY

In 1856 Darcy empirically found for laminar flow in small pores and at low gradients that the specific discharge  $Q_{\text{dis}}/A$  (*filtration velocity* = *DARCY velocity* =  $v$ ) is proportional to the hydraulic gradient  $\Delta h/z$  (Fig.3.2).  $A$  is the cross section of the aquifer.

$$v = \frac{Q_{\text{dis}}}{A} = q_{\text{dis}} = K \cdot \frac{\Delta h}{\Delta z} \quad (3.1)$$

where  $K$  is the hydraulic conductivity.

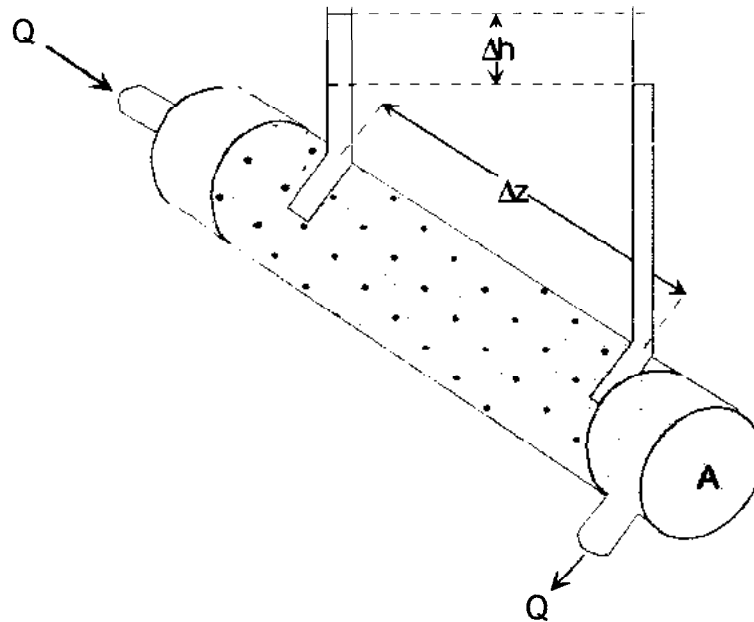


**Fig.3.2** Pressure distribution and head loss ( $\Delta h$ ) through flow in a sand column in order to demonstrate the Darcy law (after Todd 1959) (Eq.3.1).

The *hydraulic conductivity*  $K$  or *coefficient of filtration* has the dimension of a velocity as the hydraulic gradient is dimensionless (e.g. m/s, m/d).  $K$  covers a wide range (Fig.3.3)

In a porous and permeable rock environment, groundwater flows along curved pathways with an *actual velocity* or *tracer velocity*  $v_{\text{trac}}$ . The tracer velocity of groundwater changes with the width of the pores in the rock.

Between two flow cross sections of the distance  $z$ , the *tracer (travel) velocity*  $v_{\text{trac}}$  is given by

$$v_{\text{trac}} = \frac{z}{t}$$

$t$  is the time necessary for a water particle to pass this distance. The tracer velocity is determined by dye experiments or by environmental isotope dating. It describes the transport of any tracer (or contaminant) in an aquifer.

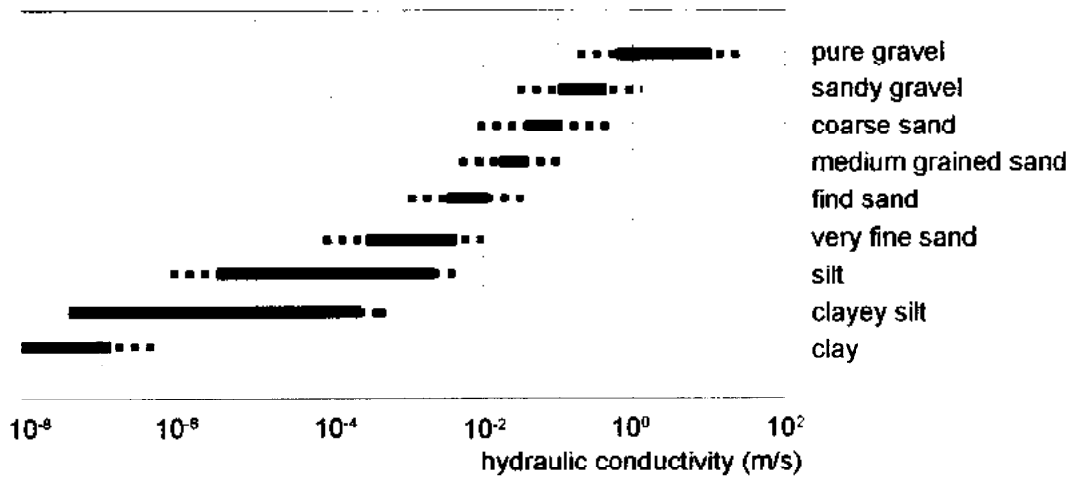


**Fig.3.3** The range of hydraulic conductivity (Eq.3.1; coefficient of filtration) in various sediments (after Dürbaum 1969).

The *filtration velocity*  $v$  (Darcy velocity) and the *tracer velocity*  $v_{trac}$  are related to each other by the total porosity  $n_{tot}$

$$v_{trac} = \frac{v}{n_{tot}} \quad (3.2)$$

The filtration velocity and tracer velocity have to be distinguished from the speed of a hydraulic pulse in a aquifer which may be caused by a storm event. This velocity cannot simply be deduced from the time lag of the discharge peaks of springs and artesian boreholes behind the peak of precipitation.

**Example:**

The filtration velocity is calculated to be  $6.3 \text{ m yr}^{-1}$  for a hydraulic conductivity of  $10^{-3} \text{ m s}^{-1}$ , and a gradient of the water table of 2 m over a distance of 1000 m. This means that  $2 \times 10^{-6} \text{ m}^3$  are passing per  $\text{m}^2$  and second or  $6.3 \text{ m}^3$  per square meter and year. The tracer velocity is  $63 \text{ m yr}^{-1}$  for a total porosity of 10%. In case of mass transport e.g. for tracer experiments the total porosity is crucial rather than the effective porosity as there is usually sufficient time for an hydrochemical and isotopic exchange between the bound and free mobile groundwater.

For an aquitard with a  $K$  value of  $10^{-10} \text{ m s}^{-1}$ , a total porosity of 50% and a vertical gradient of 4 m/50 m the filtration and tracer velocities are much smaller than  $1.6 \times 10^{-9} \text{ m s}^{-1}$  or  $5 \text{ cm yr}^{-1}$ , respectively.

**3.1.2 PRINCIPAL GROUNDWATER FLOW MODELS**

For any quantitative hydrological evaluation of the results of a tracer study (e.g. environmental isotopes) the groundwater flow in the geohydraulic system must be idealised taking account the physical properties of the isotopes employed (e.g. radioactive decay) and the flow characteristics of the carrier, i.e. that of the groundwater. For the use of isotope

hydrological data, conceptual and lumped-parameter models have specifically been developed. A detailed description is given in Volume VI for young groundwater (Zuber 1986; Maloszewski and Zuber 1993, 1996, 1998). In this section only a short summary can be given.

The simplest hydrogeological situation is represented by the *piston-flow model* (Fig.3.1). In this case the groundwater flow in the aquifer is similar to that through a tube and is described by the Darcy law (Eq.3.1; Fig.3.2). Both stable isotope and dissolved chemical compositions do not change. The activity of the radioactive environmental isotopes decreases with time or with the distance of flow according to the law of radioactive decay. The amount of groundwater in the system remains constant as recharge and discharge are balanced.

The piston-flow model usually well describes the flow in confined aquifers. When the groundwater recharge lasts longer than the maximum residence time of the groundwater in the aquifer the tracer velocity is proportional to the DARCAY velocity, and the regional total porosity can be estimated by Eq.3.2.

In natural groundwater systems, that have more than one aquifer or is subject to interactions with surface water, mixing of groundwater of different age and origin is common. The most simple cases are described by *two- and three-component mixing models*. In the plot of two parameters of two end members straight lines allow to read the proportions of the two end members. In the case of mixing of three components a triangle is obtained bordered by three two-component mixing lines (Fig.2.3). As an example, a plot of chloride and  $\delta^{18}\text{O}$  values allows to recognise whether or not salt is dissolved, or fresh water is mixed with brine or sea water. Another example is the admixture of irrigation return flow (Sect.5.2.1.1).

Two end-members I and II with the properties  $X_I$  and  $X_{II}$  are mixed with the proportions  $x_I$  and  $x_{II}$ . The mass balance equation yields

$$x_I \cdot X_I + x_{II} \cdot X_{II} = Y \quad \text{with} \quad x_I + x_{II} = 1 \quad (3.3)$$

The proportion  $x_I$  of the end-member I is calculated from the properties of the end-members I and II and that of the sample  $X_{\text{spl}}$  by

$$x_I = \frac{X_{\text{spl}} - X_{II}}{X_I - X_{II}} \quad (3.4)$$

The precision of the determined proportions of two mixing components is better than  $\pm 10\%$  for sea- and freshwater as end members, but worse than  $\pm 25\%$  for mineralised and freshwater using isotope and hydrochemical data (Geyh and Michel 1981). If a system is monitored over long periods or within very short time intervals, several groundwater and surface water components can be separated from each other (Behrens et al. 1979).

A modification of the piston-flow model also considers *dispersion* (Fig.3.1; Sect.5.1.2.2.2). This process describes the mixing of different old groundwater components moving over short distances with different velocity within the aquifer. The isotope signal becomes

smoothed. This process is important for the interpretation of the isotope composition, if the groundwater has a high velocity as in karst water systems but it is usually negligible for slowly moving groundwater which can be dated by the  $^{14}\text{C}$  method (Sect. 5.2.2.3).

Mixing of many different old groundwater components is assumed for pumped shallow groundwater and particularly for spring water from fissured aquifers (e.g. karst springs). The age distribution may be approximated by the exponential function (*exponential model*, Volume VI). The corresponding exponential model is based on the assumption of mixing of a theoretically infinite number of different old components, of which the proportions decrease exponentially with increasing age. Each component has its specific isotope composition according to the input function (Fig.3.4A). The  $^3\text{H}$  input function for karst groundwater in southern Germany is shown in Fig.3.4B. This conception has been currently confirmed especially for karst springs.

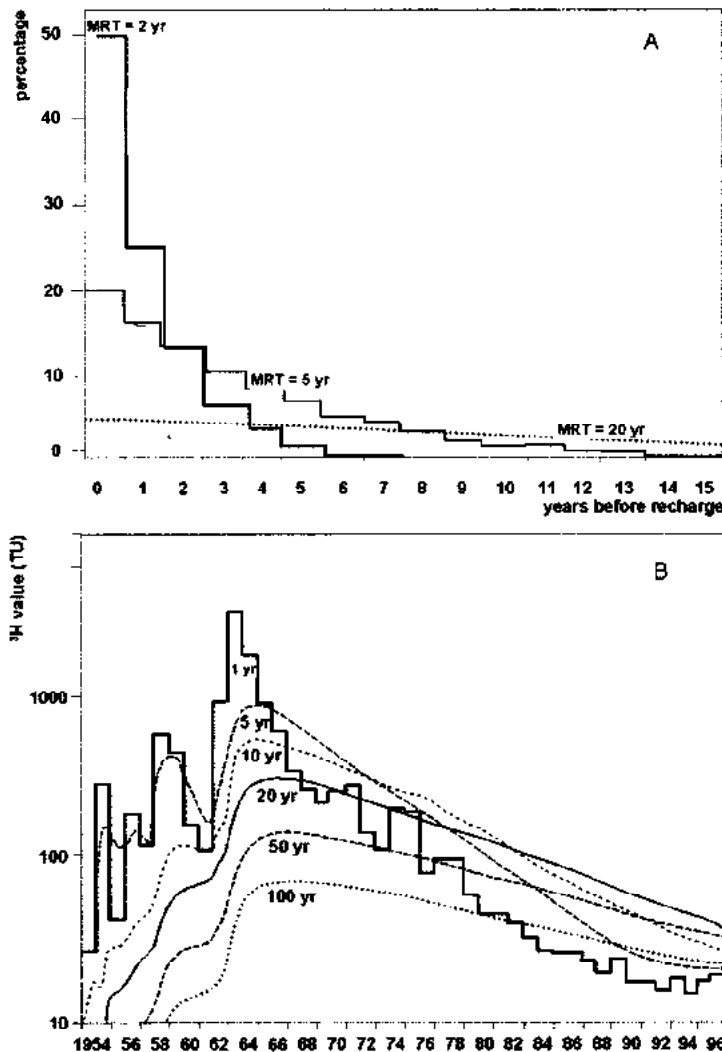


**Fig.3.4** (A) Composition of karst groundwater as mixture of different old water components and (B) relationship between the isotopic composition (e.g.  $^3\text{H}$ ) of the mixed water and the mean residence time (MRT).

For extended phreatic aquifers with a direct diffuse recharge rate  $Q_{rec}$ , the average water age was calculated by the exponential model (Vogel 1970), assuming a constant porosity and aquifer thickness  $d$ :

$$t_{avg} = \frac{n_{tot} \cdot d}{Q_{rec}}$$

For a hard rock aquifer with constant thickness and an exponentially decreasing porosity we obtain

$$t_{avg} = \frac{n_{tot}(0) \cdot d_{char}}{Q_{rec}}$$

$n_{tot}(0)$  is the total porosity at zero depth and  $d_{char}$  is the characteristic depth where the porosity has decreased by a factor of 2.72 (=  $e$ ).

### Examples: Black-Box Models

Theoretically the *piston-flow model*, the *dispersion model* and the *exponential model* can be described by the *black-box model* (Zuber, 1986; Maloszewski and Zuber 1996).

The so-called *lumped-parameter* or *black-box models* (Zuber 1986, Maloszewski and Zuber 1996) use the residence time function  $f(\bar{t}, P)$  with  $\bar{t}$  as mean residence time (turnover time) of a groundwater volume element and  $P$  as hydrogeologically relevant parameters describe the tracer (isotope) concentration (specific activity).  $C_{in}(t)$  is the specific activity of the mixed components of differing transit times. The specific activity of the mixed sample  $C_{out}(t)$  is given by It is given by the convolution integral

$$C_{out}(t) = \int_0^{\infty} C_{in}(t-t') \cdot f(\bar{t}, P) \cdot e^{-\lambda t'} dt' \quad (3.5)$$

$t$  is the time of sampling;  $\lambda = \ln 2/T_{1/2}$  is the decay constant of the environmental isotope (for stable isotopes  $\lambda = 0$ );  $t'$  is the time span between the entry of the environmental isotope from the atmosphere into the unsaturated zone and its arrival of the saturated zone. The input function  $C_{in}(t-t')$  represents the concentration or activity at which the relevant environmental isotope becomes involved in groundwater recharge (e.g. input distribution in precipitation of  $^3H$ ). Geochemical processes are not considered.

The different lumped parameter models are characterised by their residence-time distribution function  $f(\bar{t}, P)$  (Zuber 1986; Maloszewski and Zuber 1996). For the *piston-flow model* (*PFM*) (Fig.3.1)

$$f(t', P) = \delta(t'-\bar{t})$$

$\delta(t'-\bar{t})$  as Dirac function. The solution of Eq.3.5 yields for a constant  $C_{init}$

$$C_{out}(t) = C_{init} \cdot e^{-\lambda \bar{t}} \quad (3.6)$$

The residence-time response function  $f(\bar{t}, P)$  of the *exponential model (EM)* (Fig.3.1) is given by

$$f(t', P) = \frac{1}{t} e^{-\lambda t'} \quad (3.7)$$

When  $C_{init}$  is invariant with time (e.g. cosmogenic  $^{14}\text{C}$ ,  $^3\text{H}$ ,  $^{32}\text{Si}$ ) and  $t$  is the seepage time of the water from the groundwater surface to any point in the aquifer, the exponential model yields for an isotope with the decay constant  $\lambda$ :

$$C_{out}(t) = \frac{C_{mit} \cdot e^{-\lambda t}}{1 + \lambda \cdot t_{avg}} \quad (3.8)$$

The response function  $f(\bar{t}, P)$  of the *dispersion model (DM)* is given below:

$$f(t', P) = \frac{1}{t' \cdot 4\pi \frac{D}{v_{trac} \cdot z} \frac{t'}{\bar{t}}} \exp\left(\frac{(1 - \frac{t'}{\bar{t}})^2}{\frac{4D}{v_{trac} \cdot z} \frac{t'}{\bar{t}}}\right) \quad (3.9)$$

where  $z$  is the travel distance (Sect.3.1.1). Another approach to interpret isotope hydrological results are system-specific *compartmental models* or *multi-box models*. In this approach the groundwater system is divided in geohydraulically plausible boxes with an assumed uniform (well-mixed) tracer concentration and well-defined geohydraulic parameters. The volumes, the parameters, etc. are adapted iteratively until the input and output curves fit best with the obtained data points. Adar (1996) optimised this approach by a quadratic optimisation procedure in order to determine geohydraulic parameters applying isotope and hydrochemical data. These approaches are most valuable if geohydraulic knowledge of a groundwater system to be studied is scarce.

It is essential that we apply time-series of environmental isotope data with differing half-lives and that we try to interpret the data by various models. Apparently, contradictory ages or mean residence times may be obtained. The deviations will, however, allow to decipher the investigated groundwater system. In any case agreement between empirical and modelled results does not automatically mean that the model applied describes the natural reality (Oereskes et al. 1994; Maloszewski and Zuber 1993, 1998).

*Conceptional models* are individually developed for geohydraulically more complicated systems e.g. leaky aquifers. As an example Geyh et al. (1984) modelled the seepage of groundwater from a phreatic aquifer into a confined aquifer. Applying  $^{14}\text{C}$  dates of DIC, the hydraulic conductivity  $K$  of the separating aquitard and the diffuse recharge rate of the confined groundwater could be estimated. Another conceptional model was developed for the interpretation of environmental isotope data describing the seepage of water from the Nile River into the phreatic aquifer (Verhagen et al. 1991).

### 3.1.3 CONSIDERATIONS ABOUT MODELLING

The evolution of the isotopic composition within a geohydraulic system can be modelled using the equations for the movement of solutes, provided the initial and boundary conditions and other appropriate parameters are known. This is called *forward modelling*. The opposite process of interpreting field data to estimate parameters is called *inverse modelling*. The aim of isotope methods is to invert field data in order to estimate recharge rates, water ages, tracer velocities or mean residence times.

When inverting field data, it is necessary to consider two types of errors. The first is the *measurement error*. It is associated with the sampling and the spatial variability of field data, the errors involved in the chemical and isotopic analyses, those of the estimation of the input function and other parameters. Most of these errors are quantifiable.

The second type of error is associated with the *model assumptions*. If for a model steady-state, one-dimensional piston-flow is assumed and dual-pathway flow is excluded but all or several of these assumptions are wrong in some aspect, there will be an error in applying the model to field data. Generally, this second type of error is more difficult to quantify and can only be assessed by experiments under controlled conditions or by comparing estimates obtained by various methods.

If inverse modelling is done, the error of estimating recharge rates will depend partly on two types of error, but also on the model sensitivity of the measured data to the recharge rate. If the final profile of a tracer is only weakly dependent on the water fluxes, the inversion of the tracer profile will be very sensitive to measurement and model errors. In these cases, the inversion is said to be *ill-posed*. The aim of all isotope methods is a design of models which are sensitive to obtain recharge rates, water ages and geohydraulic information.

### 3.1.4 GROUNDWATER DISCHARGE

Groundwater is discharged to the surface where the zone of saturation reaches the surface. The groundwater may percolate, **effluently flow** into streambeds or discharge at **springs**. *Groundwater discharge* or *surface runoff* usually occurs at the outlet of a drainage basin long after the recharge event.

*Interflow* (also *subsurface flow* or *hypodermic flow*) is created by seeping precipitation but does not enter the groundwater. It occurs in the soil at shallow depth and lasts only shortly after the storm event. It is clearly distinguished from the surface runoff (Volume III).

Discharge of groundwater can only be detected or even measured if it is accessible at the surface e.g. as spring water. Large quantities of groundwater are discharged, however, in streambeds and becomes part of the total runoff of the discharge of streams. This is reflected by a perennial flow also during long periods of drought (*base flow*). The proportion of groundwater in the total discharge of a stream is determined by component separation techniques (Fig.3.6). The classical way is hydrograph separation evaluating the variation of



the discharge in time. Techniques using environmental isotopes are a very powerful tool (Fritz et al. 1976).

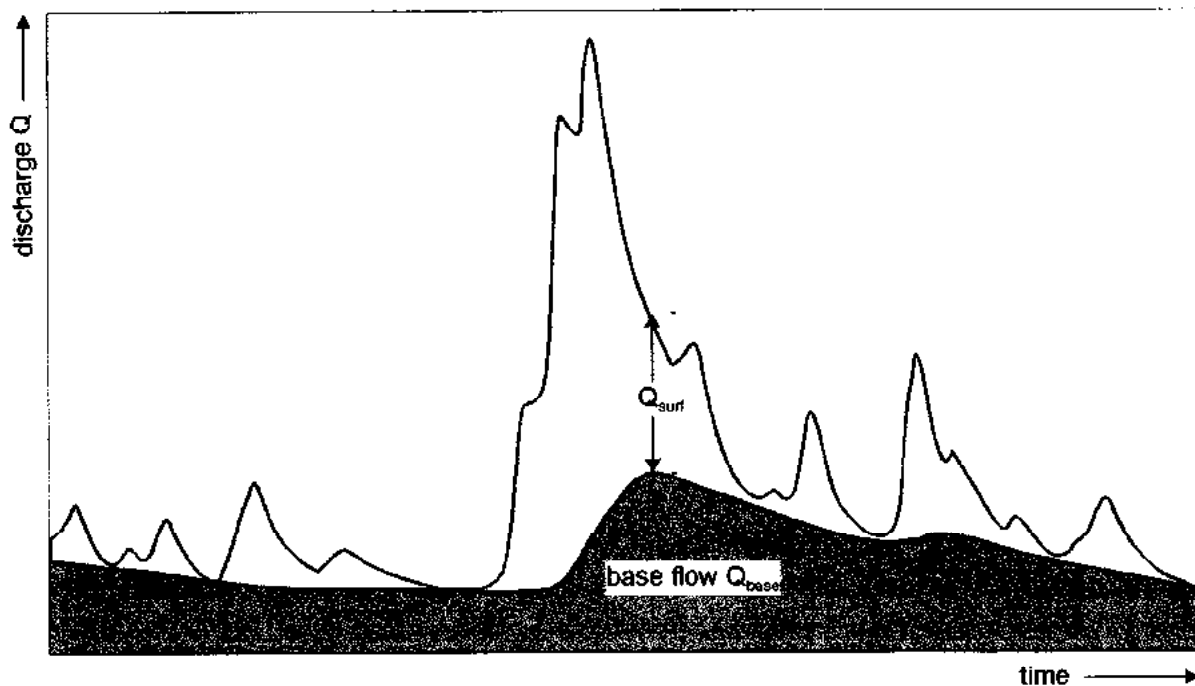


**Fig.3.6** Hydrograph of the total runoff of a basin. The white and grey areas represent the highly variable surface runoff  $Q_{surf}$  and the groundwater runoff (base flow)  $Q_{base}$ , respectively (after Fritz et al. 1976).

### 3.1.4.1 SPRINGS

A spring is a location where groundwater is discharged naturally from the rock or soil forming a superficial flow. Discharge happens into a pool, river, lake, and the sea (effluent flow). The discharge of springs in humid regions usually fluctuates with the rate of precipitation during the year.

Springs are distinguished and classified according to their seasonal discharge behaviour (magnitude and fluctuation), the duration of flow during the year, the hydraulic conditions, geological and topographic features, chemical and isotopic composition, and water temperature.

According to the duration of flow, three categories of springs are distinguished:

- 1) *perennial springs* with a continuous flow,
- 2) *periodic springs* with periodically changing flow rates. They have to be distinguished from geysers of which eruptions are caused by periodic expansion of vapour, and
- 3) *intermittent springs* with a flow which is interrupted a certain time during the year e.g. during the dry season.

The largest springs usually occur in karstified limestone terrain, in fissured lava flows, porous sandstone structures, and in large gravel and sand deposits. The discharge rate of a spring allows an estimate of the size of the recharge area, if the geological situation is known. The isotopic composition of the issued groundwater provides information on its origin and mean residence time.

*Ascending or artesian springs* issue from a level below the spring or from below the erosional base along permeable groundwater pathways, e.g. along fissures or faults. Often the discharge can be increased by tapping a borehole. Then, the isotope composition of the pumped spring water deviates from that of the naturally discharged spring water as it contains a higher proportion of old groundwater.

*Descending springs* drain above the base level of erosion. They issue from perched aquifers and partial hydrogeological structures with a limited recharge area. Their discharge is low and fluctuating (e.g. contact springs).

*Overflowing springs (barrier springs)* issue at places where the prevailing lateral component of groundwater flow in an aquifer is dammed behind an aquiclude and directed toward the surface. This may occur along an inclined contact of an aquifer with an underlying aquiclude, and along outcrops of faults and synclinal structures. Barrier springs sometimes drain groundwater basins with large groundwater resources. The water has a long residence time, while the discharge is damped with respect to fluctuations in the precipitation. The isotopic compositions cannot be interpreted with the simple well-mixed model (exponential model; Sect.3.1.2; Volume VI). Short- and long-lived isotopes as  $^{14}\text{C}$  and  $^3\text{H}$  will deliver considerably deviating mean residence times.

#### 3.1.4.2 PRODUCTION WELLS

The construction of wells has to be considered when interpreting isotope hydrological results. Detailed information are found in Clark (1988). Wells are shafts or holes which were sunk, dug or drilled into the earth to extract water (International Glossary of Hydrology 1974).

*Dug wells* are usually shallow, have a large diameter and were constructed manually. They usually catch shallow groundwater.

*Drilled wells* are constructed as boreholes and have usually small diameter. They may be several hundred to more than 1000 metres deep. They pump water from a defined layer if screens are present in the well shaft.

*Artesian wells* tap confined aquifers (Bates et al. 1980). The water head is above the level of the phreatic groundwater or even above the ground level.

If groundwater is pumped from wells, for dewatering of mines or the construction of tunnels, the natural hydrodynamics of the groundwater system is changed and adopts only slowly to the anthropogenically disturbed state of drainage. This process is often accompanied by the

disappearance of springs and always by a decline of the piezometric level. Groundwater from various parts of the aquifer may become mobilised and mixed. Even the groundwater regime may change. Such interferences are usually reflected in changes in the chemical and isotopic compositions of the water. This may also be due to the admixture of surface water from a streambed (*bank infiltration*) or of shallow groundwater from an alluvial plain (Volume III).

In arid regions without or with a limited groundwater recharge, pumping of groundwater often means groundwater mining and depletion of groundwater resources (Sect.3.2.2; Volume V).

The stable isotope compositions of oxygen and hydrogen (Sect.5.2.1.1) of the groundwater are a good tracer for new hydraulic connections. The admixture of very young water is detected by tritium (Sect.5.2.2.1 and 5.2.2.2). Radiocarbon values (Sect.5.2.2.3) are modified after many years of pumping (Sect.3.2.2). As a consequence, isotopic monitoring of short-term changes in the hydraulics of an aquifer system, due to pumping tests or groundwater abstraction, should start with  $\delta^{18}\text{O}$ ,  $\delta^2\text{H}$  and  $^3\text{H}$  determinations *before the first hydraulic disturbance*.

### 3.1.4.3 WELL CONSTRUCTION AND SAMPLING OF WATER FROM WELLS

Various techniques are used for the sinking of a well: *percussion drilling*, *rotary drilling*, *auger drilling*, and *manual construction*. During rotary drilling, drilling fluids are used to remove cuttings from the borehole, to cool and lubricate the drilling bit, and to support the borehole wall by hydrostatic pressure in order to prevent caving. A common drilling fluid in hard rocks is water. It is usually removed after completion of the borehole by well development, i. e. by removing the bentonite mud with water or the polymer by biodegradation. In spite of this, water samples from newly constructed wells often contain remains of the drilling or cleaning fluids which may falsify the natural isotopic composition of the groundwater. Bacterial decomposition of organic stabilisers used in the fluids may change the  $^{14}\text{C}$  value of DIC, while using surface water may change the tritium activity.

During or after drilling of a well a metal pipe (casing) is lowered into the borehole in order to prevent the walls from collapsing. Only in consolidated and crystalline aquifers, the boreholes may be left without support. The casing is perforated or provided with a metal screen or gravel filter within the water-bearing section.

Production wells are constructed for maximum water yield. The perforated sections stretch over the entire thickness of the aquifer and even many aquifers. In this case groundwaters of different isotope compositions may be mixed. Well logs may help to identify the positions of groundwater inflow. Stratified water samples are collected using packers or depth samples. *Depth samplers* are cylinders that are lowered to the wanted position before opening and filling with water and closing. The samples are not representative if vertical water flow exists in the well shaft. In this case the use of *packers* is recommended. These are rubber tubes that are filled with air to seal the shaft above and below the section of water. Instead of this costly

technique, *submersible small-diameter pumps* may deliver representative samples from the wanted depth. The electrical power is delivered from a generator or a car battery.

Isotope sampling of **artesian wells** is not problematic. The samples are free of any secondary contamination because the elevated piezometric pressure protects the aquifers. **Production wells** are sampled under operation. Treated water (e.g. chlorinated) should not be collected. Wells with a significant drawdown may also pump groundwater from overlying aquifers. **Observation wells** should be pumped before sampling until the EC and pH values approach a constant level or at least three times of the well volume is abstracted.

## 3.2 NON-STEADY STATE GROUNDWATER FLOW

In most isotope hydrological case studies it is assumed that the recharge and discharge of the groundwater system are balanced as usual in humid regions. Then the groundwater flow velocity, the flow direction and regional values of the porosity and hydraulic conductivity as well as boundary conditions for numerical modelling can be determined by means of the isotope hydrological results. The often cited problem of the uncertainty of the correction of the  $^{14}\text{C}$  time scale of DIC is overestimated for common fresh groundwater resources. The resulting age corrections are often constant.

For hydrogeologists the recognition of hydraulic non-steady state conditions is an important task. In short-term studies the annual periodicity of meteorological and climatic processes results in a continuous disturbance of the hydrological processes. The periodicity of the groundwater recharge and related hydrodynamic phenomena as fluctuations of the groundwater level, the discharge of springs can be used to evaluate geohydraulic parameters. They are reflected in the variation of the isotopic compositions of the surface water and shallow groundwater (Volume III). In long-term studies climatic changes might have interrupted the groundwater recharge during pleniglacial periods in the present humid region. In arid and semi-arid regions, non-steady-state hydraulic conditions dominate. The present groundwater discharge exceeds recharge and a large proportion of such resources are fossil. The palaeowater was recharged during former pluvial periods. Non-steady-state hydraulic conditions are also created by intensive groundwater abstraction.

### 3.2.1 PALAEOCLIMATIC CAUSES

In arid and semi-arid regions isotope hydrologists distinguish between steady-state and non-steady recharge/discharge conditions. In non-steady-state systems groundwater recharge was interrupted in the past as result of changing palaeohydrologic conditions, e.g. after the termination of the humid periods in the Late Pleistocene and Early Holocene (Fig.3.7; Geyh 1994). After each cessation of groundwater recharge the water head started to decline (Burdon 1977). The groundwater gradient, the groundwater velocity and the discharge rate decreased.

Groundwater ages from such regions, e.g. determined by the  $^{14}\text{C}$  method (Sect.5.2.2.3), still

reflect steady-state conditions of the former pluvial period when groundwater was recharged. The difference between  $^{14}\text{C}$  water ages of two wells are related to the past tracer velocity and direction and is not related to the actual velocity (Fig.3.8). In contrary, the present piezometric surface does not. The slopes between hydraulic heads are larger than those expected from the actual groundwater recharge. The latter gradient superimposes the gradient of the fossil relict groundwater body. However, the periods of groundwater recharge can be accurately evaluated, which is essential for numerical modelling of groundwater resources and for palaeohydrological studies. If erroneously steady-state conditions are assumed and limited periods of groundwater recharge in the past are not taken into account modelled groundwater recharge rates are very much overestimated (Verhagen et al. 1991; Geyh et al. 1995).

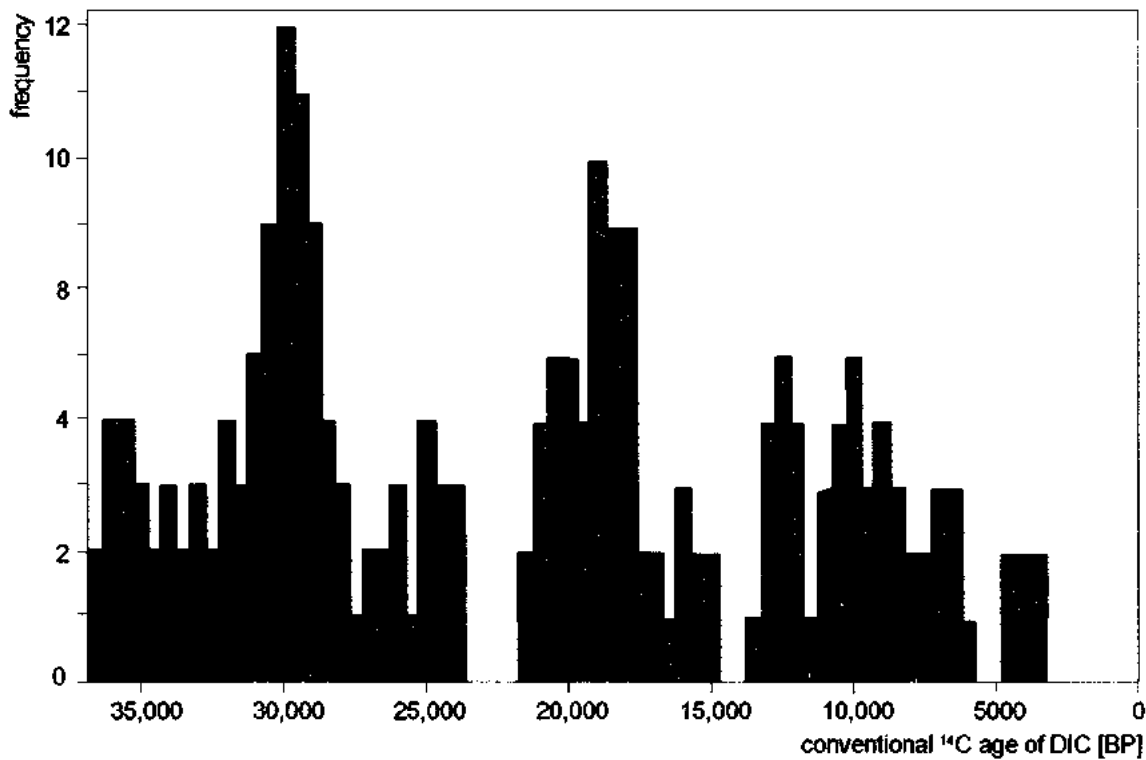


**Fig.3.7** Paleohydrological situation in the Arabic Deserts of the Hamad region (Geyh 1994).

### 3.2.2 ANTHROPOGENIC CAUSES

Non-steady state hydraulic conditions may also be caused by intensive groundwater abstraction. Leakage of reservoirs, artificial recharge and other processes may disturb the natural hydrodynamic conditions. As long the piezometric conditions are not adapted to the disturbed geohydraulic conditions, the system remains in a non-steady state. Indications are e.g. a steadily declining water table or changing hydrochemical and isotopic compositions of the pumped groundwater. As a result groundwater percolation through aquitards, separating adjacent aquifers, may become increased. Changes in the  $^{14}\text{C}$  water ages for production wells are strong indications of overexploitation and sometimes "groundwater mining" (Fig.3.9; Geyh and Backhaus 1979; Verhagen et al. 1991).

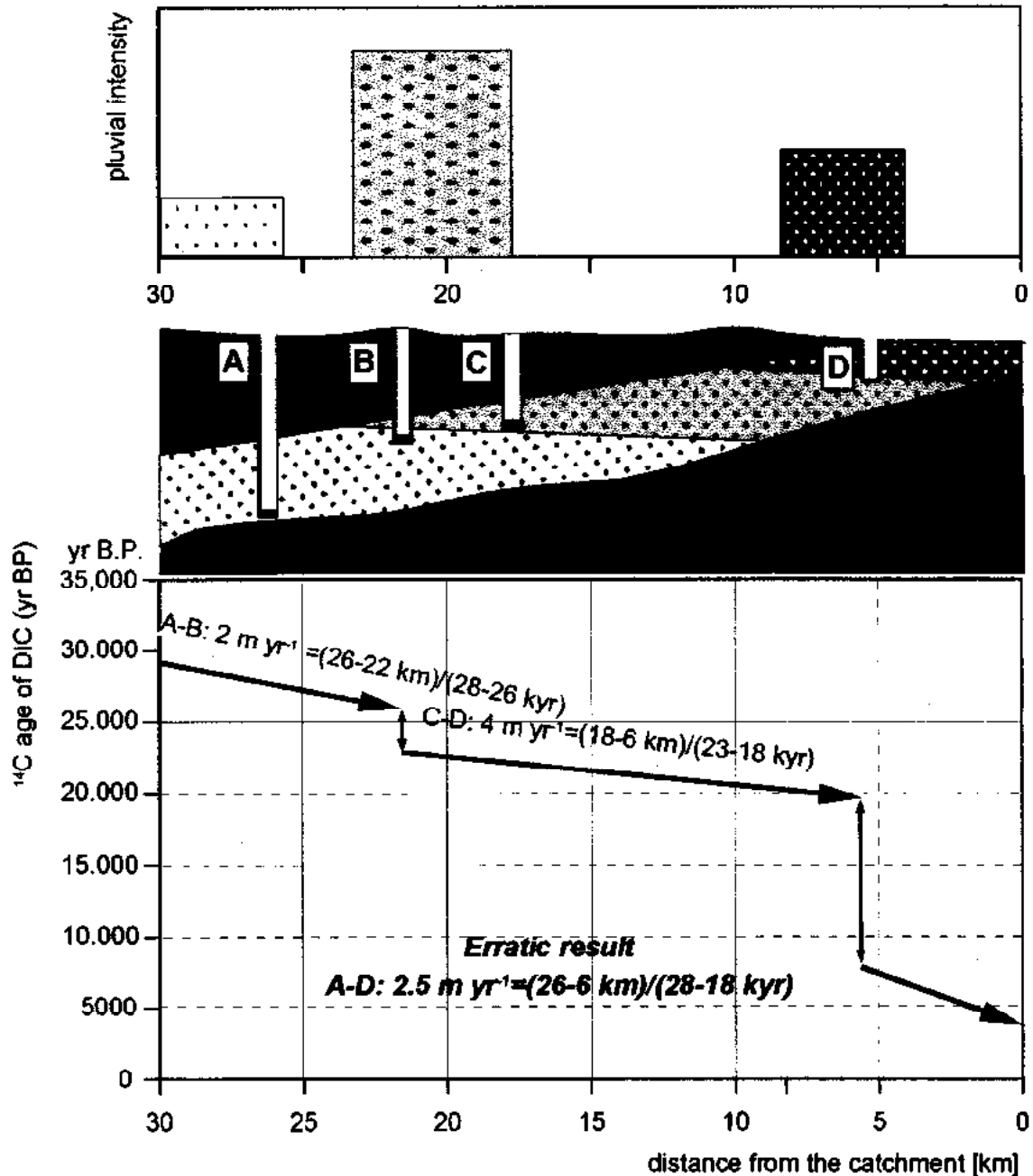


**Fig.3.8** Scheme to estimate the tracer velocity of groundwater for the arid Near East in the past (Geyh 1994). Erratic results are obtained if a tracer velocity is calculated from  $^{14}\text{C}$  dates of from different pluvial periods (e.g. for the wells A and D). The tracer velocities A–B and C–D corresponds to those during the past pluvial periods.

Under simple geohydraulic conditions, the temporal change of the conventional  $^{14}\text{C}$  dates of groundwater can be used to quantify the resulting changes in the mixing of different old groundwater as shown for the Azraq area, Jordan (Verhagen et al. 1991).

A long-term trend in  $^{14}\text{C}$  ages of groundwater in a heavily exploited aquifer reflects a complex age stratification. It is not yet understood which pumping parameters (e.g., abstraction rate, total abstraction, meteorological conditions, depth of filter and of the pump) are crucial for the

observed  $^{14}\text{C}$  changes and for what information can be derived from any similarity of long-term  $^{14}\text{C}$  trends. They may contain valuable information for optimising groundwater abstraction in well fields and for preventing groundwater pollution by admixture of young or old groundwater.

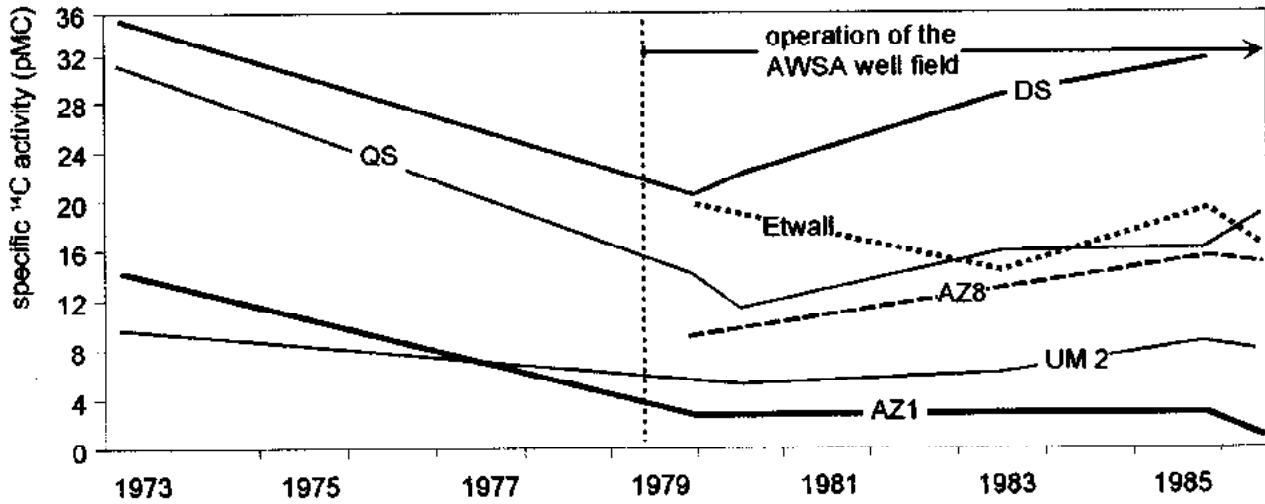


**Fig.3.9** Changes of  $^{14}\text{C}$  water ages as result of groundwater overexploitation within the Azraq area (Verhagen et al. 1991). The proportion of young basalt groundwater has increased and that of the Cretaceous groundwater has decreased.

# 4 WATER-ROCK INTERACTIONS

Isotope exchange between groundwater and minerals at temperatures of common, non-thermal groundwater bodies is slow (O'Neil 1987). Heterogeneous reactions between water and minerals with complex kinetics are usually irreversible at low temperatures. Therefore, cold groundwater rarely reaches chemical and isotopic equilibrium with minerals of the aquifer. There are, however, exceptions. The reaction between water, CO<sub>2</sub> and calcite is one example. Others examples are the oxidation of organic material as peat, and microbial metabolic processes which do not only change the chemical composition and oxidation state of dissolved nutrients (O<sub>2</sub>, C and S), but are also accompanied by large shifts in the isotope compositions (isotope fractionation) (Volume I).

The isotopic and chemical compositions of groundwater reflect the mineralogical composition of the rocks in the aquifer and can be used to localise recharge areas, and to determine the origin of groundwater (meteoric, marine, fossil, magmatic and metamorphic water) and of individual chemical components (e.g. carbonate, sulphate, nitrate and ammonium). The water compositions can also give information about processes of water-rock interaction and microbial processes in the water.

There are three major processes which are accompanied by isotope fractionation of water molecules and dissolved components in groundwater systems within the time scale of groundwater percolation:

- 1) **evaporation and condensation** leading to the fractionation of <sup>2</sup>H/<sup>1</sup>H and <sup>18</sup>O/<sup>16</sup>O (Sect.5.2.1.1) between vapour and liquid water,
- 2) **chemical reactions** between gaseous CO<sub>2</sub>, dissolved carbonate species and precipitated carbonate minerals leading to the fractionation of <sup>13</sup>C/<sup>12</sup>C (Sect.5.2.1.2), and <sup>14</sup>C/<sup>12</sup>C (Sect.5.2.2.3).
- 3) **microbial metabolic** processes such as desulfurification (Krouse 1980), denitrification and nitrification (Hübner 1986), leading to the fractionation of <sup>15</sup>N/<sup>14</sup>N (Sect.5.2.1.3), <sup>34</sup>S/<sup>32</sup>S (Sect.5.2.1.4) and <sup>18</sup>O in anions between solution and organic matter.

In geothermal systems significant isotope exchange of hydrogen and oxygen occurs between rock and water (Chapter 6), due to membrane filtration through layers of semi-permeable clays as well as hydration or dehydration of secondary minerals.

Because of the slow exchange of isotopes between cold groundwater and its surrounding rock, groundwaters of different origin can preserve their isotopic compositions over geological times. Therefore, *mixing* of different types of groundwater and the *origin of dissolved*



*components* can be evaluated using  $\delta^2\text{H}$ ,  $\delta^{18}\text{O}$ ,  $\delta^{34}\text{S}$  values and the  $^{87}\text{Sr}/^{86}\text{Sr}$  ratio (Sect.5.2.1.7), acting as conservative tracers like chloride and bromide ions. In case of mixing of more than three components it may be difficult to determine the isotopic and hydrochemical compositions of the corresponding end members.

There are various processes in the unsaturated zone which determine the qualitative change of the pore water.

#### **4.1 ANION EXCLUSION-ADSORPTION: PHYSICAL ABSORPTION**

Anions and other solutes do not move through soils similar to water because of the interaction between the ionic charge and the charge found on the surfaces of the clay minerals (and organic matter) that make up the soil or aquifer. The charges found on different minerals vary greatly. In many cases they may depend on the pH as well as the constituents and concentrations of the soil solution. Within a soil both positively and negatively charged surfaces can exist simultaneously on different parts of the same mineral as well as on different minerals.

Generally, clay minerals exhibit a negative charge, effectively excluding anions from near the mineral surface. The excluded volume is dependent on both the water content and the concentration of the soil solution. The anions are pushed out of the matrix in the main porosity, while the cations are absorbed. This phenomenon can lead to a delay in the restitution curves between anionic as well as isotopic tracers.

Significant adsorption of anions has also been found for soils containing hydrous oxide surfaces. The main compounds involved are aluminium and iron oxides (including hydroxides and oxyhydroxides) as well as the edges of layer-silicates. The surface charge of these minerals depends on the pH of the soil solution. The positive charge increases with decreasing pH. Kaolinite is one mineral that displays this behaviour. Adsorption of anions will cause the anions to be retarded with respect to the movement of water in the soil or aquifer. This may also have an effect on the environmental isotope compositions.

Johnston (1988) showed that ignoring adsorption of chloride at low pH in one profile made the concentration to be overestimated by a factor of two.

#### **4.2 CHEMICAL ABSORPTION**

The distinction between chemical and physical absorption is difficult to access in the case of clay. A distinction could be made by studying the possibility of desorption and the kinetics of the reaction.

### 4.3 EXCHANGE OF IONS

The phenomenon is linked with the crystalline structure of clay particles, that have a negative charge at the surface. The potential capacity of ion exchange depends on the nature of clay.

### 4.4 CHEMICAL INTERACTION BETWEEN SOLUTES

The chemical processes may be divided into two principal phenomena:

- 1) chemical precipitation controlled by the solubility of a substance, and
- 2) chemical alteration by e.g. oxydo-reduction and complexation processes.

These interactions may be intensified by the presence of micro-organisms such as bacteria, microscopic algae or fungi. The metabolisms may lead to absorption or destruction of the dissolved matter.

#### 4.4.1 CARBONATE-CO<sub>2</sub> SYSTEM

Determinations of the carbon isotopic composition (<sup>14</sup>C and <sup>13</sup>C) (Sect.5.2.1.2 and 5.2.2.3, Volume I), of the temperature and chemical conditions such as pH and alkalinity as well as a knowledge of associated minerals and gases may allow to decipher the chemical reactions in the carbonate systems, their mass and isotopic balance. Finally the groundwater age may be determined by the <sup>14</sup>C method (Sect.5.2.2.3, Volume I, Mook 1980; Clark and Fritz 1997). This is not a simple and straightforward procedure. Gaseous and dissolved CO<sub>2</sub>, organic and inorganic carbon constituents, individual minerals and the fossil organic matter (Sect.4.4.2) involved in these reactions between groundwater and rock may have different isotopic compositions. Moreover, chemical and isotopic equilibrium may not be approached in defined closed or open system conditions.

The isotope composition of DIC of inorganic carbonate systems containing multiple sources and sinks of carbon, and in which chemical and isotopic equilibrium prevails can be exactly modelled applying the computer program NETPATH (Plummer et al. 1994). The preset of these conditions occurs during groundwater recharge. Atmospheric precipitation infiltrates in the soil, chemical and isotopic equilibrium is established between soil carbon dioxide, dissolved carbonate species H<sub>2</sub>CO<sub>3</sub>, HCO<sub>3</sub><sup>-</sup>, CO<sub>3</sub><sup>2-</sup> in water and marine carbonate in the soil. Experimentally determined fractionation factors and thermodynamic equilibrium constants as function of temperature are used (Chapter 6 and Volume I). Complications arise if magmatic CO<sub>2</sub>, CO<sub>2</sub> from fluid inclusions, organic CO<sub>2</sub> and CH<sub>4</sub> participates. Moreover, terrestrial and hydrothermal carbonate minerals rather than marine carbonate may be components of the carbonate-CO<sub>2</sub> reaction in freshwater. Another complication of hydrochemical modelling arises if carbonate formed by feldspar decomposition is involved (Vogel and Ehhalt 1963). This carbonate is generated by atmospheric CO<sub>2</sub> and contains <sup>14</sup>C and an isotopic composition of carbon considerably deviating from that of marine carbonate.

Under the conditions just mentioned modelling is often not possible, due to the lack of reliable data. The interpretation of the stable isotope data of carbon may, however, still allow a qualitative evaluation of the constraints of water-rock interaction.

#### 4.4.2 REACTIONS WITH ORGANIC MATTER

The chemical interaction of groundwater and organic matter has an important influence on the carbon isotope composition of the dissolved inorganic carbon compounds in groundwater. The main processes are

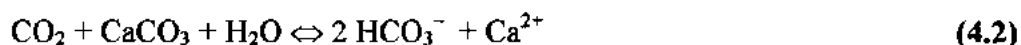
- 1) oxidation of organic matter, with the formation of CO<sub>2</sub> and successive chemical reactions with carbonate in the aquifer rock matrix, and
- 2) methane genesis.

The *oxidation of organic matter* (plant remains, coal, peat, lignite) may occur with the dissolved oxygen of freshly recharged groundwater or by sulphate reduction. The CO<sub>2</sub> – HCO<sub>3</sub><sup>-</sup> system behaves as a closed system, so that the δ<sup>13</sup>C and <sup>14</sup>C values are changed.

Organic carbon in the soil or deeper underground is being oxidised according to

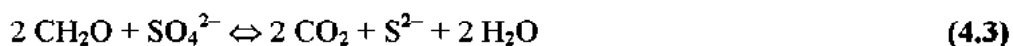


This CO<sub>2</sub> may dissolve carbonate increasing the concentration of dissolved carbon (CO<sub>2</sub> and HCO<sub>3</sub><sup>-</sup>) by up to a factor of two through:



Under organic matter containing soils fresh groundwater typically contains 12 to 24 mg C per litre in the form of dissolved inorganic carbon (Volume I).

Sulphate reduction may occur according to



100 mg/L SO<sub>4</sub> may form 91 mg/L CO<sub>2</sub> corresponding to an maximum increase of bicarbonate by a factor of 3. A detailed description of a quantitative evaluation of the isotope balance is given in Volume I and in Clark and Fritz (1997).

In the first step oxidation increases DIC due to the formation of CO<sub>2</sub> while HCO<sub>3</sub><sup>-</sup> remains constant. The <sup>14</sup>C and δ<sup>13</sup>C values decrease and the <sup>14</sup>C age increases. In the next step the CO<sub>2</sub> concentrations decreases and DIC rises. The <sup>14</sup>C value decreases while the <sup>14</sup>C age and the δ<sup>13</sup>C value increases (Fig.4.1). A detailed description of these processes is given in Volume I.

A correction scheme proposed in 1972 by Oeschger is a suitable solution for this problem. The calculation of the <sup>14</sup>C age is done by the product of the <sup>14</sup>C activity and the DIC concentration rather than by the <sup>14</sup>C activity). That means <sup>14</sup>C activity per litre of water is used rather than <sup>14</sup>C activity per gram carbon.

The process of *methane genesis* from organic matter is more complicated. It follows the

reaction (Clark and Fritz 1997)



CO<sub>2</sub> and methane are formed of which the latter may develop similar reactions as described before. The concurrent shift in δ<sup>13</sup>C is large but rather uncertain, as there is a strong but variable kinetic isotope fractionation involved. Usually the CO<sub>2</sub> becomes isotopically enriched in <sup>13</sup>C which qualitatively allows the identification of this process.

Admixture of thermocatalytic, abiogenic or mantle fossil methane is often associated with the admixture of fossil CO<sub>2</sub>. Gas will expel after exchange with the dissolved CO<sub>2</sub>, resulting in an uncontrolled loss of <sup>14</sup>C. In any case, methane is rarely found in resources of fresh groundwater (Geyh & Künzi 1981).

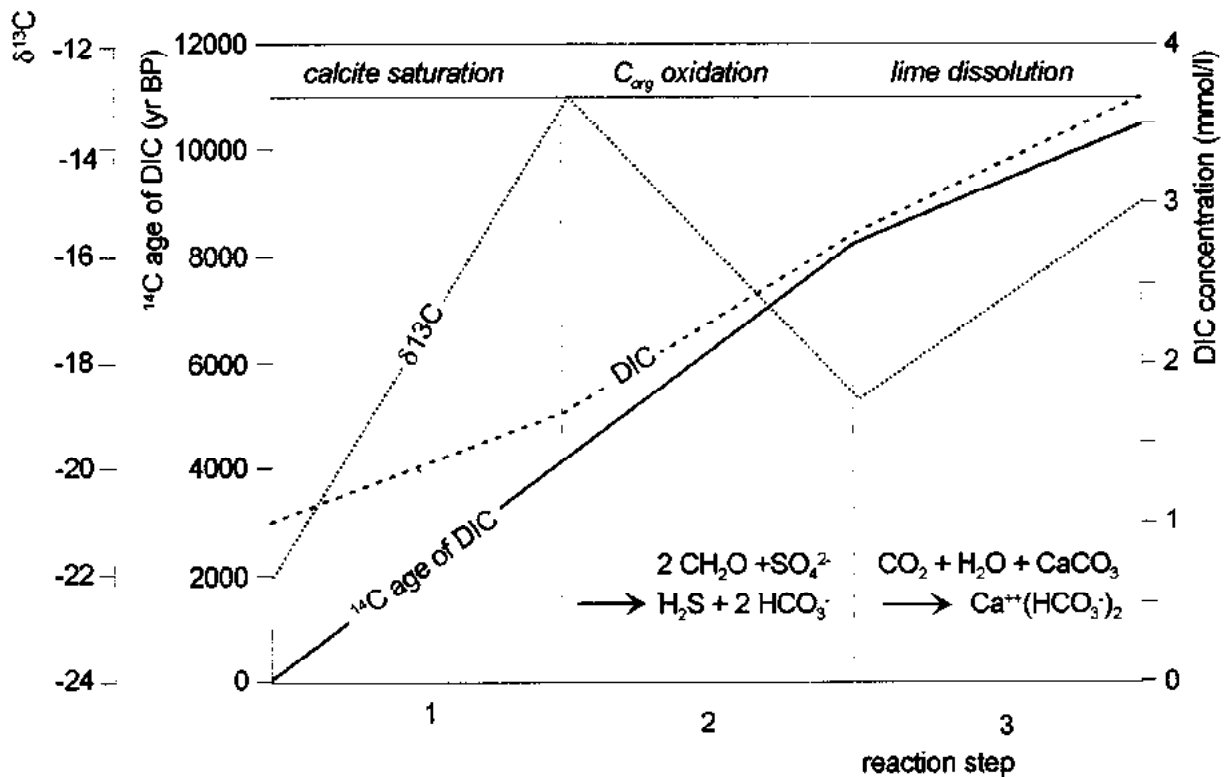


**Fig.4.1** Simplified scheme of the changes of CO<sub>2</sub> and HCO<sub>3</sub><sup>-</sup> (DIC) concentrations as well as of the <sup>14</sup>C age and δ<sup>13</sup>C value during the hydrochemical reactions until calcite saturation of the groundwater. Three reaction steps of the groundwater recharge, the oxidation of organic matter and the succeeding approach of secondary calcite saturation has to be distinguished (after Geyh and Kantor 1998).

#### 4.4.3 FATE OF DISSOLVED SULPHUR COMPOUNDS

Sulphur is found in groundwater as *sulphate* anion, SO<sub>4</sub><sup>2-</sup>. Under reducing conditions such as in peat bogs, organic bottom sediments, oilfield aquifers and in regions of active volcanism, groundwater may also contain appreciable concentrations of *sulphide* (HS<sup>-</sup> or H<sub>2</sub>S).

The most common sources of sulphur are the atmospheric wet and dry deposition of  $\text{SO}_2^{2-}$  and  $\text{H}_2\text{SO}_4$ , the admixture of seawater sulphate in seawater, oxidation of pyrite and other sulphide minerals, the dissolution of gypsum, anhydrite and other sulphate salts in marine and terrestrial evaporites, the introduction of sulphur from petroleum and coal, and finally the infiltration of sulphate from surface water bodies. The isotopic composition of sulphur in these sources, with the exception of seawater, varies in a wide range (Fig.4.2).

When sulphur from various natural and anthropogenic sources dissolves in cold groundwater, no appreciable fractionation takes place unless dissolved sulphate is microbially reduced.

Through the isotopic composition dissolved sulphur can be used as a tracer for its origin. Simple mixing concepts are sometimes sufficient to interpret the data (Schaefer and Uzdowski 1992). In more complicated cases the dissolved sulphates are distinguished by the  $\delta^{34}\text{S}$  and the corresponding  $\delta^{18}\text{O}(\text{SO}_4)$  values of the sulphate oxygen. The exchange of oxygen between  $\text{SO}_4^{2-}$  and  $\text{H}_2\text{O}$  is extremely slow at the low temperature of groundwater (Chiba and Sakai 1985). Therefore, the isotopic composition of oxygen in sulphate reflects either mixing or microbial reduction to sulphides.

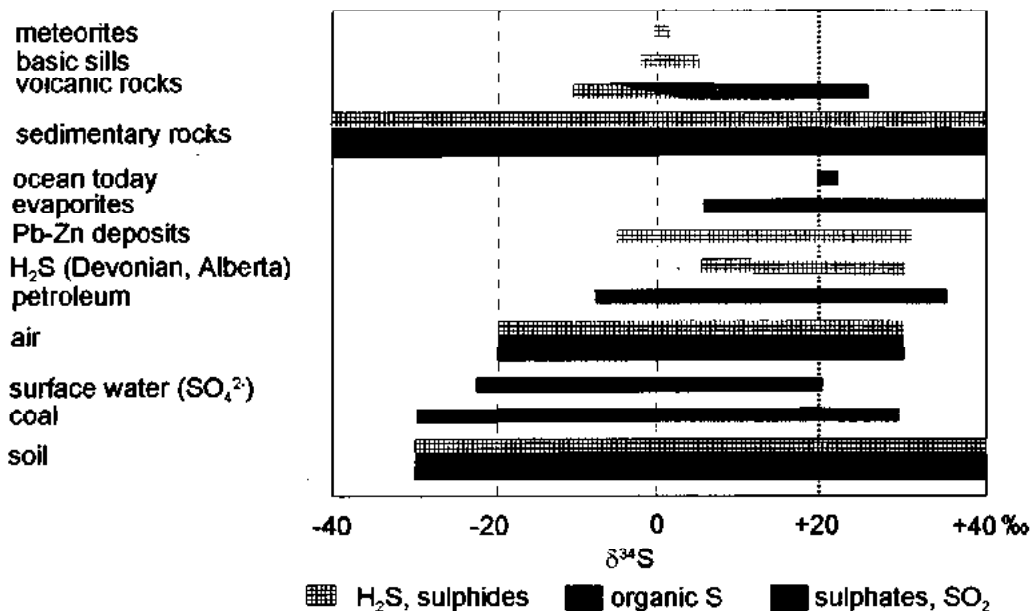
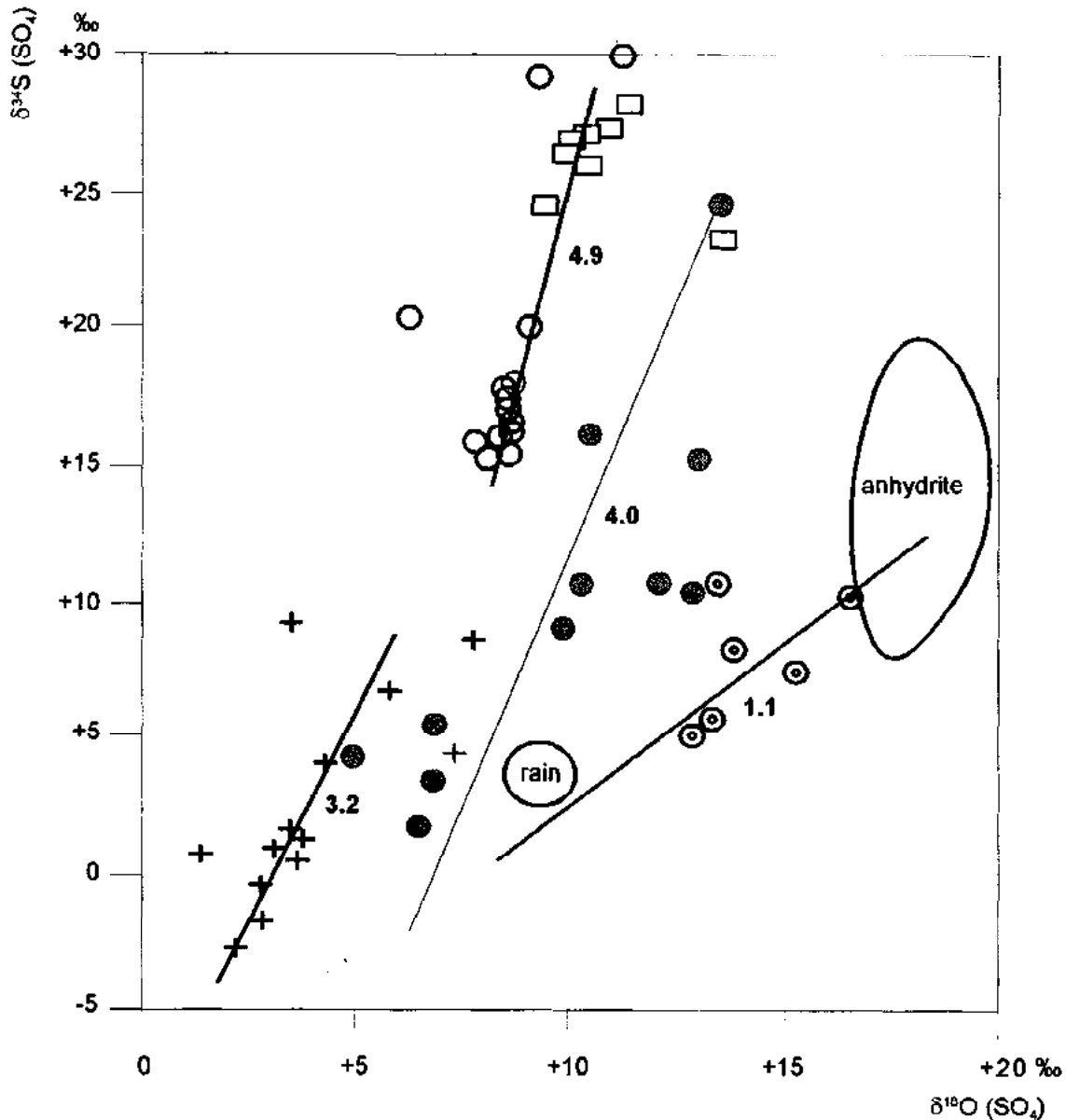


Fig.4.2 Sulphur isotope abundances in nature (after Krouse 1980)

Sulphur isotope *fractionation* is caused by various *geochemical and biochemical processes* as the formation of evaporites, microbial reduction of sulphate ions to hydrogen sulphide, inorganic oxidation of sulphide minerals and to a less extent by the adsorption of sulphate ions on colloidal particles in aquifers and soils (Krouse 1980). Changes in  $\delta^{34}\text{S}$  caused by those processes can be even several tens of per mill. Sulphide mineral that originate from the released  $\text{H}_2\text{S}$  have very negative  $\delta^{34}\text{S}$ . On the other hand, sulphate minerals originating from the isotopically heavy residual sulphate ions have positive  $\delta^{34}\text{S}$  (Smejkal 1978).



**Fig.4.3** Change of both the  $\delta^{34}\text{S}$  and  $\delta^{18}\text{O}$  values of sulphate dissolved in groundwater from the Bohemian Massif by mixing and microbial reduction of sulphides (data from Smejkal and Jetel 1990).

### Example

The plot of  $\delta^{18}\text{O}(\text{SO}_4)$  versus  $\delta^{34}\text{S}$  (Fig.4.3) represents the distribution of the  $\delta^{34}\text{S}$  of dissolved groundwater in the Bohemian Massif of central Europe (Smejkal and Jetel 1990).

The data represent four different types of groundwater. There are groundwaters tapped by a uranium mine, Vitkov II. The  $\delta^{34}\text{S}$  and  $\delta^{18}\text{O}(\text{SO}_4)$  values represent shallow groundwaters and point to mixing between sulphate derived from oxidation of sulphide minerals (pyrite and sphaerite) and sulphate in rainwater. The isotopically heaviest sulphur was found in Ca-Cl-SO<sub>4</sub> brines tapped at a depth of 500 m in the mine. This brine was sampled twice in 1972 to 1980 and in 1986 to 1989, respectively. Sulphur and oxygen became isotopically enriched. This

may be due to two stages of oxidation of reduced sulphur of volcanic origin which was preserved as a fossil brine in a volcanic playa lake of Miocene age. The existence of this lake was documented geologically, palaeontologically and by hydrochemical and isotopic data (Paces 1987). The connection between the recent groundwater and the brine represented by the line with a slope of 3.2 (Fig.4.3) is probably accidental. These two types of groundwater probably do not mix and are not genetically related.

#### 4.4.4 ON THE ISOTOPIC COMPOSITION OF STRONTIUM

Strontium isotopes (Sect.5.2.1.7) do not fractionate during dissolution, whereas biological enrichment is not known. However, due to the low strontium concentration in groundwater, water-rock interaction may approach *isotopic equilibrium* with respect to strontium. This process can sometimes be quantified by comparing the  $^{87}\text{Sr}/^{86}\text{Sr}$  values of the primary minerals of the host rock, those of the secondary minerals on the surface of fractures, joints and pores with those of the strontium constituents dissolved in the groundwater.

The strontium isotopic ratio  $^{87}\text{Sr}/^{86}\text{Sr}$  in saline water and those of the associated rocks and minerals from deep bore-holes and surface samples in the Precambrian Shield of Canada are similar (McNutt 1987), indicating isotopic equilibrium. On the contrary, the  $^{87}\text{Sr}/^{86}\text{Sr}$  ratio of oil-field water found in sedimentary rocks differs from that of the host rock. This indicates that this organic matter may not be old enough to permit the establishment of isotopic equilibration.

#### Example

There is a wide range of values for the  $^{87}\text{Sr}/^{86}\text{Sr}$  ratio of the granite minerals in the Stripa mine in Sweden, of the local groundwater and of the hydrothermal minerals on the surface of the fractures. The  $^{87}\text{Sr}/^{86}\text{Sr}$  ratio reaches from 1.8958 to 0.74529 in microcline with plagioclase of the host granite and in a fracture coating with quartz, microcline, plagioclase and chlorite, respectively. The lowest value of 0.74056 is found for the shallow groundwater (Fritz et al. 1987). Since the isotopic ratio in seawater is 0.70906 and the Rb/Sr ratio (= 0.007) in groundwater is half of the ratio of seawater (= 0.0145) the groundwater can be of meteoric rather than oceanic origin. It reacted more intensively with the coating of the fractures than with the minerals of the host rock. Knowledge of water-rock interactions on the surface of fractures is important in a rock environment which is being considered as a potential site for radioactive waste disposal.

# 5 APPLICATIONS TO LOW-TEMPERATURE SYSTEMS

Applying environmental isotope methods we have to distinguish between low-temperature ( $<90^{\circ}\text{C}$ ), medium-temperature ( $90 < T < 150^{\circ}\text{C}$ ) and high-temperature ( $>150^{\circ}\text{C}$ ) systems. In low-temperature systems many reactions and processes changing the isotopic compositions are too slow to have detectable effects. Low-temperature systems offer a wide field of applications in hydrogeology and hydrology:

- identification of the origin of groundwater and of its geogenic and anthropogenic constituents (e.g. pollution),
- tracing hydrochemical processes in groundwater and mixing processes (leakage of aquifers, mixing of groundwater with surface water from lakes or rivers (Volume III), brine, ocean water), and
- groundwater dating for the study of groundwater movement (flow pattern).

There are different aspects to be considered for the unsaturated and saturated zones.

A detailed description of the sampling for the various kinds of isotopic analyses of various kinds of water samples is given by Clark and Fritz (1997) and in Volume I.

## 5.1 UNSATURATED ZONE

Environmental isotope studies in the unsaturated zone have been carried out to obtain information on special aspects of the hydrological cycle. Special attention has been given to identify:

- the groundwater recharge rate (applying tritium and stable isotopes),
- the rate of evaporation from soils and shallow groundwater (by means of hydrogen and oxygen isotopic compositions), and
- the sources of the water used by plants.

### 5.1.1 PRINCIPAL SOIL PARAMETERS OF THE UNSATURATED ZONE

Three types of water are distinguished in the unsaturated zone:

- 1) *mobile water* (free water or gravity water), circulating through the macropores of the matrix mainly subject to gravity. The drainage of such water corresponds to the state of



the *field capacity*

- 2) *retentive water* or *absorbed water* remaining bound by capillary forces after drainage of the mobile water. This binding is strongly linked to the soil matrix by electrostatic forces and molecular attraction
- 3) *constitutive water*, an integrated part of the chemical compounds in the matrix and theoretically non-exchangeable, at least during the time of percolation. It resists a heating up to about 105°C apart from gypsum for which dehydration begins at 60°C. Some of the absorbed water in clay also resists heating above 105°C.

Qualitative parameters to describe the unsaturated zone and to investigate the movement of soil water are based on the characteristics of the sediment matrix. The most important are

- 1) the *texture* describing the grain size distribution of the soil particles
- 2) the *structure* describing the construction on aggregates or isolated or cemented particles
- 3) the *specific surface* considers the phenomena of surface absorption of water and solutes; it is defined as the total surface of the particles per unit of mass
- 4) the *mineralogic composition* of the soil.

## 5.1.2 GEOHYDRAULIC ASPECTS

### 5.1.2.1 STEADY-STATE FLOW

Steady-state mass balance models are fairly robust for the application to *intermediate depths*. This is the part of the unsaturated zone below the depth where water flow in preferred pathways (Sect. 5.1.2.2.3) and water uptake by roots affect the flux of tracers, and above the water table where flow is no longer vertical.

Steady-state solute tracer techniques completely depend on the estimate of the solute flux in the profile or region of interest. In many situations, however, redistribution of water and solute fluxes within the profile may cause uncertainties in this estimate. Surface runoff and horizontal saturated flow perched on low-permeability layers in the profile may disturb the flux into the deep profile. Vertical piston flow (water advances down the profile completely displacing older water) can be described by the convection–dispersion equations of solute transport. A particular situation arises in the unsaturated zone as the permeability and the hydraulic charge are dependent on the moisture content.

Difficulties arise if the tracer distribution at any time does not represent the long-term average conditions. In those cases water fluxes may be many orders of magnitude larger than the long-term average (steady-state). Dispersive-diffusive fluxes of solutes are probably grossly underestimated if the long-term average water flux is used in those parts of the profile where dual-flow pathways regulate the tracer flux.

### 5.1.2.2 MOVEMENT OF SOLUTES

The conceptual model of mobile-immobile water has been used to encapsulate those processes in which one part of the water phase is relatively immobile compared to the other. Hence, any solute which enters the immobile phase will cause the solute to be retarded relative to the water movement in the mobile phase. Processes that can be included in this model are anion exclusion, mixing with water in dead end pores and aggregate dispersion (Sect.5.1.2.2.2). The interaction between mobile and less mobile phases has been approximated by being proportional to the difference in the concentrations of the mobile and less mobile phases. In the event of strong interaction, the concentrations of the two phases will be equal, while for weak interaction there is virtually no time for mixing or exchange. A complete mixing may be assumed of slowly moving groundwater with ages of more than 1000 yr. This is why the total porosity is valid rather than the effective one (Sect. 1.3.1; Eq.2.1).

An example of a secondary modification of the isotopic composition of water can be expected by retardation/anion exclusion (Sect.4.1). Most clay surfaces are negatively charged. This means that there is a certain volume of water near the clay surfaces in which there are few anions. This water is generally considered to be immobile. Thus, there will be a difference in the behaviour of isotopes of water. The isotopes of water will exchange with water molecules in this excluded volume and hence will be retarded relative to the movement of the retentive and bound water. Hence, the isotopic composition in the mobile phase will differ from that of the mean soil water (Fig.5.1).

#### 5.1.2.2.1 Convection and advection

An instantaneous injection of tracer, either isotopic or chemical, in a laminar steady-state flow at point A at the starting time  $t_0$  (Fig.5.1) results in a peak displacement at a distance  $l$  (location B) at the time  $t$ . The flux  $J$  between these points is the product of the tracer concentration  $c$  multiplied by the mean tracer velocity  $v_{\text{trac}}$

$$J = v_{\text{trac}} \cdot c = \frac{l \cdot c}{t - t_0}$$

If the relative water volume (< field capacity)  $\Phi$ , present in the profile, changes during the movement of the water, the conservative equation becomes

$$\frac{\partial J}{\partial t} = \frac{\partial(\Phi \cdot c)}{\partial t} = \frac{\partial(v_{\text{trac}} \cdot c)}{\partial z} \quad (5.1)$$

#### 5.1.2.2.2 Dispersion

There is always an attenuation of the breakthrough curve with time and distance due to *dispersion* (Fig.5.1). In that case the tracer velocity is obtained by the *mean transit time*  $\bar{t}$  instead of  $t$ . Dispersion by molecular diffusion, occurring even in a less mobile liquid, is pro-

portional to the concentration gradient  $\partial c/\partial z$  and is described by Fick's law

$$J = -D_{\text{diff}} \cdot \frac{\partial c}{\partial z}$$

where  $J$  is the vertical tracer flux and  $D_{\text{diff}} [\times 10^{-5} \text{ cm}^2 \text{ s}^{-1}]$  is the molecular diffusion coefficient.  $D_{\text{diff}}$  depends on the nature and the concentration of the solution and soil type.

The *kinematic dispersion* is controlled by

- 1) differing velocities of water particles (Fig.5.1) in the same pore stream ranging from even zero near the particle surface to the maximum in the middle of the canal,
- 2) different sizes of pores and canals, and
- 3) trajectories deviating from the main direction of flow due to the tortuosity. This means that the actual velocity is higher than the mean tracer velocity.

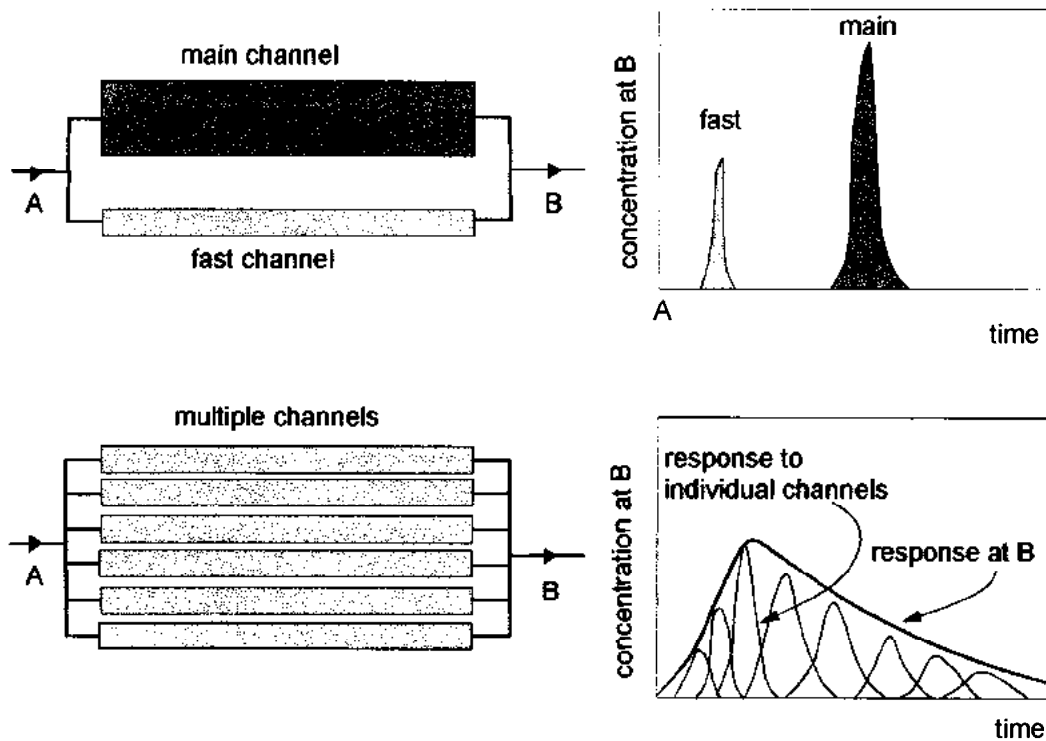


**Fig.5.1** Scheme of tracer displacement by advection for dual flow as well as for multiple channels demonstrating the effect of dispersion.

Considering both the convective and diffusive tracer transport and assuming that anion exclusion, macropore flow and immobile water is negligible, we obtain instead of Eq.5.1.

$$\Phi \cdot \frac{\partial c}{\partial t} = -v_{\text{trac}} \cdot \frac{\partial c}{\partial z} + \frac{\partial}{\partial z} \left( \Phi \cdot D_{\text{diff}} \cdot \frac{\partial c}{\partial z} \right) \quad (5.2)$$

The first and second terms on the right-hand side describe the convective and the diffusive transports, respectively.

### 5.1.2.2.3 By-pass flow (dual flow, macropore flow)

Dual-flow pathways (dual porosity) are the routes of water flow and solute movement (Black et al. 1983), arising from structures and discontinuities imbedded within the soil or aquifer matrix. These highly permeable structures are of a much larger scale than the usual representative elementary volume, that is used to average processes at the microscopic pore scale and to derive the continuum description of water and solute transport. The number of macropores connected to the surface decreases with depth, so that the role of macropores generally diminishes with depth over the top 6 m. Root channels and the pedal structure of the materials have been identified as important dual-flow pathways.

Macropores and other structures need to be in contact with a saturated zone or other source of free water to act as preferred pathways. Therefore, perching layers in the profile or ponding on the soil surface are necessary for preferred flow to occur.

A critical feature of dual-flow pathways is that they allow groundwater and solute to by-pass the matrix of the soil or aquifer (dual flow) with little or no interaction (Fig.5.1). The dual-porosity flow may be up to two orders of magnitude larger than that through the matrix. A large proportion is discharged as interface flow. This reduces the groundwater recharge on the one hand, and diminishes the influx of pollution from the surface on the other.

Flow of groundwater and solute in the profile is essentially multi-dimensional. The convection–dispersion equations of solute transport for piston flow (Volume VI) do not longer describe the tracer flux. This means that transient techniques which rely on measuring the rate of displacement cannot be applied to such situations.

Dual-flow pathways can be identified by directly applying tracers that mark the flow path and allow them to be visualised. However, the presence of non-piston flow processes can be inferred from discrepancies between travel times estimated from transient and steady-state tracer techniques.

### 5.1.3 SOLUTE TRANSPORT

In principal there are two quantitative approaches to describe solute transport:

- 1) the *tracer balance method* and
- 2) the *tracer peak-displacement method*.

Tracer studies are done to determine recharge rates rather than water fluxes. They allow recharge estimates especially by means of isotopes via the long-term observation of the soil-water flux. Classical techniques are dealing with much shorter time scales and are less sensitive.

The choice of tracer depends on the time of the passage of the root zone. This time  $t$  can be estimated by

$$t = z \cdot \frac{\Phi}{q_{\text{rec}}} \quad (5.3)$$

with  $z$  – depth of the root zone of around 1 m,  $\Phi$  - volumetric water content (ca. 0.1) and  $q_{\text{rec}}$  - recharge rate. For  $q_{\text{rec}}$  between 10 – 100 mm yr<sup>-1</sup> the time of the necessary observation becomes 1 – 10 years.

The choice of tracer depends on the likely range of recharge rates. For high recharge rates, in which the time scale associated with leaching through the root zone (Eq.5.3) is less than one year, an artificial tracer method is the most appropriate.

Soil tracer techniques usually involve soil sampling without the use of drilling fluids. In the case of Auger sampling each soil sample is weighed, preferably at the site, and immediately sealed in boxes or plastic bags and carefully labeled. The soil moisture is measured in the laboratory with gravimetric methods on an aliquot of the soil. The tracer position is usually detected by core sampling of interstitial water at different positions. If possible, comparative measurements by a neutron probe are helpful. Granulometric, mineralogic and other parameters of the soil should also be determined.

For stable *isotope analysis* the soil moisture must be extracted quantitatively to avoid any isotopic fractionation (Sect.5.2.1.1; Volume I), though it is very time-consuming. Even only some percent of water lost may falsify the isotopic composition. Azeotropic vacuum distillation of the soil samples with toluene is the most appropriate technique. Direct moisture extraction with ceramic cups or by suction probes are an alternative technique (Saxena and Dressie 1984). The soil water vapour is pumped through the probe, trapped in a molecular sieve, and extracted in the laboratory by heating to 400°C in a vacuum system. Allison et al. (1987) also tested a method to use soil CO<sub>2</sub> instead.  $\delta^{18}\text{O}$  and  $\delta^2\text{H}$  are measured mass spectrometrically.

Complementary tritium (<sup>3</sup>H) measurements allow to differentiate between transport of the vapour (followed by <sup>3</sup>H) and transport of the liquid phase (followed by stable isotopes). This technique is especially useful for case studies in arid regions.

Vegetation has little impact on the isotopic composition of soil water. Apart from this, pore water from different depth may be isotopically differently enriched due to a variable evaporation during the year. In any case, for reliable estimates of the recharge rate, soil samples for isotopic analysis should be taken from beneath the zone where water extraction by roots is occurring.

#### 5.1.4 APPLICATION

##### 5.1.4.1 RECHARGE RATE DETERMINATION BY MASS BALANCE

The first estimation of groundwater recharge rates was done with a balance study of anthro-

pogenic  $^3\text{H}$  (Münnich 1983). The *HETP model* (Height Equivalent Theoretical Plates) was developed for a better modelling of the  $^3\text{H}$  profile in the unsaturated zone. It is a simple one-dimensional multi-box model which describes the unsaturated zone as a series of soil layers with internally well-mixed soil water. The main parameter of this model is the layer thickness on the theoretical height plate controlling the simulation of the longitudinal dispersion of the tracer displacement. The initial water content is usually assumed to be constant and equal to the field capacity along the soil profile. In numerical calculations admixing of new water is assumed to be complete and instantaneous. The mixing balance is modelled for all boxes. This model can predict tracer movement in the unsaturated zone under natural conditions (Datta et al. 1973; Thoma et al. 1979).

**Example:**

Bomb  $^3\text{H}$  measurements (Thoma et al. 1979) of percolated water samples collected monthly from a lysimeter showed that the  $^3\text{H}$  response is on average delayed by 5 months in a sand lysimeter and by 2.5 years in a loess-loam lysimeter. The HETP model, adapting a variable field capacity, applied in combination with an evaporation/infiltration balance based on meteorological data showed good agreement between predicted and observed  $^3\text{H}$  concentration of the percolated water.

**5.1.4.2 RECHARGE RATE DETERMINATION BY TRACER PEAK DISPLACEMENT**

The assumption of the piston-flow model is that the tracer and all water in the soil move simultaneously. The tracer peak at the position  $z$  and the time  $t$  is the integrated result of the downward (infiltration) and upwards (evaporation) movement that occurred during the period  $t - t_0$  ( $t_0$  - starting time). The amount of water stored in the soil section between  $z$  and  $z_0$  represents the actual recharge (or the actual evaporation loss if  $z$  is above the initial position  $z_0$ ). Although the piston-flow model is an oversimplification, it has been often successfully applied.

A complication may arise by common flow through dual-flow pathways (Sect. 5.1.2.2.3). Foster and Smith-Carrington (1980) determined the interstitial piston-flow rate by the position of the bomb-tritium peak in the unsaturated chalk in various locations in England (Fig. 5.2). The low infiltration rate derived from the peak-displacement velocity is explained by an undetected rapid bypass flow through macro fissures of the chalk.

In practice, groundwater recharge must have been very low and the unsaturated zone very deep that the anthropogenic bomb- $^3\text{H}$  peak did not yet reach the saturated zone. Because the time since the injection of bomb-tritium into the hydrosphere in 1963 is too long, it is unlikely that a tritium peak can still be recognised in the unsaturated zone (Carmi and Gat 1992). Under special conditions, the specific activity of bomb  $^{14}\text{C}$  (Ousmane et al. 1983) may deliver valuable supplementary information to estimate the groundwater recharge rate, though possible water-rock interactions with the matrix (Sect. 4.4) have to be taken into account.

**Example:**

Dincer et al. (1974) determined the position of the  $^3\text{H}$  peak of 1963 in a drilled core from the arid Dahna Sand Dune area, Saudi Arabia, and estimated a recharge rate of  $23 \text{ mm yr}^{-1}$ . This is relatively high compared to the annual rainfall of 60 – 70 mm in Riyadh. Further drilling at the same location (Somntag et al. 1980a) confirmed, however, this result applying an infiltration–evaporation model.

It was assumed that the tracer-displacement methods also can be applied to *stable isotopes*. In temperate regions the stable isotopic composition of precipitation varies seasonally and may serve as environmental tracer for changes of the infiltration rate during the year. Presupposition is that this variation is conserved within the unsaturated zone (Fig.5.3). Changes of the isotopic composition can also be caused by infiltration of rainfall of different origin, by condensation, partial evaporation or partial freezing of soil water although isotope fractionation during freezing is small.

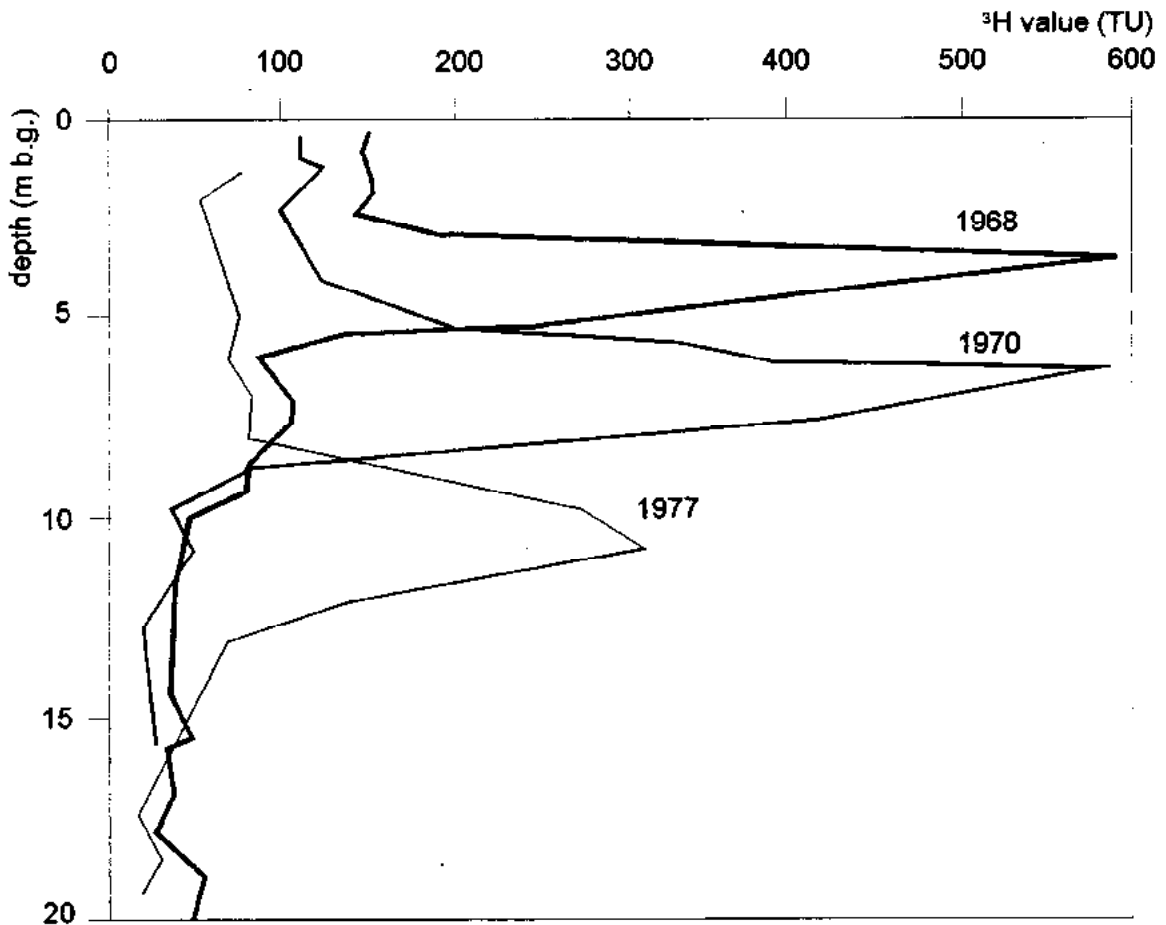
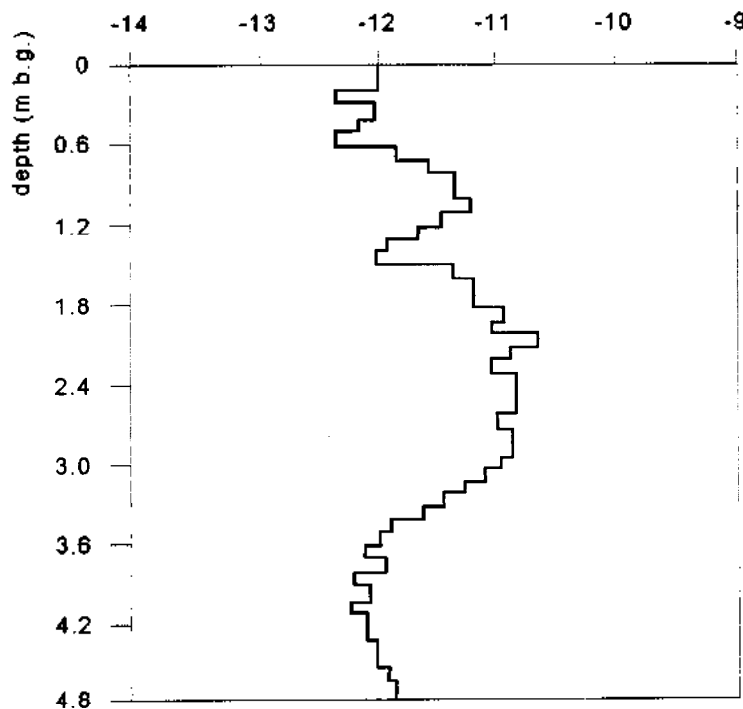


Fig.5.2 Successive bomb-tritium displacement in the unsaturated zone (after Foster and Smith-Carrington 1980).

**Example:**

Recharge studies have been most successful with seasonal changes of the stable isotopic composition when the recharge rate is relatively high ( $>200 \text{ mm yr}^{-1}$ ; Saxena and Dressie 1984) (Fig. 5.3). This makes this technique most applicable for temperate humid areas. Infiltration studies in the sand dunes of Pelat, Israel, also applied the seasonal variations of the  $\delta^{18}\text{O}$  values. The results were confirmed by the investigation of the natural  $^3\text{H}$  profile. A recharge rate of  $800 \text{ mm yr}^{-1}$  through the dunes were found, almost the total amount of rainfall (Thoma et al. 1979).

In *arid* and *semi-arid regions* the stable isotopic composition does usually not vary seasonally, though precipitation with depleted heavy isotopes may enter after short, but heavy rain events (amount effect; Volume I, Sect.5.2.1.1). Such rains more effectively contribute to groundwater recharge than the many rain events of low intensity. Soil water evaporation during the long dry season produces isotopically enriched pore water even below the evaporation front. It was assumed that repeated downward displacement of the enriched peak during the rainy season should lead to a sequence of heavy isotope peaks conserved in the unsaturated zone (Sonntag et al. 1985). These peaks would represent a certain amount of water equivalent to the recharge contribution of the individual years and should trace the groundwater movement during infiltration after the rain events. Such peaks are, however, not found. Hence, the stable isotopic composition of pore water has not been found to be a useful tracer of recharge in dry regions.



**Fig.5.3** Depth profile of the  $\delta^{18}\text{O}$  value of pore water. The annual change of the isotope composition allowed to estimate the recharge rate to approximately  $260 \text{ mm yr}^{-1}$  (after Saxena and Dressie 1984).



Allison et al. (1983a) showed that in areas of limited vegetation where transpiration is relatively unimportant and where the rate of recharge is low ( $<10 \text{ mm yr}^{-1}$ ), there is a linear relationship between the shift in isotopic composition from the meteoric water line (deuterium excess) and the inverse of the square root of the recharge rate. This relationship has, however, not yet been further tested (Fig.5.4). Limited field data pointed to agreement with this relationship.

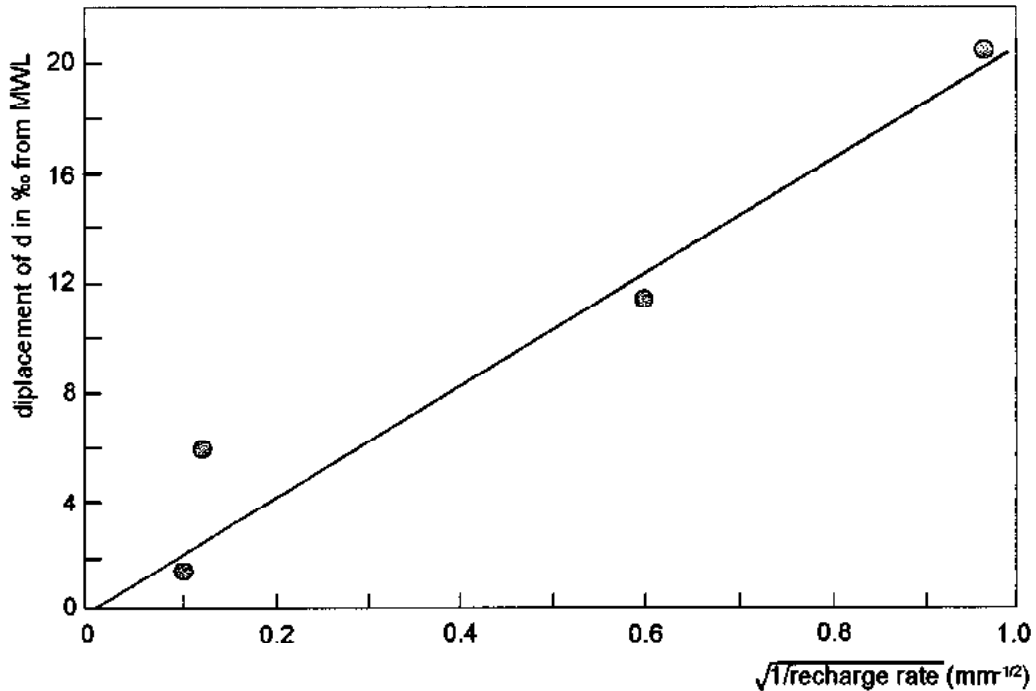


**Fig.5.4** Correlation between the displacement of the delta values from the Meteoric Water Line of deep pore water and independent estimates of the recharge rate for four dune sites in South Australia (Allison et al. 1983a).

#### **Case study: Comparison - $^3\text{H}$ balance and displacement methods**

Sukhija and Shah (1976) found that  $^3\text{H}$ -peak displacement method gave drainage estimates 20 - 40% higher than the  $^3\text{H}$  mass balance method, at field sites in northern India. This suggests either: a) that  $^3\text{H}$  fallout has consistently been overestimated, b) that  $^3\text{H}$  is being lost from the soil profiles, or c) that too much water is being counted in the peak-displacement method. The latter could be due to either i) the presence of immobile water, or ii) including water in the plant root zone, which may not become drainage.

#### **Example: $^3\text{H}$ -peak displacement, $^3\text{H}$ and chloride mass-balance methods**

At recharge rates greater than approximately  $20 \text{ mm yr}^{-1}$  the results of the  $^3\text{H}$  mass-balance, peak-displacement and chloride mass-balance studies, all appear to agree within 30 - 50%. The results of peak-displacement methods using artificial  $^3\text{H}$  tagging also compare well with those of the chloride mass-balance method. The comparison with corresponding piezometric data showed qualitative agreement in the arid area of Botswana (Beekman et al. 1996).

### 5.1.4.3 EVAPORATION RATE

The isotopic compositions of oxygen and hydrogen in soil water of the unsaturated zone vary mainly as a result of changes in the isotopic compositions of the rainfall and by evaporation. Zimmermann et al. (1967) first showed that if sand saturated with water is subject to evaporation,  $\delta^{18}\text{O}$  and  $\delta^2\text{H}$  values of the pore water decrease exponentially downwards from a maximum at the surface. Barnes and Allison (1988) presented their mathematical models describing the shape of the  $\delta^{18}\text{O}$  and  $\delta^2\text{H}$  profiles in saturated sand profiles for steady-state isothermal evaporation, under unsaturated, non-isothermal conditions and finally for non-steady state evaporation. This includes the isotope effects of partial evaporation of pore water from dry soil. The air temperature, the relative humidity and the isotopic composition of the atmospheric moisture control the enrichment process of the heavy stable isotopes. Steady-state and kinetic isotope fractionation contribute to both.

The soil profile is usually divided into two parts: in the upper shallow part down to the enrichment peak (evaporating front) only vapour moves to the surface against the diffusive flux of isotopically depleted atmospheric moisture. In the part below liquid transport is significant. The  $\delta$  values decrease approximately exponentially until the corresponding value of the groundwater of the saturated zone is approached (Fig. 5.5). Under *steady-state conditions* the ascendant flux of moisture supplied by capillary rise equals the flux of water vapour lost by evaporation. Hence, the isotopic composition of the vapour released into the atmosphere must be the same as that of the evaporated groundwater in the saturated zone.

In the evaporation front (or dry-wet interface) liquid water is converted into vapour. It remains at the same position below the soil surface. The isotopic composition at the evaporating front deviates from that of the atmospheric moisture and that of the groundwater, and depends on the following parameters:

- 1) temperature of the atmosphere (assumed to be equal to that of the water),
- 2) equilibrium fractionation between liquid and vapour,
- 3) the moisture deficit of the atmosphere,
- 4) the isotopic composition of the atmospheric vapour,
- 5) the kinetic fractionation in the dry soil layer above the evaporation front,
- 6) the isotopic composition of the reservoir water below the capillary fringe.

Above the evaporation front (eva) in the vapour transport region the delta value is given by

$$\delta_{eva} = \alpha^{-1} \left\{ \delta_{atm} + \varepsilon + \left[ \eta \cdot (1 + \delta_{res}) + (\delta_{res} - \delta_{atm}) \right] \cdot \frac{z}{z + H_{atm} \cdot z} \right\}$$

with the subscript "res" for input groundwater (reservoir water), the diffusion ratio excess  $\eta = (D_{\text{liq}}/D_{\text{isot}})^0 - 1$  ( $n = 1$  under steady-state conditions) with  $D_{\text{liq}}$  and  $D_{\text{isot}}$  as diffusion coefficients of the water and that of the corresponding isotope,  $H_{\text{atm}}$  as relative humidity of the atmosphere with  $H_{\text{atm}} = 1 - z_{\text{eva}}/z$  and  $z_{\text{eva}}$  as the depth of the evaporation front (enrichment peak) and the penetration depth  $z$

$$z = \frac{\rho_{\text{sat}}}{\rho_{\text{liq}}} \frac{(n_{\text{tot}} - \Phi) \cdot \tau_0 \cdot D_{\text{vap}}}{q_{\text{eva}}}$$

with  $D_{\text{vap}}$  as actual diffusivity of water vapour in the air,  $\rho_{\text{liq}}$  as density of the water and  $q_{\text{eva}}$  as evaporation rate.

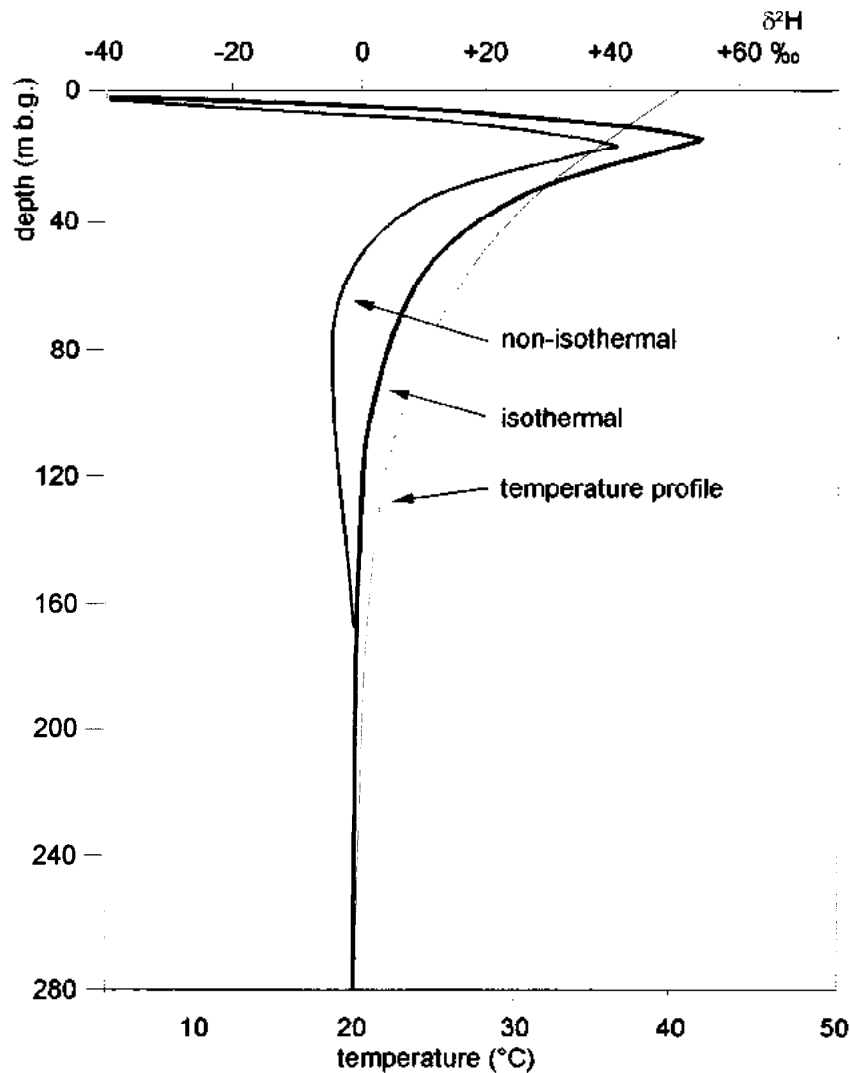


**Fig.5.5** Comparison of theoretical isothermal and non-isothermal steady-state deuterium profiles (after Barnes and Allison 1988).

Below the evaporation front where the upwards transfer of liquid is predominant, the heavy isotopes become enriched by evaporation and diffuse downward into the liquid phase. This results in an exponential relationship between isotopic composition and depth.

The  $\delta$  values along the soil profile beneath the evaporation front are given after Barnes and Allison (1983) by

$$\frac{(\delta^2\text{H} - \partial^2\text{H}_{\text{res}})}{(\delta^{18}\text{O}_{\text{eva}} - \partial^{18}\text{O}_{\text{res}})} = \left[ \frac{(\delta^{18}\text{O} - \partial^{18}\text{O}_{\text{res}})}{(\delta^{18}\text{O}_{\text{eva}} - \partial^{18}\text{O}_{\text{res}})} \right]^v$$

with 
$$v = \frac{D(^2\text{H})}{D(^{18}\text{O})} \approx 1.$$

$D(^2\text{H})$  and  $D(^{18}\text{O})$  are the isotopic diffusivities of the mentioned isotopes in the liquid phase.

Barnes and Allison (1984) showed that the effect of temperature on real isotope profiles was reasonably small but could explain a secondary minimum in the profile which is often observed in field situations. A possible explanation for this phenomenon is that under non-isothermal conditions, the isotopically light water vapour produced at the drying front moves both upwards and downwards in response to humidity and temperature gradients. The depletion observed results from this vapour condensing beneath the drying front. In real soils often an appreciable temperature gradient exists. It is caused by annual and diurnal surface temperature fluctuations.

The steady-state conditions of the isotopic profile are a final state after being wetted by infiltration from rainfall. In the first period water is freely available at the surface and the evaporation rate is relatively constant. Subsequently, the evaporation rate will decrease. The cumulative evaporation is inversely proportional to the square root of time (Eq.34 in Barnes et al. 1988). Walker et al. (1988) and Barnes and Walker (1989) modelled also non-steady state conditions. This model is now capable of representing the most general case of water and isotope movement through soils undergoing evaporation and infiltration of water. The *characteristic time*  $t$  for the development of the *steady-state profile* is given by

$$t = \frac{D}{q_{\text{eva}}^2}$$

For extremely low evaporation rates  $q_{\text{eva}}$  it results in millennia (Fontes et al. 1986), while at evaporation rates of  $q_{\text{eva}} = 10 \text{ mm d}^{-1}$  a period as short as a day may be obtained. In the field, especially in more temperate areas, profiles rarely reach steady state unless the water table is quite near the surface. However, in more arid areas, if rainfall does not penetrate to significant depth, this may be all lost by evaporation without disrupting the isotopic profile.

According to Barnes and Allison (1983) three methods exist for determining evaporation rates using stable isotopes:

- 1) interpretation of the *zone of exponential decay beneath the evaporating front*. The limiting factor is the diffusivity of soil water which may exhibit a rather complex behaviour a low water content
- 2) use of the *position of the maximum in the isotope profile* (depth of the evaporating front) combined with the diffusivity of water vapour. This technique is best for low rates of **evaporation**
- 3) use of the *shape of the isotope profile in the region above the evaporating front*. It is not likely to be successful, as there are sampling and analytical problems associated with the very low water contents usually encountered in this region.

These methods have the disadvantage of being point estimates and are subject to the natural spatial heterogeneity of the area and the corresponding evaporation rates.

Allison (1982) has experimentally shown that the slope of the relationship between  $\delta^2\text{H}$  and  $\delta^{18}\text{O}$  values can become as low as 2 for soil water in unsaturated sand subjected to evaporation below a dry layer. This is considerably lower than the value of 4 to 5 obtained during evaporation from a free water table. Barnes and Allison (1983) developed a model for predicting the enrichment. The effect is explained in terms of an increased thickness of the laminar layer through which evaporating water molecules escape. This work suggests for arid-zones that groundwater replenished by local recharge, should be characterised by low  $\delta^{18}\text{O} - \delta^2\text{H}$  slopes.

The slope of the lines is given by

$$s = \frac{\delta^2\text{H}^{\text{init}} - \delta^2\text{H}^{\infty}}{\delta^{18}\text{O}^{\text{init}} - \delta^{18}\text{O}^{\infty}} \quad (5.4)$$

with  $\delta^{\infty}$  as

$$\delta^{\infty} = \frac{\varepsilon^{\text{vap}} + h \cdot \delta^{\text{atm}} + (1-h) \left[ \eta + \left(1 + \frac{q^{\text{vap}}}{q_{\text{eva}}}\right) (1+\eta) \cdot \delta^{\text{res}} \right]}{1 + \left( \frac{q^{\text{vap}}}{q_{\text{eva}}} \right) \cdot (1-h) \cdot (1+\eta) \cdot \varepsilon^{\text{vap}}}$$

$\delta^{\text{init}}$  and  $\delta^{\text{res}}$  are the delta values of hydrogen and oxygen of the groundwater in the saturated zone and of the feed water at different depth, respectively, and  $\delta^{\text{atm}}$  the delta values of the atmospheric moisture.  $q^{\text{eva}}$  is the evaporation rate at the evaporation front,  $\varepsilon$  is the isotopic equilibrium fractionation.  $h$  the relative humidity of the free air and  $\eta$  the ratio of the diffusivities of the isotopically heavy and light water vapour in the gas phase.

There is a relationship between the evaporation rate  $q_{\text{eva}}$  and the slope  $s$  of the evaporation line in the  $\delta^{18}\text{O} - \delta^2\text{H}$  plot as well as the thickness of the dry layer (Fig.5.6).

Whenever evaporation takes place, two types of fractionation give rise to enrichment of isotopes at the evaporating surface. These are:

- 1) the equilibrium effect due to small differences in the chemical potential between the isotopic species
- 2) the kinetic effect due to different rates of diffusion of the isotopic species in the vapour phase. In this case both isotopic species behave in a similar fashion (Merlivat 1978).

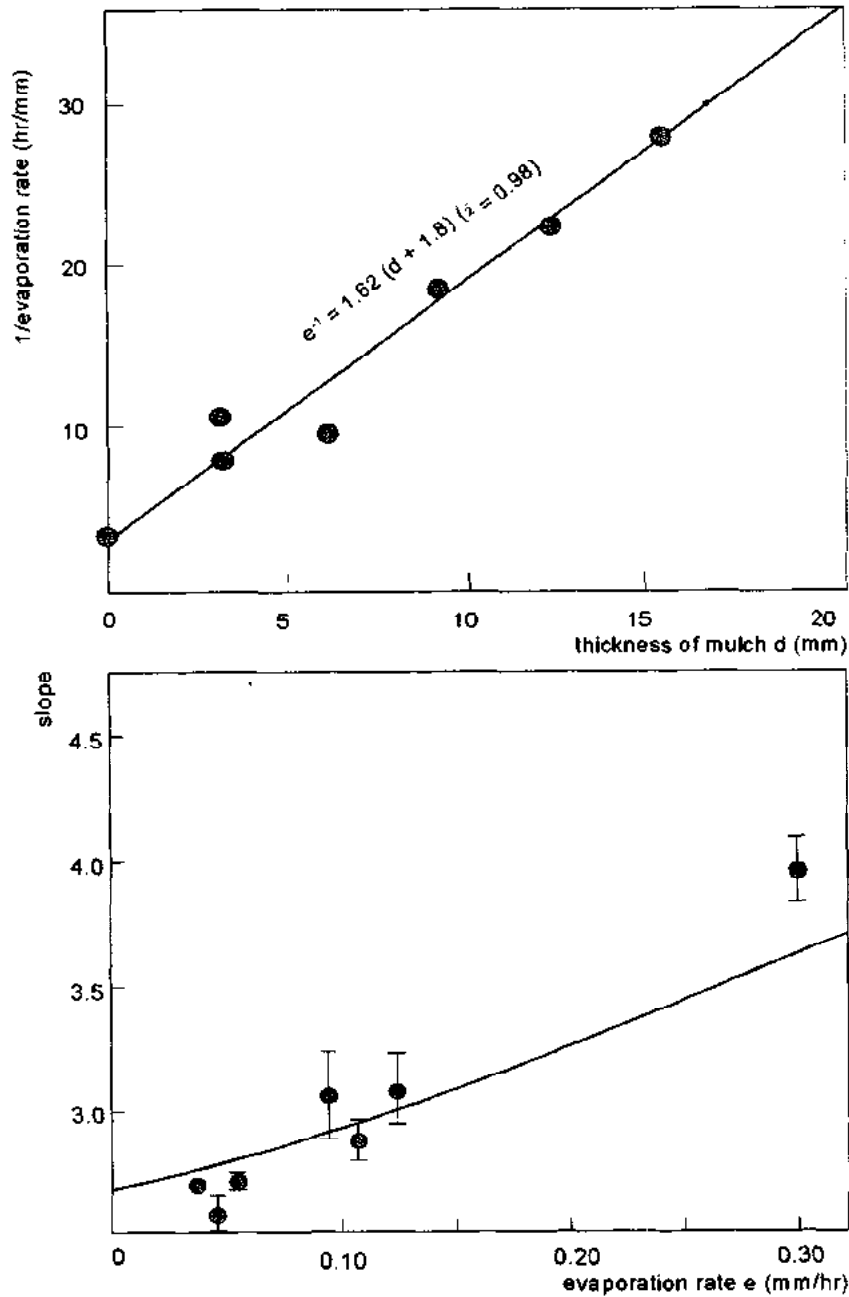


**Fig.5.6** Upper part: Relationship between the evaporation rate  $q_{\text{eva}}$  and the slope of the line in the  $\delta^{18}\text{O}/\delta^2\text{H}$  plot (Eq.5.4). The solid line is calculated using the data shown. Lower part: Relationship between the thickness of the dry layer and the inverse of the evaporation rate (after Allison et al. 1983a).

As the evaporating front moves further into the soil profile, the relative importance of the kinetic effect increases because of the development of a superficial dry layer where diffusive transport of water vapour dominates, leading to a reduction in the slope of the  $\delta^2\text{H} / \delta^{18}\text{O}$  relationship (Eq.5.4; Allison et al. 1983a).

These results were confirmed by Sonntag et al. (1985) who found (Fig.5.7) that:

- 1) the slope of the  $\delta^{18}\text{O} / \delta^2\text{H}$  line increases with increasing humidity in the climate chamber,
- 2) and with increasing grain size,
- 3) the slope of the evaporation line for grain sizes  $> 1$  mm corresponds to that for open water bodies.

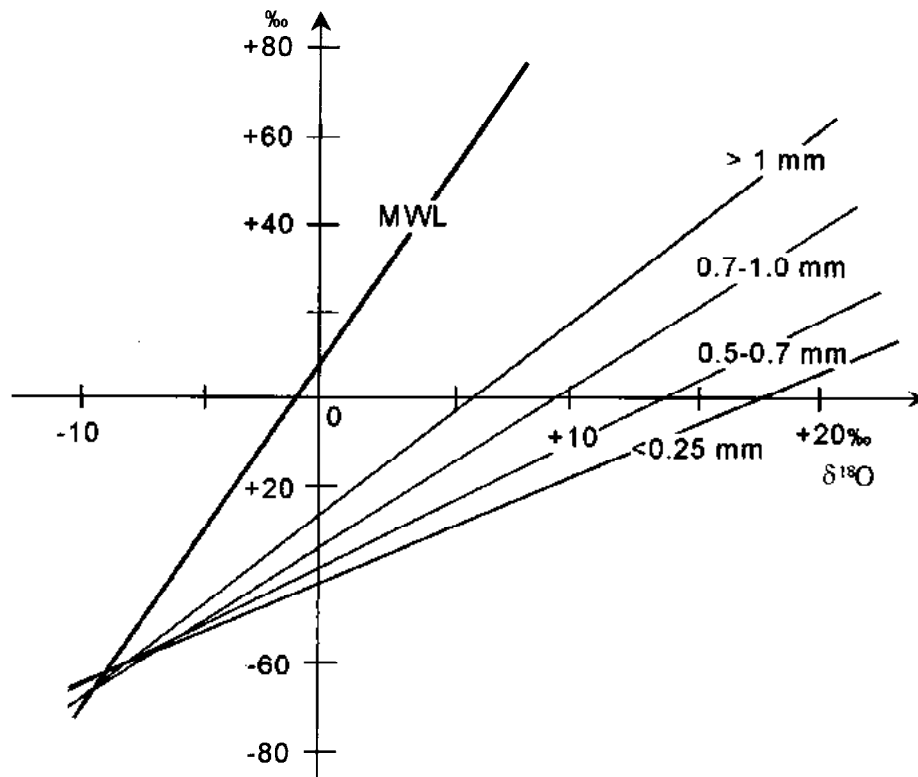


**Fig.5.7** Differing slopes of the evaporation lines in the  $\delta^{18}\text{O} / \delta^2\text{H}$  plot for sand of different grain sizes. The pore water evaporated into dry air (after Sonntag et al. 1985).

**Example:**

*Diffuse discharge* is often an important component of the water balance of groundwater systems - for example, the aquifers beneath the Sahara (Aranyossy et al. 1991) and the Great Artesian Basin (GAB; Woods 1990). Such discharge may be an important component of the water balance and may need to be evaluated to estimate the sustainable yield of some groundwater systems. Diffuse discharge from a part of the GAB was approximately four times the discharge from springs, the generally accepted outflow points of this aquifer.

#### 5.1.4.4 WATER LOSS BY PLANT EXTRACTION

Plant roots are not capable to produce isotope fractionation under saturated and unsaturated conditions (Allison et al. 1983b; Zimmermann et al. 1967; Volume I). Stable isotopes provide possibly the only way to determine the source of water used by vegetation in the field. The isotopic composition of water in small twigs, for instance, is representative of that of the water taken up by roots. Usually however the pore water has more positive delta values than groundwater (Volume I, Sect.5.2.1.1).

Thornburn and Walker (1994) showed that mature Eucalyptus trees took up soil water from deep rather than water which had infiltrated into the surface soil as a result of flooding, even though the inundation lasted for several months. Both these data and those mentioned in the preceding paragraph show that at least for mature vegetation roots must not approach the saturated zone of groundwater.

A quantitative approach was attempted by Adar et al. (1995). He studied two Tamarisk trees in Israel and surprisingly found that the ratio of the proportions of water drawn off from the saturated and unsaturated zones remained remarkably similar during the dry and wet seasons, though the total extraction rate changed by a factor of two.

## 5.2 SATURATED ZONE

There is a wide field of applications for environmental isotope techniques in the saturated zone. The best source for corresponding studies are the proceedings of the numerous international conferences on the application of isotope hydrological techniques organised by IAEA since the early sixties (see Recommended Literature).

### 5.2.1 ORIGIN OF GROUNDWATER

The numerous applications of isotope hydrological methods applying stable isotopes encompass the entire hydrosphere. One of the main fields of application is concerned with the origin and mixing of groundwater and of its dissolved natural and anthropogenic constituents. Most comprehensive information is obtained from stable isotope abundances. They can be measured quickly and cheaply and can be reliably interpreted as a largely conservative tracer (Gat and Gonfiantini 1981; Volume I).

#### 5.2.1.1 OXYGEN ( $^{18}\text{O}/^{16}\text{O}$ ) AND HYDROGEN ( $^2\text{H}/^1\text{H}$ )

##### Physical Fundamentals

(See Volume I). The most abundant isotopes of oxygen,  $^{16}\text{O}$  (ca 99.7 %) and  $^{18}\text{O}$  (ca. 0.2 %), and those of hydrogen,  $^1\text{H}$  and  $^2\text{H}$  (or deuterium; D), combine and produce water molecules of differing molecular mass between 18 and 22, of which the most abundant are  $^1\text{H}_2^{16}\text{O}$ ,  $^1\text{H}^2\text{H}^{16}\text{O}$ , and  $^1\text{H}_2^{18}\text{O}$ . As constituents of the water molecules, they can act as conservative



tracers. The natural atomic ratios are  ${}^2\text{H}/{}^1\text{H} = {}^2\text{R} \cong 1.5 \times 10^{-4}$  and  ${}^{18}\text{O}/{}^{16}\text{O} = {}^{18}\text{R} \cong 2 \times 10^{-3}$ . These ratios are expressed as delta values (Eq.2.1; Sect.2.3.1). Ocean water has  $\delta^{18}\text{O}$  and  $\delta^2\text{H}$  values of  $\pm 0\text{‰}$ , as V-SMOW (Standard Mean Ocean Water) has been chosen as the standard. Most freshwaters have negative values.

### Occurrence

Most cold groundwater resources are of meteoric origin (*meteoric groundwater*). There is a strong relationship between the  $\delta^{18}\text{O}$  and  $\delta^2\text{H}$  values of precipitation reflected in the Meteoric Water Line (MWL, Dansgaard 1964). The slope is 8 and the so-called deuterium excess is  $+10\text{‰}$  (Fig.5.8). The deuterium excess (d) is defined as

$$d_{\text{excess}} = \delta^2\text{H} - 8 \delta^{18}\text{O}$$

The *deuterium excess (d excess)* near the coast is smaller than  $+10\text{‰}$  and approximately  $0\text{‰}$  only in Antarctica. In areas where, or during periods in which, the relative humidity immediately above the ocean is or was below the present mean value, d is greater than  $+10\text{‰}$  (Merlivat and Jouzel 1979). An example is the deuterium excess of  $+22\text{‰}$  in the eastern Mediterranean (Gat and Carmi 1970). The value of d is primarily a function of the mean relative humidity of the atmosphere above the ocean water (Merlivat and Jouzel 1979). The coefficient d can therefore be regarded as a palaeoclimatic indicator.

### Processes

Evaporation from surface water may cause the slope to be as low as 4. The slope can be as low as 2 for soil water in the unsaturated zone (Sect.5.1.4.3). Thus, groundwater that has previously been subjected to evaporation can be identified on this basis.

There are deviations from the MWL indicating various processes of isotopic exchange and fractionation. The best known examples are departures due to evaporation observed in brines from sedimentary marine aquifers, exchange of oxygen between water molecules and silicate minerals observed in geothermal systems with active exchange of oxygen between water molecules and silicate minerals (Chapter 6), and mixing between meteoric groundwaters and fossil residual brines in crystalline rocks (Fig.5.8).

The *evaporation effect* which results in an enrichment of the heavy isotopes in the liquid phase with respect to the vapour phase allows to identify quantitatively the admixture of superficial water as lake water and river water to groundwater (e.g. Darling et al. 1996). Water balance studies of lakes have successfully been applied with a precision of less than  $\pm 20\%$  (Zuber 1983). In arid regions it is possible to estimate the evaporation rate through the unsaturated zone (Sect.5.1.4.3).

**Temperature effect:** As water molecules with differing molecular mass have different vapour pressure, the lighter isotopes will become enriched in the more volatile phase as opposed to the less volatile phase during a change of phase (evaporation, condensation, sublimation). This effect, known as isotope fractionation, is strongly temperature dependent (Volume I).

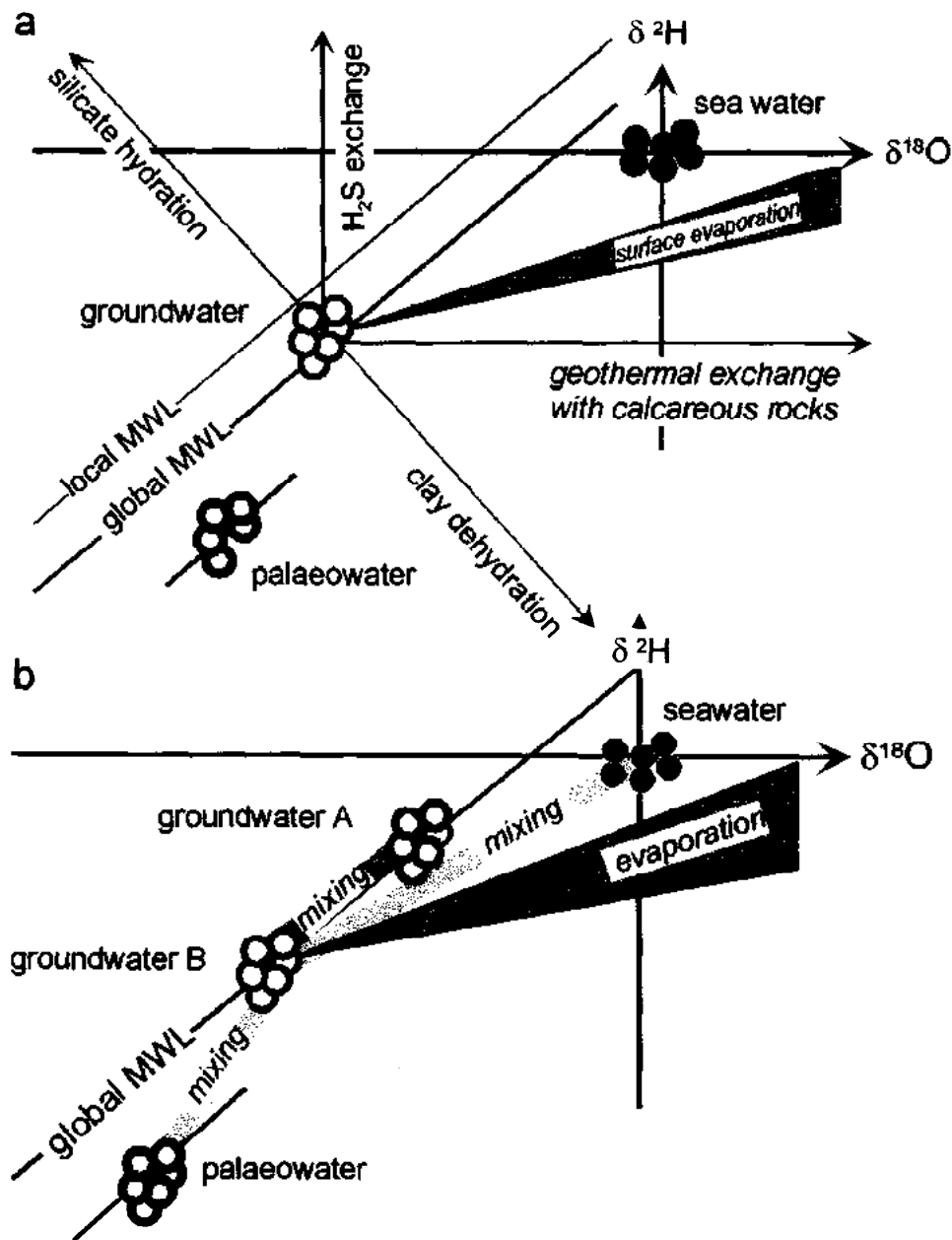


**Fig.5.8** (a) Various processes which shift the  $\delta^{18}\text{O}$  and  $\delta^2\text{H}$  values from the MWL: evaporation shifts both  $\delta^{18}\text{O}$  and  $\delta^2\text{H}$  values; the former are displaced as a result of isotopic exchange with volcanic  $\text{CO}_2$  and limestone, the latter due to exchange with  $\text{H}_2\text{S}$  and silicate hydration. (b)  $\delta^{18}\text{O}/\delta^2\text{H}$  plot for continental precipitation (MWL = Meteoric Water Line; local corresponds to the Mediterranean precipitation) with examples of various mixing lines. The MWL of Pleistocene palaeowater may be apart from the MWL.

The precipitation in winter is isotopically lighter than that of the summer (Fig.5.10). The temperature coefficient of the  $\delta^{18}\text{O}$  value for continental precipitation is  $\approx 0.7 \text{‰}$  per  $^\circ\text{C}$  or less, that of the  $\delta^2\text{H}$  value is about  $5.6 \text{‰}$  per  $^\circ\text{C}$  or less. In coastal areas, this gradient may be much smaller, e.g.  $0.2 \text{‰}$  per  $^\circ\text{C}$  for  $\delta^{18}\text{O}$  (Gat and Gonfiantini 1981; Volume II).

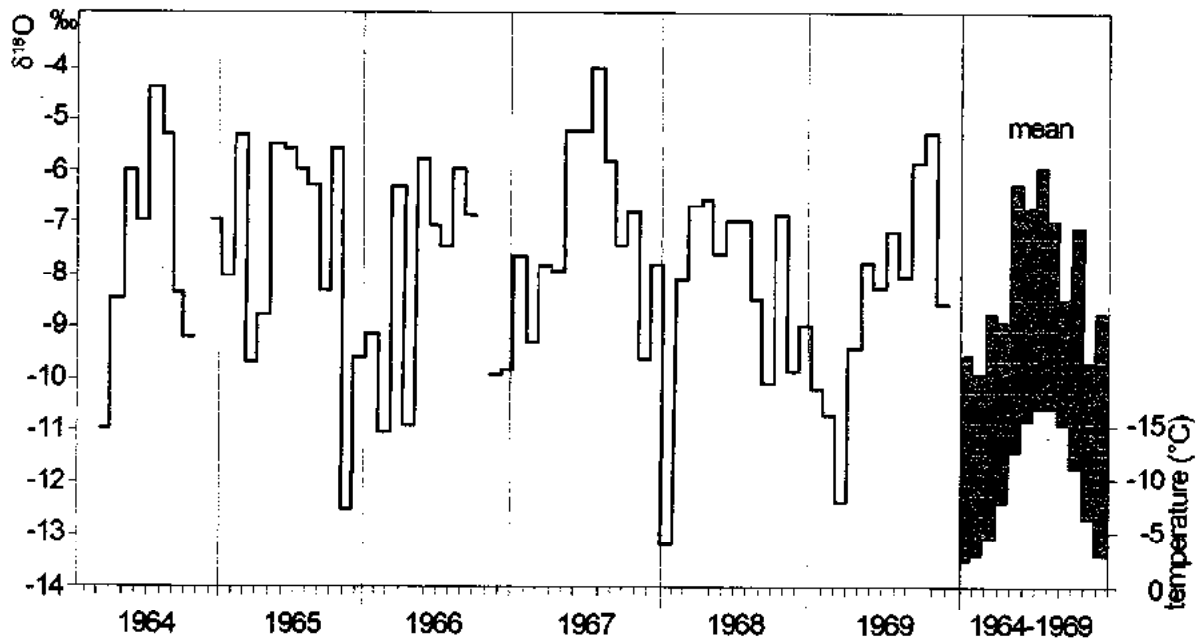


**Fig.5.9** Seasonal variation of the  $\delta^{18}\text{O}$  value in precipitation at Groningen and the correlation of the mean values with the mean monthly temperature (from Mook 1970).

The seasonal isotopic trend in precipitation may be approximated by a sine curve, which can be observed in very young groundwater, albeit that the response is damped and phase-shifted. This effect allows to estimate the mean residence time of shallow groundwater and of karst water up to about 5 years according to the exponential model (Stichler and Herrmann 1983):

$$\bar{t} = \frac{1}{2\pi} \sqrt{\frac{A_{\text{in}}^2}{A_{\text{out}}^2} - 1}$$

where  $A_{\text{in}}$  and  $A_{\text{out}}$  are the amplitudes of the sinusal  $\delta^{18}\text{O}$  trend of the precipitation and the discharged water (water from a shallow well, spring), respectively. The phase shift of both curves is maximum 3 months (Fig.5.10).

In tropical regions, a strong correlation exists between low  $\delta^{18}\text{O}$  and intensity of the rainfall (*amount effect*), resulting in a seasonal variation of the  $\delta^{18}\text{O}$  values of the shallow groundwater.

The local and temporal variability of the isotopic compositions of hydrogen and oxygen in precipitation (temperature effect, altitude effect) may be used to study even more complicated hydrologic systems. This has been done to separate *hydrograph* of *surface streams* and *run-off* into individual hydrological components of infiltrated groundwater (Mook et al. 1974; Fritz et al 1976). Behrens et al. (1979) separated even four different components: base flow = groundwater, snow meltwater, ice meltwater and longer retained glacier meltwater).

The temperature dependence of the isotopic composition for precipitation is preserved in fossil groundwater of Pleistocene and Holocene age (Fig.5.11), recharged under different climatic conditions. During the glacial period the precipitation was isotopically lighter because of a lower temperature of about 5°C (Stute and Deak 1989). In Europe the  $\delta^{18}\text{O}$  values for groundwater of these two periods differ by 1.5 to 2.0‰ (Bath et al. 1979). This can be used as a first glance dating tool.

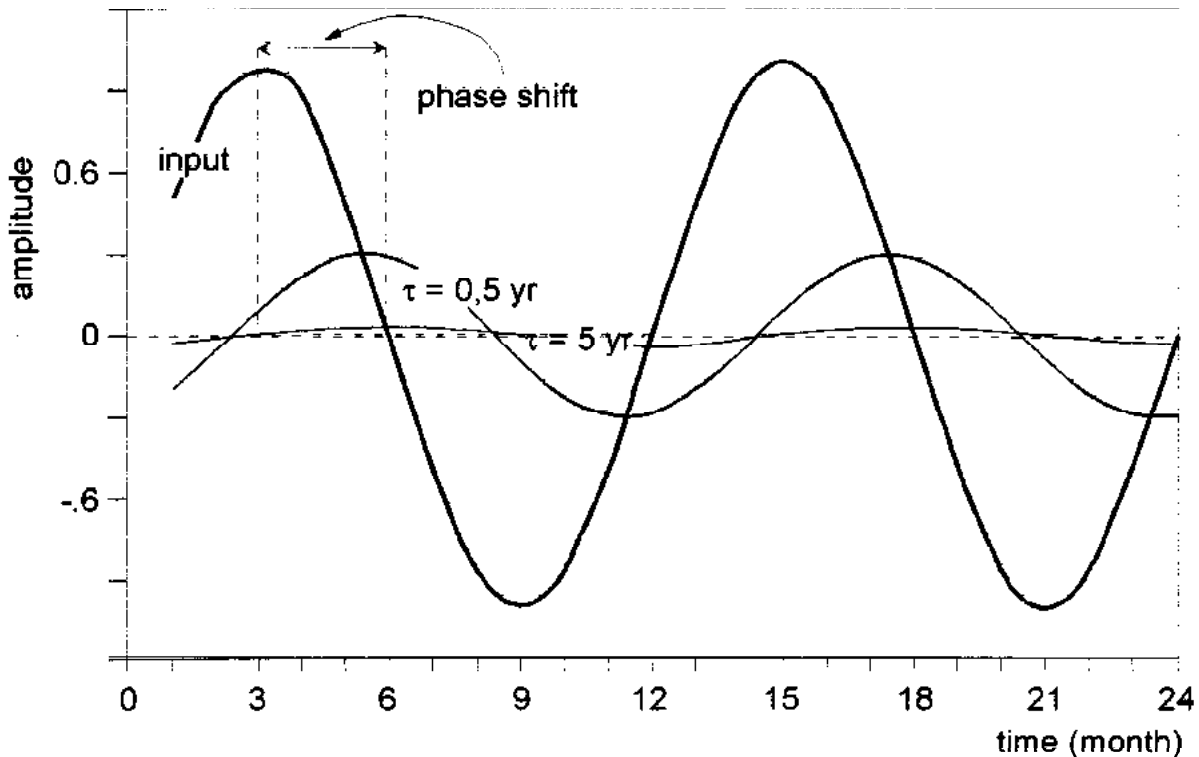


**Fig.5.10** Interrelationship between the amplitude of the seasonal change of the  $\delta^{18}\text{O}$  values of both groundwater and precipitation as input and the mean residence time (MRT) according to the exponential model. The phase shift rises up to three months with the MRT.

**Altitude effect:** As temperature usually decreases with increasing altitude, the delta values will correspondingly drop. Gradients in  $\delta^{18}\text{O}$  of -0.15 to -0.40 ‰/100 m are observed (Gat and Gonfiantini 1981; Fig.5.12), while according to Eq.2.1 the gradients for  $\delta^2\text{H}$  are about 8 times larger. With the aid of the altitude effect recharge areas of spring water can be localised. The elevation of the recharge areas for springs has been estimated from the orographic  $\delta^{18}\text{O}$  gradient. It is important to note that the hydrogeologically estimated altitude of the catchment is compared with the  $\delta^{18}\text{O}$  value of the corresponding spring water rather than the altitude of the spring-discharge site. An estimate of the altitude effect in a certain region may be misleading if  $\delta^{18}\text{O}$  values are used of precipitation and spring water from sites located far from each other. The continental effect may truncate the altitude information (e.g. Kattan 1996a).

**Continental effect:** On their track across a continent clouds produce rain; the heavier molecules preferentially enter the condensed phase. The  $\delta^{18}\text{O}$  and  $\delta^2\text{H}$  correspondingly decrease towards the interior. Complex isotopic patterns are established (Sonntag et al. 1980b), that reflect the morphology of the landscape and the pathways of cyclones. Present-day precipitation and palaeowater are isotopically different (Fig.5.13), insofar as the climatic situation has changed (Stute and Deak 1989).

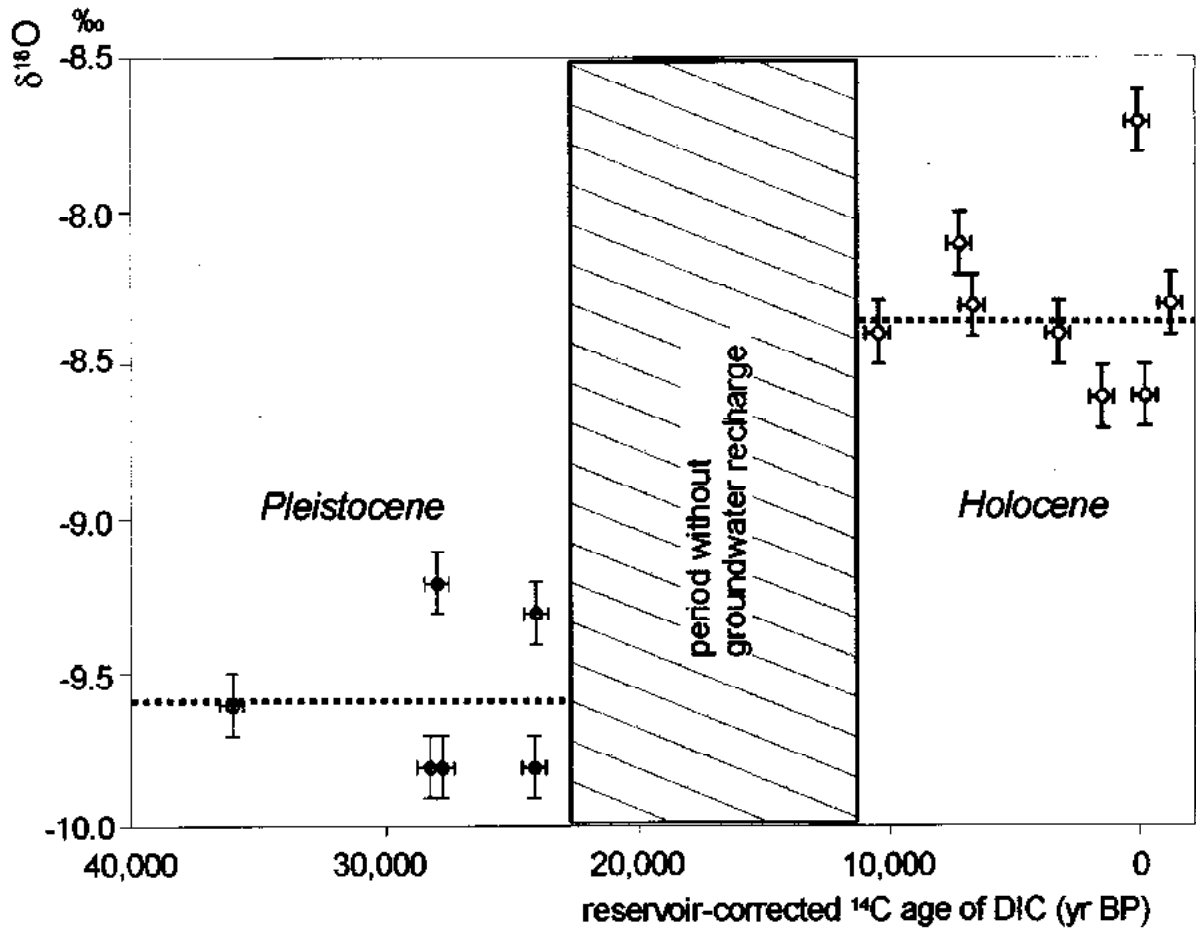


**Fig.5.11** Deviating of  $\delta^{18}\text{O}$  values of Pleistocene and Holocene groundwaters in southern England (after Bath et al. 1979).

By the continental effect, diffuse direct recharge of groundwater is distinguished from groundwater recharged in restricted recharge areas. In the Sahara Desert (diffuse recharge is reflected), while groundwater recharge in the Great Artesian Basin of Australia is restricted to the mountain range in the east (Calf and Habermehl 1984).

**Meteorological studies:** Stable isotope analysis of precipitation and humidity has provided information on their spatial and temporal distribution, their origin, and the trajectories of water vapour in the troposphere (Hübner et al. 1979). Such information has also been obtained for the past (Rozanski 1985; Volume II).

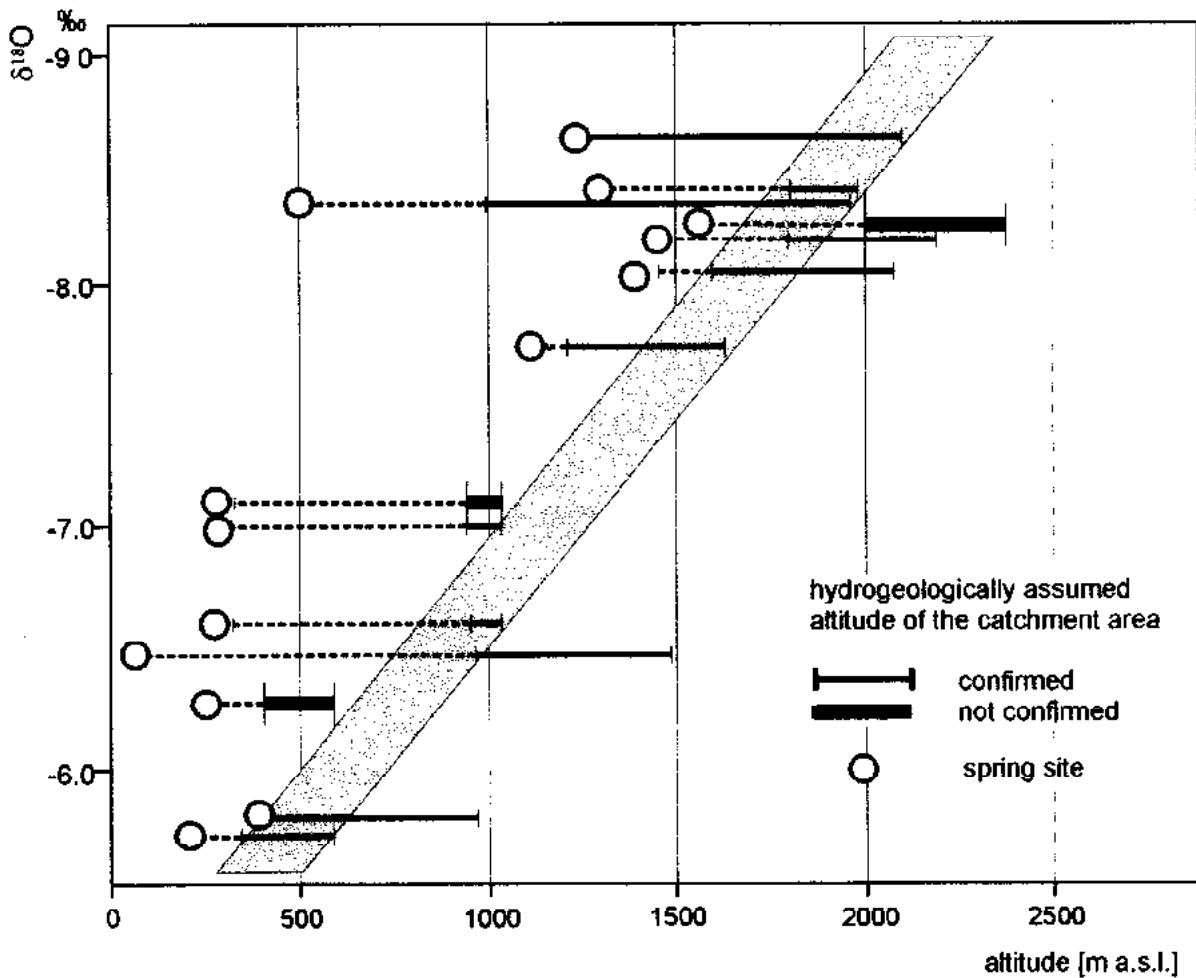


**Fig.5.12** Altitude effect in the Antilebanon Mountains, Syria. The altitude of the discharge sites is lower than that of the corresponding recharge area. In several cases the geologically assumed recharge area had to be revised.

**Mixing studies:** Groundwater is usually a mixture of two or more genetically and chemically distinct groundwater components, often of different age. Isotopic combined with hydrochemical analyses (preferentially with conservative tracers as chloride or the bromide/chloride ratio) allow to distinguish between different kinds of groundwater and often to set up a mixing balance (Fig.2.3). Two- or three-component models are applied for obtaining rough estimates. In the case of time series more complex models can be applied (Zuber 1986; Maloszewski and Zuber 1993, 1996, 1998).

During *pumping tests* occasionally the question arises whether or not groundwater bodies, separated by a horizontal aquitard, are connected via "windows", in other words, whether leakage plays a role. This question can be answered if the groundwaters in the aquifers have different  $\delta^{18}\text{O}$  values and are hydrochemically distinct (Bertleff et al. 1985).

The *admixture of surface water (dam, lake) to the groundwater* (Volume III) was studied on river alluvions in Cyprus. The isotope signal was provided by isotopically enriched water be-

hind a dam released once a year. The movement of this signal (Fig.5.14) was used to determine the tracer velocity in this valley and the extension of the artificial discharge (Plöthner and Geyh 1991).

*Leakage* from a *water pipeline* into a local urban aquifer was traced by means of the oxygen and hydrogen isotopic compositions (Butler and Verhagen 1997).

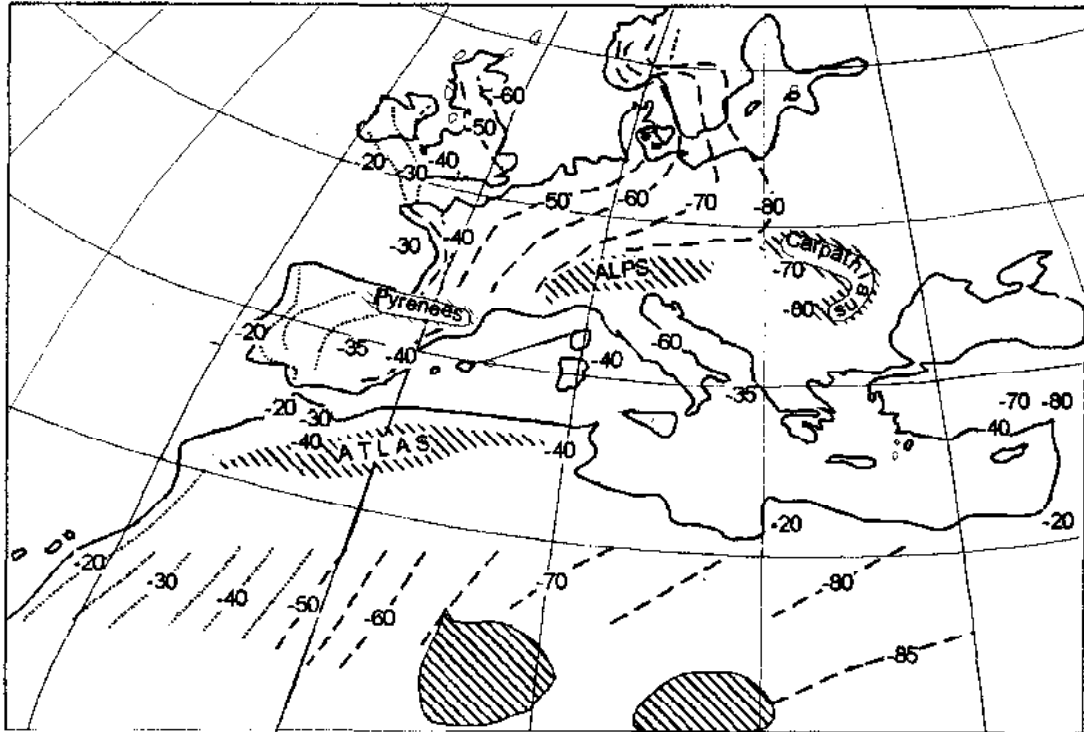


**Fig.5.13** Isolines of equal  $\delta^2\text{H}$  values of Holocene groundwater in Europe and those of Pleistocene groundwater in North Africa. The isotope pattern reflects direct recharge of groundwater by local rain storms approaching from the Atlantic Ocean (after Sonntag et al. 1980b).

The *source* of *salination* of brackish to highly mineralised groundwater and thermal water can be definitely detected by a  $\delta^{18}\text{O}/\text{Cl}^-$  plot. Processes as dissolution and leaching of salt, enrichment by evaporation or mixing of fresh water with saline water or seawater can be clearly and quantitatively distinguished (Fig.5.15).

#### 5.2.1.2 CARBON ( $^{13}\text{C}/^{12}\text{C}$ )

##### Physical fundamentals

The stable isotopes of carbon,  $^{13}\text{C}$  and  $^{12}\text{C}$ , have an average ratio of about 1 : 100. The actual number plays an important role in quantifying the water-rock interaction for  $^{14}\text{C}$  age correction (Sect.4.4.1; Volume I). Moreover, it allows to identify the sources of  $\text{CO}_2$  involved in the carbonate- $\text{CO}_2$  system.

Low-Temperature Systems

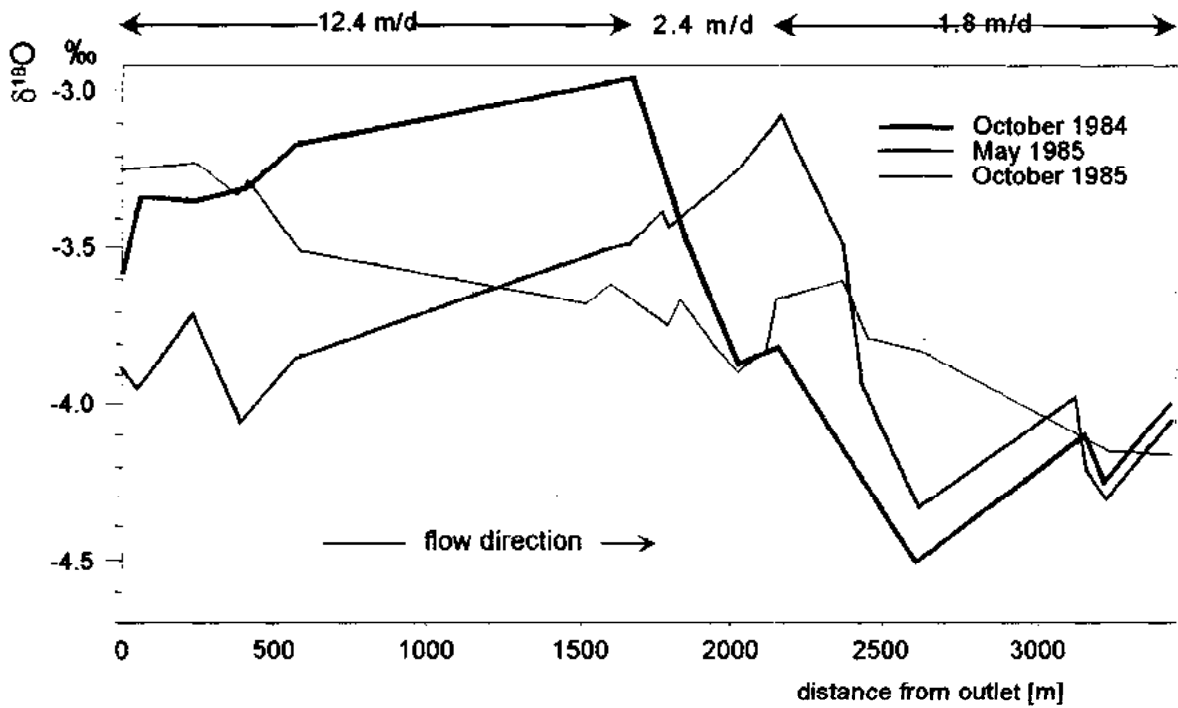


Fig.5.14 Groundwater movement from an superficial reservoir in a valley of Cyprus (after Plöthner and Geyh 1991) and estimation of the tracer velocity by tracing the  $\delta^{18}O$  shift of evaporated dam water.

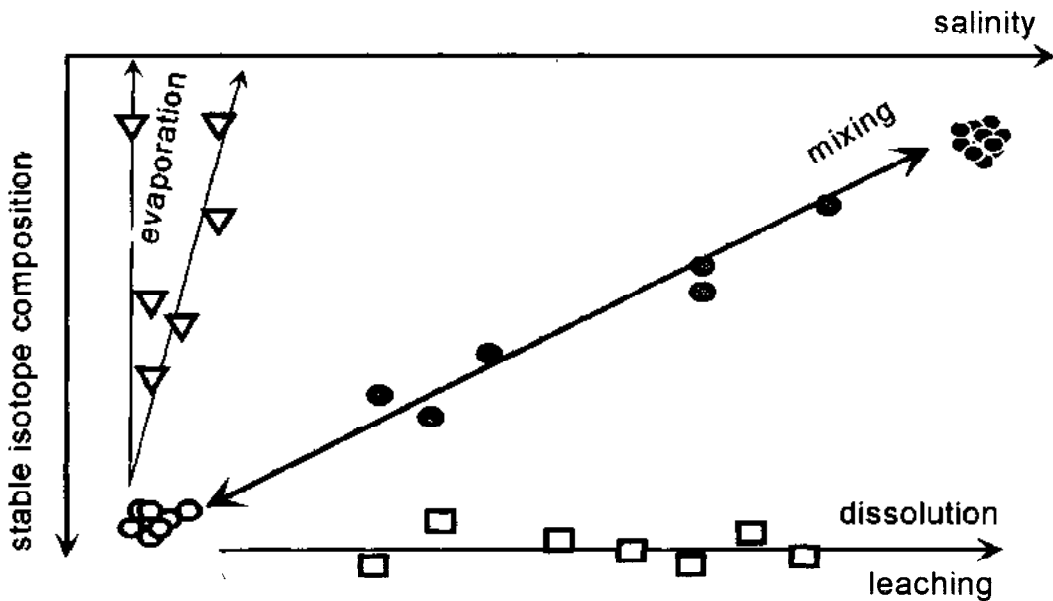


Fig.5.15 Stable isotope composition vs. salinity for the identification of different salination processes: mixing (gray circles) of fresh (open circles) and mineralised water (black circles), dissolution of salt and leaching (open squares), and evaporation (open triangles).

CO<sub>2</sub> assimilation causes considerable carbon isotope fractionation. Isotope fractionation processes are also relevant for studying the carbonic acid and calcite system in water. The  $\delta^{13}C$



values of CO<sub>2</sub> originating from C<sub>3</sub> and C<sub>4</sub> vegetation differs by 12‰.

### Occurrence

The isotopic composition of carbon in the dissolved carbon constituents of groundwater is very variable. The sources of carbon dissolved in groundwater are soil CO<sub>2</sub>, CO<sub>2</sub> of geogenic origin or from magmatic CO<sub>2</sub> (from deep crustal or mantle sources) or in fluid inclusions, living and dead organic matter in soils and rocks, methane, and carbonate minerals. Each of these sources has a different carbon isotopic composition and contributes to total dissolved carbon in various proportions. Therefore, the isotopic composition of dissolved inorganic carbon compounds in groundwater has a wide range of δ<sup>13</sup>C values. Soil carbon dioxide usually has a value of about -22‰, in tropical soils it may be more positive to about -11‰. Carbon dioxide of an endogenous or magmatic origin has δ<sup>13</sup>C values of about -6‰, metamorphic carbon from sedimentary rocks is usually close to zero if it is derived from marine carbonates. The organic carbon of terrestrial plants has δ<sup>13</sup>C values between -30 and -20‰. The heaviest carbon isotopic composition is found in evaporate carbonates with +10‰. Such carbonates occur in sedimentary basins where the δ<sup>13</sup>C values of DIC of fresh groundwater might have elevated δ<sup>13</sup>C values (Volume I).

### Applications

Measurement of the abundance ratio of the stable carbon isotopes, <sup>13</sup>C/<sup>12</sup>C is indispensable for <sup>14</sup>C dating of groundwater (Vogel and Ehhalt 1963). The δ<sup>13</sup>C values reflect chemical interaction with the aquifer rock. This has to be taken into account when interpreting <sup>14</sup>C values (Sect. 5.2.2.3; Volume I). A prerequisite is that the reactions are restricted to CO<sub>2</sub> from the top soil and the lime in the unsaturated zone. Open and closed systems have to be distinguished (Fontes 1992).

Numerous hydrochemical models have been developed in order to determine the initial <sup>14</sup>C value C<sub>init</sub> (Eq. 2. 2) based on the δ<sup>13</sup>C value of DIC needed to calibrate the <sup>14</sup>C time scale for groundwater (Mook 1980). The NETPATH model (Plummer et al. 1994) includes the whole chemistry of the groundwater and delivers the most reliable absolute water ages (e.g. Phillips et al. 1989; Geyh 1992). Its application is, however, limited as only results of water samples from the same flow path can be used. Whatever model is used the correction of the <sup>14</sup>C water ages by the δ<sup>13</sup>C values of DIC introduces large uncertainties (Sect. 5.2.2.3).

Although theoretically not appropriate the most often used correction procedure of the <sup>14</sup>C value using the δ<sup>13</sup>C value has been introduced by Gonfiantini (Salem et al. 1980):

$$A_{\text{init}} \approx \frac{(\delta^{13}\text{C}_{\text{DIC}} - \delta^{13}\text{C}_{\text{lime}})}{\delta^{13}\text{C}_{\text{CO}_2} - \delta^{13}\text{C}_{\text{lime}} + \epsilon_{\text{CO}_2\text{-lime}}} \times 100 \text{ pMC} \quad (5.5)$$

It takes into account the mixture of soil CO<sub>2</sub> and soil lime and the isotopic difference between CO<sub>2</sub> and CaCO<sub>3</sub>. Closed system conditions are assumed.

Geyh and Michel (1982) applied the  $\delta^{13}\text{C}$  values of DIC from groundwater to distinguish between groundwater recharged in a sandstone aquifer from that of a limestone aquifer (Fig.5.16). The  $\delta^{13}\text{C}$  value of the groundwater in the sandstone aquifer is commonly more negative.

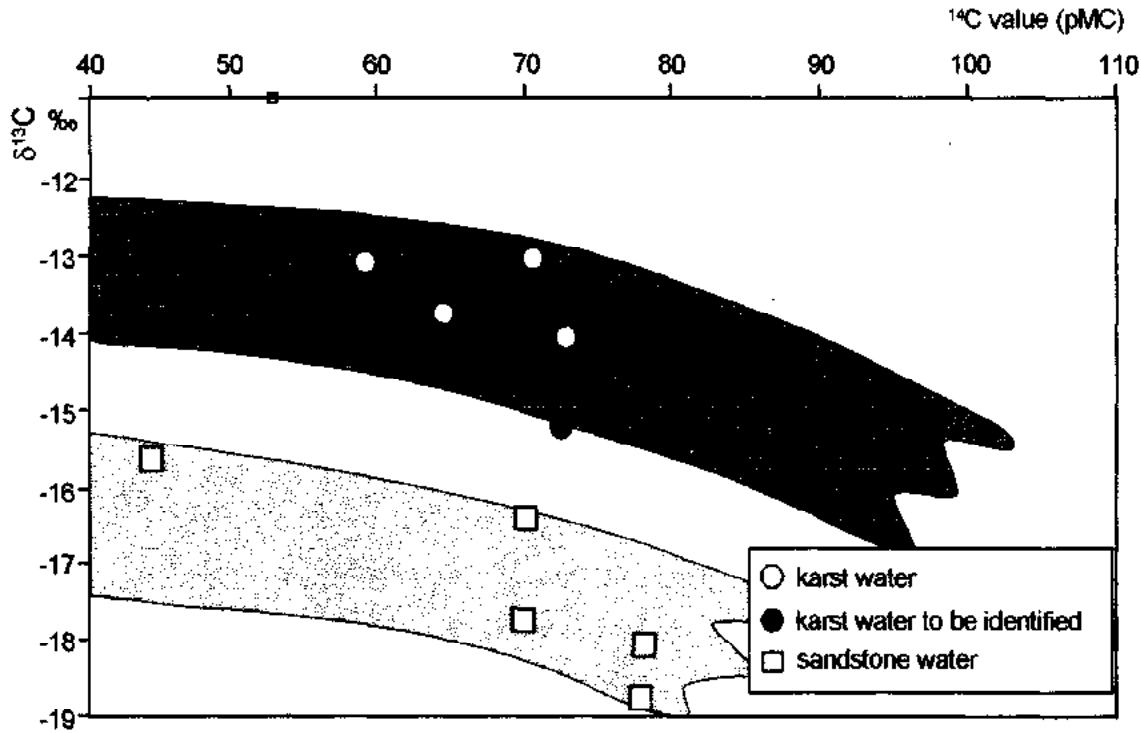


**Fig.5.16** Distinction of groundwater pumped from a sandstone and a limestone aquifer in Höxter, Germany, by the corresponding  $\delta^{13}\text{C}$  and  $^{14}\text{C}$  values of DIC (after Geyh and Michel 1982) and identification of the used groundwater as karst water.

### 5.2.1.3 NITROGEN ( $^{15}\text{N}/^{14}\text{N}$ )

#### Physical fundamentals

In nature there are two stable nitrogen isotopes:  $^{14}\text{N}$  ( $\approx 99.6\%$ ) and  $^{15}\text{N}$  ( $\approx 0.36\%$ ).  $\delta^{15}\text{N}$  values are referred to air nitrogen as standard (Eq.2.1).

#### Occurrence

The nitrogen and oxygen isotopic compositions of the three most important nitrogen compounds are summarised in Table 5.1. Nitrogen in groundwater may be from atmospheric origin and from wet and dry pollution ( $\text{N}_2$  and  $\text{NO}_x$  pollution), from mineral fertilisers, and from living and dead organic matter (animal waste and domestic sewage). Water-rock interaction is usually not involved in the biogeochemical cycle of nitrogen.

#### Processes

Important microbial processes are nitrification, denitrification, biological fixation and mineralisation of organic nitrogen. Because of the complexity of the biogeochemical nitrogen cycle,

a quantitative interpretation of  $\delta^{15}\text{N}(\text{NO}_3)$ ,  $\delta^{18}\text{O}(\text{NO}_3)$  and  $\delta^{15}\text{N}(\text{NH}_4)$  is rarely possible. It is always difficult to relate the isotopic composition of nitrate in groundwater to atmospheric and agricultural inputs without considering nitrification and denitrification processes as well as mixing of nitrates and ammonium from soil and atmospheric sources. Fig.5.17 shows that the nitrogen isotopic composition of the nitrate dissolved in groundwater frequently is similar to that of soil nitrogen rather than with that of fertilisers ( $\delta^{15}\text{N}(\text{NO}_3) < 2.5\text{‰}$ ) or of animal and domestic wastes. Nitrate from fertilisers is consumed by soil biota and isotopically enriched in  $^{15}\text{N}$  ( $\delta^{15}\text{N}(\text{NO}_3) > +5\text{‰}$ ). On the other hand, nitrate resulting from *nitrification* of animal and domestic wastes is isotopically heavier ( $\delta^{15}\text{N}(\text{NO}_3) > +9\text{‰}$ ).

There are three fundamental processes which control the isotopic composition of nitrogen compounds: isotopic equilibrium fractionation, kinetic fractionation and mixing.

Isotopic equilibrium fractionation controls dissolution of ammonium. Reversible reaction  $\text{NH}_3(\text{gas}) + \text{H}^+ = \text{NH}_4^+$  has a isotopic fractionation factor  $\epsilon(\text{NH}_4 - \text{NH}_3)$  of 25 and 35‰ (Mariotti 1984) while the irreversible dissolution of ammonia in water has a negative isotopic fractionation factor (Freyer 1978).

Kinetic isotope fractionation is not important in fixation of organic nitrogen. Bacterial denitrification ( $\text{NO}_3^-$  to  $\text{N}_2$ ) fractionates isotopes substantially ( $\epsilon(\text{N}_2 - \text{NO}_3) \approx -25$  to  $-35\text{‰}$ ; Heaton 1986) and can be described by the Rayleigh distillation equation for an open system. The residual nitrate has a larger  $\delta^{15}\text{N}(\text{NO}_3)$  value than the initial component. Soil mineralization of organic nitrogen to nitrate ions proceeds in steps via ammonium and nitrite ions. The overall isotopic fractionation factor  $\epsilon(\text{NO}_3 - \text{N}_{\text{org}})$  of this complex reaction is between 0 and  $-35\text{‰}$ , depending on which of the reaction steps is rate controlling (Heaton 1984, 1986).

Mixing of groundwater with different sources of nitrate can be detected by the  $\delta^{15}\text{N}(\text{NO}_3)$  versus  $\delta^{18}\text{O}(\text{NO}_3)$  plot manifested in straight mixing line between the two end-members. A hyperbolic function is obtained in the plot of  $\delta^{15}\text{N}(\text{NO}_3)$  versus the concentration of  $\text{NO}_3$  (Mariotti 1984). The hypothetical relationships are shown in Fig.5.18 (Heaton 1986). There is no simple trend other than complex mixing of various sources and microbial denitrification.

The isotope fractionation of nitrogen in soil ammonium is controlled by nitrification, dilution with atmospheric ammonium and adsorption-desorption processes in the soil-water system (Fig.5.19, Buzek et al. 1998). Exchangeable ammonium ions in soil are nitrified during which  $\delta^{15}\text{N}(\text{NH}_4^+)$  increases (fractionation factor  $\epsilon(\text{NO}_3^- - \text{NH}_4^+) \approx -10$  to  $-24\text{‰}$ ).

The residual ammonium is isotopically diluted by lighter atmospheric ammonium ( $\delta^{15}\text{N}(\text{NH}_4^+)$  between  $-12$  and  $3\text{‰}$ ). Since the concentration of adsorbed soil ammonium is low after denitrification, the  $\delta^{15}\text{N}(\text{NH}_4^+)$  in the residual ammonium drops to negative values due to the admixture of isotopically lighter atmospheric nitrogen.

**Table 5.1** Isotope abundances of nitrogen compounds depending on their origin.  $\delta^{15}\text{N}$  values as AIR standard,  $\delta^{18}\text{O}$  values as SMOW standard. Sources:  $\text{O}_2$ :  $\delta^{18}\text{O} = +23.5\text{‰}$ ,  $\text{H}_2\text{O}$ :  $\delta^{18}\text{O} = -10.5\text{‰}$ ,  $\text{N}_2$ :  $\delta^{15}\text{N} = 0\text{‰}$ .

Molecule	Origin	$\delta^{15}\text{N}$ expected	$\delta^{15}\text{N}$ measured	$\delta^{18}\text{O}$ expected	$\delta^{18}\text{O}$ measured
$\text{N}_2$	Air	0‰	0‰		
	Denitrification	-3 to +15‰ <sup>c</sup>	-5 to +2‰		
	$\text{NO}_x$ emission	-5 to +5‰			
bound N	organic soil matter		+4 to +9‰		
	particulate matter in rivers		0 to +3‰		
$\text{NO}_3^-$	tech. synth. fertiliser	0‰	-5 to +7‰	+18 ± 2‰ <sup>a</sup>	+17 to 23‰
	nitrification	<-10 -	-30 to +10‰	1‰ <sup>b</sup>	-1.5‰
	rainwater	+10‰	-12 to +2‰	>+23.5‰	+50 to 60‰
	surface water	0‰	-4 to +15‰		
	groundwater		+1 to +15‰		
animal waste and sewage		-4 to +5‰			
$\text{N}_2\text{O}$	denitrification/nitrification	>0‰		>>0‰	+36 to +5‰
		>0‰		0 to +2‰	+22‰
$\text{NH}_4$	rain		-15 to 0‰		
	fertiliser		-4 to +5‰		

<sup>a</sup>) Calculated on the base of:  $\text{N}_2 + 2.5 \times \text{O}_2 + \text{H}_2\text{O} \rightarrow 2 \text{HNO}_3^-$ ; <sup>b</sup>) Basing on  $\text{H}_2\text{O}$  as the main oxygen source; <sup>c</sup>) Assuming a shift of 18‰ relative to the original  $\text{NO}_3^-$ .

### Application

Combined isotope analyses of nitrogen and oxygen in  $\text{NO}_3^-$  leaves fingerprints on natural and anthropogenic sources of nitrate, on the microbial denitrification, nitrification and biological fixation processes and the nitrogen budget in the groundwater (Volume I, Heaton 1986; Böttcher et al. 1990; Aravena et al. 1996). Therefore, the  $\delta^{15}\text{N}$  values of the dissolved nitrates, ammonium and organic nitrogen in soil water are well distinguished from one region to another one (Fig.5.19).

The isotopic composition of nitrates which percolate to groundwater is the result of complex processes. Therefore, it is difficult to relate the isotopic composition of the various nitrogen compounds in groundwater to atmospheric and agricultural inputs without considering the isotope fractionation caused by nitrification and denitrification processes as well as mixing of nitrates and ammonium from soil and atmospheric sources.

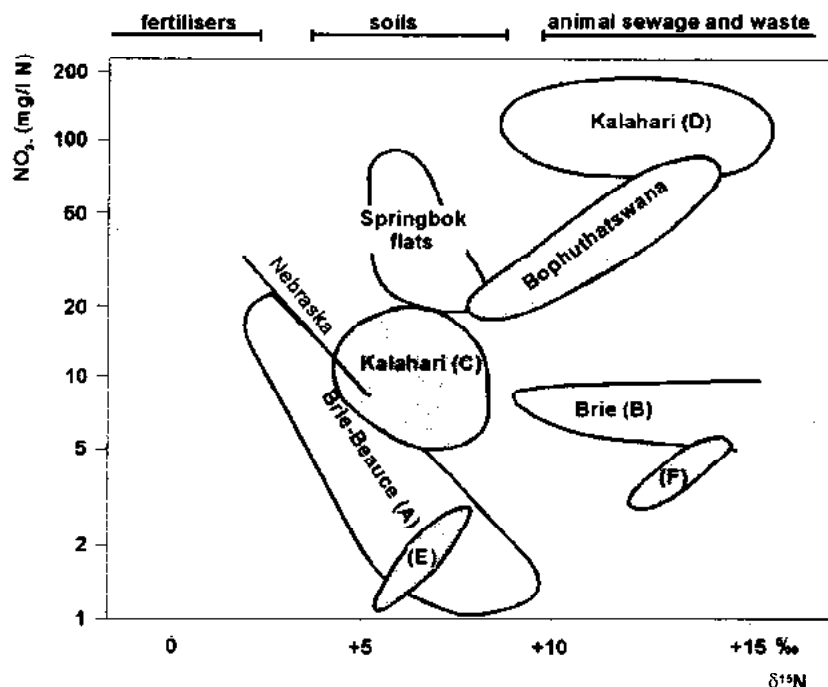


**Fig.5.17** Differentiation of various sources of nitrate by its  $\delta^{15}\text{N}(\text{NO}_3^-)$  value and its concentration in groundwater (after Heaton 1986).

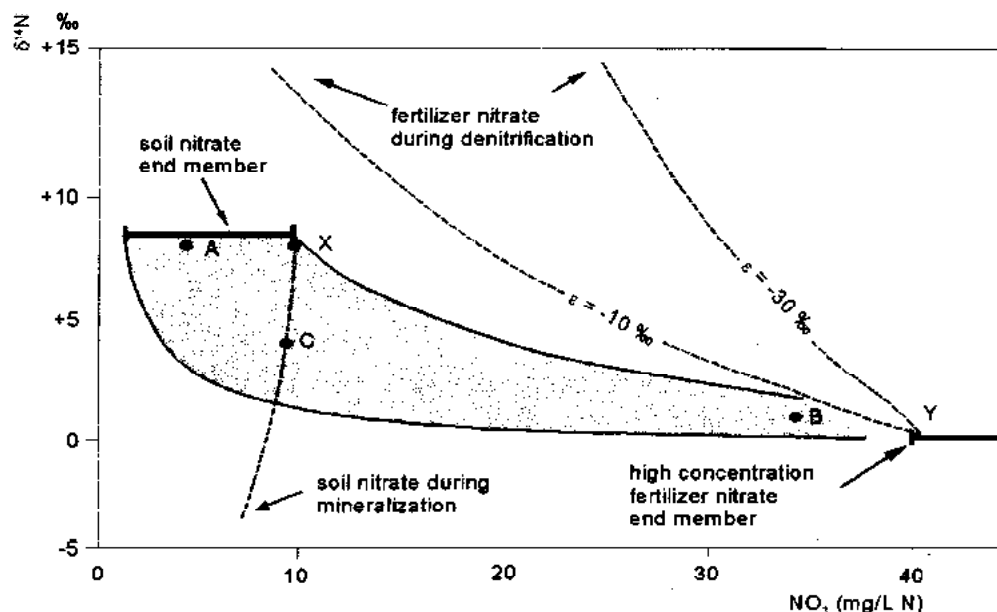


**Fig.5.18** Hypothetical relationship between the  $\delta^{15}\text{N}$  value and the concentration of dissolved nitrate derived from soil and fertilisers (after Mariotti 1984). Solid bars (X and Y) represent soil and fertiliser mixing end members. The grey area shows the effect of mixing. The broken lines were calculated and stand for the fractionation during denitrification of fertiliser nitrate ( $\epsilon(\text{N}_2 - \text{NO}_3^-) = -30$  and  $-10$ ‰ with the initial point Y) and due to mineralization of soil organic nitrogen (line X - C using  $\epsilon(\text{NO}_3^- - \text{N}_{\text{org}}) = -30$ ‰). A, B, C are hypothetical isotopic compositions of nitrate resulting from mixing and/or nitrogen mineralisation (after Heaton 1986).

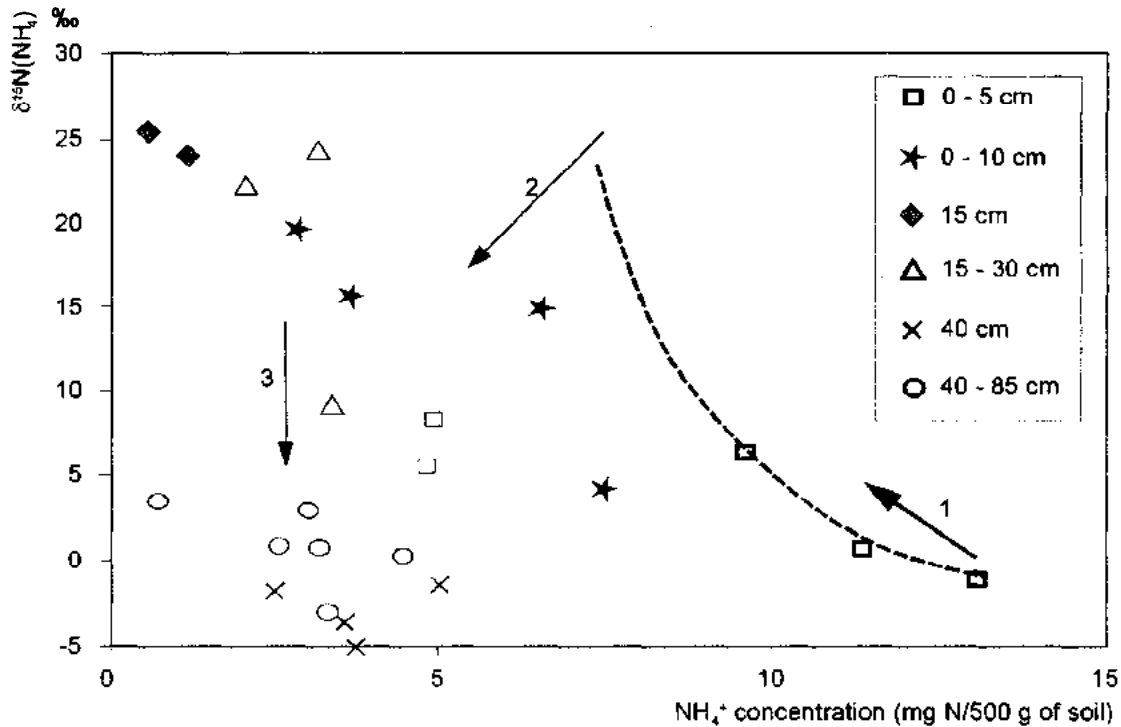


**Fig.5.19** Change of the isotopic composition of ammonium ions in subsurface water as a result of mixing and denitrification during the downwards passage (1 – 2 – 3) in a forest soil (after Buzek et al. 1998).

#### 5.2.1.4 SULPHUR ( $^{34}\text{S}/^{32}\text{S}$ )

##### Physical fundamentals

Sulphur has four stable isotopes:  $^{32}\text{S}$  (95.02 %),  $^{33}\text{S}$  (0.75 %),  $^{34}\text{S}$  (4.21 %), and  $^{36}\text{S}$  (0.02 %). The abundance ratio of  $^{34}\text{S}$  and  $^{32}\text{S}$  is generally given as a  $\delta^{34}\text{S}$  value, defined analogously to Eq 2.1. Iron sulphide from the troilite phase of the Diablo Canyon iron meteorite (DCT) (with a  $^{32}\text{S}/^{34}\text{S}$  ratio of 22.220) is conventionally used as standard (Volume I).

##### Occurrence

There are three main reservoirs of sulphur: evaporite sulphate (with  $\delta^{34}\text{S}$  values of +10 to +30‰, mean +17‰), dissolved sulphate in ocean water ( $\delta^{34}\text{S}$  value of +21‰), balanced by the largest of the three, the sedimentary sulphides (roughly -12‰). In recent and fossil volcanic systems the sources of sulphur are magmatic volatiles. Organic sulphur plays usually a minor role in common groundwater. The isotopic composition of most important sources of sulphur is illustrated in Fig 5.20 (Fritz et al. 1994).

During the course of the Earth's history, the  $\delta^{34}\text{S}$  value of the world's oceans, and consequently, of marine evaporite sulphate has varied between +10 ‰ (Permian) and +35‰ (Cambrian) (Fig.5.21). Sulphur and carbon isotope fractionation ( $\delta^{34}\text{S}$  and  $\delta^{13}\text{C}$  values) appears to correlate inversely with one another in the long term.

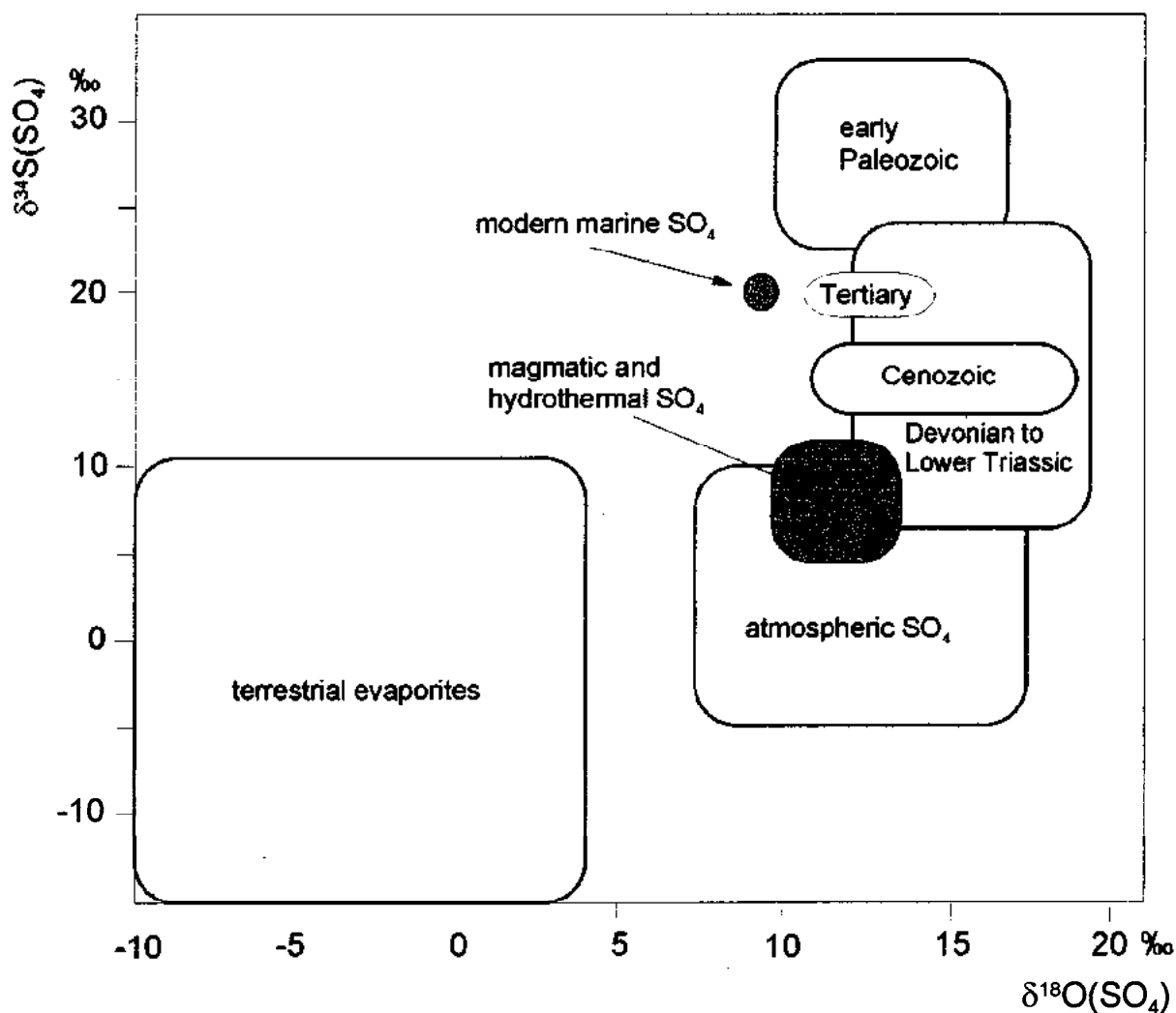


**Fig.5.20** Ranges of  $\delta^{34}\text{S}$  and  $\delta^{18}\text{O}$  values of sulphates of various origin dissolved in groundwater (after Clark and Fritz 1997).

Groundwater contains *dissolved sulphate* ions in concentrations from few mg/L in shallow subsurface waters to tenths of a g/L in fossil brines. These sulphur sources can be divided in atmospheric contribution, mineral or rock contribution, marine and playa lake sources, volcanic sources and biological contributions. Atmospheric contribution includes atmospheric wet precipitation ( $\text{H}_2\text{SO}_4$ ), atmospheric dry deposition ( $\text{SO}_2$ ) and sea-spray aerosols. Mineral contribution contains recent and fossil evaporite sulphates (gypsum and anhydrite), barite in veins and fracture fillings in rocks, pyrite and other sulphidic minerals. Their isotopic compositions expressed in  $\delta^{34}\text{S}_{\text{CDT}}(\text{SO}_4)$  and  $\delta^{18}\text{O}_{\text{SMOW}}(\text{SO}_4)$  are important characteristics when *origin of water* and sulphates are discussed.

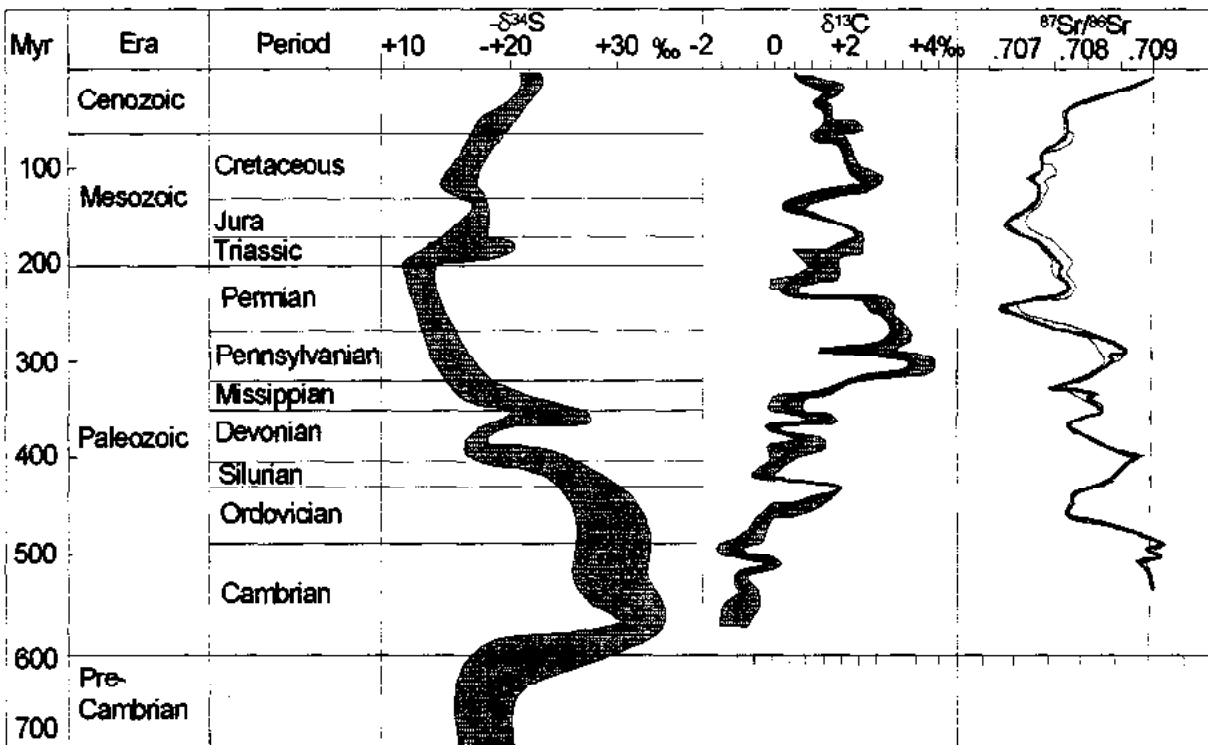


Fig.5.21 Composite  $\delta^{34}\text{S}$  curve for sulphate of marine evaporites (after Claypool et al. 1980) and corresponding  $\delta^{13}\text{C}$  values, as well as  $^{87}\text{Sr}/^{86}\text{Sr}$  values from carbonate and apatite in marine sediments (after Holser et al. 1986).

The isotopic composition of the sulphate of atmospheric origin is determined today either by sea-water spray near cost lines or by the composition of sulphur in burned fossil fuels.  $\delta^{34}\text{S}$  in oil, natural gas and coal is mostly between  $-5$  and  $+10\text{‰}$  while marine sulphur has uniform  $\delta^{34}\text{S}$  of  $+21\text{‰}$ . Isotopic composition of oxygen in *atmospheric sulphate* is a result of mixing of molecular oxygen in atmosphere ( $\delta^{18}\text{O} = +23.5\text{‰}$ ), oxygen in water molecules ( $\delta^{18}\text{O}$  is negative and oriented to the meteoric water line) and *marine sulphate* ( $\delta^{18}\text{O} \approx +9.5\text{‰}$ ). A complex oxidation of  $\text{SO}_2(\text{g})$  to  $\text{SO}_4^{2-}$  may be accompanied by a low oxygen isotopic fractionation. In accordance with the tree sources,  $\delta^{18}\text{O}(\text{SO}_4)$  in atmospheric sulphates usually varies from slightly negative values to  $+10\text{‰}$  (see also Volume I).

### Processes

Stable isotope ratios of sulphate are strongly affected by isotopic fractionation caused by microbial activity as well as water-rock interactions (Chapter 4).

During complex geochemical and biochemical transformations of sulphate, fractionation processes affect the stable isotopic compositions of sulphur ( $^{34}\text{S}/^{32}\text{S}$ ) and oxygen ( $^{18}\text{O}/^{16}\text{O}$ ). These processes are: *sulphur reduction* and oxidation, *crystallisation* of sulphate minerals and *adsorption* of sulphate ions in sediments. The relatively low temperature of groundwater prevents most of the isotopic fractionation processes to reach isotopic equilibrium and signifi-



cant isotopic exchange of oxygen between  $\text{SO}_4^{2-}$  and  $\text{H}_2\text{O}$ .

The trends in the isotopic shift due to the fractionation are illustrated in Fig.5.22 (Krause 1987).

Sulphate and  $\text{H}_2\text{S}$  formed through *oxidation of sulphides* or bacterial reduction, respectively, are isotopically significantly lighter at about +10 ‰. The most effective isotopic fractionation is caused by microbial *reduction of dissolved sulphate to sulphide*. The fractionation factor  $\epsilon(\text{SO}_4/\text{H}_2\text{S})$  is about +30‰. After major bacterial decomposition to  $\text{H}_2\text{S}$ , the residual sulphate remaining has  $\delta^{34}\text{S}$  values is often far above +20‰.

*Terrestrial sulphate* as well as sulphate in atmospheric precipitation have  $\delta^{34}\text{S}(\text{SO}_4) < +10\text{‰}$  and  $\delta^{18}\text{O}(\text{SO}_4) < +4\text{‰}$ . Microbial reduction of sulphate enriches both the residual sulphur and oxygen with their heavier isotopes. The shift due to the microbial reduction has a slope of

$$2 < \frac{\delta^{34}\text{S}(\text{SO}_4)_{\text{residual}} - \delta^{34}\text{S}(\text{SO}_4)_{\text{initial}}}{\delta^{18}\text{O}(\text{SO}_4)_{\text{residual}} - \delta^{18}\text{O}(\text{SO}_4)_{\text{initial}}} < 4$$

in the plot of  $\delta^{34}\text{S}(\text{SO}_4)$  vs.  $\delta^{18}\text{O}(\text{SO}_4)$  (IAEA 1987). Newly formed sulphide has  $\delta^{34}\text{S}(\text{SO}_4) < 7\text{‰}$ . Oxidation of sulphide yields sulphate with  $\delta^{18}\text{O}$  larger than that of the oxygen in water molecules by +4 to +20‰. (Taylor et al. 1984). This reflects the mixing of isotopically light oxygen in water molecules ( $\delta^{18}\text{O} < 0\text{‰}$ ) and isotopically heavier atmospheric oxygen ( $\delta^{18}\text{O} \approx +23.5\text{‰}$ ). During biological oxidation of sulphidic minerals  $^{32}\text{S}$  reacts faster and this lowers  $\delta^{34}\text{S}(\text{SO}_4)$  by +2 to +5.5‰ (Toran and Harris 1989).

Crystallisation of gypsum favours heavier isotopes of S and O in the precipitate. In oil field waters the reduction of sulphate by methane and other hydrocarbons will also lead to isotopic fractionation.

Sulphate in groundwater is diluted by precipitation and removed by crystallisation of evaporite sulphate minerals, by microbial reduction to volatile or dissolved hydrogen sulphide, COS, CS<sub>2</sub> or sulphidic amorphous precipitates and minerals. Fine-grained soils and sediment particles adsorb small quantities of sulphate ions, while vegetation takes up sulphur as a indispensable nutrient.

*Mixing* of groundwater with modern seawater, with brines of playa lakes and with fossil formation water, modifies the isotopic composition of sulphate along the lines between the end members of mixing.

The dissolution of evaporite minerals does not change the isotopic signature. However, sulphate reduction may occur and exclude the application of simple mixing models to explain precisely the observed sulphate isotopic composition.

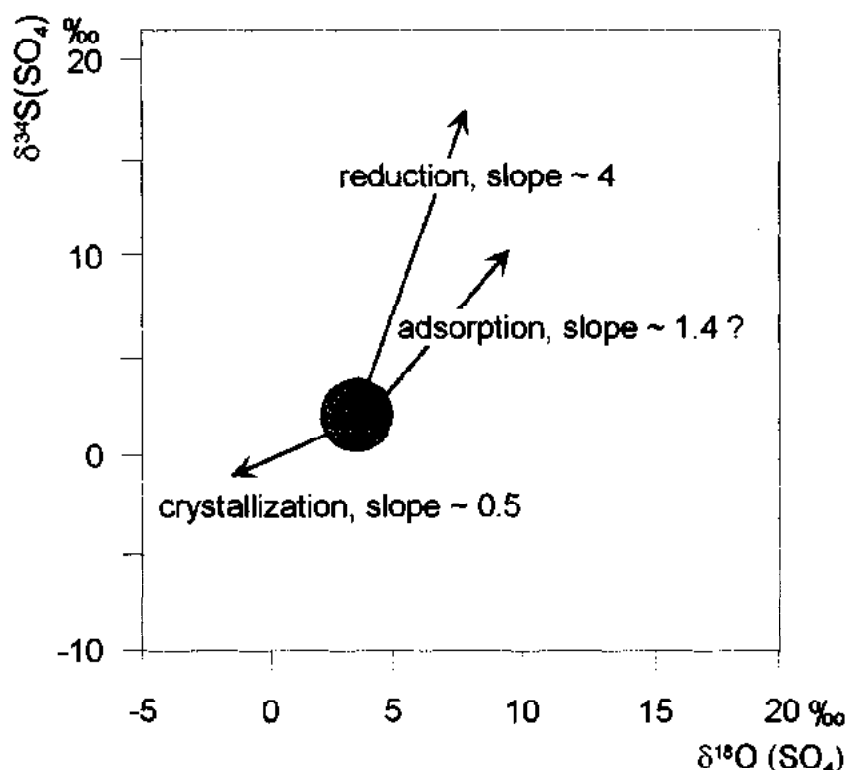


**Fig.5.22** Trends in the isotopic shift of sulphur and oxygen due to the most important fractionation mechanisms occurring in nature (after Krause 1987).

Mixing of recent and fossil sea water or fossil playa-lake brines is difficult to interpret, though the isotopic composition of the recent seawater end-member is well defined ( $\delta^{34}\text{S}(\text{SO}_4) = +21\text{‰}$ ;  $\delta^{18}\text{O}(\text{SO}_4) = +9.5\text{‰}$ ). The isotopic composition of fossil seawater depends upon the complex geological history of the marine sulphate (Fig.5.22).

### Application

The isotopic composition of sulphur and oxygen in sulphates helps to differentiate between marine, evaporitic and volcanic sources of dissolved sulphate (Krouse 1980; Pearson and Rightmire 1980) and to elucidate its fate in the groundwater. The variety of possible sources of dissolved sulphates, complex fractionation mechanisms, non-equilibrium state and uncertainties about the degree of openness of the groundwater systems make, however, the interpretation of isotopic composition of the sulphate and the bound oxygen a difficult task.

### Example:

The isotopic composition of sulphates in groundwater and its evolution is demonstrated by a brief discussion of three groundwater systems.

#### Case study 1: Simple mixing

A simple mixing with negligible fractionation is indicated by groundwater from Zechstein sediments in the Harz mountain in Germany (Schaefer and Usdowski 1992). Four springs (FOR 1 to FOR 4) were sampled and  $\delta^{34}\text{S}(\text{SO}_4)$  measured in the sulphate ions as well as in

gypsum and anhydrite of the associated sedimentary rocks. The evaporites showed a very narrow range of  $\delta^{34}\text{S}(\text{SO}_4)$  values from +9.9 to +12.4‰. Sulphate ions in three of the springs (FOR 1 to FOR 3) have their isotopic compositions within the limits of the minerals (+10.6 to +11.6‰) indicating that the dissolved sulphate originates from the rock. On the other hand,  $\delta^{34}\text{S}(\text{SO}_4)$  in spring FOR 4 is less positive (+8.3‰), indicating a mixing with sulphate from an isotopically lighter source. An obvious choice is the mixing with local rain water and snow melt with  $\delta^{34}\text{S}(\text{SO}_4)$  equal to +4.5‰. Using those values of  $\delta^{34}\text{S}(\text{SO}_4)$ , the mixing proportions of the atmospheric and evaporite components in sulphates of the spring FOR 4 are estimated to be 46 and 54%, respectively.

### Case study 2: Mixing of sulphates of different origin and process interference

The isotopic composition of sulphur of the groundwater from the Permo-carboniferous and crystalline basement of Cretaceous basin in the Bohemian Massif (Central Europe) reflects a complex fate of the sulphate. The relationship between  $\delta^{34}\text{S}(\text{SO}_4)$  and  $\delta^{18}\text{O}(\text{SO}_4)$  is shown in Fig 5.23. Chloride brines with a low and an elevated concentration of sulphate from the basement of the Cretaceous basin were analysed (Smejkal and Jetel 1990). The data points of the brines with high sulphate concentration are located along the line between local rain and gypsum and may be interpreted as dissolution of local evaporites. The water of the brines is of meteoric origin according to the  $\delta^2\text{H}$  and  $\delta^{18}\text{O}$  values.

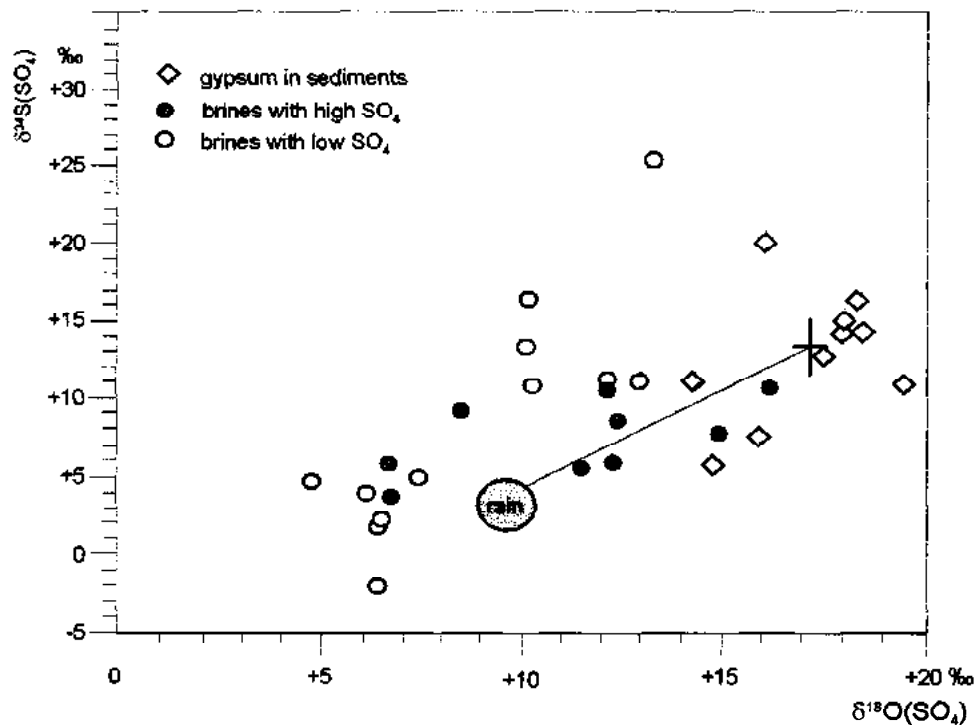


**Fig.5.23** The tie line of the  $\delta^{34}\text{S}(\text{SO}_4)$  and  $\delta^{18}\text{O}(\text{SO}_4)$  values indicates mixing of rainwater with groundwater and brines containing dissolved evaporite sulphate in the Cretaceous Basin of the Bohemian Massif (Central Europe) (after Smejkal and Jetel 1990).

The brines with low sulphate concentration contain isotopically heavier sulphate. A slope of the  $\delta^{34}\text{S}(\text{SO}_4)$  vs.  $\delta^{18}\text{O}(\text{SO}_4)$  diagram of nearly 4 may indicate bacterial reduction and removal of  $^{32}\text{S}$  via  $\text{H}_2\text{S}$ . This interpretation is in contradiction with the increase of the sulphate concentration (Fig.5.24). Therefore, a more complex history of sulphate has to be assumed for the brines with low sulphate concentration. One explanation is dissolution of gypsum and anhydrite present in the Permo-carboniferous sediments. The sulphate of brines which came in contact with organic matter became reduced and its concentration decreased. The isotopic composition shifted to heavier sulphur and sulphate oxygen.

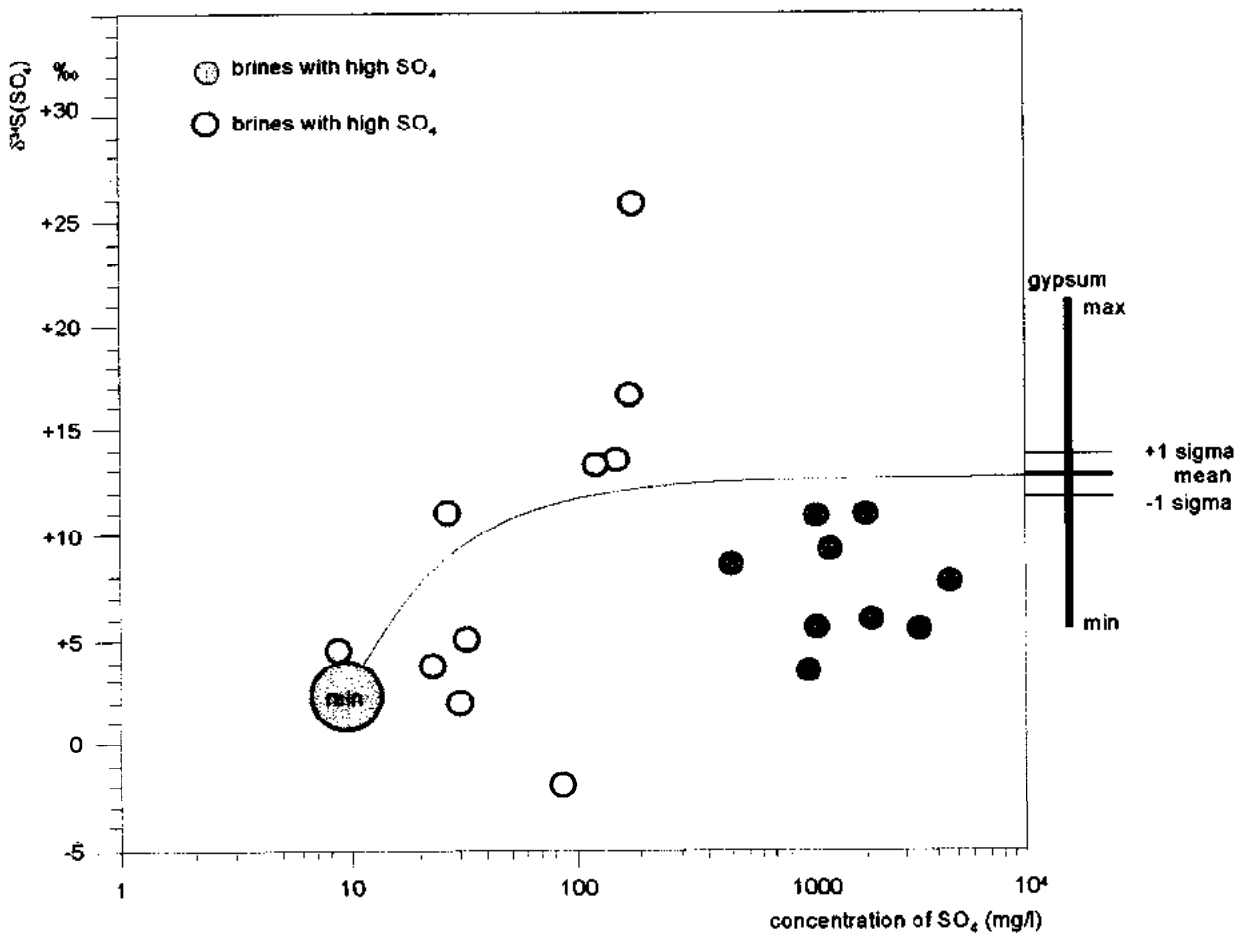


**Fig.5.24** Relationship between  $\delta^{34}\text{S}(\text{SO}_4)$  and the concentration of sulphate ions (log scale) in groundwaters and brines from the basement of the Cretaceous basin in the Bohemian Massif, Central Europe. As the mixing line  $\delta^{34}\text{S}(\text{SO}_4) = \{[c(\text{SO}_4)_{\text{rain}} \times (\delta^{34}\text{S}(\text{SO}_4)_{\text{rain}} - \delta^{34}\text{S}(\text{SO}_4)_{\text{evaporitic}})] / c(\text{SO}_4)\} + \delta^{34}\text{S}(\text{SO}_4)_{\text{evaporitic}}$  does not fit the data, the sulphate must have a more complex fate (data from Smejkal and Jetel 1990).

The isotopic composition of sulphate in the groundwater of the Variscian Bor granodiorite in the Bohemian massif (V. Smejkal, unpublished results) indicates that a fossil brine has remained in fractures of the rock though the sulphate concentration and the isotopic composition might have been modified by microbial reduction. The data points follow a linear trend

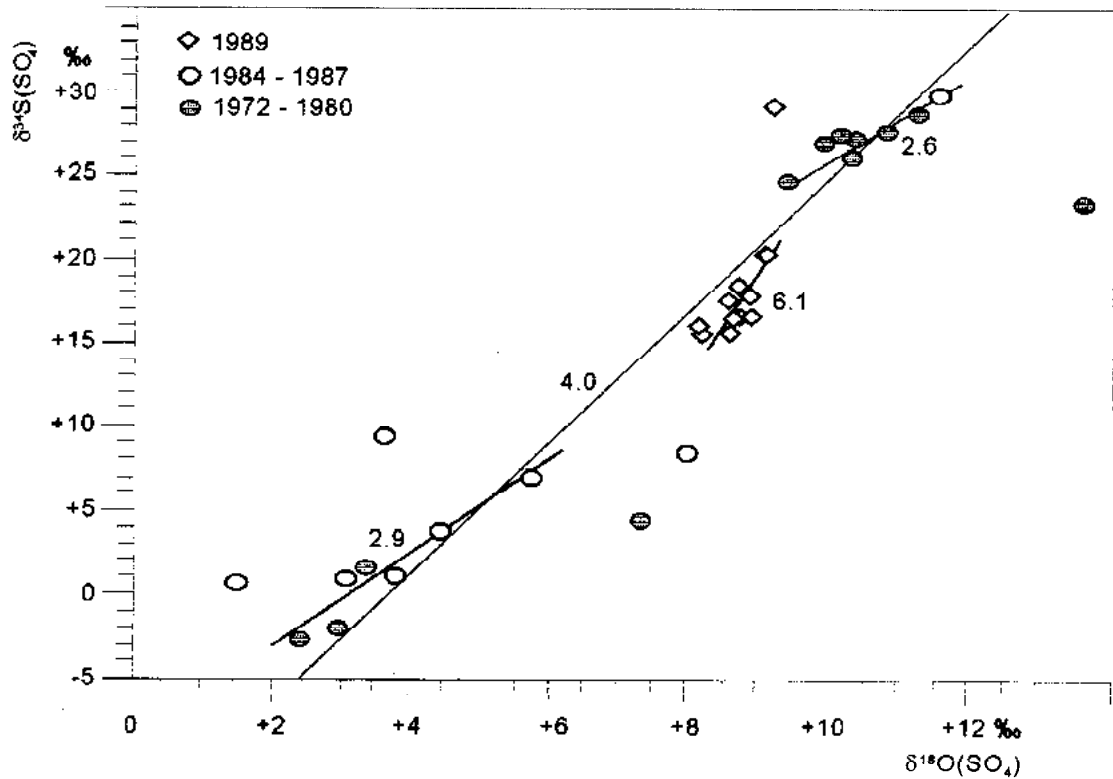


Fig.5.25 Plot of  $\delta^{34}\text{S}(\text{SO}_4)$  vs.  $\delta^{18}\text{O}(\text{SO}_4)$  for groundwaters and brines from the Variscian Bor granodiorite (Bohemian massif) (V. Smejkal, unpublished data).

along lines with a slope between 2.6 and 6.1 which can be explained by a Rayleigh distillation process in a closed system according to (Fig.5.25; Volume I).

$$\frac{R_s(\text{SO}_4)_t}{R_s(\text{SO}_4)_{t=0}} = f_s(\text{SO}_4)^{\alpha-1}$$

with the fractionation factor  $\alpha = R_s(\text{H}_2\text{S})/R_s(\text{SO}_4)$  and that of the residual sulphate  $\varepsilon = 1 - \alpha$  ( $\times 10^3\text{‰}$ ).  $f_s(\text{SO}_4)$  is the residual fraction of dissolved sulphate. Substitution with  $\delta^{34}\text{S}(\text{SO}_4)$  yields

$$\begin{aligned} \delta^{34}\text{S}(\text{SO}_4)_t &= \delta^{34}\text{S}(\text{SO}_4)_{t=0} + (\alpha - 1) \cdot \ln f_s(\text{SO}_4) \\ &= \delta^{34}\text{S}(\text{SO}_4)_{t=0} - \varepsilon \cdot \ln f_s(\text{SO}_4) \end{aligned}$$

Fig.5.26 presents the results of this hydrogeological conception. Two source members were considered: fossil Tertiary sulphate brine of the Bohemian Massif with 800 mg/L  $\text{SO}_4^{2-}$  and  $\delta^{34}\text{S}(\text{SO}_4)_{t=0} = 5.4\text{‰}$  (curve A) and of the Cheb Tertiary basin with a maximum sulphate concentration of 54 g/L and  $\delta^{34}\text{S}(\text{SO}_4)_{t=0} = 5.4\text{‰}$  (curve B). The enrichment factor of 22‰ corresponds relatively well to the observed isotopic composition of sulphur and the sulphate concentration to that of the first end member. The isotopic composition of the second end member cannot be explained by sulphate reduction or any other known fractionation process.

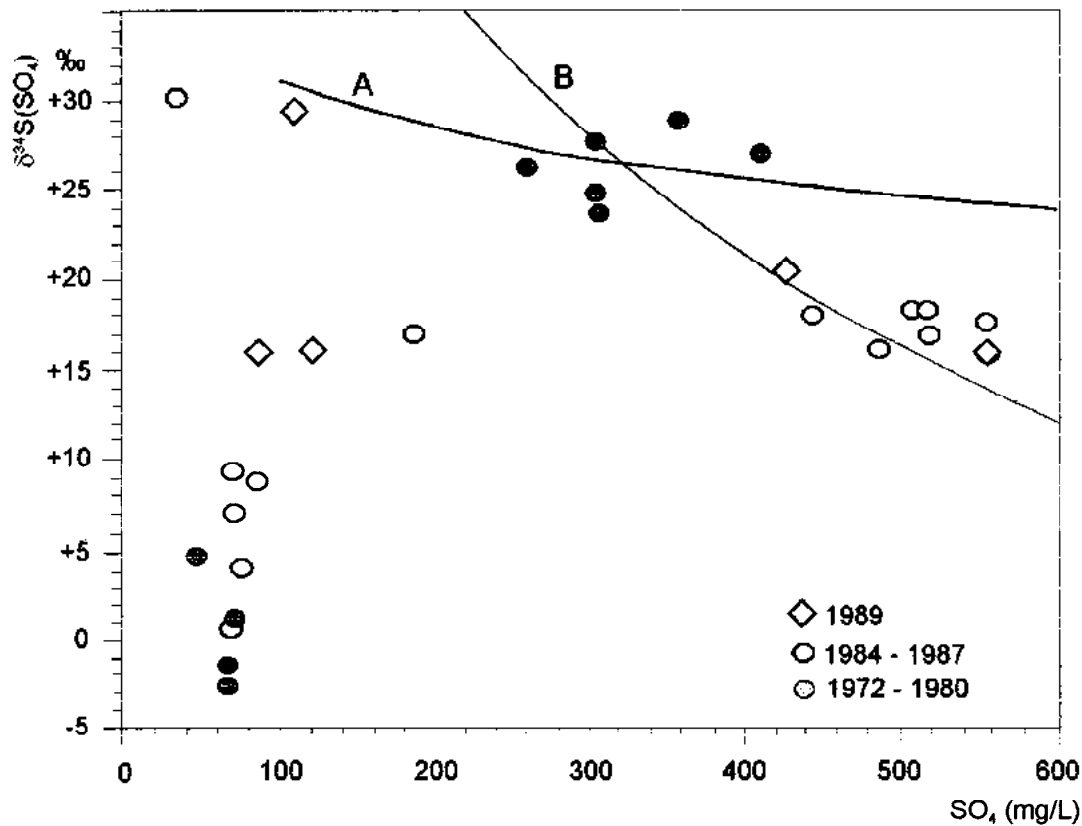


**Fig.5.26** Plot of  $\delta^{34}\text{S}(\text{SO}_4)$  vs.  $c(\text{SO}_4)$  for groundwaters and brines from the Variscian Bor granodiorite (Bohemian massif) (V. Smejkal, unpublished data). Curve A represents isotopic fractionation by sulphate reduction in a fossile brine with 800 mg/L  $\text{SO}_4^{2-}$  and  $\delta^{34}\text{S}(\text{SO}_4) = +5.4\text{‰}$ . Curve B reflects isotopic fractionation after sulphate reduction in a fossile brine from a neighbouring Cheb Tertiary basin, Czech Republic, with 56 g/L  $\text{SO}_4^{2-}$  and a  $\delta^{34}\text{S}(\text{SO}_4) = +5.4\text{‰}$  (after Paces 1987).

### Case study 3: Anthropogenic pollution

The isotopic composition of sulphate can also be an indicator of anthropogenic pollution of groundwater. Sulphate formed during high-temperature oxidation in technological processes contain heavy sulphate oxygen derived from the atmosphere. The sulphate isotopic composition was determined from groundwater collected from an aquifer in the vicinity of a settling pond with ash from power plants at Sulkov, Czech Republic (Smejkal 1990).

Three sources of sulphate were identified (Fig. 5.27):

- 1) high sulphate concentration enriched with heavy oxygen and sulphur isotopes are derived from the ash,

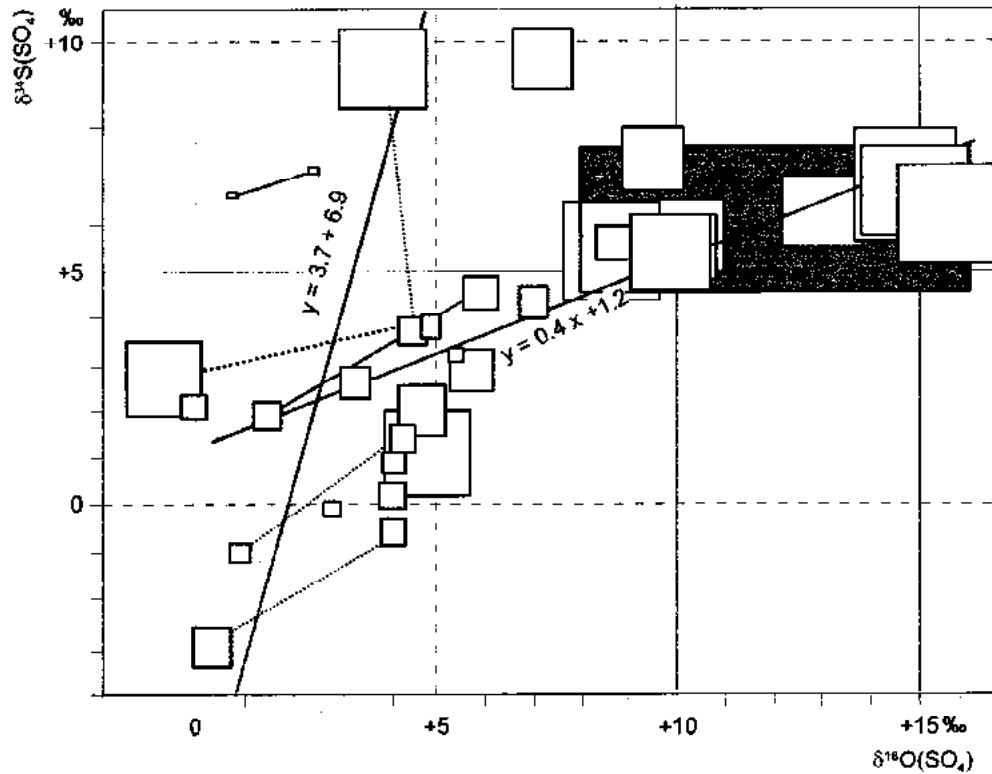


**Fig.5.27** Various mixing lines of the isotopic compositions of sulphur and oxygen of sulphate as indicator of anthropogenic pollutions in groundwater. The area of the squares is proportional to the sulphate concentration in groundwater. The grey area represents samples from an region with ash deposited in the settling ponds of the power plant in Sulkov, Czech Republic. The points of samples from different depth but of the same well or drill hole are connected by broken lines. The regression line  $y = 0.4x + 1.2$  is a mixing line between fresh groundwater and water unpolluted with sulphate from the ash. The slope of the regression line  $y = 3.7x - 6.9$  indicates microbial reduction of sulphate (after Smejkal 1990).

- 2) elevated sulphate concentrations enriched with light oxygen and light sulphur isotopes are derived from oxidised local pyrite,
- 3) sulphate with low concentrations, enriched light sulphur isotopes and  $\delta^{18}\text{O}(\text{SO}_4)$  between +1 and +7‰ belong to groundwater containing atmospheric sulphate. Many of the samples in Fig.5.27 represent mixtures of these three types of groundwater.

In conclusion, sulphur and oxygen isotopic analyses of sulphate dissolved in groundwater may yield information on the origin of water and its constituents. The interpretation requires a careful consideration of the various hydrochemical and biochemical processes, including mixing of two or more water components. Geochemical and hydrogeological data on groundwater may be a welcome supplement.

### 5.2.1.5 CHLORINE ( $^{37}\text{Cl}/^{35}\text{Cl}$ )

#### Physical fundamentals

Chloride has two stable isotopes:  $^{35}\text{Cl}$  ( $\approx 75.7\%$ ) and  $^{37}\text{Cl}$  ( $\approx 24.2\%$ ). They do not participate in biological processes and act as conservative tracer. Data are expressed as  $\delta^{37}\text{Cl}$  with respect to the standard mean oceanic chloride (SMOC). The ratio  $^{37}\text{Cl}/^{35}\text{Cl}$  is measured by isotope ratio mass spectrometry (IRMS). The precision must be better than  $\pm 0.1\%$  (Volume I).

#### Occurrences

$\delta^{37}\text{Cl}$  values contain information on the origin of chloride ions in fresh and polluted groundwater as well as in subsurface brines (Eggenkamp 1994, Frape et al. 1995, 1998; Van Warmerdam et al. 1995). They are not always well distinguished and scatter within a range of  $-1.6$  to  $+2\%$  (Fig.5.28). Therefore, major sources of chlorine cannot easily be distinguished by their isotopic composition (Volume I).

#### Processes

Isotope fractionation of the chloride isotopes occurs in geothermal systems (Chapter 6) under crustal temperatures and pressures (Eastoe and Guilbert 1992). Ion filtration, diffusion, geothermal boiling, brine evaporation and salt deposition appear to be the most important physical processes (Eggenkamp 1994).

#### Applications

##### Example:

The chloride concentration increases from shallow groundwater, to deep groundwater and the brine in the Stripa mine, Sweden (Fig.5.28). Correspondingly the  $\delta^{37}\text{Cl}$  values increase. The occurrence of transient values indicate mixing of deep and shallow groundwater (Frape et al. 1998). The available data do not yet allow a definitive decision about whether or not the chloride isotopic composition has a potential in such groundwater studies.

### 5.2.1.6 BORON ( $^{10}\text{B}/^{11}\text{B}$ )

#### Physical fundamentals

Natural boron has two stable isotopes  $^{11}\text{B}$  ( $\approx 80\%$ ) and  $^{10}\text{B}$  ( $\approx 20\%$ ). The variation in the ratio of these two isotopes is expressed in  $\delta^{11}\text{B}$  (‰) with respect to SRM-951 NBS standard (Ven-gosh et al. 1998).  $\delta^{11}\text{B}$  is determined by thermal ionisation mass spectrometry (TIMS) (see also Volume I).



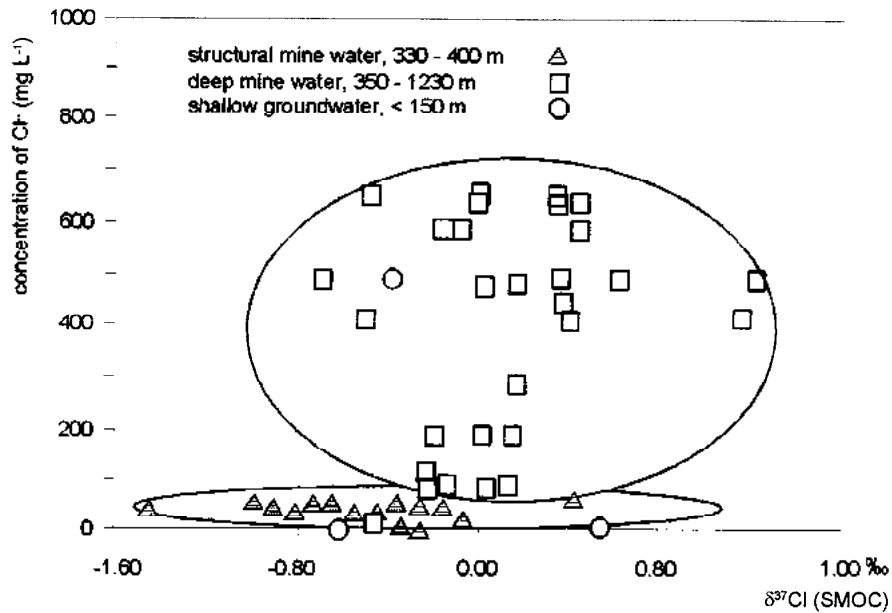


**Fig.5.28** Ranges of chloride concentration and stable isotopic composition of chlorine for fresh and brackish groundwaters and brine from the crystalline rocks of the Stripa mine area, Sweden (after Frapé et al. 1998).

### Occurrence

Boron is a minor constituent of groundwater with a concentration of usually less than 0.1 mg/L, in seawater it is 4.6 mg/L, and in oil-field brines >100 mg/L (White et al. 1963). An increased concentration of boron in groundwater is usually related to enrichment with substances of marine and volcanic origin or they are related to anthropogenic pollution. Sodium perborate is a component of detergents so that boron is present in sewage and in industrial waste (Hem 1985). It is also a constituent of fertilisers (Vengosh et al. 1998).

Natural sources of boron in groundwater are atmospheric deposition, tourmaline, biotite and amphiboles in crystalline rocks, colemanite, kernite and borax in evaporites, illite in marine shales, residual seawater in isolated aquifers and magmatic volatiles in volcanically active and geothermal areas.

There is a wide range of  $\delta^{11}\text{B}$  values in rain from +0.8 to +35‰ (Vengosh et al. 1998). Freshwater  $\delta^{11}\text{B}$  is controlled by the atmospheric deposition, consisting of marine aerosols, volcanic gases, and soil particles. Isotopically heavy boron originates from the sea ( $\approx +39\text{‰}$ ), isotopically light boron from volcanic sources as well as rock forming minerals (+1.5 to +6.5‰). Terrestrial dust supplies small quantity and has a  $\delta^{11}\text{B}$  value between -6.6 and +15.0‰. Brines contain isotopically extreme heavy boron (+25 to +60‰) (Barth 1993). Anthropogenic sources are characterised by isotopically light boron and allow their differentiation (+10 to -15‰; Vengosh et al. 1998).

The isotopic composition of boron in groundwater shows a continental effect. Uncontaminated groundwater from coastal plains of Israel has a  $\delta^{11}\text{B}$  of around +30‰, water in Alpine lakes between +0.9 and +6.2‰ (Jurasko 1994). The lowest  $\delta^{11}\text{B}$  is found in groundwater from Great Artesian Basin in Australia, between -16 to +2‰ (Vengosh et al. 1991).

A generalisation on possible sources of boron in groundwaters is in Fig.5.29. The wide range of  $\delta^{11}\text{B}$  values from -20 to +60‰ and several orders of magnitude differences in the B/Cl ratio indicate that the isotopic composition of boron has a future potential for identification of natural sources as well as of pollution sources in groundwater systems (see also Volume I).

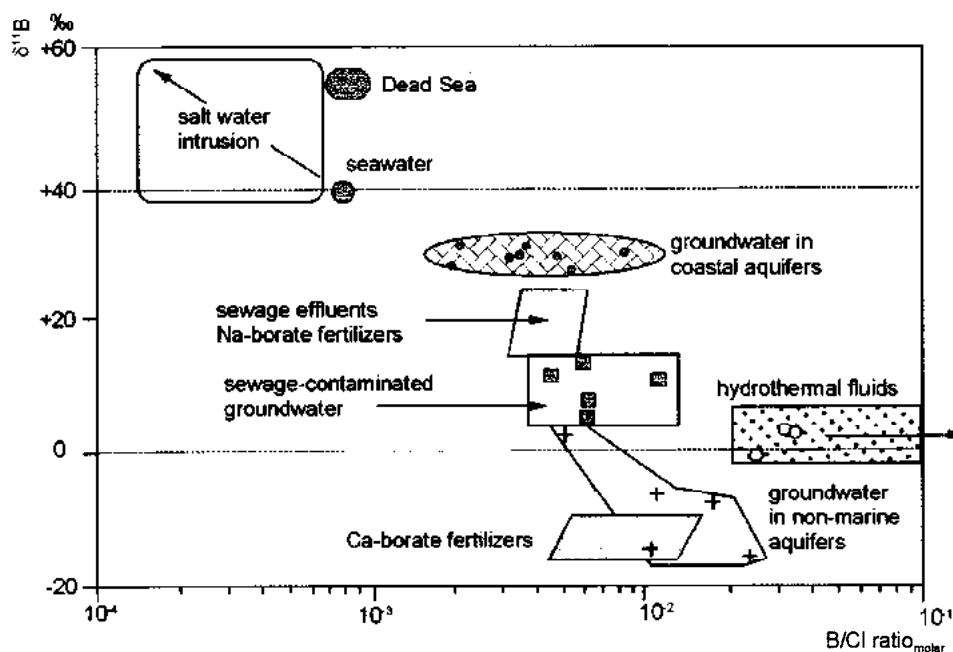


**Fig.5.29** Isotopic composition of boron and B/Cl molar ratio in various sources of boron in groundwater (after Vengosh et al. 1998).

### Processes

The most common dissolved species in groundwater is non-dissociated boric acid ( $\text{H}_3\text{BO}_3$ ). Polyborate ions and molecules are formed in highly saline solutions. The crystallographic orientation of dissolved boron is trigonal, whereas in crystals the structure is governed by a tetragonal co-ordination. The transformation in atomic co-ordination symmetry is accompanied by a large isotopic fractionation with a characteristic enrichment factor  $\epsilon_{\text{tri-tetra}}$  of about -20‰. Heavy isotopes are preferentially partitioned to non-dissociated boric acid in groundwater. Even *adsorption of boron* onto clay minerals may remove  $^{10}\text{B}$  from solution (Vengosh et al. 1994). Boron is removed from soil water by biological uptake.

In spite of the wide range of  $\delta^{11}\text{B}$  in groundwater (from -7 to +60‰, Vengosh et al. 1998), a quantitative interpretation of data is often difficult and uncertain due to *mixing* of various

sources of boron and isotopic fractionation. A suitable graphical interpretation of mixing is with the use of a diagram showing  $\delta^{11}\text{B}$  vs. B or B/Cl (see also Volume I).

### Applications

Boron stable isotope ratios have a potential to play a role in pollution studies (e.g. Davidson and Bassett 1993). They have also applications in the characterisation of brines and geothermal waters (Eggenkamp and Coleman 1998; Chapter 6).

### Case study:

Fig.5.30 shows two mixing lines. One is between fresh groundwater and seawater in the Coastal Plain of Israel. The second line reflects mixing between fresh groundwater and sewage effluent (Vengosh et al. 1998). The high values of  $\delta^{11}\text{B}$  in waters from the saline plumes in Be'er Toviyya and Shiller, Israel, are explained by adsorption of boron and preferential fractionation of the heavier  $^{11}\text{B}$  to solution.

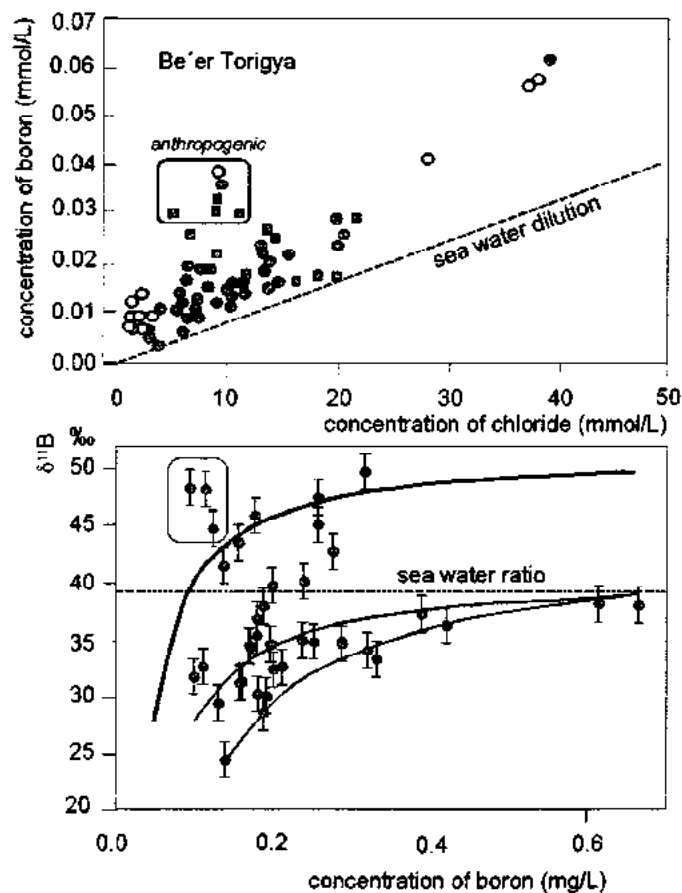


**Fig.5.30** Boron and chloride in brackish waters from saline plumes in the coastal aquifer of Israel. Mixing between boron of terrestrial groundwater and seawater is suggested by the linear mixing line in the plot of boron vs. chloride concentration and by the hyperbolic relation of  $\delta^{11}\text{B}$  vs. boron concentration (after Vengosh et al. 1998).

### 5.2.1.7 STRONTIUM ( $^{87}\text{Sr}/^{86}\text{Sr}$ )

#### Physical fundamentals

The  $^{87}\text{Sr}/^{86}\text{Sr}$  atomic ratios are measured mass spectrometrically (TIMS) and are given as atomic ratios. That of seawater is 0.70906 and as reference (Volume I).

#### Occurrence

Strontium is a minor constituent of groundwater. It readily substitutes calcium ions in calcium, sulphate, feldspar and other rock-forming minerals. Hence it participates in the water-rock interactions (Chapter 4; Volume I).

#### Processes

No natural fractionation of stable strontium isotope was observed during natural processes. This property makes the isotopic ratio of strontium a reliable candidate for tracing strontium of different *origin*, for evaluating *mixing* of ground waters and for studying a state of isotopic equilibrium between groundwater and strontium bearing minerals and rocks. A precise mixing balance can be set up for two aqueous end members with different  $^{87}\text{Sr}/^{86}\text{Sr}$  values. Information on this process and on the extend of water-rock interactions is obtained from comparing the  $^{87}\text{Sr}/^{86}\text{Sr}$  values in the primary minerals of the host rock with those in the groundwater and in the secondary minerals on the surface of fractures, joints and pores. Strontium and calcium have similar geochemical properties. Therefore, the strontium isotopic composition serves to study the weathering of calcium bearing rocks and the biogeochemical recycling of calcium (Volume I).

#### Applications

It is a tracer for the origin of salinity, groundwater movement and water-rock interactions (Chapter 4).

#### Case study 1: Source of Sr in spring water

The  $^{87}\text{Sr}/^{86}\text{Sr}$  ratio of spring water in the Mont-Dore region in Massif-Central, France, depends upon the source rocks and ranges from 0.704408 to 0.714226 (Pauwels et al. 1997). Granitic rocks contain more radiogenic  $^{87}\text{Sr}$  (0.722282 and 0.733804) while basaltic rocks less (0.703844 to 0.704215). Groundwater with low radiogenic strontium apparently dissolved strontium from basaltic rocks being richer in the element than the granitic rocks. The fact that the  $^{87}\text{Sr}/^{86}\text{Sr}$  ratio of the spring water from granitic rock does not approach the characteristic value may be explained as isotopic equilibrium with the rock not having been reached, by the occurrence of mixing or by the possibility that an isotopic equilibrium is related to an unknown soluble rock-forming mineral.

### Case study 2: Weathering studies

In weathering studies (Aberg et al. 1989; Wickman and Jacks 1992) strontium serves as a chemical analogue to calcium. The weathering rate of release of calcium from rocks is calculated from the strontium isotopic mass balance, applying a simple two-component mixing approach according to Eq. 5.5 (Wickman and Jacks 1992). The subscripts  $_{\text{runoff}}$ ,  $_{\text{weath}}$ , and  $_{\text{atm}}$  indicate the strontium isotope ratios of strontium of the input by runoff, weathering, and atmospheric deposition;  $x_{\text{weath}}$  and  $x_{\text{atm}}$  are proportions of weathering and atmospheric deposition inputs. It follows for the rate of weathering  $q_{\text{weath}}$

$$q_{\text{weath}} = \frac{\left(\frac{{}^{87}\text{Sr}}{{}^{86}\text{Sr}}\right)_{\text{runoff}} - \left(\frac{{}^{87}\text{Sr}}{{}^{86}\text{Sr}}\right)_{\text{atm}}}{\left(\frac{{}^{87}\text{Sr}}{{}^{86}\text{Sr}}\right)_{\text{weath}} - \left(\frac{{}^{87}\text{Sr}}{{}^{86}\text{Sr}}\right)_{\text{atm}}} \quad (5.6)$$

It is assumed that strontium weathering rate  $Q_{\text{Sr}}$  ( $\text{kg ha}^{-1} \text{ yr}^{-1}$ ) is proportional to that of calcium so that it can be referred to that of ( $Q_{\text{Ca}}$ ). Then

$$Q_{\text{weath}} = Q_{\text{atm}} \cdot \frac{q_{\text{weath}}}{1 - q_{\text{weath}}}$$

where  $Q_{\text{atm}}$  is the atmospheric deposition rate of calcium in ( $\text{kg ha}^{-1} \text{ yr}^{-1}$ ).

For example, the  ${}^{87}\text{Sr}/{}^{86}\text{Sr}$  ratios of precipitation, river water and soil from the catchment in Svartberget, northern Sweden, are 0.7168, 0.7398, and 0.7402. Then, 98% of the strontium in the runoff is due weathering. As the annual atmospheric deposition rate of Sr amounts to 0.76 ( $\text{kg ha}^{-1} \text{ yr}^{-1}$ ) the corresponding rate for calcium is 38 ( $\text{kg ha}^{-1} \text{ yr}^{-1}$ ).

### Case study 3:

The effects of the interaction between infiltrating meteoric water into soils and plants on the calcium-strontium system was studied by changes of the strontium isotopic composition at a soil profile in forests of the Black Triangle in Czechoslovakia (Bendl 1992). Fig. 5.31 illustrates how the  ${}^{87}\text{Sr}/{}^{86}\text{Sr}$  ratio changes due to atmospheric acid deposition following the increase in the calcium content and the decrease of pH. Continental precipitation contains more radiogenic  ${}^{87}\text{Sr}$  (0.70999) than marine strontium (0.70906). The throughfall (0.71013) under the spruce canopy dissolves a mixture of soil dust (increasing with depth from 0.71379 to 0.740425) and limestone (0.707859). The water infiltrating into the soil has a ratio of 0.71197 and that of the runoff in local small streams ranges from 0.72095 to 0.72160. The gradual increase of the  ${}^{87}\text{Sr}/{}^{86}\text{Sr}$  ratio from the lowest value in atmospheric water to the highest value in the runoff indicates that a strontium isotopic equilibrium cannot be reached during the relatively short residence time of the water in the soil.

Another case study about water-rock interaction at rock fractures in the Stripa mine granite in Sweden is given in Sect. 4.4.4.

## 5.2.2 GROUNDWATER DATING

The *residence time* of groundwater in an aquifer or the *groundwater age* is an important parameter in any palaeohydrologic and geohydraulic study. The chemical and isotopic compositions of groundwater usually represent steady-state conditions which develop after a certain time. Water-rock interactions (Chapter 4) occur during groundwater recharge within days/weeks and during flow in the aquifer within years to even millions of years. Isotope hydrological studies give at least an idea about approximate ages of the various groundwaters.

The radiogenic isotopes of hydrogen ( $^3\text{H}$  – tritium; Sect.5.2.2.1 and 5.2.2.2) and carbon ( $^{14}\text{C}$  radiocarbon; Sect.5.2.2.3) and in special cases krypton ( $^{81}\text{Kr}$ ; Sect.5.2.2.7,  $^{85}\text{Kr}$ ; Sect.5.2.2.8), argon ( $^{39}\text{Ar}$ ; Sect.5.2.2.6) and chlorine ( $^{36}\text{Cl}$ ; Sect.5.2.2.5) with very different half-lives are being used to evaluate relative or absolute groundwater ages (see Volume I).

**Dating by radioactive decay.** The physical process of radioactive decay is the basis of the age determination of groundwater. Radioactive decay of a certain nuclide is completely independent of any environmental parameter such as pressure, temperature, pH or chemical bonds, and only depends upon a characteristic degree of instability, expressed into a half-life. There are, however, physical processes and geochemical reactions which secondarily change the specific activity (= activity per L or per g) (Volume I, Chapters 3 and 5).

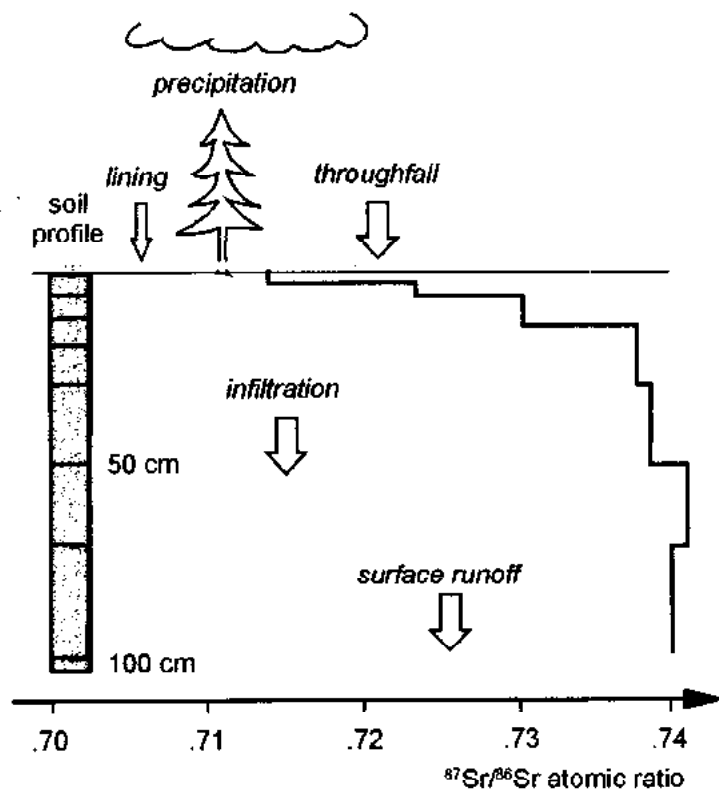


**Fig.5.31** Change of the  $^{87}\text{Sr}/^{86}\text{Sr}$  ratio in a soil profile below a forest damaged by acidic deposition in the Black Triangle of Europe, Czech Republic. The calcium content is increased and the pH decreased. The change reflects the different  $^{87}\text{Sr}/^{86}\text{Sr}$  ratios for continental precipitation (= 0.70999) and marine sources (0.70906) (after Bendl 1992).

### Complications:

**Hydrochemical reactions:** The initial activity  $A_{\text{init}}$  of a radioactive isotope present in the groundwater at the time of recharge may not be 100 % as defined for the atmosphere (e.g.  $^{14}\text{C}$ ,  $^{39}\text{Ar}$ ) (cf. Volume I, Chapter 8: for  $^{14}\text{C}$  defined as the relative activity  $^{14}\text{a}$  in % or pMC). Hydrochemical processes as the dissolution of fossil limestone without  $^{14}\text{C}$  lower the  $^{14}\text{C}$  activity apart from radioactive decay. As a result  $^{14}\text{C}$  ages calculated conventionally with  $A_{\text{init}} = 100\%$  are apparently too large. The actual initial  $^{14}\text{C}$  activity  $A_{\text{init}}$  of the groundwater must be used in Eq. 2.2 (see Volume I).

**Underground production:** Mainly neutrons produced by the decay of uranium and thorium and the daughter products create nuclear reactions with chemical elements of the rock matrix. Radioactive nuclides as  $^{39}\text{Ar}$ ,  $^{36}\text{Cl}$  and other may be formed (Florkowski et al. 1988). If this underground production of environmental isotopes is not taken into account, apparently too small groundwater ages would result.

**Water-Rock interaction** (Chapter 4): Exchange between the dissolved constituents of the groundwater and the rock matrix, congruent and incongruent precipitation and dissolution may have lowered the activity of the isotope used for dating and results in apparently too large ages (Wigley et al. 1978).

**Anthropogenic tracing of the hydrosphere:** The hydrosphere has become polluted with anthropogenic radiocarbon, tritium,  $^{36}\text{Cl}$  and others isotopes by nuclear weapon tests during the 1950s and early 1960s and later by the release of environmental isotopes as  $^{85}\text{Kr}$  by the nuclear energy industry, and the use of isotopes in industrial applications. The occurrence of these "artificial" isotopes in nature can be used to estimate *mean residence times* (Volume VI) or *absolute ages* of groundwater (Sect. 5.2.2.3).

The presuppositions of any age determination is that the dated samples belong to groundwater resources that behave as closed systems. In freshwater systems, this presupposition is seriously prevented by *geohydraulic mixing*. The seepage of surface water into a phreatic aquifer and the leakage between adjacent aquifers results in mixing of different old groundwaters. In such cases the isotope data have to be interpreted by conceptual or lump-parameter models (Chapter 3; Volume VI).

#### 5.2.2.1 TRITIUM

##### Physical fundamentals

The radioactive hydrogen isotope, tritium, has a half-life of 12.43 years. The tritium activity is given in tritium units [TU]. One TU corresponds to one  $^3\text{H}$  atom to  $10^{18}$  hydrogen atoms or 1.185 Bq/L (Volume I).

$^3\text{H}$  acts as a conservative tracer as it is a constituent of the water molecule itself. Only in highly saline groundwater with high uranium, thorium, and lithium contents, underground production via boron results in  $^3\text{H}$  activity levels of up to 0.5 TU (Florkowski et al. 1988). A slight retardation of the  $^3\text{H}$  movement has been observed at clay by anion exclusion (Sect.4.1).

### Occurrence

The natural cosmogenic level of  $^3\text{H}$  in precipitation is a few TU. Since the fifties the level in precipitation rose up to about 2000 TU due to nuclear weapons testing primarily on the Northern Hemisphere until 1963/1964. After the atom bomb moratorium it dropped exponentially to about 10 TU in the northern hemisphere at present (Fig.2.1). On the southern hemisphere the time course of the  $^3\text{H}$  levels was similar though on a lower level and retarded by about 2 years. Seasonal  $^3\text{H}$  fluctuations are less important for groundwater dating. One reason may be that summer rainfall hardly contributes to groundwater recharge.

In order to record this change of  $^3\text{H}$  in precipitation IAEA established a global network of about 125 stations to collect precipitation for isotope analysis. The measured isotopic abundances have regularly been published in the IAEA Technical Reports Series since 1969 (IAEA 1969 – 1994). For more recent data contact <http://www.iaea.org/worldatom>. This data bank provides sufficiently reliable input curves for extrapolation to nearly any site on the globe. Samples which behaved as closed systems during the past century as cold ice, deep groundwater, and deep ocean water may reflect this record.

There is a pronounced continental effect. Lower  $^3\text{H}$  values are found in coastal areas than inland.

On the conditions for sampling and the detection techniques the reader should consult Volume I. The sample size ranges between 2000 and 15 mL. The detection limit is 0.1 TU applying electrolytic enrichment of  $^3\text{H}$ .

### Applications

**Dating** by  $^3\text{H}$  determines the residence time of shallow groundwater and of spring water in fissured and fractured rocks less than about 150 years. The classical  $^3\text{H}$  method (Libby 1953) was based on the environmental cosmogenic  $^3\text{H}$  activity in rain water. It had a very limited applicability due to the drastic increase of the  $^3\text{H}$  level by up to four orders of magnitude, between the early fifties and 1963/64 as a result of nuclear weapons tests (Fig.2.1). This input of  $^3\text{H}$  to the hydrosphere can, however, be used to estimate mean residence times applying lumped-parameter models (exponential model, dispersion model, linear model; Sect.3.1.2; Volume VI). In most cases the  $^3\text{H}$  activity of shallow groundwater and spring water is interpreted by the exponential model (Sect.3.1.2; Fig.3.5; Volume VI). It is assumed that spring water consists of water of different aged components whose proportions decrease exponentially with increasing age. The MRT may be between years and decades, implying short turnover times of the groundwater. Time-series of data provide the most precise and reliable re-



sults and allow to test whether or not a used model was able to describe the system (Zuber 1986; Malozewski 1994). An alternative is applying the analysis of several isotopes as  $^{85}\text{Kr}$  (Sect.5.2.2.8) (Grabczak et al. 1982; Zuber 1986). Appropriate models for routine evaluation of  $^3\text{H}$  data are commercially available (e.g. MULTIS; Richter et al. 1993). Single  $^3\text{H}$  values mostly yield ambiguous mean residence times, to be discarded because of geohydraulic reflections.

Other applications of  $^3\text{H}$  is studying lake dynamics, and the estimation of groundwater *recharge rates* in humid, arid and semi-arid regions. In regions with low precipitation samples from dug wells offer a unique possibility to estimate upper limits of the groundwater recharge. If the water table has a thickness  $d$  the measured  $^3\text{H}$  value of the water and the recharge rate  $q_{\text{rec}}$  is given by

$$q_{\text{rec}} = \frac{{}^3\text{H}_{\text{spl}} \cdot d \cdot n_{\text{tot}}}{\sum_{1955}^{\text{now}} {}^3\text{H}_{\text{in}}(t) \cdot e^{-\lambda(\text{now}-t)}}$$

The  *$^3\text{H}$ -interface method* is an example of estimating groundwater recharge areas that are heavily urbanised and have a high density of wells (Fig.5.32; Andres and Egger 1985; Deak et al. 1995, Bertleff et al. 1993).

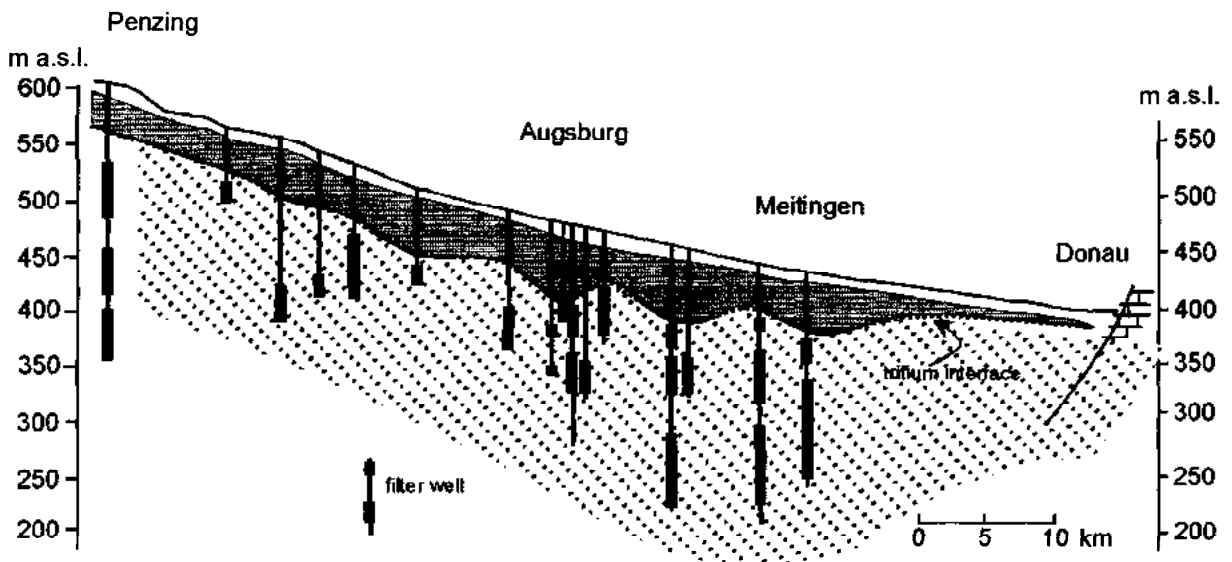


Fig.5.32 Application of the  $^3\text{H}$  interface method to estimate the groundwater recharge in heavily populated areas in southern Germany (after Egger and Andres 1985).

*Geohydraulic* information on the mixture of groundwater from different sources and of different age – an old  $^3\text{H}$ -free groundwater with a young groundwater containing  $^3\text{H}$  – is a routine application. It is related to the current hydrological problem of estimating the pollution potential of groundwater resources pumped for the drinking water supply. It has been found

that elevated nitrate concentrations make  $^3\text{H}$  analyses useless because of the much lower mean life of nitrate.

### Case studies

The shape of the input function of  $^3\text{H}$  since 1963/1964 as shown in Fig 2.1 is preserved in the fast moving groundwater in the alluvial deposits of the Danube River, Hungary, for over 30 years. The flow is radially away from the river over a horizontal distance of 12 to 15 km and at a vertical depth of about 140 m. Due to radioactive decay and the preferential infiltration of winter precipitation with relatively low  $^3\text{H}$ , the peak activity in the groundwater should be 200 to 300 TU. The measured values of 80 to 90 TU are due to hydrodynamic dispersion (Fig 5.33).

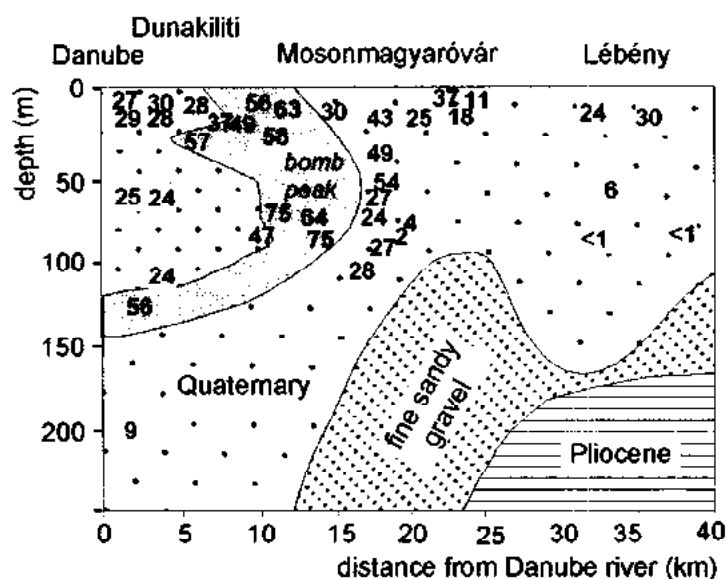


**Fig.5.33** Spatial  $^3\text{H}$  distribution in a depth profile at the Danube River, Hungary. The bomb peak of  $^3\text{H}$  (grey area) travelled with about  $500 \text{ m yr}^{-1}$  from W to E and approached a depth of 50 – 100 m at 1993 (after Deak et al. 1995).

#### 5.2.2.2 $^3\text{H}/^3\text{He}$ AND $^3\text{He}$ METHODS

##### Physical fundamentals

$^3\text{H}$  decays with a half-life of 12.43 yr into the daughter isotope  $^3\text{He}$ . By measuring both the mother and daughter activity actual water ages can be calculated, provided the samples were unmixed and collected from an aquifer with a piston-flow like groundwater movement (Chapter 3). The input function of  $^3\text{H}$  need not be known.

The activity of  $^3\text{H}$  is given by (Volume I):

$$^3\text{H}_{\text{spl}} = ^3\text{H}_{\text{init}} e^{-\lambda t} \tag{5.7}$$

The growth of  $^3\text{He}$  in a sample is given by

$$^3\text{He}_{\text{spl}} = ^3\text{H}_{\text{init}} (1 - e^{-\lambda \cdot t}) \quad (5.8)$$

Combining Eq. 5.7 and 5.8 the unknown and variable initial  $^3\text{H}$  activity  $^3\text{H}_{\text{init}}$  is eliminated and the absolute age is obtained by

$$^3\text{He}_{\text{spl}} = ^3\text{H}_{\text{spl}} (e^{-\lambda \cdot t} - 1)$$

The  $^3\text{He}$  concentration has to be corrected for admixed  $^3\text{He}$  from the Earth's crust and from the atmosphere.

Until now the high cost of the mass spectrometer analysis prevented a wide application. An methodical problem of this method is diffusive gas loss, either due to natural processes or during sample treatment and storage (Volume I; Schlosser et al. 1989; Ekwurzel et al. 1994).

The required high-precision measurement of  $^3\text{H}$  is obtained by the so-called  *$^3\text{H}$ -ingrowth technique* (Volume I). The  $^3\text{H}$  activity is determined through measuring the stable  $^3\text{He}$  produced by the  $^3\text{H}$  decay. Water samples (typically ca. 45 ml) are thoroughly degassed and then stored for at least a half year in a tightly sealed aluminosilicate container under vacuum. The  $^3\text{H}$  value  $C(^3\text{H})$  is calculated from the concentration  $c(^3\text{He})$  of  $^3\text{He}$  produced during the storage time  $t$  by Eq. 5.7. The detection limit for  $^3\text{H}$  of this method is  $> 0.005$  TU (Volume I).

### Application

Schlosser et al. (1989) used this method to absolutely date *shallow groundwater* in an alluvial aquifer in Germany. The precision of the dating was  $\pm 10\%$ , the loss of  $^3\text{He}$  by diffusion was estimated to  $\approx 20\%$ . This is small enough to consider  $^3\text{He}$  as conservative tracer. The method is found to be a very valuable complementary tool for the dating by CFC and  $\text{SF}_6$ .

Owing to its sensitivity, the  $^3\text{H}/^3\text{He}$  method is used for *absolute groundwater dating* up to about 40 yr (Schlosser et al. 1989). The application may increase in the future as the application of the conventional  $^3\text{H}$  method is temporarily limited (Carmi and Gat 1992) due to the largely declined  $^3\text{H}$  activity in precipitation.

### 5.2.2.3 RADIOCARBON

#### Physical fundamentals

Radiocarbon ( $^{14}\text{C}$ ) is the radioactive isotope of carbon with a half-life of 5730 years. It occurs in atmospheric  $\text{CO}_2$ , living biosphere and the hydrosphere after its production by cosmic radiation. Underground production is negligible. The  $^{14}\text{C}$  activity is often given as an activity ratio relative to a standard activity, about equal to the activity of recent or modern carbon. Therefore, the  $^{14}\text{C}$  content of carbon containing materials is often given in percent modern carbon (pMC): 100 % or 100 pMC (or 100 % Modern Carbon) corresponds by definition to the  $^{14}\text{C}$  activity of carbon originating from (grown in) 1950 AD (Volume I).

Fallout  $^{14}\text{C}$  (in carbon dioxide) from the nuclear tests (Fig.2.1) offers the possibility – analogous to  $^3\text{H}$ – to date young groundwater with mean residence times of up to 150 years of the long-term components of karst spring-water and shallow groundwater applying suitable interpretation models (Volume VI).

$^{14}\text{C}$  is measured radiometrically using samples with an equivalent of 25 mg to 5 g carbon (corresponding to about 5 to 100 L of groundwater) and mass spectrometrically (AMS accelerator mass spectrometry) with less than  $< 1$  mg carbon (details in Volume I).

### Occurrence

$^{14}\text{C}$  may not behave as a conservative tracer in groundwater as it is a constituent of the dissolved inorganic carbon (DIC) compounds undergoing hydrochemical reactions with the rock matrix of the host aquifer (Sect.4.4; Volume I; Clark and Fritz 1997).

$^{14}\text{C}$  also occurs in the dissolved organic carbon compounds (DOC). The dissolved organic carbon (DOC) in groundwater consists of organic liquids, hydrocarbons, methane and humic components. It is produced by microbial activity from humic matter in the top soil, peat layers and lignite. The youngest dissolved constituents in groundwater are fulvic acids (FA) which are most promising for groundwater dating (Geyer et al. 1993; Wassenaar et al. 1991). Humic acids (HA) are less suitable.

The concentration of FA in groundwater is as low as 1 mg/L carbon. As the fulvic acids are composed of variable-age organic carbon of pedogenic and geogenic origin with an age range of many hundreds to thousands of years.  $A_0$  is usually lower than 100 pMC. Geyer et al. (1993) found a range of 34 – 100 pMC but most frequently between 75 and 100 pMC. The initial  $^{14}\text{C}$  activity can only empirically be estimated. The expectation that  $^{14}\text{C}$  dating of DOC may overcome the hydrochemically involved problems of  $^{14}\text{C}$  dating of DIC has not been fulfilled though sometimes the contribution of old sedimentary organic carbon can be estimated (Aravena and Wassenaar 1993).  $^{14}\text{C}$  dating of DOC is, however, a useful supplement to  $^{14}\text{C}$  dating of DIC (Volume I).

### Processes and Reactions

*Dating of groundwater*, initially considered as the main purpose of isotope hydrology, applies the  $^{14}\text{C}$  method developed by Libby (1946) for organic samples with ages up to some 50 000 years. According to Libby's model, the  $^{14}\text{C}$  produced by cosmic rays is oxidised to  $\text{CO}_2$  in the atmosphere and is mixed into the  $\text{CO}_2$  cycle. Through the assimilation by plants and their consumption by animals and man,  $^{14}\text{C}$  enters the biocycle and thus the various earth reservoirs of  $^{14}\text{C}$  (atmosphere, biosphere and hydrosphere), for each of which a different specific initial specific activities  $A_{\text{int}}$  applies (reservoir effect). Within the time span of the  $^{14}\text{C}$  dating method the production rate and therefore also the global  $^{14}\text{C}$  reservoir, is taken as approximately constant. Cosmogenic production of  $^{14}\text{C}$  is balanced by radioactive decay. As soon as an organism dies the assimilation of  $^{14}\text{C}$  ceases and the specific  $^{14}\text{C}$  activity ( $^{14}\text{C}$  value) de-

creases with a half-life of 5730 years. In order to determine the age by Eq.2.2 it is therefore necessary to measure the specific  $^{14}\text{C}$  activity of a reference material  $A_{\text{init}}$  of known age (standard) and of the sample  $A_{\text{sp}}$  to be dated.

Münnich (1957, 1968) recognised that groundwater can be dated based on the carbonate/bicarbonate chemistry.  $^{14}\text{C}$  is present in groundwater in the form of  $\text{CO}_2$ , mainly as  $\text{HCO}_3^-$ .  $\text{CO}_2$  in soil air (up to 3 vol.%), which is produced by the respiration of roots and the decomposition of organic material that has recently died ( $^{14}\text{C}$  activity = 100 pMC,  $\delta^{13}\text{C} = -25\text{‰}$ ) is dissolved by infiltrating rainwater and dissolves marine and fossil carbonate in the topsoil (assumed to be 0 pMC,  $\delta^{13}\text{C} = 0\text{‰}$ ) as carbonic acid forming bicarbonate (Eq.4.1). There is a large difference between open and closed systems (Volume I; Clark and Fritz 1997).

After hydrochemical equilibrium between the  $\text{CO}_2$  and carbonate has been reached  $A_{\text{init}}$  in newly regenerated groundwater is in the range of 55 to 65 pMC, corresponding to a reservoir correction of -4500 to -3500 yr. Consequently,  $A_{\text{init}}$  increases with increasing DIC.

There are various models to estimate  $A_{\text{init}}$  by applying the concentrations of bicarbonate and  $\text{CO}_2$  or the isotopic composition of carbon including isotopic fractionation and mixing (Sect.4.4.1; Volume I; Mook 1980; Clark and Fritz 1997). Most common is the estimation of the initial  $^{14}\text{C}$  activity ( $C_{\text{init}}$ ) by means of the Gonfiantini model (Salem et al. 1980; Eq.5.5). It relates the  $\delta^{13}\text{C}$  of the DIC in groundwater ( $\delta^{13}\text{C}_{\text{DIC}} = 0 \pm 0.3\text{‰}$ ) to mixing of carbon from calcite ( $\delta^{13}\text{C}_{\text{calc}} = 0 \pm 2\text{‰}$ ) with carbon from soil  $\text{CO}_2$  ( $\delta^{13}\text{C}_{\text{CO}_2} = -22 \pm 1.5\text{‰}$ ) and isotopic fractionation factor  $\epsilon$  between dissolved bicarbonate and gaseous  $\text{CO}_2$  is a function of temperature and pH and amounts to 8 to 9‰. The model yields the initial activity of  $^{14}\text{C}$  for closed carbonate- $\text{CO}_2$  systems, and the calculated model age  $t$  according to Eq.5.9.

Experience with these models shows that using the same hydrochemical and isotope hydrological information they produce corrections varying by up to many thousands of years (Geyh 1992). The best results are obtained with the program NETPATH, provided chemical and isotopic data are available from samples taken from wells along the same flowpath of the groundwater. This presupposition cannot easily be fulfilled. A mayor problem of all modelling remains that the isotopic compositions of the chemical components – limestone and  $\text{CO}_2$  are rarely accurately known, while isotopic equilibrium is usually not attained (Geyh 1992). In any case, the time scales of the different models for most fresh groundwater resources are linearly related to each other (Fig.5.34). Therefore, the numerous possible secondary changes in  $^{14}\text{C}$  values of fresh groundwater, due to water-rock interactions in the saturated zone and unrelated to radioactive decay (Chapter 4), appear to play a minor role. The  $^{14}\text{C}$  values of DIC thus represent reliable time differences producing reliable flow rates in solute transport modelling.

One problem of the estimate of  $A_{\text{init}}$  by hydrochemical or isotopic models is that a thorough error analysis, adopting the ranges of initial  $^{14}\text{C}$  activity and  $\delta^{13}\text{C}$  of the hydrochemically involved components, considerably lowers the precision of groundwater dating. This becomes

the more pronounced the more components are used in the model. In the case of the relative simple Gouffier model (Eq.5.5) the precision rises from  $\pm 100$  yr to  $\pm 2700$  yr. Fortunately, the results of many case studies show that the  $^{14}\text{C}$  groundwater dates scatter less than  $\pm 500$  yr (Geyh 1992). The reason is that the range of the initial  $\delta^{13}\text{C}$  values of the participating hydrochemical constituents from restricted recharge areas are smaller than the global ranges though not accurately known.

A possibility to overcome the problems in selecting the appropriate correction model and determining representative regional parameters are empirical approaches to estimate  $A_{\text{init}}$  and to calibrate the  $^{14}\text{C}$  ages of DIC. Frequently the *fixed correction value* of 85 pMC (Vogel & Ehhalt 1963) is applied. Geyh (1972) evaluated a differentiated array of  $A_{\text{init}}$  for different geological settings of the recharge area (Table 5.2).

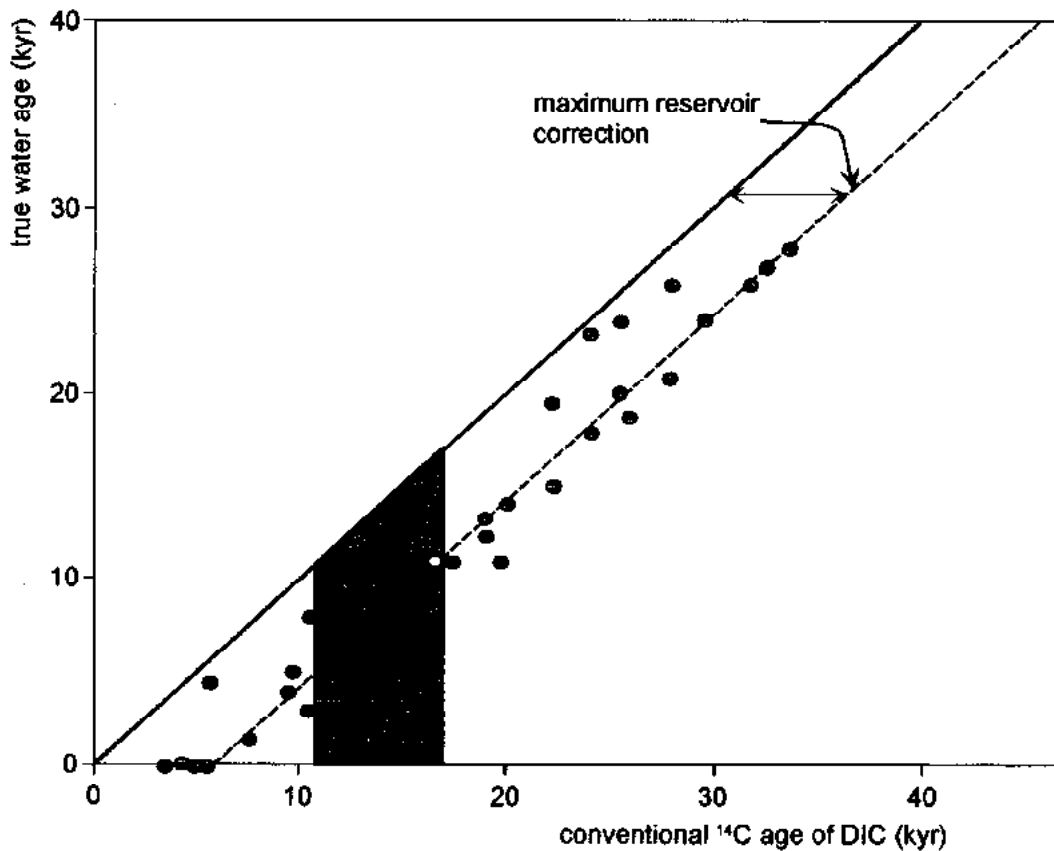


**Fig.5.34** Example of an interrelationship between true water ages and conventional  $^{14}\text{C}$  ages of DIC from central USA. It shows that secondary  $^{14}\text{C}$  changes during groundwater flow cannot play a dominant role as the slope of the best-fit line is near unity. Moreover, the interruption of the groundwater recharge during the last pleniglacial period is well documented by the gap (grey area) of the  $^{14}\text{C}$  dates. The reservoir correction amounts maximum to 5000 yr (data from Phillips et al. 1989).

A very effective way is to plot the  $^{14}\text{C}$  ages of DIC along the flow path and to extrapolate them towards the recharge area where the actual water age is assumed to be zero (Vogel 1970; Fig.5.35).

A very reliable approach is to plot the  $^3\text{H}$  value (alternatively  $^{85}\text{Kr}$ ) versus the  $^{14}\text{C}$  activity (Fig.5.36; Verhagen et al. 1991). The initial  $^{14}\text{C}$  activity is found where the curve hits the detection limit of  $^3\text{H}$ . This approach is based on the assumption that a groundwater which does not contain bomb  $^3\text{H}$  may also not contain bomb  $^{14}\text{C}$  (Fig.2.1).

**Table 5.2** Empirically estimated initial  $^{14}\text{C}$  values  $A_{\text{init}}$  and corresponding reservoir corrections for different geological settings (Geyh 1972).

geology of the catchment	$A_{\text{init}}$ (pMC)	reservoir correction (yr)
crystalline	90 to 100	-1000 to 0
loess covered	85	-1300
uncovered karst, dunes	55 to 65	-5000 to -3500

Palaeohydrological, palaeoclimatological and prehistoric information (Geyh 1992; Clark et al. 1996) may always be used to check the reliability of the estimated initial  $^{14}\text{C}$  activity or to check its accuracy. An example is given by Clark et al. (1996) who applied supplementary correction models for carbonate dissolution and sulphate reduction (Clark & Fritz 1997) until the  $^{14}\text{C}(\text{DIC})$  dates fit with the palaeohydrological situation (Fig.5.37).

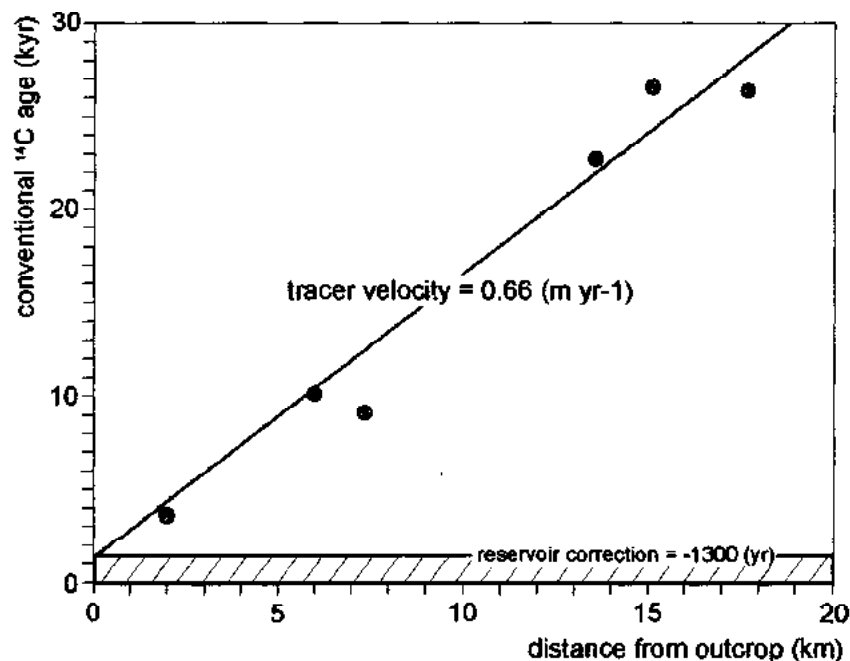


**Fig.5.35** Increase of  $^{14}\text{C}$  water ages of DIC over the distance from the recharge area used to estimate the initial  $^{14}\text{C}$  activity of 85 pMC or the corresponding reservoir correction of -1300 yr (after Vogel 1970).

There are several hydrochemical reactions of water-rock interaction (Sect.4.4.1) and processes which may change the  $^{14}\text{C}$  value after the groundwater recharge, resulting in apparently too large water ages. Concurrent dissolution and precipitation of carbonate is one process (Wigley et al. 1978), matrix diffusion and isotopic exchange within the aquifer another, but more important the oxidation of fossil organic matter by sulphate reduction and subsequent dissolution of additional carbonate as well as the admixture of magmatic and crust  $\text{CO}_2$  (Sect.4.4.1). All these processes lower the  $^{14}\text{C}$  activity, accompanied with an increase of the DIC concentration,  $C_T$ . As shown in Sect.5.2.2.3 the resulting dissolution of the  $^{14}\text{C}$  activity cannot be corrected by means of the changes of the  $\delta^{13}\text{C}$  values. A solution is the so-called Oeschger correction applied instead of Eq.2.2 for the age determination:

$$t = \frac{5730}{\ln 2} \cdot \ln \frac{A_{\text{init}} \cdot C_{T\text{init}}}{A_{\text{spl}} \cdot C_{T\text{spl}}} \quad (5.9)$$

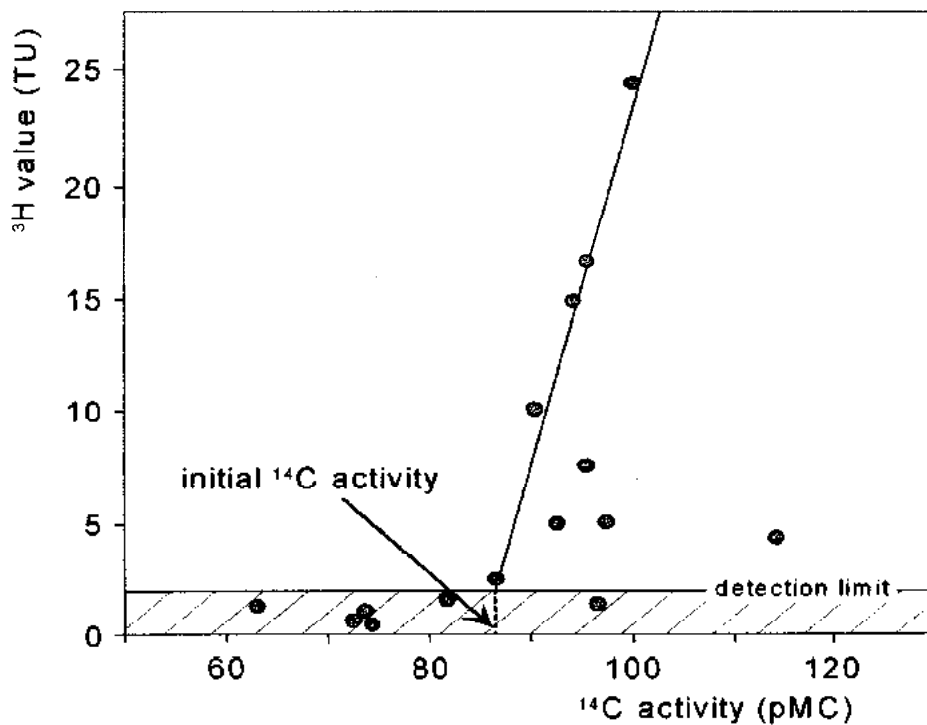
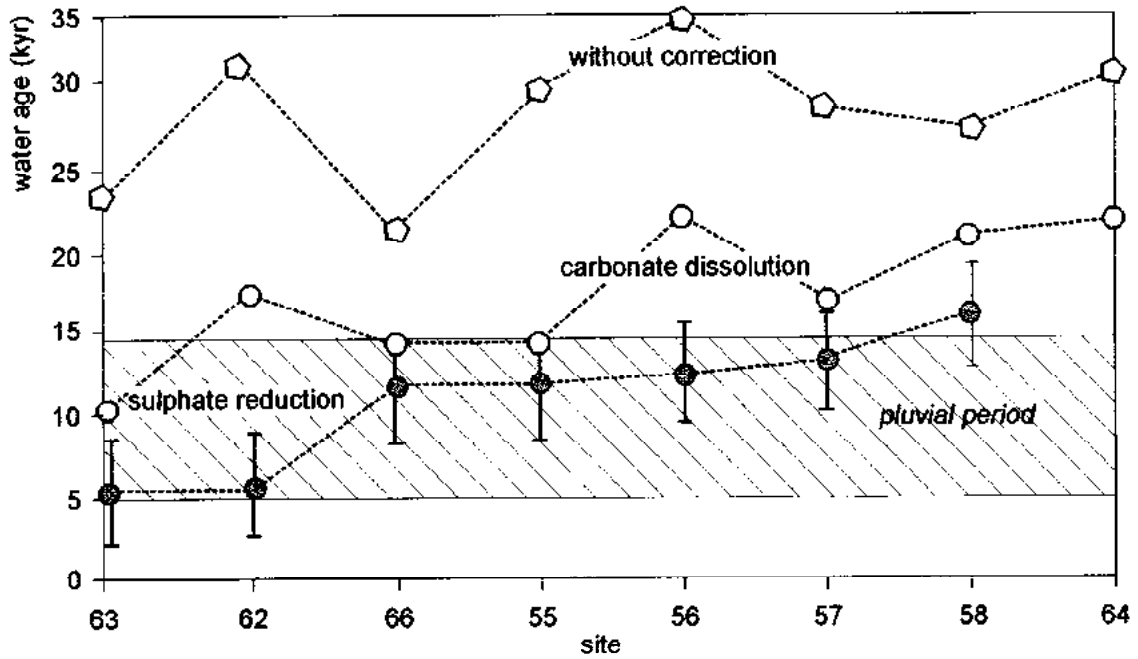


Fig.5.36  $^{14}\text{C}$ - $^3\text{H}$  plot to estimate the initial  $^{14}\text{C}$  activity of groundwater in the northern Kalahari (after Verhagen et al. 1974). Samples at or below the  $^3\text{H}$  detection limit should not contain bomb  $^{14}\text{C}$ .

In summary the hydrochemical reactions before and after groundwater recharge as well as several physical processes may change the  $^{14}\text{C}$  activity as well as DIC concentration, and influence the  $^{14}\text{C}$  time scale of the groundwater. This is shown in Fig.5.38.





**Fig.5.37** Application of different hydrochemical correction models to estimate the initial  $^{14}\text{C}$  value of DIC of groundwater in the Ad Rhuma aquifer, Oman. The validity of the results is proved by the agreement with the palaeohydrological situation (after Clark et al. 1996).

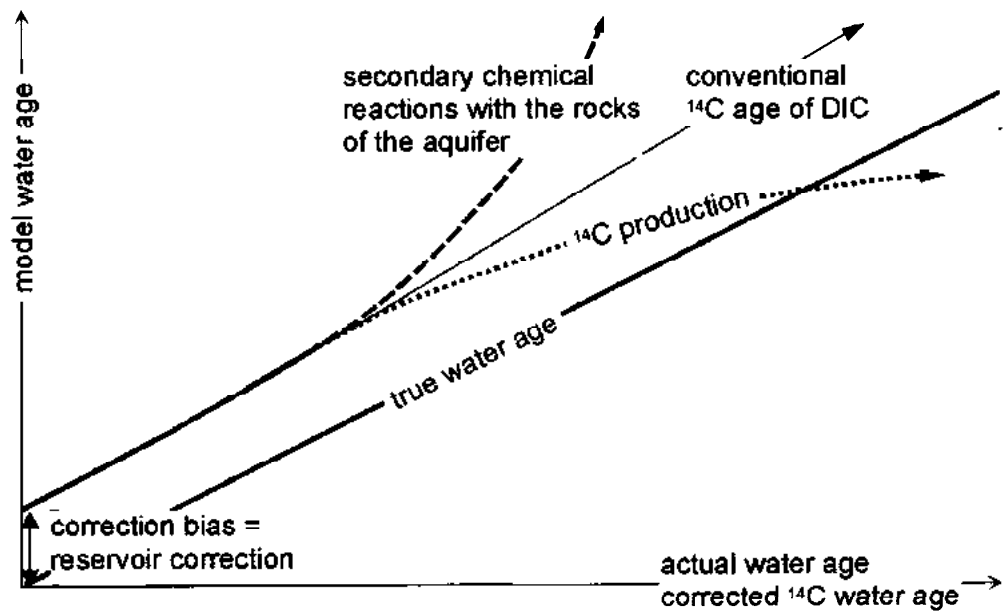


**Fig.5.38** Changes of the  $^{14}\text{C}$  time scale of DIC as result of radioactive decay (conventional ages), hydrochemical reactions due to water-rock interactions and  $^{14}\text{C}$  production after groundwater recharge.

## Applications

The broad application of the  $^{14}\text{C}$  dating method to hydrological problems and the interpretation of the results is largely covered by the proceedings of the international conferences on hydrology organised by the IAEA and reviewed by a number of publications mentioned in the section on Recommended Literature. Palaeohydrogeological and quantitative geohydraulic aspects have been treated in Verhagen et al. (1991). In spite of the above mentioned limitations of the method,  $^{14}\text{C}$  age determinations on DIC in groundwater are in demand in various ways. This field covers the age determination for palaeohydrological and palaeoclimatological studies (Geyh 1994), the determination of flow rates and flow direction of groundwaters (Fig.5.35), the search for arid or pluvial periods in present semi-arid and arid regions (Fig.3.7), the estimation of recharge rates in phreatic deep aquifers (Verhagen et al. 1991), the determination of regional geohydraulic parameters as porosity and hydraulic conductivity (Geyh et al. 1984), and a check on and improvement of hydrological conceptions (Verhagen et al. 1991).

### 5.2.2.4 SILICON-32

$^{32}\text{Si}$  is the radioactive isotope of silicon with a half life of about 140 yr. It is cosmogenically produced and shows high variations during the season (Morgenstern et al. 1996). Biochemical processes result in an uncontrolled uptake of silicon by plants in the unsaturated zone and seriously accelerate the decrease of the  $^{32}\text{Si}$  activity with time, apart from radioactive decay. Moreover, mixing with natural resources in the subsoil complicate the evaluation of the  $^{32}\text{Si}$  activity. The geochemical and biochemical processes in the soil, modifying the  $^{32}\text{Si}$  activity are not yet well known. They are responsible that  $^{32}\text{Si}$  does not behave as a conservative tracer in groundwater. Thus, dating of groundwater in a theoretical range between 100 and 1500 yr has not (yet) been successful (Volume I).

### 5.2.2.5 CHLORINE-36

#### Physical fundamentals

$^{36}\text{Cl}$  is the radioactive isotope of chlorine and has a half-life of 300 000 years. Its specific activity is given in disintegrations per minute and litre water ( $\text{dpm L}^{-1}$ ) or as the atomic ratio between  $^{36}\text{Cl}$  and  $\text{Cl}$ . The initial  $^{36}\text{Cl}/\text{Cl}$  ranges from 5 to  $30 \times 10^{-15}$  for young groundwater (Volume I).

If  $^{36}\text{Cl}$  is measured by AMS, 1 to 2 mg  $\text{AgCl}$  are analysed. This can be obtained from a few litres of water (Bentley et al. 1986).

#### Occurrence and processes

$^{36}\text{Cl}$  is produced cosmogenically, by natural underground production and by nuclear weapon tests. The subsurface production by radionuclide-derived neutron fluxes on  $^{35}\text{Cl}$  depend heav-

ity of the variable geological settings (e.g. Andrews and Fontes 1992). As radioactive decay and underground production on the one hand, and dilution by dissolution of salt or salt enrichment by evaporation on the other interfere, the interpretation of  $^{36}\text{Cl}$  data in terms of groundwater ages remains ambiguous (Mazor 1992). If uranium-rich or chlorine-bearing minerals are present, apparently too low  $^{36}\text{Cl}$  groundwater ages may be obtained (Bentley et al. 1986).

The relative  $^{36}\text{Cl}$  abundance in groundwater is not changed by evaporation of the water, mineral interactions or secondary mineral formation, but it is influenced by dissolving of chloride. Therefore, the total chloride concentration has to be always determined. The plot of  $^{36}\text{Cl}/\text{Cl}$  versus the chloride concentration yields information on groundwater mixing, evaporation, remobilisation of chloride, and radioactive decay and subsurface production of  $^{36}\text{Cl}$  (Florkowski et al. 1988). The complex situation of the interpretation of chlorine isotope data is shown in Fig.5.39.

### Applications

$^{36}\text{Cl}$  is applied to groundwater with transit times of  $>40\,000$  yr up to  $3\,000\,000$  yr (Fabryka-Martin et al. 1987).  $^{36}\text{Cl}$  is also a bomb tracer and was used for dating young groundwater in the unsaturated zone and in unconfined aquifers recharged during the last four decades. However, AMS analyses are expensive compared to  $^3\text{H}$  and  $^{14}\text{C}$  measurements.

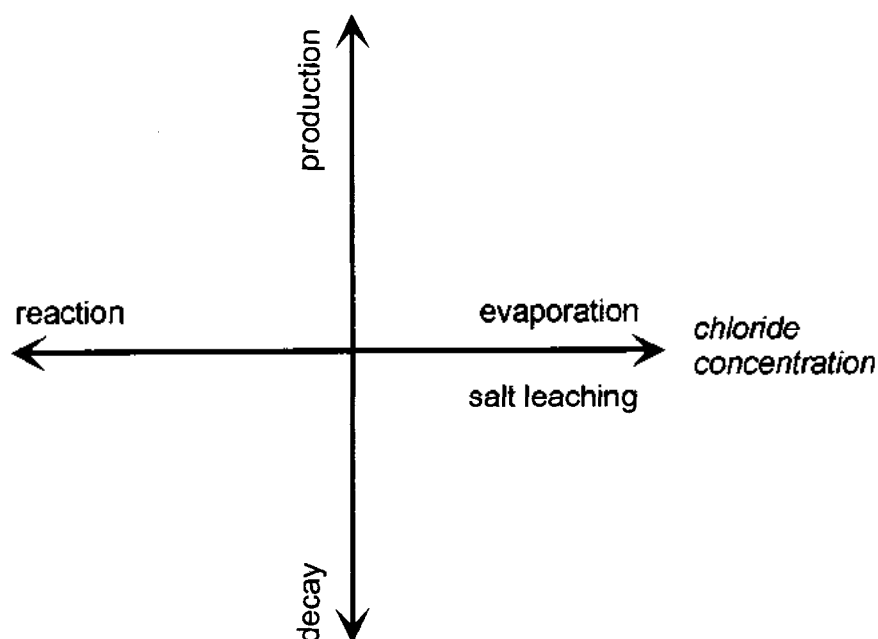


**Fig.5.39** Physical processes which change the chlorine-36 activity in groundwater and complicate the interpretation of the isotope data (after Mazor 1992).

**Case study 1: Great Artesian Basin, Australia**

$^{36}\text{Cl}$  dating is limited to fresh groundwater resources in large basins as the Great Australian Basin. The results confirmed the geohydraulically estimated water ages of up to 1 Myr (Fig. 5.40). The initial  $^{36}\text{Cl}/\text{Cl}_{\text{init}}$  ratio was estimated to be around  $100$  to  $120 \times 10^{-5}$  (Bentley et al. 1986; Herczeg et al. 1999). There is, however, a large difference to the estimated  $^{81}\text{Kr}$  water ages which has not yet been explained (Sect. 5.2.2.7; Lehmann et al. 1999).

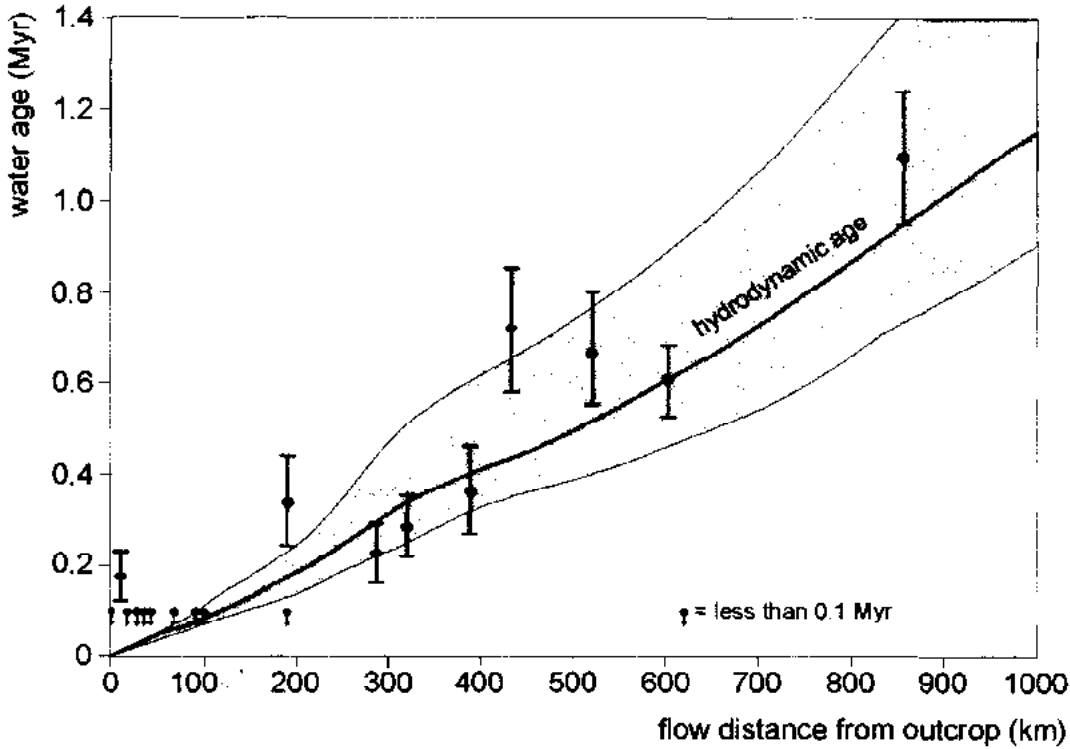


**Fig.5.40** Concordant  $^{36}\text{Cl}$  ages and geohydraulically estimated groundwater ages along the southern flow line in the Great Artesian Basin in Australia (after Bentley et al. 1986).

**Case study 2: Milk River Aquifer, Canada**

The problematics of hydrogeological  $^{36}\text{Cl}$  studies was recognised by  $^{36}\text{Cl}$  dating attempts in the Milk River aquifer in Alberta, Canada, in which the chloride concentrations cover a range of two orders of magnitude (Phillips et al. 1986). It is the general reason why the application of the  $^{36}\text{Cl}$  method is still very limited.

**Case study 3: Mixing studies**

There is a potential to apply  $^{36}\text{Cl}$  analyses to differentiate between *mixing* components, to set-up a chloride balance for geothermal fluids in hydrothermal systems (Chapter 6), for old groundwater systems with extensive water-rock interaction as well as with a high input of endogenous  $\text{CO}_2$  (Phillips et al. 1984a, Balderer 1993; Balderer and Synal 1995; Yechieli et al. 1996).

#### Case study 4: Young groundwater

$^{36}\text{Cl}$  produced by the nuclear bomb tests has also been used to determine the vertical velocity of soil water. Reasonable flow rates of  $2.5 \text{ mm}\cdot\text{yr}^{-1}$  were found in arid regions (Bentley et al. 1982; Elmore et al. 1982, Phillips et al. 1984b; Clark and Fritz 1997). This application may have been overlived, as most of such young groundwater has already discharged.

#### 5.2.2.6 ARGON-39

##### Physical fundamentals

$^{39}\text{Ar}$  is the radioactive isotope of argon and has a half life of 269 yr. Its activity is given in pMAR (equivalent to the definition for  $^{14}\text{C}$ : % Modern Argon) referring to the  $^{39}\text{Ar}$  activity in atmospheric argon which is by definition 100 pMAR.  $^{39}\text{Ar}$  is cosmogenically produced. Groundwater ages are calculated by Eq.2.2 analogous to  $^{14}\text{C}$  if the groundwater system behaved as closed system in the age range of several decades to about 1000 yr (Loosli 1992). Hydrochemical water-rock interaction of noble gas can be excluded. The occurrence of underground production, however, may considerably increase the  $^{39}\text{Ar}$  activity (Florkowski et al. 1988).

The extraction of samples of about  $15 \text{ m}^3$  of water in the field is complicated and the radiometric measurement is time-consuming with 5 to 30 days counting time (Volume I).

##### Occurrence and processes

In granitic and other rocks having a high uranium concentration the production of  $^{39}\text{Ar}$  by neutron reaction with  $^{39}\text{K}$  [ $^{39}\text{K}(n, p)^{39}\text{Ar}$ ] (Florkowski et al. 1988) explains the too small  $^{39}\text{Ar}$  ages (Loosli 1992). In leaky aquifer systems  $^{39}\text{Ar}$ -saturated pore water from the aquitards may falsify  $^{39}\text{Ar}$  dates of groundwater (Geyh et al. 1984). An indication of underground produced  $^{39}\text{Ar}$  is obtained from the measurement of  $^{37}\text{Ar}$  ( $T_{1/2} = 35 \text{ d}$ ). In old groundwater the contribution of  $^{40}\text{Ar}$  produced by the decay of  $^{40}\text{K}$  must be taken into account.

##### Applications

#### Case study 1: Concordant $^{14}\text{C}$ and $^{39}\text{Ar}$ water ages

Forster et al. (1992) presented concordant  $^{39}\text{Ar}$ ,  $^{14}\text{C}$ ,  $^3\text{H}$ ,  $^{39}\text{Ar}$ , and  $^{85}\text{Kr}$  ages of groundwater for the range of 120 to 800 yr. In two sandstone aquifers in Germany underground production could be excluded. In all cases maximum  $^{85}\text{Kr}$  and  $^3\text{H}$  ages were obtained, whereas  $^{14}\text{C}$  resulted in minimum ages.

#### Case study 2: Discrepancy between $^{39}\text{Ar}$ and $^{14}\text{C}$ (DIC) ages

$^{39}\text{Ar}$  water ages deviated by as much as one order of magnitude from the  $^{14}\text{C}$  ages of DIC in groundwater from a leaky, confined sandstone aquifer in southern Germany. Underground production of  $^{39}\text{Ar}$  in the sandstone aquifer was excluded. In spite of this, a high specific  $^{39}\text{Ar}$

activity was found for groundwater of more than several 1000 yr of age. This was explained by contributions of groundwater seeped from the shallow aquifer, becoming saturated in  $^{39}\text{Ar}$  during the passage of the aquitard. The high thorium content causes a high underground production (Geyh et al. 1984). This process may partly be responsible for other deviating  $^{14}\text{C}$  and  $^{39}\text{Ar}$  water ages (Loosli 1992; Andrews et al. 1984).

#### 5.2.2.7 KRYPTON-81

##### Physical fundamentals

$^{81}\text{Kr}$  is the long-lived radioactive isotope of the noble gas krypton and has a half-life of 230,000 yr. It is cosmogenically produced and considered to be a conservative tracer. Most likely underground production is negligible. The concentration is given in  $\text{dpm L}^{-1}$   $^{81}\text{Kr}$  (Rozanski and Florkowski 1979). The atmospheric  $^{81}\text{Kr}/\text{Kr}$  ratio is about  $5 \times 10^{-13}$  and independent from climatic conditions in the past.

Krypton is degassed from  $15 \text{ m}^3$  of groundwater and obtained by fractionated vacuum techniques. The measurement is done by AMS. Contamination with modern atmospheric krypton during sampling must be avoided (Volume I; Collon et al. 1999).

##### Occurrence

$^{81}\text{Kr}$  enters the groundwater during the recharge by dissolution of atmospheric gases.

##### Application

$^{81}\text{Kr}$  has the potential for dating old and saline groundwater with isolation ages of 50 ka to 1 Ma (Andrews et al. 1989; Collon et al. 1999). First datings of fresh groundwater was carried out in the Great Artesian Basin, Australia (Collon et al. 1999). The results were compared with  $^{36}\text{Cl}$  dates (Sect. 5.2.2.5; Lehmann et al. 1999). The agreement is reasonable within the age range of 1 000 000 yr though in both methods methodical problems may exist.

#### 5.2.2.8 KRYPTON-85

##### Physical fundamentals

$^{85}\text{Kr}$  is the short-lived radioactive isotope of the noble gas krypton with a half-life of 10.76 yr. The  $^{85}\text{Kr}$  specific activity is given in  $\text{dpm L}^{-1}$  of  $^{85}\text{Kr}$ . The detection limit is about  $100 \text{ dpm L}^{-1}$  of Kr, while the present level is around 5500 (Fig. 2.1). As a chemically inert gas, krypton offers nearly ideal possibilities for studying hydrodynamic movement and mixing of groundwater into which it has diffused (Salvamoser 1986).

For the analysis  $^{85}\text{Kr}$  is extracted from about 100 L of groundwater within a vacuum chamber and measured in a small proportional counter over a week (Volume I; Salvamoser 1986).

## Occurrence

The specific activity of  $^{85}\text{Kr}$  in the atmosphere has been monotonously increasing world-wide since the beginning of the 1950s (Fig.2.1; Weiss et al. 1983). The primary source of  $^{85}\text{Kr}$  is the nuclear reprocessing industry.

## Applications

The  $^{85}\text{Kr}$  method allows to estimate mean residence times in the range of 10 to 50 years by means of lump-parameter models. The results are more precise and less ambiguous than those obtained by the  $^3\text{H}$  method (Salvamoser 1986) (Fig.5.41). Presupposition is the analysis of unmixed samples. The limiting factor of this dating method is that the input function is not precisely known (Forster et al. 1992), but analysing this isotope serves as a valuable supplement to other tracer studies with CFC,  $\text{SF}_6$ ,  $^3\text{H}$ ,  $^3\text{He}/^3\text{H}$ .

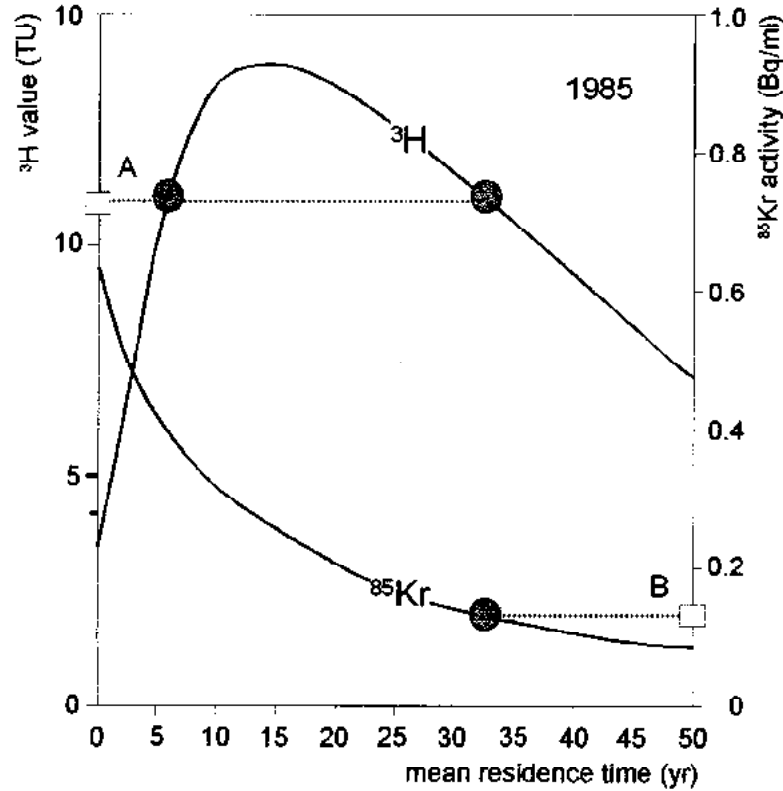


**Fig.5.41** Theoretical relationship between the mean residence times (MRT) of  $^3\text{H}$  and  $^{85}\text{Kr}$  calculated with the exponential groundwater model for 1985 (Fig.3.5) and southern Germany. The  $^3\text{H}$  value A yield two MRT values of 6 and 32 yr, the  $^{85}\text{Kr}$  value B yields an even more precise MRT of 33 yr (after Salvamoser 1986).

Case studies are given by Forster et al. (1992), the potentials of the method are discussed by Ekwurzel et al. (1994).

### 5.2.2.9 IODINE-129

#### Physical fundamentals

$^{129}\text{I}$  is radioactive and has a half-life of 15.7 Ma. It is cosmogenically formed in the upper atmosphere and anthropogenically by nuclear weapons tests (Paul et al. 1987). In addition,  $^{129}\text{I}$  is present in gaseous emissions from nuclear reactors and reprocessing plants. Its concentration is usually given as atomic ratio to the stable  $^{127}\text{I}$ .

Samples are extracted from a few litres of water and measured by AMS (Volume I).

#### Applications

Hydrogeological applications are being proposed for the age range of 3 to 80 Myr (e.g. Fabryka-Martin et al. 1987),  $^{129}\text{I}$  is applied for dating and tracing slow-moving groundwater but also for the detection of young groundwater. As for the other environmental isotopes, mixing of groundwater from different sources can be monitored (Fabryka-Martin et al. 1987). The nuclear  $^{129}\text{I}$  bomb pulse was also detected (Paul et al. 1987).

In groundwater, the  $^{129}\text{I}/^{127}\text{I}$  atomic ratio is mainly controlled by the rate of its recharge, the leaching from the aquifer rock and of the amount of in-situ uranium fission. Except for underground production, the  $^{129}\text{I}/^{127}\text{I}$  ratio is quite constant.

Most probably due to the expensive analytical technique case studies are not known.

### 5.2.2.10 URANIUM/HELIUM AND K/Ar METHODS

#### Physical fundamentals

The parent nuclides of the natural  $^{238}\text{U}$ ,  $^{235}\text{U}$ , and  $^{232}\text{Th}$  decay series and many of the subsequent daughter nuclides (Volume I) are  $\alpha$  emitters, i.e. producers of  $^4\text{He}$ . For example, during the decay of  $^{238}\text{U}$  to  $^{206}\text{Pb}$  8 helium atoms are produced, seven are produced by the decay of  $^{235}\text{U}$  to  $^{207}\text{Pb}$  and 6 by the decay of  $^{232}\text{Th}$  to  $^{208}\text{Pb}$ . Hence, the helium content increases in a closed system (e.g. in a confined aquifer) as a function of the uranium concentration and age. Provided loss and gain of helium does not occur, the water age  $t$  can be calculated from the production rates of  $^4\text{He}$  by the  $^{235}\text{U}$ ,  $^{238}\text{U}$  and  $^{232}\text{Th}$ . If radioactive equilibrium in a rock has been established,  $1.19 \times 10^{-13} \text{ cm}^3 \text{ STP He}/\mu\text{g U}$  and  $2.88 \times 10^{-14} \text{ cm}^3 \text{ STP He}/\mu\text{g Th}$  are produced annually (Volume I).

The helium content of groundwater is determined using 100 L samples. After degassing and separation of the noble gases, helium is isolated by fractional distillation. The argon concentration is used to correct for disturbing concentration of atmospheric helium.

#### Applications

The U/He method is recommended to determine groundwater ages between several thousand years up to 400 Ma (Andrews et al. 1982). The growth of  $^4\text{He}$  can be used to estimate resi-



dence times of up to 100 000 yr by comparing the Ne/He ratio of the groundwater to that of atmospherically equilibrated recharge water (e.g. Bottomley et al. 1990).

For groundwater dating, the uranium and thorium concentrations are roughly estimated via their  $\alpha$  activities, because the error due to loss of helium predominates. This is sometimes corrected for by measurement of the  $^{20}\text{Ne}$  or  $^{40}\text{Ar}$  isotopes.

### **Case studies in England and Austria**

The results showed a linear increase of the helium concentration with  $^{14}\text{C}$  groundwater age. However, this increase was larger than the expected excess by helium ingrowth from uranium and thorium decay. This is obviously due to migration of helium from adjacent strata. The  $^3\text{He}/^4\text{He}$  ratio would have yielded information on the proportion of crustal helium, that is often degassed from fracture zones in active tectonic regions (Andrews 1985, Torgersen and Clarke 1987).

An analogous dating method is based on the ingrowth of  $^{40}\text{Ar}$  by the decay of the frequently occurring  $^{40}\text{K}$  ( $T_{1/2} = 1.28$  Gyr) in rocks (Geyh and Schleicher 1990).

### **Case study: Great Artesian Basin, Australia**

In the Great Artesian Basin the  $^4\text{He}$  concentration increases due to in-situ production, resulting in a water age of up to 50 kyr. For ages above 100 kyr, an additional helium flux equivalent to the entire crustal production has been taken into account (Torgersen and Clarke 1985, Torgersen and Ivey 1985).

## **5.2.2.11 RADIUM/RADON DATING METHOD**

### **Physical fundamentals**

$^{222}\text{Rn}$ , the daughter of  $^{226}\text{Ra}$ , is a radioactive noble gas with a half-life of 3.6 days. Radium is easily soluble in water and is gained by dissolution from rock and alpha recoil of  $^{230}\text{Th}$ . The enrichment of  $^{226}\text{Ra}$  in groundwater approaches radioactive equilibrium after about 8000 yr (Volume I) (Andrews et al. 1989), and theoretically allows dating up to 5000 yr (Hillaire-Marcel et al. 1997).

Sampling for Rn is straightforward, and relatively simple counting devices can measure the activities. Because of its short half-life, Rn must be analysed within a few days after sampling to obtain the maximum measurement precision (Volume I).

### **Applications**

The presence of the short-lived radon in groundwater always means that the source radium is not too distant. A fast turn-over time of the groundwater in the aquifer system can be assumed. Rn concentration approaches radioactive equilibrium in the aquifer after a few weeks. Radon degasses completely after its discharge to the surface. This allows the detection of dis-

charge zones of groundwaters into rivers and lakes (e.g. Corbett et al. 1997). Also pumping tests profit from radon measurements.

The radon method can also be applied in areas of karstic flow and in fractured rocks. If the Rn concentration in groundwater is known and the Rn flux from the rock surface can be estimated for a particular flow system, the mean fracture width in the system can be estimated (Andrews 1991).

### Case Studies: Artificial recharge

Hoehn et al. (1992) obtained residence times of up to 15 days for artificially recharged river water in the aquifer used for the drinking water supply of the town Dortmund, Germany. Also the proportion of admixed lake water and pipe leakage could be estimated.

In *hydrothermal systems* the [ $^{226}\text{Ra}/^{222}\text{Rn}$ ] activity ratio has been shown to be a sensitive indicator of low-temperature interactions of hydrothermal solutions with crustal rocks along the Galapagos Rift. Information was gained about the mixing and flow history of these hydrothermal solutions (Dymond et al. 1983).

#### 5.2.2.12 $^{234}\text{U}/^{238}\text{U}$ DATING METHOD

##### Physical fundamentals

$^{234}\text{U}$  is produced by radioactive decay ( $T_{1/2} = 247,000$  yr) of  $^{238}\text{U}$ , the most abundant uranium isotope.

Uranium is extracted from 2 – 10 L of groundwater either by precipitation with  $\text{Fe}(\text{OH})_3$  or aluminium phosphate or by adsorption on a strongly basic anion exchange resin (Gascoyne 1981). The activities of the uranium isotopes are determined alpha-spectrometrically or mass-spectrometrically (Volume I).

##### Processes

In solid lattices  $^{234}\text{U}$  is bound less tightly than  $^{238}\text{U}$ . In the  $\text{U}^{\text{VI}+}$  state it is more easily dissolved (Petit et al. 1985). As a result there is a wide range of  $^{234}\text{U}/^{238}\text{U}$  activity ratios between 0.5 and 40 in sediments and rocks and consequently also in groundwater with uranium concentrations between 0.1 and 25 ppb.

There are three zones of differing uranium chemistry. In the oxidising zone near the catchment area, uranium occurs in the chemically stable, highly soluble +6 oxidation state. Here, uranium acts as a conservative tracer and becomes enriched like  $^{234}\text{U}$ . This is due to  $\alpha$  recoil ejection of  $^{234}\text{Th}$  (from the disintegration of  $^{238}\text{U}$ ; Volume I) at the rock-water interface and the preferential leaching of  $^{234}\text{U}$  due to lattice radiation damage. Leaching of uranium from the rocks of the aquifer results in a nearly linear increase in uranium concentration and in an increase of the  $^{234}\text{U}/^{238}\text{U}$  activity ratio (Rogojin et al. 1998).

In the transition zone (downstream from the oxidising zone), both this ratio and the uranium concentration pass through a maximum (Fig. 5.42). Further downstream, in the reducing zone, the  $^{234}\text{U}/^{238}\text{U}$  activity ratio decreases slowly and more or less linearly as a function of the residence time, while the uranium concentration remains relatively constant at a very low level (Pearson et al. 1983).

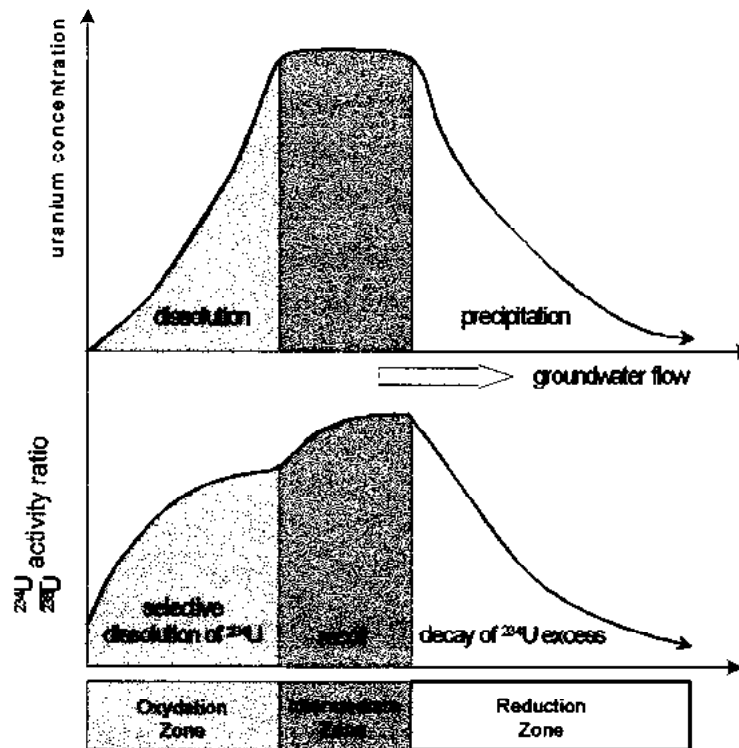


**Fig.5.42** Illustration of the changes of the uranium concentration and  $^{234}\text{U}/^{238}\text{U}$  activity ratio in the oxidising, transition, and reducing zones of an aquifer (after Osmond et al. 1983; Pearson et al. 1983; Fröhlich and Gellermann 1986). The rise in the oxidation zone seems to be suitable for water age determination (Fig.6.43; Rogojin et al. 1998).

Andrews et al. (1982) developed a model for closed systems to calculate the evolution of the  $^{234}\text{U}/^{238}\text{U}$  activity ratio and the uranium concentration of the water as function of the density, the water-rock surface and the leachable uranium concentration of the rock. The width of the fractures is the most sensitive parameter. The inhomogeneity of the corresponding distribution does not allow absolute age determinations but yield valuable information on changes in the flow regime.

### Applications

The first attempt to *date groundwater* with the  $^{234}\text{U}/^{238}\text{U}$  activity ratio was concentrated on the oxygen-free part of aquifers. They were all not successful mainly due to complicated and not yet fully understood chemical reactions of uranium with the aquifer rocks (Andrews et al. 1982). However, the  $^{234}\text{U}/^{238}\text{U}$  activity ratio allows to study hydrodynamic mixing processes

from rock joints and flow regimes (Osmond et al. 1983). Additionally, it yields valuable information on the hydrogeological history of the aquifer. Values around one confirm that the aquifer was not tectonically disturbed since many hundred thousands of years. Higher values indicate relative young rock surfaces that are formed after earthquakes or tectonic movement (Wakshal and Yaron 1974).

Groundwater datings of samples from the oxidising zone in a limestone and a sandstone aquifer in Israel were successful. A reasonable agreement was found between  $^{14}\text{C}$  water ages and those of the  $^{234}\text{U}$  excess (Rogojin et al. 1998) (Fig.5.43).

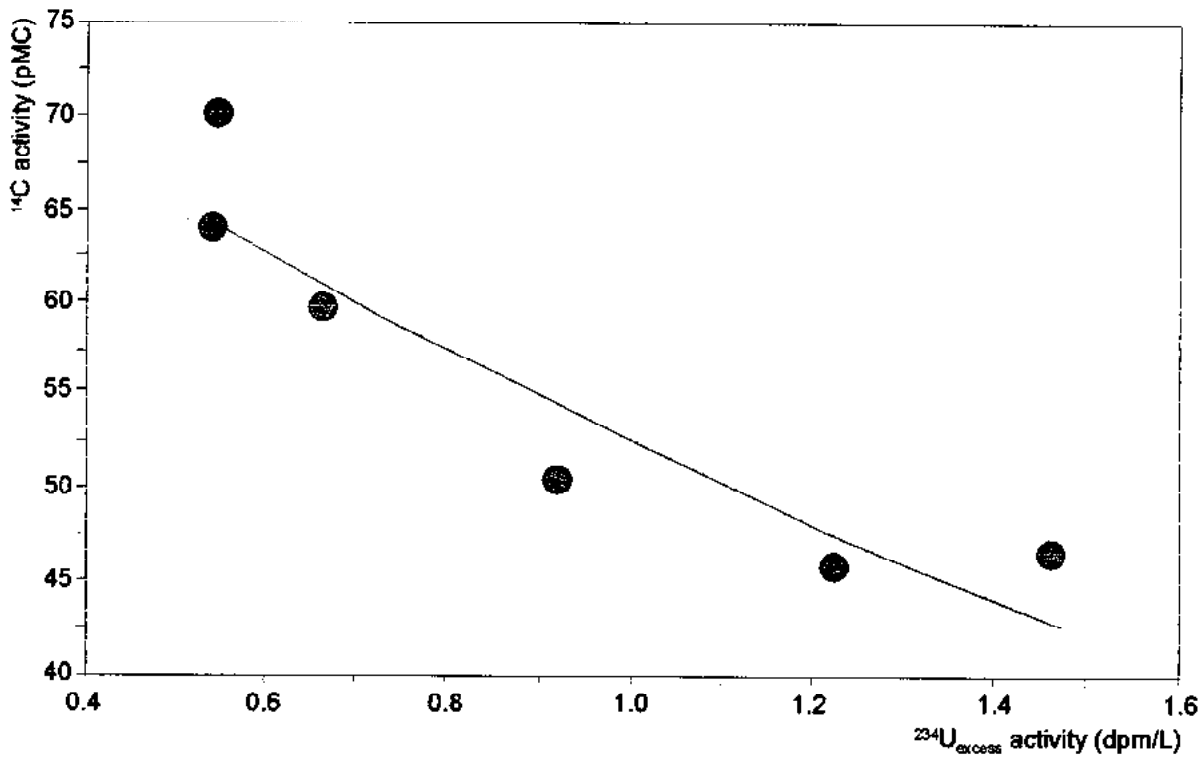


**Fig.5.43** Exponential fit between the specific  $^{14}\text{C}$  activity of groundwater DIC from the Judea Group aquifer, Israel, and the corresponding specific  $^{234}\text{U}$ -excess activity (after Rogojin et al. 1998).

# 6 APPLICATIONS TO HIGH-TEMPERATURE SYSTEMS

In natural systems (gas-water-rock assemblages) variations in the isotopic composition occur as a result of natural and anthropogenic processes. In geothermal systems mainly the isotopic ratios of the four elements – hydrogen, oxygen, carbon and sulphur – are of interest (Volume I). These elements are important constituents of geothermal fluids and rocks.

Techniques based on natural variations of the isotopic compositions are now common tools in the geochemical survey during the stages of exploration and exploitation of a geothermal resource. Two opposite properties of isotopes are used:

- 1) the change in the isotopic composition due to temperature-dependent, fast, incomplete or uni-directional processes associated with water-rock interactions, steam separation, dilution and mixing, and
- 2) the constancy of the isotopic composition, largely unaffected by physical and chemical processes during the movement of the water from the source area to the sampling point.

Isotopic tracing is used to unravel hydrological problems. Essential to the interpretation of the change in the stable isotopic composition is our knowledge of the magnitude and temperature dependence of the isotopic fractionation factors  $\alpha$  between the common minerals and fluids (gases and water).

Because of the high exchange rate between the liquid and vapour phases (Giggenbach 1971), the isotopic composition can usually be assumed to be close to equilibrium and, therefore, strongly governed by the isotopic equilibrium constant  $\alpha$ . The determined isotope delta values (Eq.2.1)  $\delta_{\text{liq}}$  and  $\delta_{\text{vap}}$  for oxygen and hydrogen of the liquid and vapour phases are related to  $\alpha$  through

$$\delta_{\text{liq}} - \delta_{\text{vap}} \approx \varepsilon_{\text{lv}} = (\alpha_{\text{lv}} - 1) \cdot 10^3\text{‰} \approx \ln \alpha_{\text{lv}} (\times 10^3\text{‰}) \quad (6.1)$$

The corresponding isotopic fractionation factors are compiled in Table 6.1. The thermodynamic fractionation factors  $\varepsilon$  for both  $^2\text{H}$  and  $^{18}\text{O}$  for temperatures  $>100^\circ\text{C}$  and  $< 100^\circ\text{C}$  are given by Truesdell et al. (1977) and Majoube (1971), respectively.

The fractionation factors  $\alpha$  are obtained in three ways: (i) semi-empirical calculations using spectroscopic data or methods of statistical mechanics, (ii) laboratory calibration studies, and (iii) measurements of natural samples whose formation conditions are well-known or highly constrained.

**Table 6.1** Temperature dependence of equilibrium isotope fractionation ( $\epsilon$  values in ‰) between liquid water and vapour (liq-vap) for  $^{18}\text{O}$  and  $^2\text{H}$ . The enthalpies of liquid water,  $H_{\text{liq}}$ , and steam,  $H_{\text{vap}}$ , are given in (J/g). The vapour fractions  $x_{\text{vap}}$  are given for fluid mixtures at temperatures of first boiling at 300° and 260°C as a function of temperature: data >100°C (Truesdell et al. 1977) and < 100°C (Majoube 1971).

Temp. °C	$\epsilon(^{18}\text{O}_{\text{liq-vap}})$ ‰	$\epsilon(^2\text{H}_{\text{liq-vap}})$ ‰	$H_{\text{liq}}$ J/g	$H_{\text{vap}}$ J/g	$x_{\text{vap}}$	
					300°C	260°C
0	11.68	112.3	0	2499	0.538	0.454
20	9.81	85.1	84	2538	0.513	0.428
40	8.22	64.5	168	2574	0.489	0.402
60	6.95	48.6	251	2610	0.463	0.374
80	6.03	36.8	355	2644	0.437	0.346
100	5.25	28.2	419	2676	0.410	0.317
120	4.53	21.5	504	2706	0.382	0.286
140	3.91	16.3	589	2734	0.352	0.254
160	3.37	11.7	676	2758	0.321	0.220
180	2.90	7.4	763	2778	0.288	0.184
200	2.48	3.5	853	2793	0.253	0.145
220	2.10	0.1	944	2802	0.215	0.102
240	1.77	-2.2	1037	2804	0.174	0.055
260	1.46	-3.6	1134	2797	0.126	0.000
280	1.19	-4.0	1236	2780	0.070	-
300	0.94	-3.4	1344	2749	0.000	-
320	0.70	-2.2	1462	2700	-	-
340	0.45	-1.3	1594	2622	-	-
360	0.19	-0.5	1761	2481	-	-

Isotopic analyses of water from springs and wells yield information on the origin and the evolution of geothermal fluids such as underground mixing between waters of different origin, on effects of water-rock interaction (Chapter 4), on the isotopic geothermometry (Sect.6.1.2), and on steam separation processes (Sect.6.2.2). Studies of the stable isotopic compositions of geothermal gases may offer particular advantages with respect to studies of aqueous fluids, as the gases and their stable isotopes will be less affected by near surface conditions. From the hydrochemical and isotopic composition of geothermal fluids information is gained on their origin, the recharge area and the flow patterns, on the temperature in the depth, the molar fraction of vapour and vapour saturation. The cooling mechanism undergone by the fluid during its ascent to the surface, including heat conduction, mixing with shallow

groundwater and steam loss, may be quantitatively evaluated. Last but not least the effects of re-injection and the evolution of geothermal fields can be studied.

Criteria for the sampling strategy, information on sampling techniques and arising problems are discussed by Paces (1991).

## 6.1 NATURAL PROCESSES

Local meteoric water from different geothermal areas has usually different isotopic composition. The mean annual isotopic  $\delta$  values of precipitation are, in fact, largely related to the local mean annual *air temperature* – the lower the temperature, the lower the content of heavy isotopes, corresponding to more negative  $\delta^{18}\text{O}$  and  $\delta^2\text{H}$  values in colder regions. This is also reflected in the *altitude effect* (Sect.5.2.1.1). The rainfall at a higher altitude is isotopically lighter than in plains (Volume II). Last but not least, the *continental effect* may play a role if the distance between the studied areas is large.

The origin of the groundwaters in high-temperature geothermal systems can be distinguished by their geochemical and isotopic compositions. The following major water types are found in geothermal systems worldwide:

- *andesitic water* – recycled sea water which has been subducted in regions with andesitic volcanism or convergent plate volcanism (Giggenbach 1992). The  $\delta^{18}\text{O}$  and  $\delta^2\text{H}$  values are about  $+10 \pm 2$  and  $+20 \pm 10$  ‰, respectively, while the chloride concentration is similar to that of the sea water,
- *juvenile water* – water coming from the Earth's mantle or core that has never been part of the hydrospheric cycle. Because of mantle-crust interactions and subduction processes, juvenile water has never been knowingly recognised,
- *magmatic water* – water that equilibrated with magma, regardless of its initial origin; only the separated aqueous phase is magmatic water but not the water physically dissolved in the magma,
- *meteoric water* – originated from precipitation and of any age (rain, snow, ice, river water, lake water, groundwater),
- *ocean water* or sea water – water in the open oceans which may enter the geothermal systems.

In most geothermal fields the isotopic composition of the water is relatively constant and equals to that of the local meteoric water of the area. The  $\delta^{18}\text{O}$  often shows a characteristic enrichment of the heavy isotope ("*oxygen-isotope shift*") with respect to the isotopic composition of the local meteoric water. Oxygen-isotope shift is the significant property of any geothermal water in high-temperature systems. There are two physical processes which might have produced such isotopic pattern:

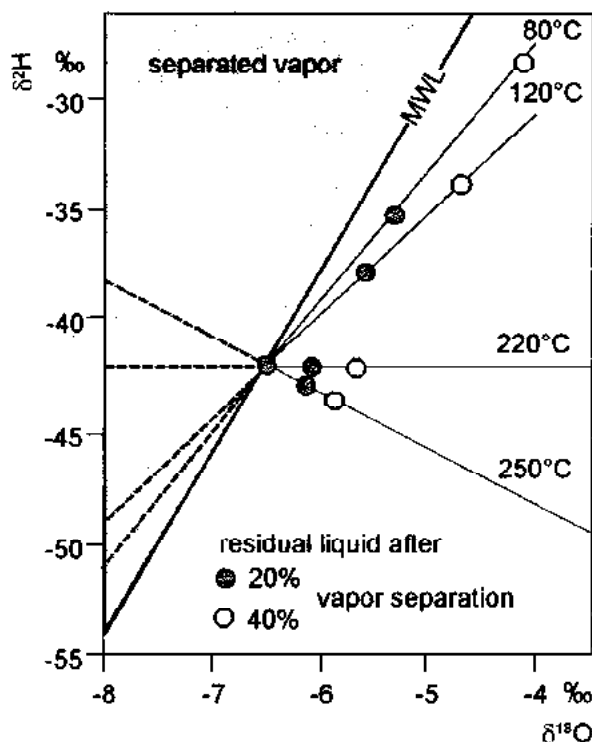


**Fig.6.1** Scheme of the shift in  $\delta^{18}\text{O}$  and  $\delta^2\text{H}$  values between the residual water and the vapour after separation.

- 1) **liquid-vapour isotopic exchange** at 220°C (Fig 6.1). At this temperature the two phases at equilibrium have the same hydrogen isotopic composition while there is still appreciable oxygen isotope fractionation. The heavy oxygen isotope becomes enriched in the liquid phase. This phenomenon is only observed if the temperature of any water did exceed 220°C in the area.
- 2) Oxygen-isotope shift due to **isotopic exchange** with minerals forming the rock matrix through which the water has moved. Meteoric water that infiltrated to depth and formed a geothermal reservoir is in isotopic disequilibrium with the rock: oxygen-isotope exchange with the surrounding rocks results in an enrichment of the heavy isotopes with respect to the initial water, controlled by the temperature of the geothermal reservoir. The fast continuous removal of heavy isotopes leads to a steady depletion in  $^{18}\text{O}$  of the rock (Clayton and Steiner 1975; Fig.6.2). The  $\delta^{18}\text{O}$  value of a groundwater in isotopic equilibrium with quartz or albite at 300°C is  $\approx +3\text{‰}$  and  $\approx +4.5\text{‰}$ , respectively. A quantitative approach to estimate the oxygen-isotopic shift in water was made by Taylor (1977).

Not all geothermal systems are exclusively fed by meteoric water. In some systems deep fossil marine (connate) water may be present (e.g. Salton Sea, California). Systems near the coast may be fed by both meteoric water and seawater (e.g. Svartsengi, Iceland). Other geothermal fields may be fed by already evaporated waters. In these cases the phenomenon of the oxygen-isotope shift is still visible on a horizontal alignment but the intercept with the MWL will be less negative than that found for meteoric water.



**Example:**

The slope of the lines in the  $\delta^{18}\text{O}/\delta^2\text{H}$  plot is controlled by the temperature of steam separation (Fig.6.1): the black dot and the open circles represent the initial water and the residual liquid after loss of 20% and 40% as steam, respectively. Dashed lines represent the isotopic composition of the separated vapour.

**6.1.1 WATER-ROCK INTERACTION AT HIGH TEMPERATURE**

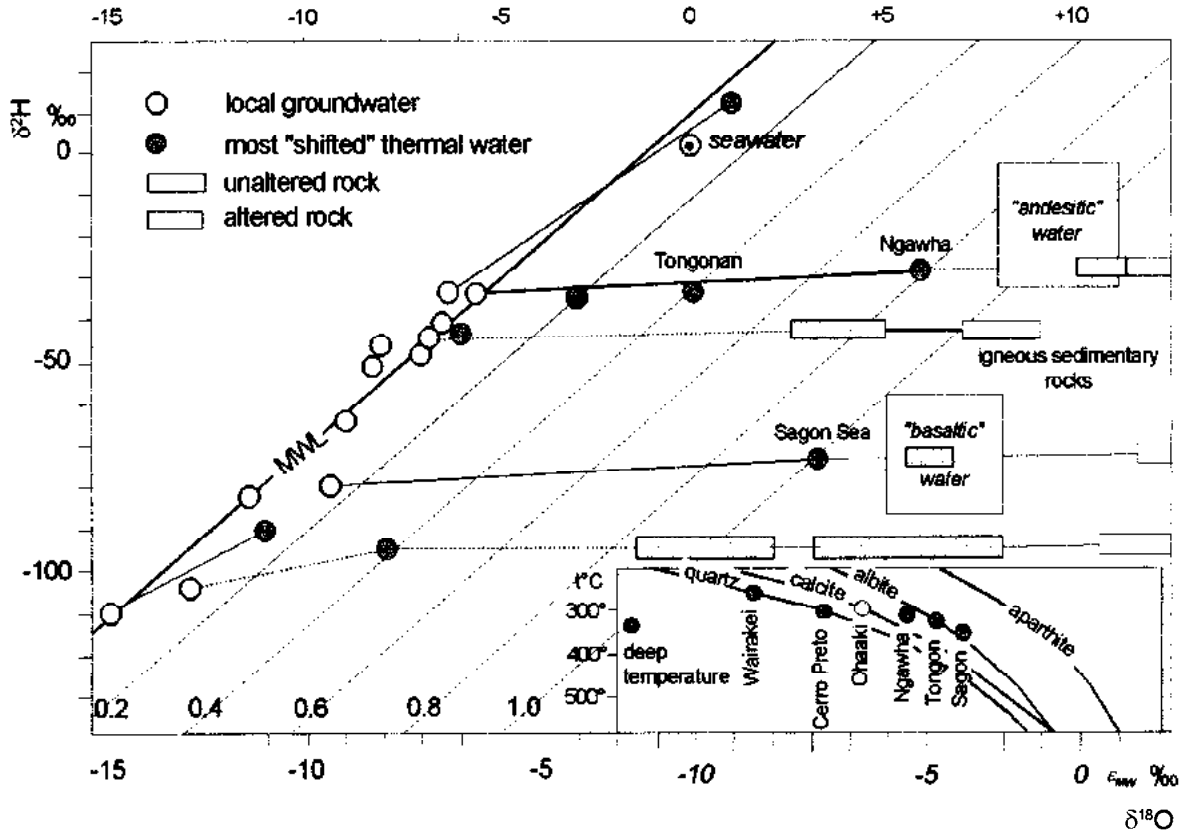
The thermodynamic equilibrium fractionation factor  $\alpha$  for mineral-water  $^{18}\text{O}$  exchange reactions increases with increasing strength of the oxygen bonds within a specific mineral. Matsu-hisa et al. (1979) determined values of  $\alpha$  as a function of temperature for the major "geothermal" minerals quartz, calcite and two feldspars (Giggenbach 1991). The highest fractionation shows oxygen tightly bound in quartz; the fractionation factor for feldspars is considerably smaller.

Fig.6.2 shows the isotopic compositions of oxygen and hydrogen for surface water and deep thermal water and those of the corresponding altered and unaltered rocks from geothermal systems. The  $\delta^2\text{H}$  values of the rocks equal that of the corresponding thermal water and do not reflect those of any hydrous minerals actually present. Lines parallel to the meteoric water line belong to fractions of andesitic vapour possibly contributing to the formation of the thermal water. Fig.6.2 allows to compare the actually observed isotopic fractionation between thermal water and the coexisting altered rock and that expected for isotopic equilibrium with the major minerals at the measured temperature of the deep groundwater.

The rate of oxygen-isotopic exchange between water and rock decreases rapidly with declining temperature. The presence of an  $^{18}\text{O}$  shift in water is, therefore, usually taken as evidence for a present or former high temperature ( $> 250^\circ\text{C}$ ) within the geothermal system. However, the magnitude of any oxygen-isotope shift depends, beside on temperature, on the degree of isotopic exchange and the proportions and  $\delta^{18}\text{O}$  values of the exchanging water and rock.

**Case studies:**

In *Ngawha*, New Zealand, the isotopic compositions of both altered and unaltered rock are visually indistinguishable, pointing to a very low degree of water-rock exchange (Blattner 1985). The least diluted water has a  $\delta^{18}\text{O}$  value of around +6‰, which is about 5‰ lower than that of the rock. The 5‰ difference in  $\delta^{18}\text{O}$  corresponds to an isotopic exchange temperature of  $>350^\circ\text{C}$  or  $300^\circ\text{C}$  if equilibrium with quartz or albite is assumed, respectively. The temperatures encountered in a deep drillhole (2255 m) were  $320^\circ\text{C}$ . The large oxygen-isotope shift of the water suggests that the relative proportions of water and rock involved in isotopic exchange were small. The water has almost completely isotopically equilibrated with the predominant sedimentary rocks at the temperature measured over the deep parts of this essentially stagnant system (Giggenbach and Lyon 1977).



**Fig.6.2** Isotopic compositions of oxygen and hydrogen of surface water and deep thermal waters and those of the altered and unaltered rocks from geothermal systems. The  $\delta^2\text{H}$  values of the rocks correspond to those of the corresponding thermal waters and do not represent those of any hydrous minerals actually present. Lines parallel to the meteoric water line represent fractions of andesitic vapour possibly contributing to the formation of the thermal water (after Giggenbach and Lyon 1977).

The reverse is observed at *Wairakei*. The  $\delta^{18}\text{O}$  shift is only 1.2‰ (Stewart 1978) which is interpreted as an indication of large amounts of local meteoric water having passed through the system (Clayton and Steiner 1975; Blattner 1985). The altered rocks are isotopically considerably lighter (+2.5 to +5‰) than fresh rock (+7 to +9‰; Clayton and Steiner 1975). The prevailing temperature within the Wairakei system is 260°C, corresponding to the observed  $\delta^{18}\text{O}$  shift of about 8.5‰ for an isotopic equilibrium with the dominant mineral quartz.

Based on the likely component dominating the water-rock interaction process, the examples of Fig.6.2 may be split into two groups:

- 1) essentially stagnant, rock-dominated systems with large  $\delta^{18}\text{O}$  shift, indicating adjustment of the isotopic composition of water to those of the unaltered, generally sedimentary rock (Ngawha, New Zealand; Salton Sea),
- 2) dynamic, fluid-dominated systems with comparatively small  $\delta^{18}\text{O}$  shift of the water. The isotopic composition of the altered, generally igneous rocks reflect isotopic equilibrium with the ascending groundwater.

The  $\delta^{18}\text{O}$  values of altered rocks, encountered at comparatively shallow levels in drillholes, are thus likely the product of an interaction with waters already isotopically modified with a  $\delta^{18}\text{O}$  shift. The dominant water-rock isotopic exchange, reflected by the isotopic composition of the ascending groundwater, may already have occurred well below the drilled depth, possibly within the zones of primary neutralisation of initially magmatic fluids or other deep, high temperature zones of major water-rock equilibration (Giggenbach 1988).

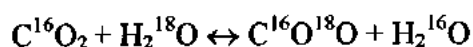
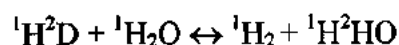
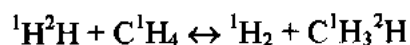
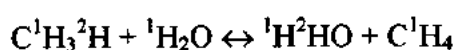
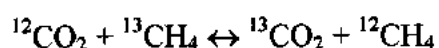
This example is representative for many geothermal systems. The major processes responsible for the  $\delta^{18}\text{O}$  shift in the water occurred well below the presently accessible depth. The actually observed wide range of the  $\delta^{18}\text{O}$  shift may, in many cases, simply reflect varying degrees of dilution of a highly shifted end-member component by local meteoric groundwater.

### 6.1.2 ISOTOPIC GEOTHERMOMETRY

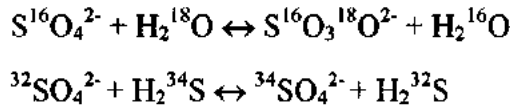
The gas component of geothermal fluids always contains carbon dioxide, methane, hydrogen and, of course, water vapour. As the relative distribution of isotopes between the components of the geochemical system is solely a function of temperature, any pair of these compounds may in principle act as an isotopic geothermometer. In order to apply this, the equilibrium fractionation factor  $\alpha$  of the isotopic exchange reactions must be known. The deciphering of the thermal history of a geothermal system by any isotopic geothermometer depends critically on whether or not isotopic equilibrium has been approached between the considered species. The following requirements must be fulfilled:

- 1) in the temperature range of interest, the regular temperature gradient of the isotopic fractionation factor  $\alpha$  must be large enough to be easily measurable; mixing with the same chemical species of different origin is to be excluded,
- 2) the isotopic equilibrium achieved in the geothermal reservoir is not altered at the sampling point, the rate of isotopic exchange is slow enough to prevent isotopic re-equilibration between the time of sampling and the time of analysis.

The following isotopic geothermometers are well developed:



In systems where the concentration of gas species is too low for an isotopic temperature determination, sulphate water/sulphate-sulphide isotopic exchange can be used for geothermometry:



If the temperature of the fluid remains constant sufficiently long to establish isotopic equilibrium, all geothermometers should give the same isotopic temperature. However, a change of the fluid temperature towards the point of discharge will result in different isotopic temperatures as indicated by the different geothermometers.

**Example:**

The kinetics of the reaction  $\text{CO}_2\text{-H}_2\text{O}$  is, for instance, very fast. Thus, the continuous isotopic re-equilibration does not permit to determine the maximum temperature of the system. The slowest reaction rate is for the  $\text{CO}_2\text{-CH}_4$  geothermometer.

The best geothermometers are those for which the temperature coefficient of the fractionation factor is large. Quartz and magnetite are a proper choice. Quartz is the most  $^{18}\text{O}$  rich, isotopically stable mineral and magnetite is the most  $^{18}\text{O}$  deficient mineral (Becker and Clayton 1976). On the other hand, quartz and feldspar are not suitable because the  $\delta^{18}\text{O}$  temperature gradient is small and particularly feldspar is susceptible to isotopic exchange with post-formational fluids.

There is a generalised temperature relation for all geothermometers for the component pair I and II (T in Kelvin):

$$\ln \alpha_{\text{I-II}} = \ln \frac{R_{\text{I}}}{R_{\text{II}}} = A + \frac{10^3 B}{T} + \frac{10^6 C}{T^2} \quad \text{‰} \quad (6.2)$$

In Table 6.2 the coefficients A, B and C of Eq.6.2 are given for the most common geothermometers.

**Table 6.2.** Coefficients of the most common geothermometers according to Eq.6.2.

		temperature range (°C)	phase		A	B	C
quartz–magnetite	$\delta^{18}\text{O}$	>500		empirical			4.8
$\text{CO}_2\text{-CH}_4$	$\delta^{13}\text{C}$	100 – 400		theoretical	-9.560	15.25	2.432
$\text{H}_2\text{O - H}_2$	$\delta^2\text{H}$	100 – 400	vapour	theoretical	-217.4	396.8	11.76
			liquid		-294.0	396.8	25.196
$\text{CO}_2\text{-H}_2\text{O}$	$\delta^{18}\text{O}$	100 – 400	vapour	theoretical	-8.87	7.849	2.941
			liquid		1961	18.29	7.626
$\text{SO}_4^{2-}\text{-H}_2\text{O}$	$\delta^{18}\text{O}$	0 – 300	quartz	Lloyd 1968	-5.6	0	3.251
				Mizutani and Rafter 1969	-4.1	0	2.880

The isotope equilibrium fractionation factor of the *carbon dioxide - methane isotopic geothermometer* at different temperatures (Fig.6.3) has been calculated from spectroscopic data by Richet et al. (1977). Lyon and Hulston (1984) found that the temperature T in °C may be estimated with a precision of about 2°C for a temperature range of 150 to 500 °C by:

$$T = -173 + \frac{15.79}{\delta^{13}\text{C}_{\text{CO}_2} - \delta^{13}\text{C}_{\text{CH}_4} + 9\text{‰}}$$

where the  $\delta$  values are small numbers (in ‰; 9‰  $\equiv$  0.009). This geothermal method has since been applied to most of the major geothermal fields in the world (e.g. Lyon and Hulston 1984; Nuti et al. 1985).

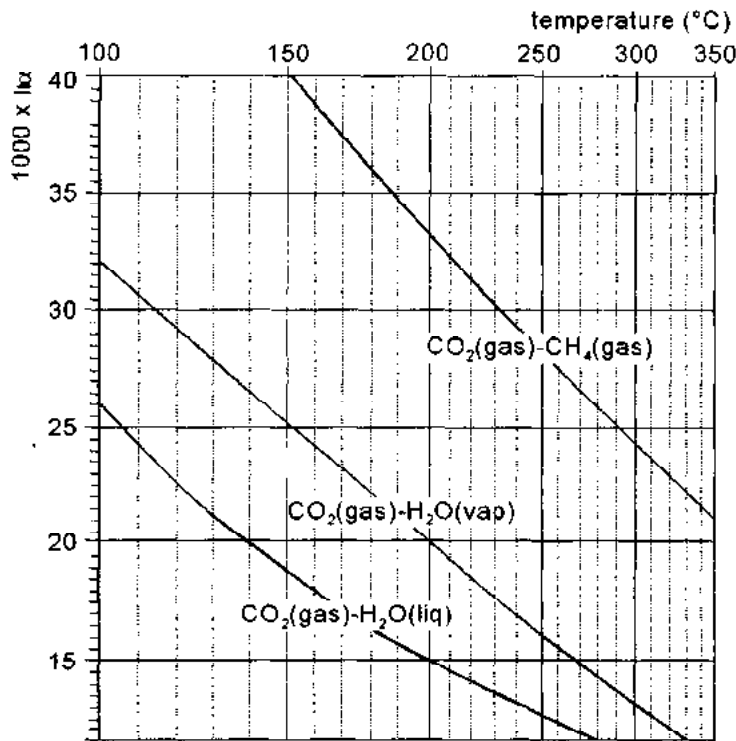


**Fig.6.3** Isotopic equilibrium factor  $100 \times \ln \alpha$  of the  $\text{CO}_2 - \text{CH}_4$  and  $\text{CO}_2 - \text{H}_2\text{O}$  geothermometers as function of the temperature calculated by Richet et al. (1977).

As the  $^{13}\text{C}$  equilibration reaction is by several orders of magnitude slower than that of the silica geothermometer (Truesdell and Hulston 1980), the  $^{13}\text{C}$  temperature may probably reflect earlier periods of the gas history than the present conditions of the exploited reservoir (Lyon and Hulston 1984). The experimentally determined reaction half-lives of the  $\text{CO}_2\text{-CH}_4$  geothermometer are 3, 75, 3000 and  $10 \times 10^6$  years at temperatures of 600°C, 500°C, 400°C and 300°C. Due to the slow rates, the temperature as determined by this geothermometer refers to a depth of a cooling magma body well below the actual productive horizon.

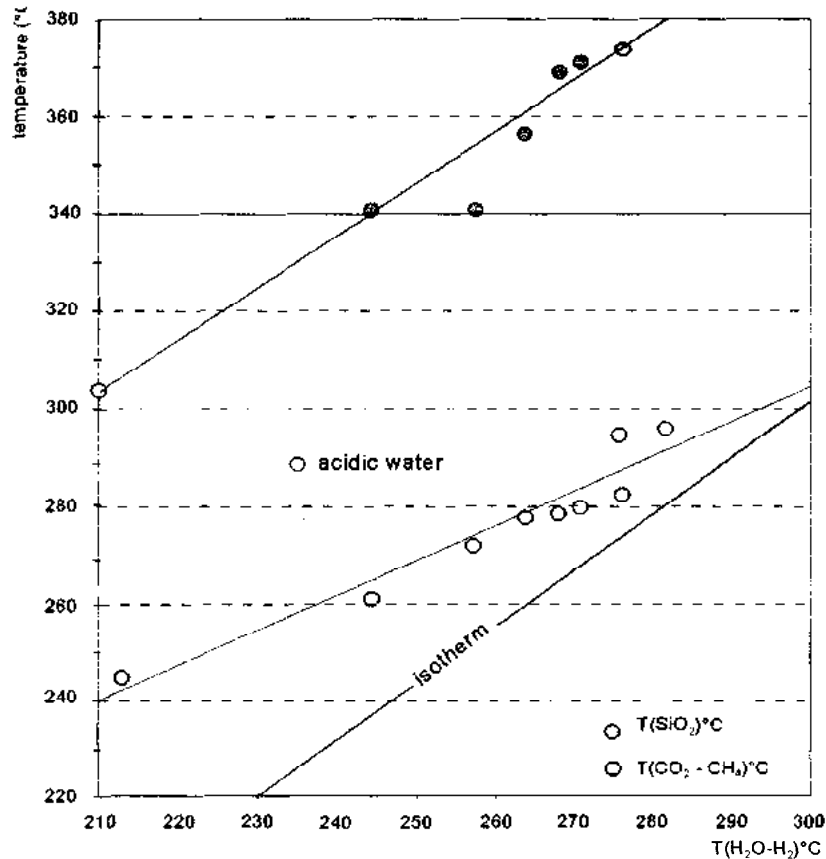


**Fig.6.4** Isotope temperatures computed from the CO<sub>2</sub>-CH<sub>4</sub> pair and the silica content (quartz) versus that of the H<sub>2</sub>O-H<sub>2</sub> pair for the Palinpinon field, Philippines.

### Case studies

Gunter and Musgrave (1971) applied the CO<sub>2</sub>-CH<sub>4</sub> geothermometer to a vapour system in the Yellowstone Park at Broadlands, Panichi et al. (1979) to the geothermal field of Larderello, Italy, and Nuti et al. (1985) to the Phlegraean Fields. The temperatures obtained were usually higher than observed probably due to conditions of equilibration temperatures at deep horizons below the productive zone.

The *water-hydrogen geothermometer* based on theoretical data by Richet et al. (1977) is well calibrated experimentally and theoretically and yields the best agreement between estimates and observed underground temperatures in geothermal exploration. This may be due to the relatively high exchange rate between water and hydrogen with less than one year to reach 90% equilibrium (Hulston 1973).

### Case study: Palinpinon field, Philippines

Fig.6.4 shows the good correlation between the temperatures computed from the pairs H<sub>2</sub>O-H<sub>2</sub> and CO<sub>2</sub>-CH<sub>4</sub> pairs for the Palinpinon field, Philippines, though the temperature computed from the pair CO<sub>2</sub>-CH<sub>4</sub> is by more than 70°C higher. The temperatures computed

from the silica content and the  $H_2O-H_2$  pair agree well.

For the vapour-dominated field of Larderello the *carbon dioxide-water geothermometer* (Ri- chet et al. 1977) yielded a temperature comparable to the one observed for the wellhead. This is due to high reaction rate of the isotopic exchange.

The use of the *sulphate-water geothermometer* for water-dominated geothermal fields is well proven. Two equations by Lloyd (1968) and Mizutani and Rafter (1969) are valid for the tem- perature range of 0 to 300°C. The results differ by about 10°C. The corresponding isotopic-exchange reaction rate is inversely proportional to the pH. Under neutral conditions the time required to reach 90% isotopic equilibrium is 500 and 2 years at 100°C and 300°C, respec- tively. Residence times of water in most geothermal reservoirs are larger.

The draw-back of this geothermometer is that mixing with sulphate-bearing, shallow ground- water oxidation of  $H_2S$  by atmospheric  $O_2$  and evaporation may modify the isotopic composi- tion of the dissolved sulphate. In these cases the isotopic signature does no longer reflect that of the deep geothermal sulphate.

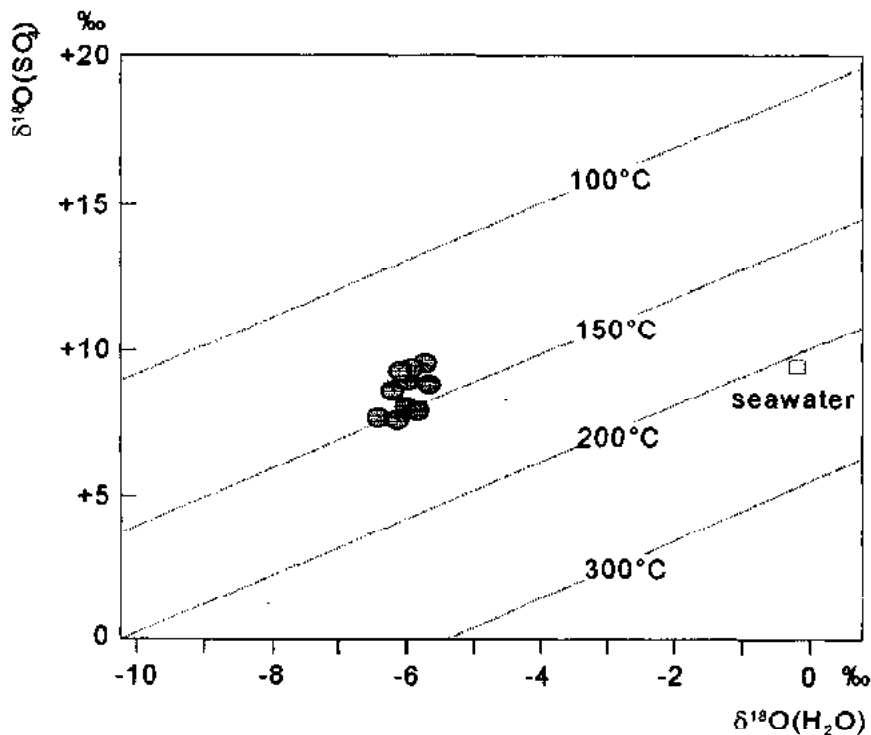


**Fig.6.5** Oxygen isotope geothermometer based on the  $SO_4-H_2O$  pair (Mizutani and Rafter, 1969). Open circles represent samples of geothermal water from the Zhangzhou geothermal field, China (from Pang and Wang, 1995).

**Case study: Zhangzhou field, China**

The Zhangzhou geothermal field is located in a Quaternary fault basin with a Mesozoic gran- ite basement. The deeply circulating thermal water has a temperature of 114°C at the well- head and 122 °C at a depth of 90 m. The water is highly saline: 12g/L of total dissolved solids

and 6g/L of  $\text{Cl}^-$ .  $\text{SO}_4$  is mainly of marine origin. Fig.6.5 shows the geothermometry results based on the  $\delta^{18}\text{O}$  values of the  $\text{SO}_4\text{-H}_2\text{O}$  pair. The estimated reservoir temperature (140–150°C) (Mizutani and Rafter 1969) is in good agreement with that obtained by geochemical modeling (Pang and Reed 1998).

### 6.1.3 TRACING THE ORIGIN AND HISTORY OF FLUIDS

Apart from geothermometry, the isotopic composition of stable isotopes in geothermal fluids and their constituents may sometimes be used to trace their origin and history.

The  $^{13}\text{C}$  value of the carbon dioxide discharged from geothermal and volcanic systems, usually in the range of -8‰ to -3‰ can be distinguished from that of  $\text{CO}_2$  from organic sediments (<-20‰) or marine limestone ( $0 \pm 1\%$ ). The  $\delta^{13}\text{C}$  value of geothermal methane usually ranges between -25 ‰ and -35‰, well above that of organically produced natural gas (-100 to -40‰). According to Galimov (1973) the carbon isotopic composition of methane depends on the stage of coalification of organic matter. Methane with  $\delta^{13}\text{C}$  values less negative than -35‰ would derive from carbonaceous matter of the late stage of catagenesis.

The  $\delta^{34}\text{S}$  values of  $\text{H}_2\text{S}$  and  $\text{SO}_4$  of the geothermal discharge also contain information on their origin. Sulphur of the primordial mantle, usually originated from basalts, has a  $\delta^{34}\text{S} \approx 0\%$  close to that of meteoritic sulphur (Rye and Ohmoto 1974). Sulphur from the crust has  $\delta^{34}\text{S}$  values ranging from +2 to +6‰; the lower values correspond to andesitic sources and the higher to rhyoliths (Giggenbach 1977). In Icelandic geothermal systems, where sulphur originates partly from seawater, higher  $\delta^{34}\text{S}$  values were found (Sakai et al. 1980).

### 6.1.4 MIXING WITH GEOTHERMAL FLUIDS

Deviations of the isotopic composition of geothermal waters from that the local meteoric water usually results from mixing of waters of different origin. Admixture of highly saline formation water or of connate water is frequently detected in lower temperature mineral springs, but may also play an important role in high temperature systems situated in sedimentary rocks. Another component may be isotopically ill-defined metamorphic water produced by dewatering of sediments (White et al. 1973).

#### Case study:

For the vapour-dominated fields of *Larderello*, Italy, and *The Geysers* a schematic model was designed of the main processes generating the observed isotopic compositions of the steam and water (Fig.6.6). It may be also applicable to other geothermal fields.

Magmatic water is the most common source for geothermal systems with close volcanic-magmatic associations. Because of the very small fractionation factor governing isotope exchange at magmatic temperatures, the  $\delta^{18}\text{O}$  value of any magmatic water is likely to be near that of the parent magma (+5 to +10‰). The  $\delta^2\text{H}$  values of basaltic water associated with



magmatic activity along divergent plate margins are between  $-60\text{‰}$  and  $-90\text{‰}$  (Allard 1983).

*Andesitic water* typical for volcanic discharges along convergent plate boundaries has  $\delta^2\text{H}$  values in the range of  $-10$  to  $-30\text{‰}$  (Sakai and Matsubaya 1977; Taran et al. 1988). The oxygen shift is often only due to simple mixing of local groundwater with  $^{18}\text{O}$  enriched "magmatic" water (Fig.6.7; Giggenbach 1989).

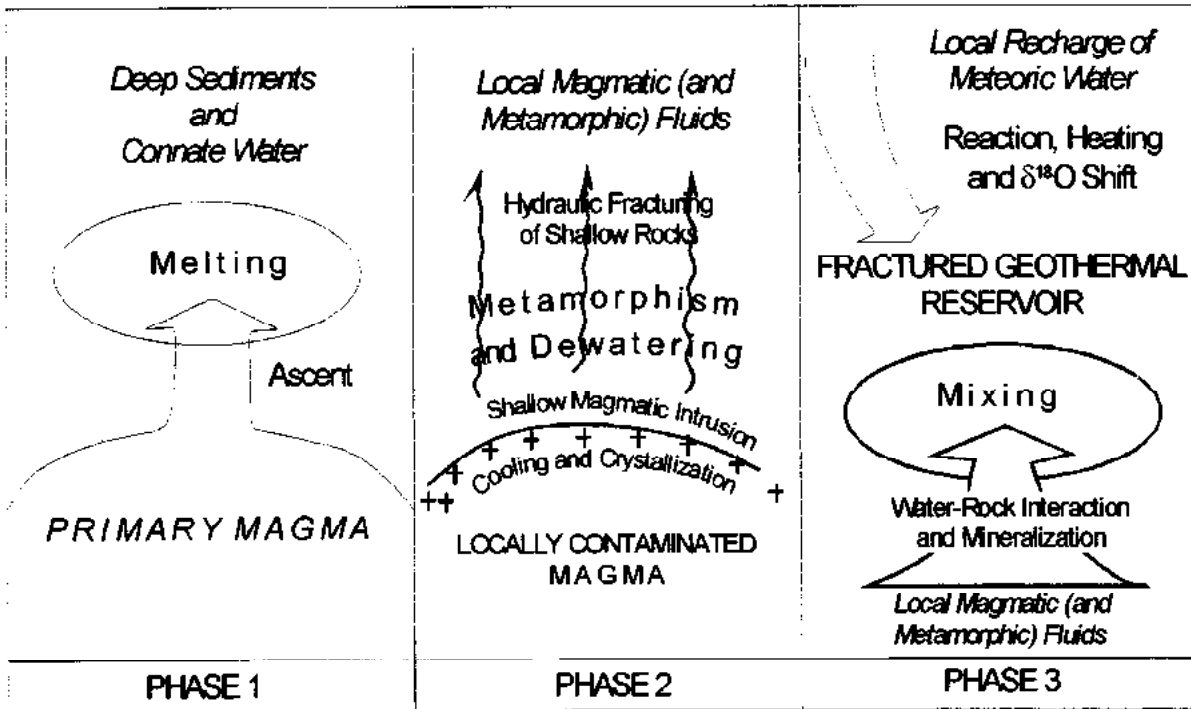


**Fig.6.6** Schematic model of the main proposed processes generating the observed isotopic composition of the steam at Larderello and The Geysers geothermal systems.

In volcanic, topographically highly variable mountainous areas, geothermal and meteoric waters may originate from different altitudes, and therefore may have different isotopic compositions. A  $\delta^{18}\text{O}$ -chloride mixing-line may allow to recognise fresh groundwater as one end member locally recharged at the highest parts of the associated volcanic structures and geothermal water as the second end member derived from precipitation onto the surrounding low altitude areas (Fig.6.7).

Assuming that the oxygen-isotope shift of a geothermal system along convergent plate boundaries is due to admixture of andesitic water, its fraction  $x_{\text{and}}$  can be estimated. The  $\delta_{\text{and}}$  value as assumed to be known ( $X_i$ ; e.g.  $\delta^2\text{H} \approx -20\text{‰}$  and  $\delta^{18}\text{O} \approx +10\text{‰}$ ) and the  $\delta_{\text{mct}}$  ( $Y$ ) and  $\delta_{\text{therm}}$  ( $X_{II}$ ) values for the meteoric water and the geothermal discharge, respectively, are measured. The two-component mixing model yields  $x_{\text{and}}$  (Eq.3.4).

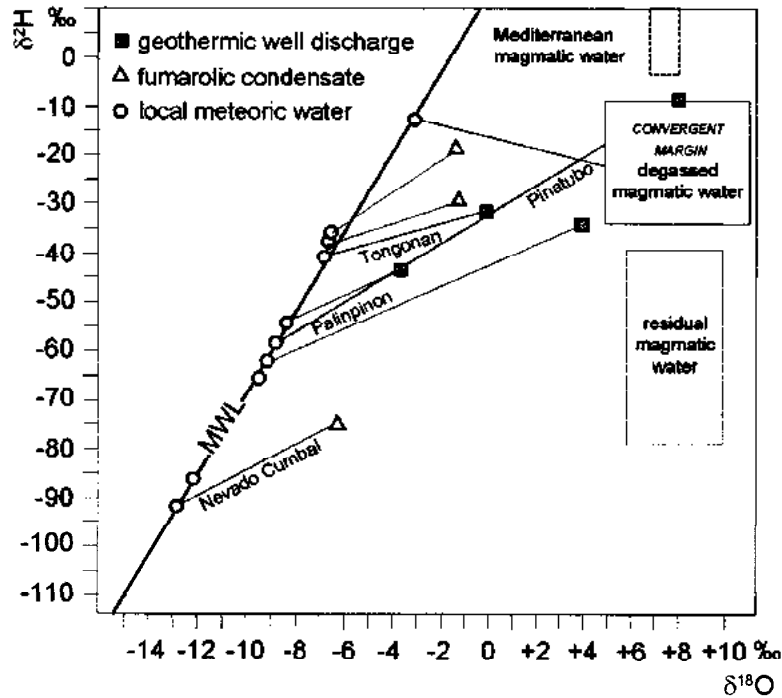


**Fig.6.7** The oxygen-isotope shift of the steam of high temperature fumaroles is often only the result of single two-component mixing shown for various areas.

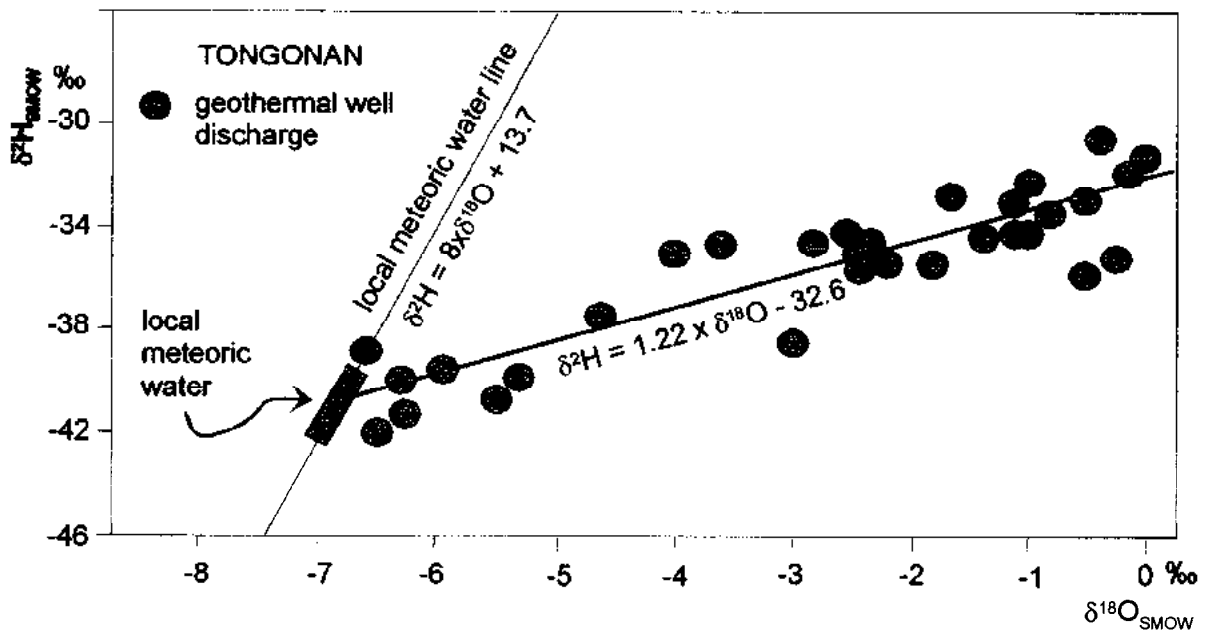


**Fig.6.8** Isotopic compositions of the steam of wells from Tongonan geothermal field, Philippines (after Alvis-Isidro et al. 1993).

**Case study:**

The slope of the  $\delta^2\text{H}/\delta^{18}\text{O}$  line is so low that is explained by mixing rather than by evaporation because of the high temperature (250 – 300°C) of the water pumped from the wells.

According to Eq.3.4, the fraction  $x_{\text{and}}$  in the least diluted waters from *El Ruiz, Amatitlan*, Wairakai, Philippines, and Ohaaki, Japan, is equal to 5 to 12%, to about +20% for Zunil and Miravalles, and to about +40% for Tongonan, Philippines.

Further downstream entries all parameters varied quite regularly: the  $\delta^{18}\text{O}$  value shifts towards less negative values, the gas/steam ratios decreased strongly and the computed temperature increased. The molal steam fraction dropped to nearly zero, corresponding with a liquid saturation of almost 100%. The presence of liquid water in the matrix rock with a temperature of up to 250°C is interpreted as condensate layer. According to the isotopic composition of the steam from the gas cap and that of the condensate layer, steam separation occurs at about 200°C. Below this layer fluids of different characteristics belong to a typical two-phase reservoir: (i) a gas/steam ratio of more than 3 times the value observed for the condensate layer, (ii) an increased steam molal fraction indicating liquid saturation as result of mixing between condensate and the two-phase layers. The isotopic composition corresponds to that of the local meteoric water.

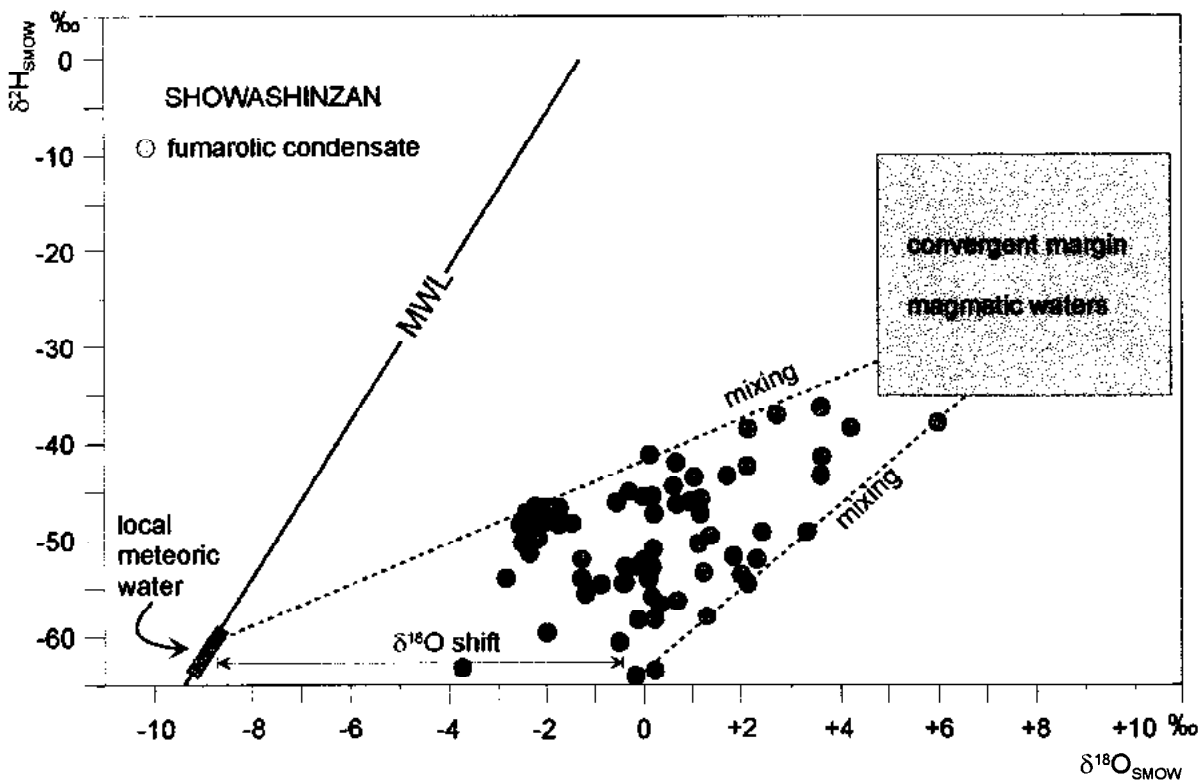


**Fig.6.9** Isotopic composition of the high-temperature fumarolic steam ("Convergent margin magmatic waters ") from Showashinzan volcano, Japan.

**Case study: Showashinzan volcano, Japan**

The isotopic composition of the high-temperature fumarolic steam from Showashinzan vol-

cano is consistent with a  $\delta^{18}\text{O}$  shift due to water-rock interaction and an admixture of local convergent margin andesitic water (Fig.6.9). A similar situation exists in the vapour-dominated fields of Larderello, Italy, and The Geysers.

Fig.6.10 shows a schematic cross section of the Volcano Island, Sicily, with fluid types and mixing from the hydrothermal system. Fig.6.11 shows the isotopic compositions of oxygen and hydrogen of water samples from shallow wells and of the condensate of high temperature fumaroles (up to 500°C) located at the rim of the crater for different years of observation. The changing temperature is explained by dilution of the magmatic vapour supported by the temporal shift of the  $\delta^{18}\text{O}$  values. The two-component mixing concept of a parent geothermal water and locally recharged freshwater is supported by the linear relationship between tritium values and chloride concentration well as the  $\delta^{18}\text{O}$  and  $\delta^2\text{H}$  values (Fig.6.12).

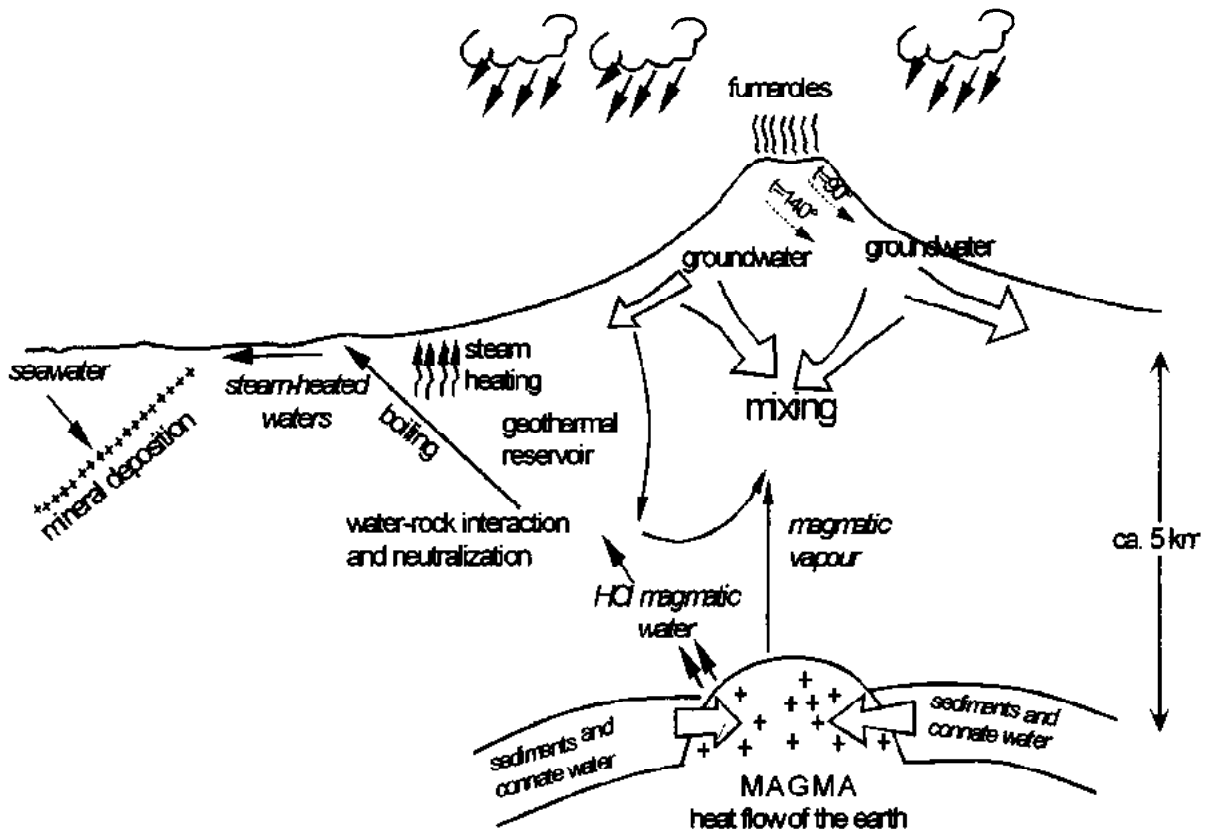


Fig.6.10 Schematic cross section (not to scale) showing fluid types, processes and regions of fluid mixing in the volcanic hydrothermal system of Vulcano Island.

## 6.2 ANTHROPOGENIC PROCESSES

### 6.2.1 STEAM LOSS

Boiling and steam loss are the most important cooling processes in geothermal systems with large surface discharge. The amount of heat loss by a phase shift is greater than that by con-

duction which is often hindered by mineral deposition in the upflow paths of the descending cold groundwater. In low temperature environments two physical processes are mainly responsible for isotopic fractionation:

- 1) subsurface evaporation and
- 2) evaporation on the surface.

Subsurface evaporation has been discussed by Giggenbach (1971) and Truesdell et al. (1977). In natural systems the convective rise of hot water to the surface produces steam as pressure decreases. Adiabatic steam production in its turn determines a decrease in temperature. The resulting isotopic compositions of the steam and water phases depend greatly on the mode of the phase separation. "*Single-step steam separation*" shows the largest isotopic effect. During fluid ascent steam coexists with the liquid phase. The two are separated at the surface in the well at the separator. This conception is also valid for hot springs and fumaroles. "*Continuous steam separation*" requires a continuous steam removal immediately after its formation (Henley et al. 1984). The isotopic fractionation effect is minimal.

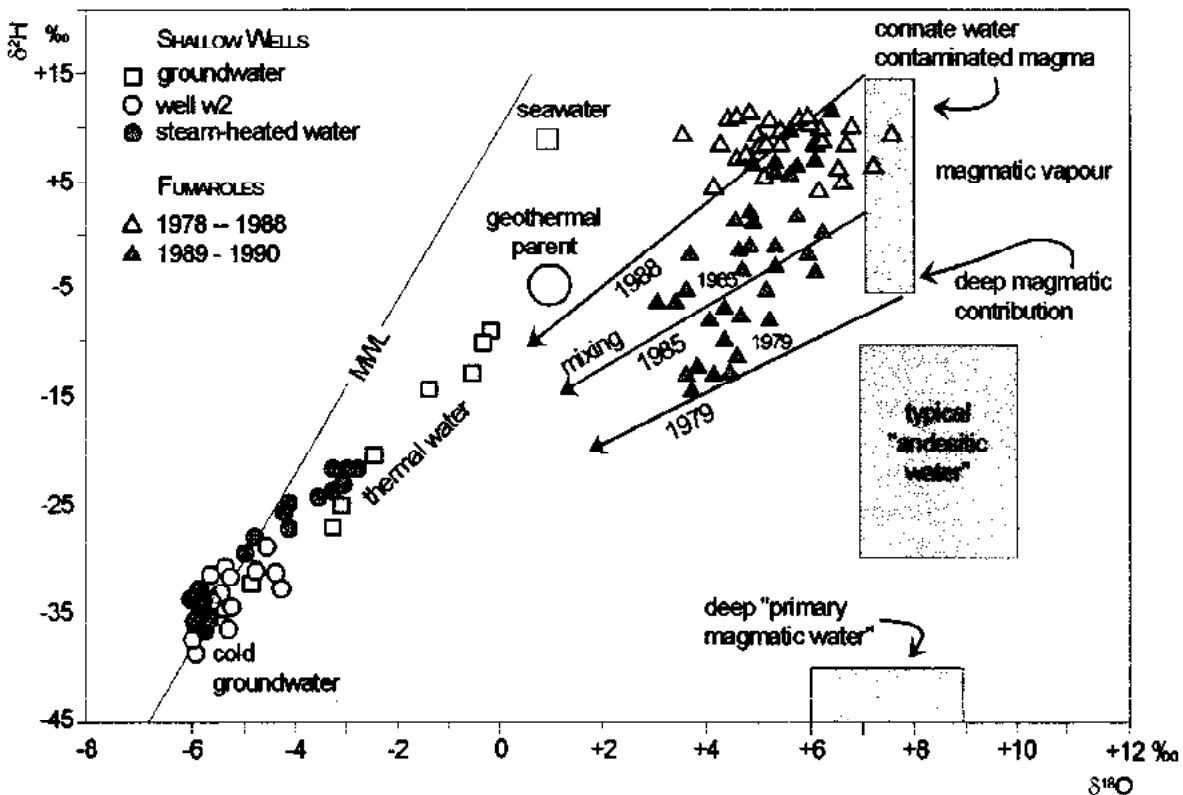


Fig.6.11 Isotopic compositions of the water from shallow wells (triangles for the condensate of the Gran Catere fumaroles). Three mixing lines are shown for different years of observation of "primary magmatic water" and andesitic water (Giggenbach 1992). The isotopic composition of the condensate of the Gran Cratere fumaroles for the period 1978 - 1990 reflects changes in the discharge temperature due to dilution of magmatic vapour (Taylor 1974).

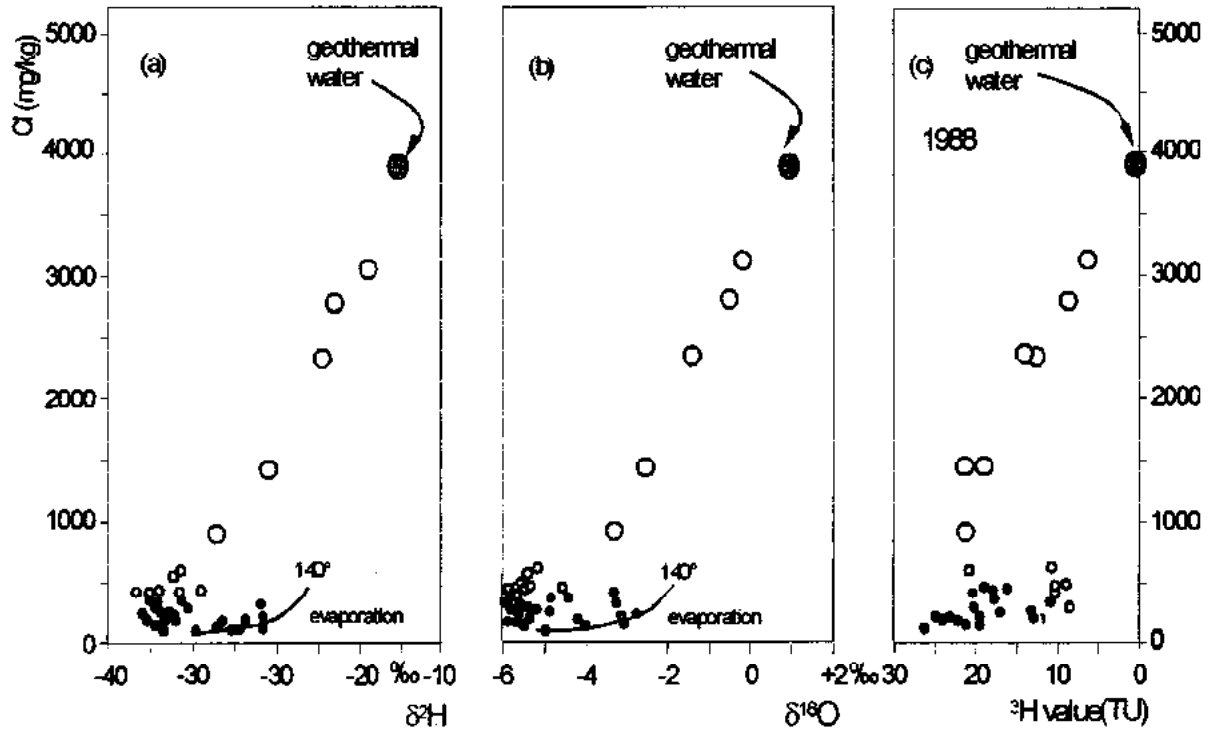


Fig.6.12  $\text{Cl}^-$  concentration versus  $\delta^2\text{H}$ ,  $\delta^{18}\text{O}$  and  $^3\text{H}$  values in well water of the Volcano Island, Sicily. The grey open circles representing the isotopic compositions of the parent geothermal water have been obtained by linear extrapolation to zero TU.

Both separation modes can be considered as extreme situations. Many examples of intermediate natural processes have been discussed for Yellowstone (Truesdell et al. 1977) and El Tatio (Giggenbach 1978) though single-step steam separation was predominant. Intermediate effects are also called "*multi-stage steam separation*" (Henley et al. 1984).

The isotopic composition of the separated steam ( $\delta_{\text{vap}}$ ) and the water ( $\delta_{\text{liq}}$ ) for the single-step process may be evaluated by the isotope balance equation (Eq.3.3) with the proportions  $x_{\text{vap}}$  and  $x_{\text{liq}}$ :

$$\begin{aligned} \delta_{\text{vap}} \cdot x_{\text{vap}} + \delta_{\text{liq}} \cdot x_{\text{liq}} &= \delta_{\text{vap}} \cdot x_{\text{vap}} + \delta_{\text{liq}} (1 - x_{\text{vap}}) = \delta_{\text{init}} \\ \text{with } x_{\text{vap}} + x_{\text{liq}} &= 1 \end{aligned} \quad (6.3)$$

where  $\delta_{\text{init}}$  represents the initial isotopic composition of the single liquid phase fluid before separation of the steam fraction  $x_{\text{vap}}$ . At the initial stage (before evaporation)  $x_{\text{vap}}$  can also be computed by the corresponding enthalpy (H) balance of the fluid and for the separation temperature of the water and steam.

$$x_{\text{vap}} = \frac{H_{\text{init}} - H_{\text{liq}}}{H_{\text{vap}} - H_{\text{liq}}} \quad (6.4)$$

Combining Eq.6.1 with Eq.6.3 allows to calculate the isotopic compositions  $\delta_{\text{liq}}$  and  $\delta_{\text{vap}}$  of

the liquid and vapour phases for different fractions  $x_{\text{vap}}$  of steam after its separation (see also Eq. 6.7).

**Example:**

Underground liquid-vapour separation in liquid dominated systems effectively is a single-step process (Giggenbach and Stewart 1982) as isotopic equilibration between water and steam is rapidly established (Giggenbach 1971). The slope  $s$  of the relationship between  $\delta^{18}\text{O}$  and  $\delta^2\text{H}$  can be approximated by

$$s = \frac{(\alpha^{2\text{H}} - 1) \cdot (\delta^2\text{H} + 1)}{(\alpha^{18\text{O}} - 1) \cdot (\delta^{18}\text{O} + 1)} \quad (6.5)$$

We assume an infiltration of meteoric water into the underground. The initial  $\delta^{18}\text{O}$  and  $\delta^2\text{H}$  values are  $-6.5\text{‰}$  and  $-42\text{‰}$ , respectively. The calculated  $\delta^{18}\text{O}$  and  $\delta^2\text{H}$  values after steam separation at different temperatures are compiled in Tab.6.3. An example is given. In the  $\delta^{18}\text{O}/\delta^2\text{H}$  plot the delta values of the residual liquid and separated vapour after loss of a fraction of steam at  $80^\circ\text{C}$  lie on a line with a slope 5.8. The  $\delta^{18}\text{O}$  value of the residual liquid will be  $-5.3\text{‰}$  and  $-4.1\text{‰}$  in the case of 20% or 40% of separated vapour, respectively.

**Table 6.3** Change of the  $\delta^{18}\text{O}$  and  $\delta^2\text{H}$  values by water/steam separation as function of the temperature and the percentage of the separated steam fraction.

temp °C	residual liquid		slope	separated steam fraction			
	$\delta^{18}\text{O}$ ‰	$\delta^2\text{H}$ ‰		20%		40%	
				$\delta^{18}\text{O}$		$\delta^2\text{H}$	
80	6.03	36.8	5.8	-5.3	-4.1	-34.8	-27.6
120	4.54	21.7	4.6	-5.6	-4.7	-37.7	-33.4
220	2.10	0.1	0.0	-6.1	-5.7	-42.0	-42.0
260	1.46	-3.6	-2.4	-6.2	-5.9	-42.7	-43.5

Column 1 contains the separation temperature of the steam, columns 2 and 3 list the  $\delta^{18}\text{O}$  and  $\delta^2\text{H}$  values of the residual liquid, respectively. Column 4 compiles the slope and the columns 5 and 6 as well as 7 and 8 contain the  $\delta^{18}\text{O}$  and  $\delta^2\text{H}$  values for separated steam fractions of 20% and 40%, respectively.

At  $220^\circ\text{C}$  and above the fractionation factor of hydrogen isotopes shows an "inversion" while the isotopic fractionation of oxygen further decreases.

Truesdell et al. (1977) and Henley et al. (1984) developed an approach for the more complex situation of a continuous steam separation to compute the isotopic enrichment of residual liquid water with respect to initial water. The isotopic composition of the residual liquid water differs for the single step and continuous steam separation modes if the initial and final temperatures differs by more than 150°C.

While the subsurface evaporation is governed by the equilibrium constant  $\alpha$ , evaporation from surface water is controlled by kinetic fractionation (Volume I). The isotopic compositions of rapidly flowing thermal water as usual in thermal springs are not greatly affected by evaporation. During the initial exploration phase, steam-heated pools may be present of which isotopic composition is indirectly related to those of the deep supply water. Steam-heated water is also common in the superficial zone of geothermal systems where boiling occurs in the reservoir as indicated by high sulphate to chloride ratios and low pH. This water originates from the condensation of rising steam from the underlying reservoir into deep groundwater. This steam-heated water may boil and lose mass. A steady-state model allows to calculate the isotopic composition.

A pool with initially cold shallow groundwater is heated by geothermal steam. The isotopic composition of this groundwater ( $\delta_{\text{init}}$ ) and that of the water leaving the pool ( $\delta_{\text{dis}}$ ) allow to calculate the delta value of the steam ( $\delta_{\text{vap}}$ ) entering the pool for heating:

$$\delta_{\text{vap}} = \delta_{\text{init}} + (\delta_{\text{dis}} - \delta_{\text{init}}) \cdot x_{\text{vap}} + (1 - \beta) \quad (6.6)$$

where  $x_{\text{vap}}$  is the fraction of vapour entering the pool (considered equal to that leaving the pool) and  $\beta$  is the overall fractionation factor given by

$$\beta = \alpha_{\text{liq-vap}} \cdot \left( \frac{D_{\text{H}_2\text{O}}}{D_{\text{isot}}} \right)^n$$

where  $\alpha$  is the equilibrium fractionation factor between liquid water and steam,  $D/D_{\text{isot}}$  the ratio between the diffusion coefficients in air of  $\text{H}_2\text{O}$  and  $^1\text{H}^2\text{HO}$  or  $\text{H}_2^{18}\text{O}$ , respectively.  $n$  is an exponent related to the Rayleigh distillation. For a temperature below 100°C  $\alpha = 1.024$  and  $= 1.028$  for O and H, respectively (Merlivat 1970). The exponent  $n$  ranges from 0 (equilibrium) to 0.578 for kinetic fractionation (Stewart 1975). More complex models considering Rayleigh distillation and even more complicated processes are discussed by Giggenbach and Stewart (1982).

### 6.2.2 UNDERGROUND LIQUID-VAPOUR SEPARATION PROCESSES

During the temperature rise to values in excess of 100°C the vapour pressure will at a certain stage exceed the hydrostatic pressure, and the geothermal water will start to boil. The associated vapour separation process is accompanied by isotopic fractionation. The heavy isotopes,  $^2\text{H}$  and  $^{18}\text{O}$ , become enriched in the liquid phase and the separated vapour phase becomes



isotopically depleted. For deuterium this holds true for each temperature below 220°C. At higher temperature <sup>2</sup>H remains preferentially in the vapour phase.

Apart from the temperature, the isotopic compositions of the separated liquid depend on the fraction  $x_{\text{vap}}$  of the formed vapour, and can be calculated for single mode separation of vapour at a given temperature, continuous vapour separation, a separation process which is described by the Rayleigh fractionation or isothermal batch evaporation (Giggenbach and Stewart 1982). The latter process is active for sudden decompression or in vapour-dominated systems with small fraction of liquid suspended in pores (D'Amore and Truesdell 1979).

**Case Studies: Wairakei Geothermal Field, Philippines**

Fig.6.13 illustrates the theoretically expected and actually observed effects of vapour separation in natural water and steam discharged from the Wairakei geothermal field (Giggenbach and Stewart 1982).

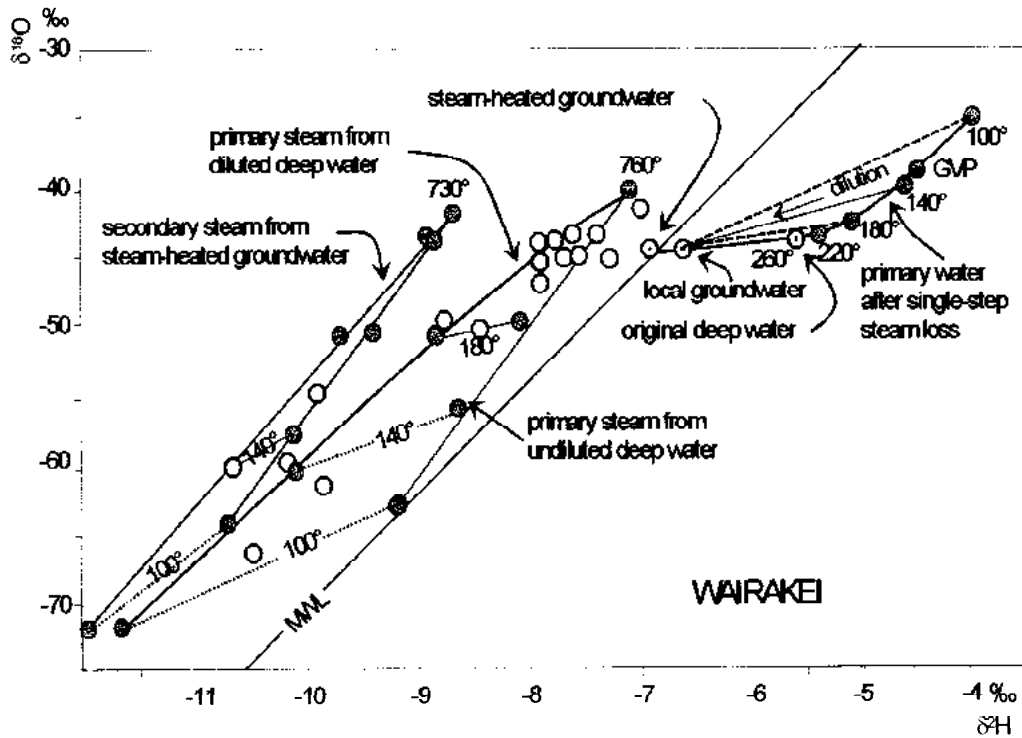


**Fig.6.13** The isotopic compositions of steam and water formed from an initial 260°C warm deep groundwater at various temperatures after dilution with local groundwater from the Wairakei geothermal field, Philippines. Single-step vapour separation is assumed. Open circles are data points for fumarolic steam samples (Giggenbach and Stewart 1982).

The isotopic compositions of the residual water after removal of steam at 220°, 180°, 140° and 100° from a deep water with an initial temperature of 260°C are shown by the curved line marked "primary water" after single-step steam loss. The effect of dilution by surface water is indicated by lines connecting the separated water to the local groundwater. The isotopic com-

position of the dominant natural chloride-water discharge from the Wairakei field, Geyser Valley Pool, GVP, prior to exploitation, plots on the steam-loss line at a temperature of about 135°C. For such a surface discharge, a separation temperature of about 100°C would be expected. Preservation of the deeper separation composition is likely to be due to some conductive cooling, reducing the amount of steam produced from the boiling pool.

The lower  $\delta$  values for fumaroles point to secondary processes as e.g. steam separation from pre-diluted water. In this case, the separation temperature is likely lower, though the isotopic composition of the water before steam separation is shifted to lower  $\delta$  values (connecting "dilution" line between the deep primary water and local groundwater). The line "primary steam from diluted deep water" represents the isotopic composition of the steam formed from a pre-diluted water. Most of the data points fall within the area representing steam from undiluted to diluted primary water. The few samples with even stronger isotopic depletion represent secondary steam separated from steam-heated bicarbonate water frequently formed at the margins of geothermal fields (Hedenquist 1990).

Fig. 6.14 shows the effect of steam loss at 280 - 290°C from a primary deep geothermal water in the Cl/ $\delta^{18}\text{O}$  diagram for some wells of the *Berlin geothermal field*, El Salvador. Mixing with fresh shallow groundwater is obvious.

The above examples demonstrate the wide range of isotopic compositions of natural geothermal surface discharge. It may come from a single source of deep groundwater and caused by underground steam-vapour separation and dilution. The wide range provides the basis for a powerful tool to reconstruct deep hydrological processes active within a geothermal system during the early stage of exploration when only surface water can be sampled and analysed.

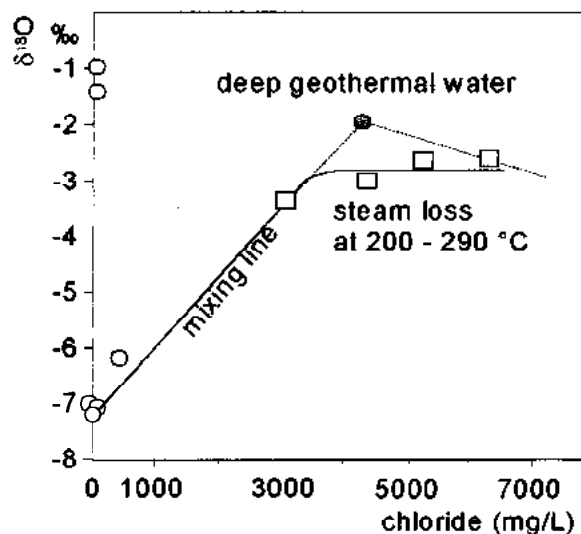


**Fig.6.14** The relationship between chloride concentration and  $\delta^{18}\text{O}$  value of the geothermal fluid from the Wairakei geothermal field, Philippines, may be interpreted as mixing between shallow groundwater and deep andesitic groundwater.

Geothermal groundwater of high temperature cools as it rises to the surface by conduction, mixing and boiling. Each of these processes is separately traced by the isotopic (and chemical) composition. The process of boiling can be easily monitored by a change in the isotopic composition.

**Conductive heat loss.** During ascent of liquid water with conductive heat loss the hydrogen composition is not changed as there is no other hydrogen containing material. The oxygen isotopic composition may slowly change due to water-rock interaction with oxygen bound in the rocks (e.g. carbonate, sulphate) at a temperature well below 220°C. Conductive cooling is assumed to be important for springs with discharge rates of less than 1 L/sec.

**Mixing with cold water.** Admixture of cold groundwater can be identified by an isotopic composition falling along the meteoric water line. It is very common in hot spring systems before or after boiling. The source may be locally recharged groundwater of large depth and from far away (up to 100 km).

**Boiling and steam loss** are the most important cooling processes in high temperature geothermal systems with large surface discharge. The loss of heat is greater than by conduction, and because mineral deposition seal supflow paths from invading cold groundwater.

For the calculation of the effect of single stage separation at spring water at a temperature of 100°C we assume a temperature of the reservoir water of 260°C and  $\delta^{18}\text{O}$  and  $\delta^2\text{H}$  values of -5‰ and -40‰, respectively. From Table 6.1 follows  $1000 \times \ln \alpha_{100^\circ\text{C}}$  equals 5.24 and 27.8 for oxygen and hydrogen isotopes, respectively.

The enthalpy and isotopic balances are given analogous to Eq.3.3 by:

$$H_{1260^\circ\text{C}}^* = x_{\text{vap}} \cdot H_{1100^\circ\text{C}}^* + (1 - x_{\text{vap}}) H_{1100^\circ\text{C}}^*$$

$$\delta_{1260^\circ\text{C}} = x_{\text{vap}} \cdot \delta_{1100^\circ\text{C}} + (1 - x_{\text{vap}}) \delta_{1100^\circ\text{C}}$$

Using the figures in Table 6.4 we calculate the steam fraction  $x_{\text{vap}}$  at the surface by combining the isotope balance equations with the equations derived earlier and obtain

$$\delta_{\text{liq}}(100^\circ\text{C}) = \delta_{\text{liq}}(260^\circ\text{C}) + x_{\text{vap}} \ln \alpha \quad (\times 1000\text{‰}) \quad (6.7)$$

From the value of  $x_{\text{vap}}$  and  $\ln \alpha$  we obtain  $\delta^{18}\text{O}_{\text{liq}}(100^\circ\text{C})$  and  $\delta^2\text{H}_{\text{liq}}(100^\circ\text{C})$  of -3.33‰ ( $\equiv -0.00333$ ) and -31.3‰ ( $\equiv -0.0313$ ), respectively.

### 6.2.3 ISOTOPE TECHNIQUES IN RE-INJECTION STUDIES

The chemical composition of the waste water produced in large quantities from geothermo-electric power-plants is such (high concentrations of ammonia, boric acid and sulphides) that it cannot be discharged into the runoff of rivers. The problem of getting rid of these polluting effluents has been solved by re-injecting the waste water back to the underground at some suitable sites of the geothermal field. This procedure may also be useful for an artificial re-

charge of the field. It partly compensates the natural fall of the reservoir pressure caused by the negative hydrological balance between exploited groundwater and the often limited natural recharge.

In order to avoid eventually irreversible negative effects of re-injection in the field, some experiments must be made prior launching the full-scale re-injection. Apart from radioactive isotopes the stable isotopes of oxygen and hydrogen are suitable to trace quantitatively the underground pathways of the re-injected waste water within the geothermal field (Nutti et al. 1981).

The turbine steam is partly condensed in cooling towers but a considerable part is lost to the atmosphere. During this process the residual water is enriched in the heavy isotopes  $^2\text{H}$  and  $^{18}\text{O}$ . As the isotopic composition of the injected water differs from that of the local groundwater the system can be systematically monitored throughout the re-injection test.

The isotopic compositions of the undisturbed groundwater are variable with time due to a variable contribution of the steam sources (condensate layer, two-phase layer) and areal fluid redistribution. In previously non-exploited areas, the isotopic effect of re-injection are overlapped by the natural temporal evolution of the  $\delta^{18}\text{O}$  value towards more negative values, and of the gas/steam ratio (= *steam saturation G/S*) towards higher values (Box et al. 1987).

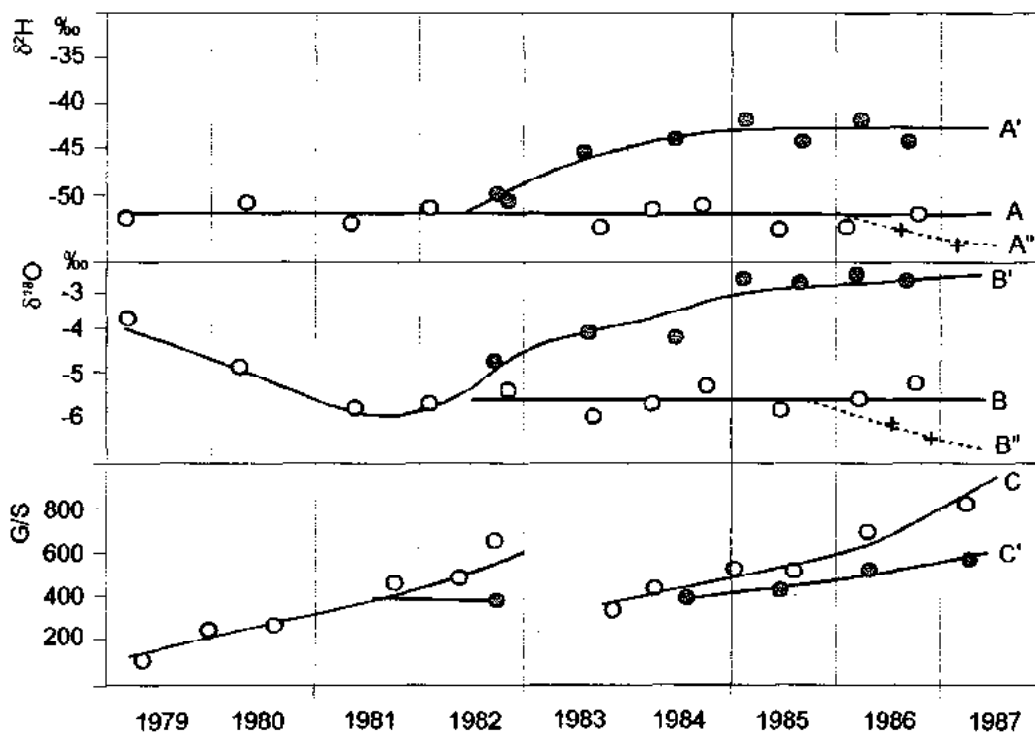


**Fig.6.15** Temporal and re-injection induced variations of the  $\delta^{18}\text{O}$  and  $\delta^2\text{H}$  values as well as the G/V ratio. Lines A, B and C (open circles) represent the variation in wells not affected by re-injection. Lines A', B' and C' (full circles) represent the variation in wells affected by re-injection. Lines A'' and B'' represent the variation induced by cooling.

The isotopic compositions of the other component of the admixed injected waste water is also variable (mass loss in the cooling tower and isotopic fractionation due to partial re-evaporation of re-injected water). Under such a complex situation it is likely to obtain data which do not fit simple straight mixing lines (Fig.6.15).

$^2\text{H}$  is the parameter least affected by fractionation (fractionation factor  $\alpha$  is close to 1 at boiling temperatures near  $220^\circ\text{C}$ ), by any kind of water-rock interaction, or by areal fluid displacement. As a consequence,  $\delta^2\text{H}$  values allow to evaluate the relative contribution of the original vapour and injection-derived steam. They also trace the flow paths of steam produced by injected water and the relative contribution to production of this steam (Nuti et al. 1981).

D'Amore et al. (1988) studied the following phenomena in a reservoir:

- 1) mixing of original steam with re-injected steam, and the isotopic fractionation during steam production from re-injected water,
- 2) effects of fluid redistribution (displacement), where areal gradients of the isotopic composition and gas/steam ratio exist, and
- 3) cooling of the rock matrix.

All these processes have to be taken into account when the proportion of the injected water is estimated for the surrounding wells. Depending on the number of measurements available  $\delta^{18}\text{O}/\delta^2\text{H}$  and gas/steam/ $\delta^2\text{H}$  diagrams may permit a quantitative calculation of the contribution of steam from the different sources and an assessment of eventual cooling effects in the reservoir matrix.

#### **Case Studies: Larderello geothermal field, Italy**

The temporal variation of the isotopic compositions and the gas/steam ratio in the Larderello geothermal field during three experiments of re-injection is shown in Fig.6.16. These experiments yielded mixing lines for the  $\delta^2\text{H}$  and  $\delta^{18}\text{O}$  values of the initial water and those of the steam separated from the re-injected condensate (Fig.6.17).

#### **6.2.4 VARIABILITY OF THE ISOTOPIC COMPOSITION IN GEOTHERMAL FLUID**

In any geothermal field the isotopic composition of the discharged water and/or steam varies locally. Rain water infiltrated through permeable rocks, spring water and groundwater pumped from wells are usually of meteoric origin. Along the underground flow in a geothermal field the  $\delta^{18}\text{O}$  value of the groundwater may increase due to progressive isotopic exchange with increasing distance from the recharge area. Differences in the chemical and isotopic compositions at different localities in the Larderello geothermal field are interpreted in such a way for the lateral steam flow from central boiling zones (upflow points) toward the edges of the system before the start of exploitation.

Fig.6.18 shows a scheme of the lateral steam movement and condensation in vapour dominated systems. During this lateral flow partial condensation occurs as well as conductive heat loss through the surface. Gases are concentrated in the residual steam, while volatile salts are slowly removed into the condensate ( $H_3BO_3$ ,  $HCl$ ). This process is modelled as a Rayleigh

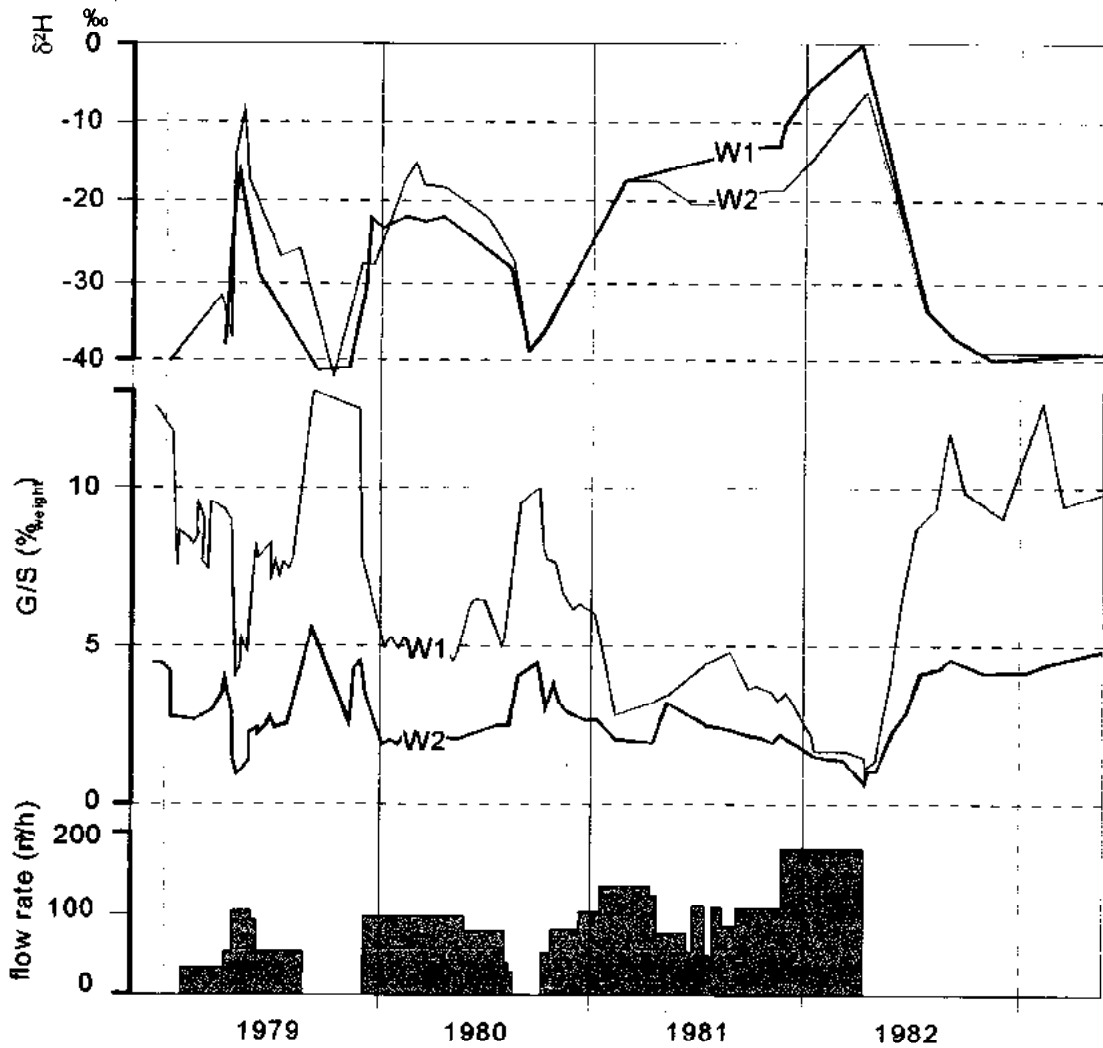


**Fig.6.16** Temporal variation of the  $\delta^2H$  and  $\delta^{18}O$  values as well as of the gas/steam ratio monitored in two wells W1 and W2 of the central area during and after re-injection tests. Undisturbed pre-reinjection values and low-rate of injected water are shown. I, II and III refer to the three re-injection periods.

condensation obeying the equation

$$C_{\text{vap}} = C_{\text{init}} \cdot \left( \frac{\Gamma_{\text{vap}}}{\Gamma_{\text{init}}} \right)^{\frac{1}{k-1}} \quad (6.7)$$

where  $c_{vap}/c_{init}$  is the ratio of the concentration of a steam component to its original concentration at any point, and  $r_{vap}/r_{init}$  the ratio of the corresponding fractions  $r$  of condensed steam.  $k$  is the distribution coefficient of the component between steam and water ( $c_{vap}/c_{init}$ ).

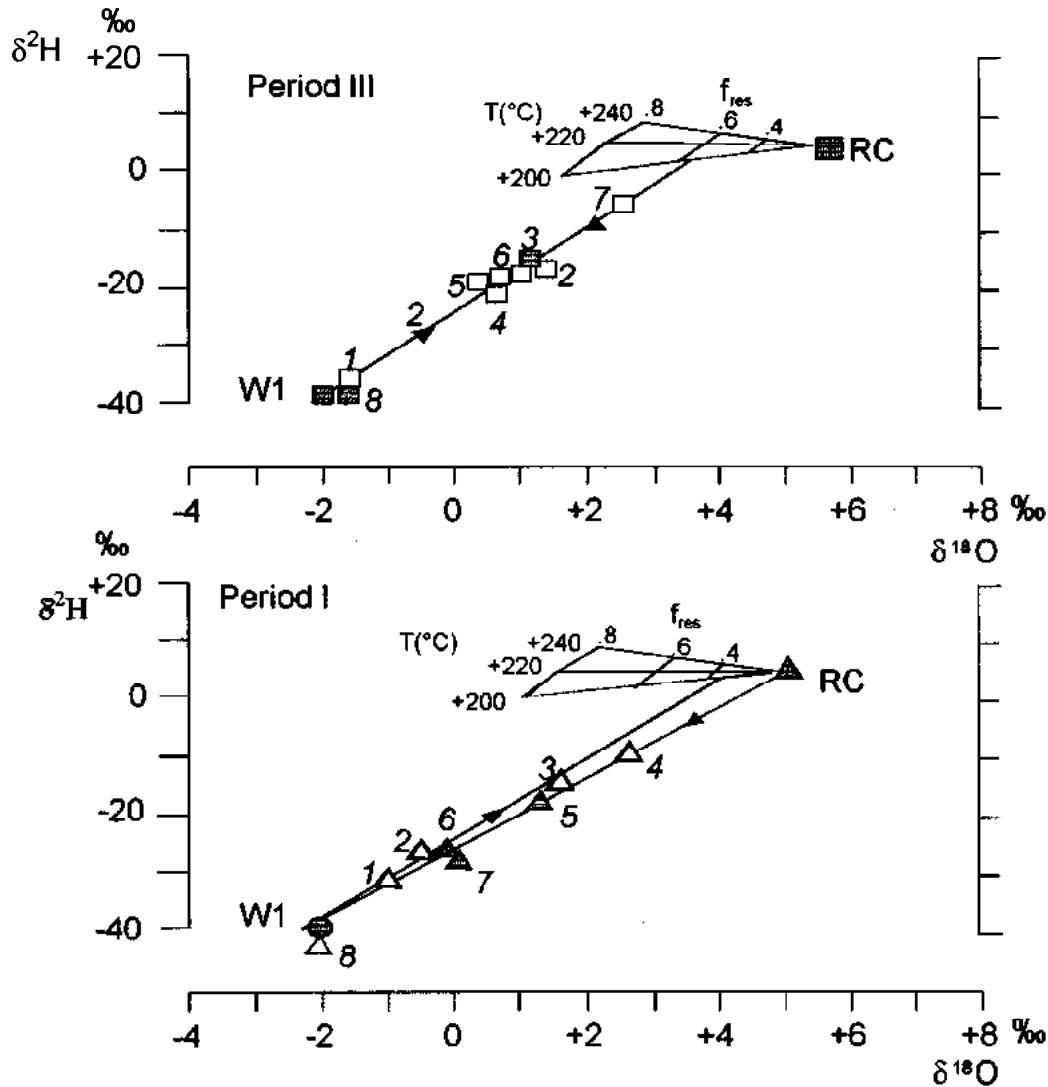


**Fig.6.17** Variation of the  $\delta^{18}O$  and  $\delta^2H$  values of the fluid pumped from well W1 during three succeeding test periods shown in Fig.6.16 for well RC (central area). The different isotopic compositions of the monitored waters are reported together with the theoretical isotopic pattern of the steam produced by re-injected water, assuming continuous steam separation at depth:

$$\delta_{vap} = \delta_{init} + \{(1 - f_{res})^{\alpha - 1} - 1\}$$

Since the actual evaporation temperature and the fraction of residual water are unknown, calculations were made for three different temperatures and fractions  $f_{res}$  of residual liquid water after boiling. Progressive numbers indicate the chronological sampling order during the test (open symbols) and after the test (solid symbols).

For  $\delta^{18}\text{O}$  the equation of condensation can be expressed as:

$$\delta_{\text{vap}} - \delta_{\text{liq}} = \left[ \left( \frac{r_{\text{vap}}}{r_{\text{liq}}} \right)^{\alpha_{\text{liq-vap}} - 1} - 1 \right] \times 1000\text{‰}$$

Fig.6.19 shows the calculated results (Eq.6.7) for  $k = 0.05$  to 1000. The magnitude of the variation at Larderello geothermal field, Italy, (-3‰ in  $\delta^{18}\text{O}$ , 5 and 3 times in  $\text{CO}_2$  and  $\text{NH}_3$  concentrations) suggests that the productive field is limited by excessive liquid water and non-condensable gas after 80% of the original steam flow has condensed. At The Geysers, a 7‰ decrease in  $\delta^{18}\text{O}$  and a 17 times increase in  $\text{CO}_2$  are expected at 95% condensation.

Fig.6.20 shows the observed concentration profiles of different species in steam along a line through the northern Larderello Field, far from recharge areas. It reflects the disturbance due to the well discharge.

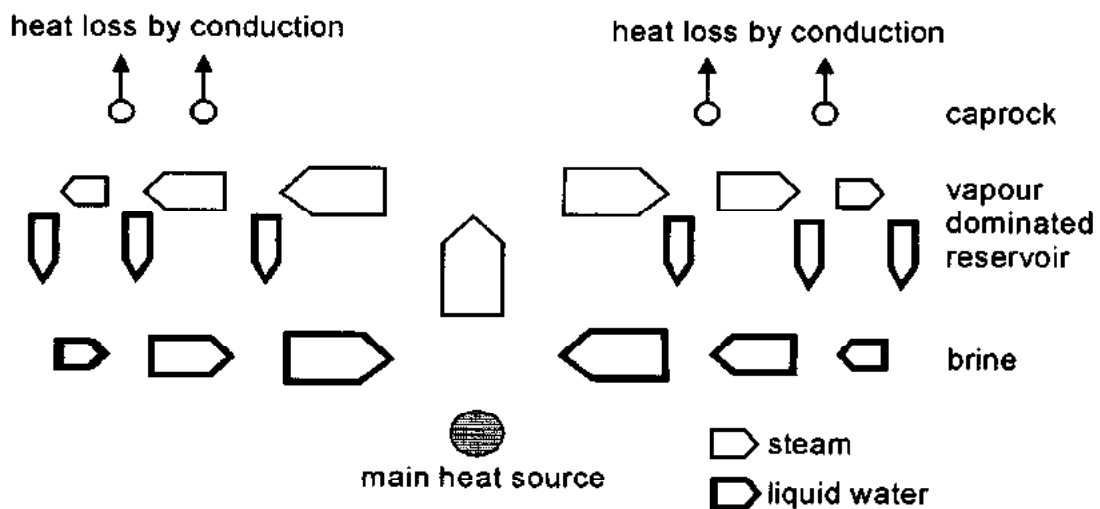


**Fig.6.18** Lateral steam movement and condensation in vapour-dominated geothermal systems.

Another common process in geothermal spring systems is mixing of the ascending geothermal water with varying proportions of local groundwater. The former will be enriched in heavy isotopes because of the  $\delta^{18}\text{O}$ -shift and/or steam loss as described before. An additional process resulting in isotopic changes is artificially caused by re-injection of waste water from geothermal power plants (Sect.6.2.3).

A variation of the isotopic composition of the steam with time is observed in exploited geothermal fields mainly due to re-injection. It may be, however, also be caused by the mode of fluid production. As in geothermal fields strong spatial variation of the isotopic composition is observed, the widening of the area affected by steam production has the same effect.



The  $\delta^{18}\text{O}/\text{Cl}$  relationship of the waters in the Palinpinon field, Philippines (Fig.6.21) after several years of exploitation reflects mixing processes due to re-injection of water, admixture of meteoric water and acidic- $\text{SO}_4^{2+}$  water.

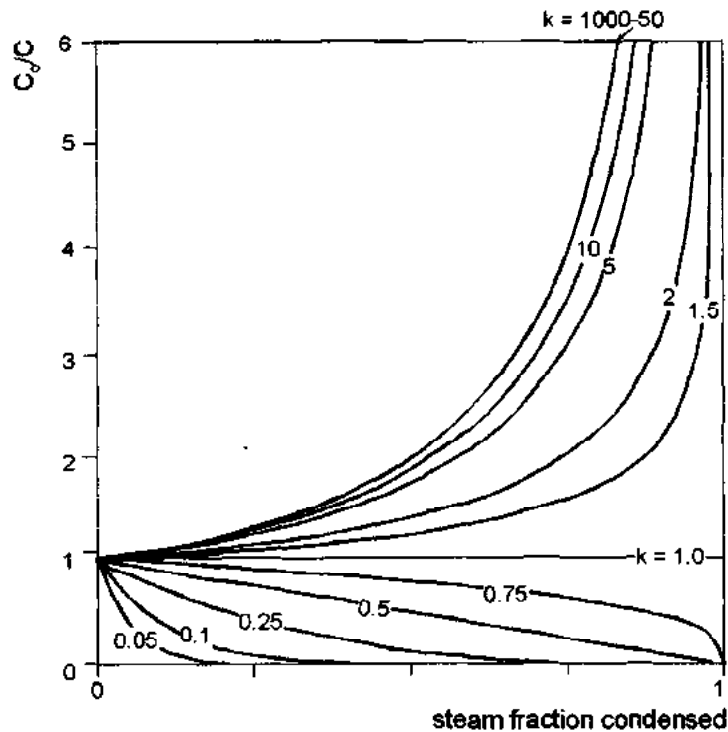


Fig.6.19 Results obtained from the Rayleigh condensation equation for  $k=0.05$  to 1000 for the Larderello Geothermal Field.

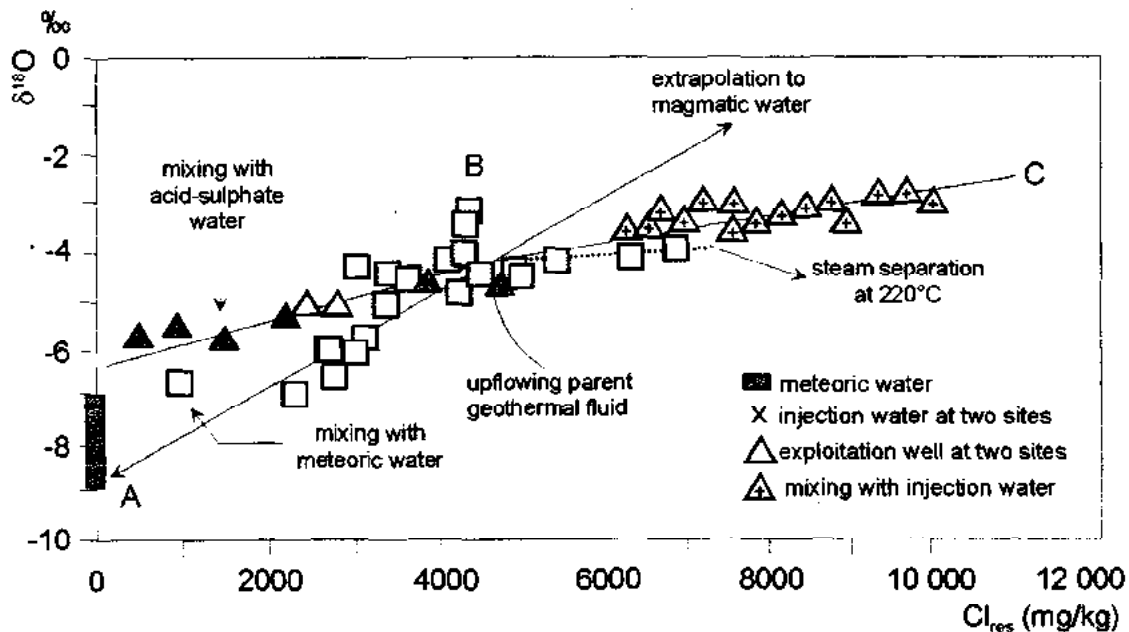
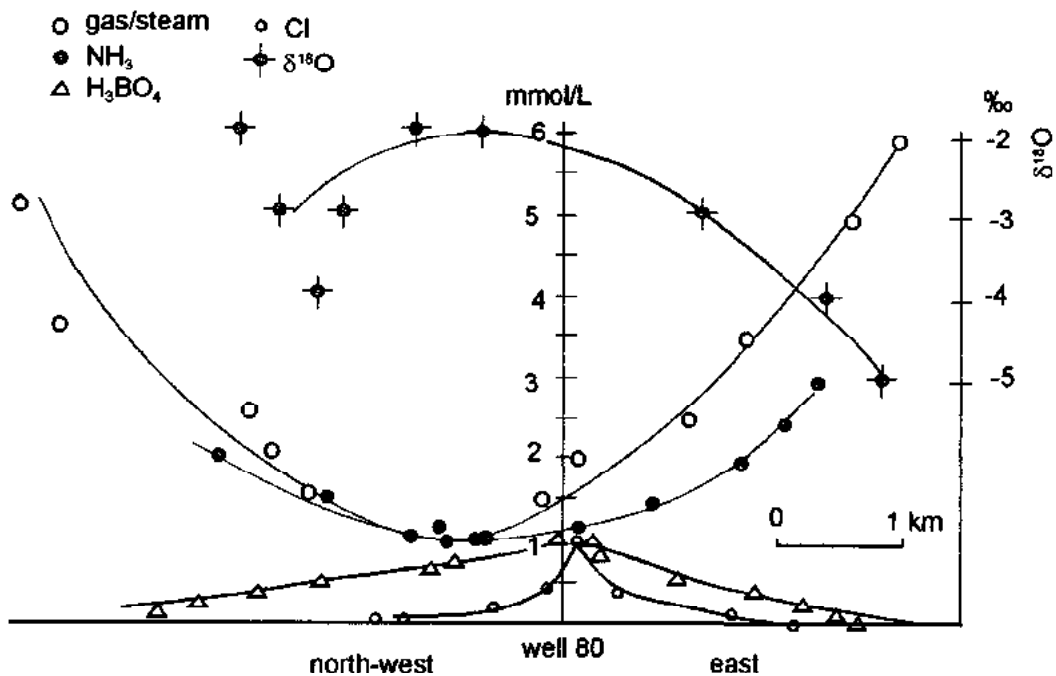


Fig.6.20 Measured and calculated vertical distributions of the  $\delta^{18}\text{O}$  value, the gas/steam ratio, the temperature  $T$  and the proportion  $x_{\text{vap}}$ .

During drilling in exploited and previously non-exploited parts of The Geysers geothermal field, the steam chemistry was monitored in six new wells at different depths down to 2000 m. Samples were taken from steam entries at non-connected fractured zones. A vertical zonation of the chemical and isotopic compositions in the reservoir fluids were found (Fig.6.22).

In the short interval of the first steam entry, both  $\delta^{18}\text{O}$  and  $\delta^2\text{H}$  values were more negative than in the surrounding productive wells. The gas/steam ratio and the temperature were measured at the well head. The molal steam fraction was computed from the chemical gas analyses (D'Amore and Truesdell 1985). The gas/steam ratio was at least one order of magnitude higher than that of the fluids normally delivered by productive wells. The calculated temperature was  $< 200^\circ\text{C}$ , while the molal steam fraction was close to 100%, indicating an extremely low liquid saturation. The reactive gases are in chemical equilibrium at relatively low temperature. This observation has been interpreted as a local upper gas cap.



**Fig.6.21** Chloride/ $\delta^{18}\text{O}$  relationship of geothermal water reflecting admixture of ascending parent water (near B), dilution and steam separation prior to exploitation of The Geysers geothermal field. The origin of the parent water is mixed meteoric (indicated by detectable  $^3\text{H}$ ) and magmatic waters (trend line AB:  $\delta^{18}\text{O} = 8.16 \times 10^{-4} \text{Cl} - 7.9$ ). During exploitation mixing between geothermal fluids, injected water (trend line BC:  $\delta^{18}\text{O} = 3 \times 10^{-4} \text{Cl} - 5.8$ ), and acidic  $\text{SO}_4$  fluids occurs.

Further down steam entries all parameters varied quite regularly: the  $\delta^{18}\text{O}$  value shifts towards less negative values, the gas/steam ratios decreased strongly and the computed temperature increased. The molal steam fraction dropped to nearly zero, corresponding with a liquid saturation of almost 100%. The presence of liquid water in the matrix rock with a temperature of up to  $250^\circ\text{C}$  is interpreted as condensate layer. According to the isotopic composition of the

steam from the gas cap and that of the condensate layer, steam separation occurs at about 200°C. Below this layer fluids of different characteristics belong to a typical two-phase reservoir: (i) a gas/steam ratio of more than three times the value observed for the condensate layer, (ii) an increased steam molal fraction indicating liquid saturation as result of mixing between condensate and the two-phase layers. The isotopic composition corresponds to that of the local meteoric water.

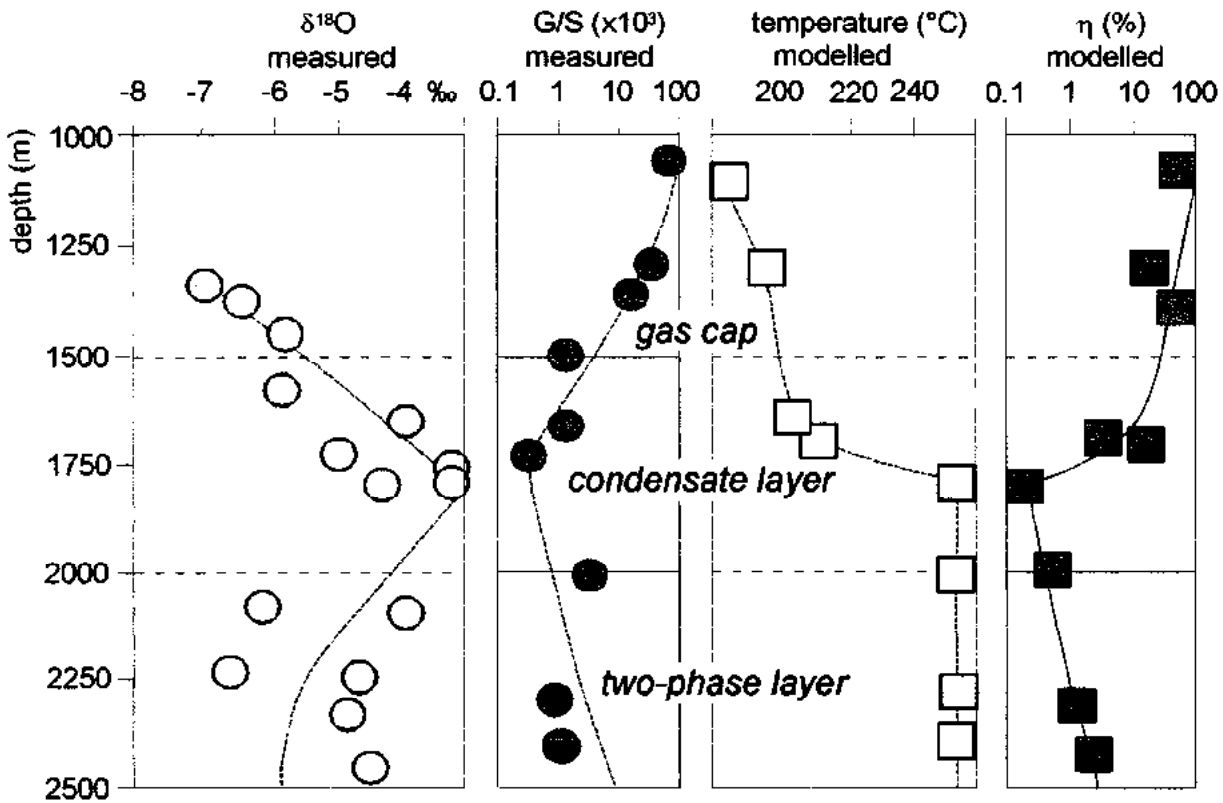


**Fig.6.22** Measured and calculated vertical distributions of the  $\delta^{18}\text{O}$  value, the gas/steam ratio, the temperature  $T$  and the relative molar steam fraction  $\eta$  for the The Geysers geothermal field.

D'Amore and Truesdell (1979) hypothesised different fluid sources at different depths which may contribute in different and time-dependent proportions to the total production. Usually the gas cap is exhausted after a short time. As the contribution from the condensate layer decreases in new wells in previously exploited areas, the two-phase reservoir gradually becomes the most important productive level. The temporal variation of the isotopic compositions in steam of wells located in the south-eastern area of The Geysers geothermal field is interpreted as a result of a changing contribution of fluid from admixed different sources.

# 7 PLANNING AND PERFORMANCE OF MULTIPLE ISOTOPE STUDIES

In Fig.3.1 (Chapter 3) the most simple geohydraulic conditions are shown, described by the piston-flow model and the exponential model. In nature the conditions are generally more complicated. Young water may be admixed to very old water. Leakage between aquifers may result in mixtures of differently old groundwaters. In such cases measured and modelled isotope data often deviate from each other. To overcome this problem trial and error procedures are applied using different model conceptions (e.g. by applying the MULTI program; Richter et al. 1993). A final agreement between these two values does not mean that the model is a good reflection of natural conditions (Oereskes et al. 1994; Maloszewski and Zuber 1993, 1998).

There are many attempts to express a close agreement between modelled and measured isotope data as a good approximation of the actual situation. An example is the long-term record of the stable isotopic composition of the Fijeh spring in the Antilebanon mountains (Kattan 1996b). Even a slight disagreement shows that a model cannot be applied and a completely deviating geohydraulic constellation may exist. In this case the approximate estimate of a mean residence time is hydrogeologically misleading. The proposed explanation of the deviation between the model and the observed isotopic composition is then unsatisfactory (Fig.7.1).

In order to understand the hydrogeological system two or even more independent isotope determinations are required, combined with hydrochemical analyses. The fact is that the applicability of the model is not proven by an apparent agreement between the model result and the data obtained. As the above mentioned example demonstrates that a long-term monitoring of one isotope instead of multiple isotope analyses may give evidence for such disagreement. On the other hand, it still may not allow to understand the actual geohydraulic situation of the system. Hence serious case studies in isotope hydrogeology usually consist of a wide spectrum of techniques (e.g.  $^3\text{H}$ ,  $^{14}\text{C}$ ,  $^{36}\text{Cl}$ ,  $^{85}\text{Kr}$ ; Bath et al. 1979; Andrews et al. 1984; Phillips et al. 1989; Verhagen et al. 1991), in order to describe a realistic geohydraulic situation with more than one groundwater component. The occurrence of groundwaters of different age in the same hydraulic system requires independent information on different time scales. That is why *multiple-isotope analyses* are usually essential. An example is the determination of the mean residence time (MRT) of young groundwater by means of the exponential model or any other lump-parameter model (Sect.3.1.2; Volume VI). Using complementary  $^{14}\text{C}$  and  $^3\text{H}$  analyses of the same water samples, two unknowns exist – the

mean residence time (MRT) and the initial  $^{14}\text{C}$  activity  $C_{\text{init}}$ . Time-series of these isotope data yield more accurate and reliable estimates. Moreover, it is recommended to analyse samples of as many as possible sites of the same catchment, in order to check which interpretation model yields the best fit to the data.

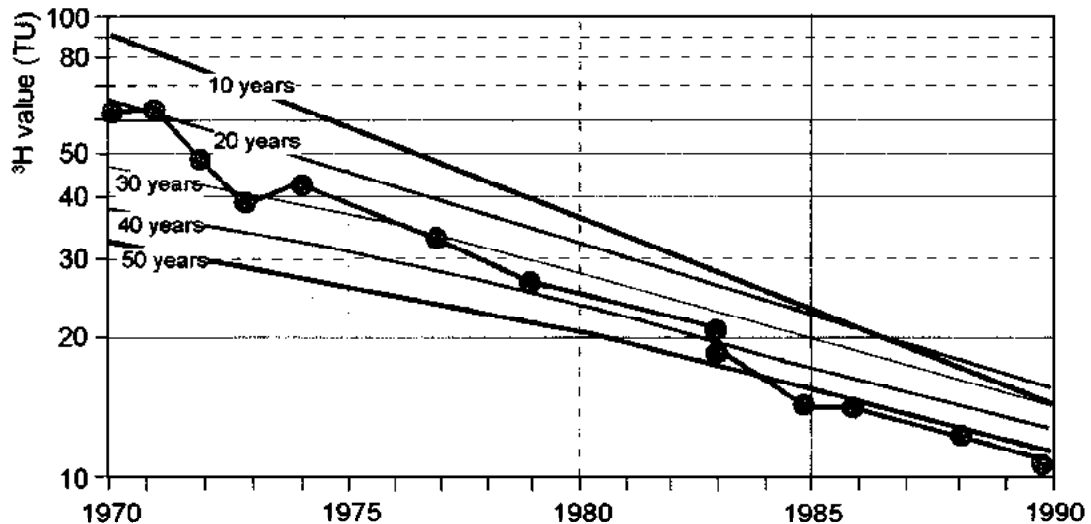


**Fig.7.1** Temporal trend of the  $^3\text{H}$  value of groundwater discharged from the Fijeh spring in the Antilebonaon mountains. The discrepancy between modelled (lines) and the measured  $\delta$  values (open circles) shows (Kattan et al. 1996b) that the exponential model cannot be applied to estimate a mean residence time which would be geohydraulically misleading.

Any multiple isotope hydrological study can only develop its full potential if there is a lack of hydrogeological information or the hydrogeological questions are very specific. When planning such an *applied hydrological study* the first question is if there are sufficient funds and time.

In case of a *scientific study* as many as possible isotopic and hydrochemical analyses are to be carried out and The time of sampling should be extended over at least one hydrological cycle of 12 months. The goal is usually to understand the whole system without answering specific hydrological questions. One of the best examples is the most comprehensive multi-isotope study which was conducted in the marly sandstones of southern England (Andrews et al. 1984). The aim was to assess the value of individual environmental isotopes for establishing hydrogeological data. The results confirmed that  $^3\text{H}$  and  $^{14}\text{C}$  activity measurements along with the determinations of the stable isotopic composition of carbon, hydrogen and oxygen provide practically all information of hydrogeological interest to be expected from environmental isotope methods, provided hydrochemical analyses are implemented.

The applied *isotope hydrological studies* usually suffer from the shortness of the period available for sampling and often also from restricted financial resources (Verhagen et al. 1991). On the other hand, the hydrogeologically interesting questions are often well-defined.

The limitations require a thorough planning including all information on the site to be studied:

The *size* of the region and the distance of the sampling sites defines the required age resolution and possible influence of the continental effect on  $\delta^{18}\text{O}$  (Sect. 5.2.1.1).

The *morphology* determines whether or not the altitude effect on  $\delta^{18}\text{O}$  (Sect. 5.2.1.1) may play a role, allowing a rough estimate of the tracer velocity of groundwater in relation to the required age resolution.

The *sampling sites* may be drilled or dug wells. The pumping rate and the totally abstracted amount of groundwater may be important to estimate if groundwater mining has occurred that may have modified the  $^{14}\text{C}$  ages of groundwater DIC (Sect. 5.1.2.3). In the case of springs the fluctuation of the spring discharge during one hydrological cycle may allow to decide whether or not a spot sampling is sufficient or sampling and analysis is required in short distances (e.g. month or weeks).

The *hydrogeological situation* of the study region (unconsolidated sediments, fractured rocks, phreatic or confined aquifers, leaky aquifer systems) allow to resolve what age range of the groundwater has to be expected, how many groundwater components with what estimated age have to be expected in order to decide how many and which isotopes should be analysed.

The *geohydraulic conditions* are reflected by the piezometric surface of the groundwater in different aquifers and allows reliable estimates of the tracer velocity and expected flow directions. Based on this the minimum and maximum distance of the sampling sites can be determined.

The *palaeohydrologic situation* of the study is important to set up the spatial distribution of the sampling sites, this in order to get an impression whether or not steady-state or non-steady-state geohydraulic conditions have to be taken into account in the interpretation of the isotope date (Verhagen et al. 1991).

The *hydrochemistry of the groundwater resources* is important in order to recognise if hydrochemical analyses are indispensable for a hydrochemical correction of the isotope compositions ( $^{14}\text{C}$ ,  $^{13}\text{C}$ ) (Volume I, Clark and Fritz 1997), in order to correct and to calibrate the time scale of groundwater.

Based on this information and on the hydrogeological questions an optimum sampling and analytical program is to be established. The main aims are determining:

- 1) the *age* of the *groundwater* where the determination of relative water ages is sufficient for checking or calibrating the geohydraulic model results. Tracer velocities, groundwater recharge rates, regional aquifer parameters (hydraulic conductivity, total porosity), mixing proportions, or contributions to the groundwater budget can be obtained with

conventional  $^{14}\text{C}$  ages of the groundwater DIC. Palaeoclimatic information to be used for numerical model calibration requires absolute ages. This requires the estimating the initial  $^{14}\text{C}$  activity and thoroughly making hydrochemical analyses in order to exclude or to correct secondary changes of the isotopic composition. This is also necessary if the pollution potential of an aquifer has to be substantiated.

- 2) the *origin* of the *groundwater*, possibly allowing to make mixing balance studies, to localise the recharge areas or to determine and distinguish between the participating groundwater components.

Comparing the estimated costs of sampling and analysis, and possibly of data interpretation, an optimal *multiple-isotope programme* can be set up. The quality finally determines the hydrogeological value of the isotope hydrological contribution.

# REFERENCES

- Aberg, G.G., Jacks, G. and Hamilton, P.J., 1989. Weathering rates and  $^{87}\text{Sr}/^{86}\text{Sr}$  ratios: An isotopic approach. *Jour. Hydrology*, 109: 65-78.
- Adar, E.M., Gev, I., Berliner, P. and Issar, A.S. 1995. The effect of forestation on a shallow groundwater reservoir in an arid sand dune terrain. *J. Arid Studies*, 55: 259-262.
- Adar, E.M., 1996. Quantitative evaluation on flow systems groundwater recharge and transmissivities using environmental tracers. *Manual on Mathematical Models in Isotope Hydrogeology*. IAEA-TECDOC-910, IAEA Vienna: 113-154.
- Allard P. , 1983. The origin of hydrogen, carbon, sulphur, nitrogen and rare gases in volcanic exhalations: evidence from isotope geochemistry. In: H. Tazieff and J.C. (Editors), *Forecasting Volcanic Events*, Elsevier, Amsterdam, New York: 337-386.
- Allison, G.B., 1982. The relationship between  $^{18}\text{O}$  and deuterium in water and sand columns undergoing evaporation. *J. Hydrol.*, 55: 163-169.
- Allison, G.B., Barnes, J.B., Hughes, M.W. and Leaney, F.W.J., 1983a. The distribution of deuterium and  $^{18}\text{O}$  in dry soils, 2. Experimental. *J. Hydrol.*, 64: 377-397.
- Allison, G.B., Barnes, J.B., Hughes, M.W. and Leaney, F.W.J., 1983b. The effect of climate and vegetation on oxygen-18 and deuterium profiles in soils. In: *Isotope Hydrology 1983*, IAEA Vienna: 105- 123.
- Allison, G.B., Colin-Kaczala, C., Filly, A. and Fontes, J.Ch. , 1987. Measurement of isotopic equilibrium between water, water vapour and soil  $\text{CO}_2$  in arid zone soils. *J. Hydrol.*, 95: 131-141.
- Alvis-Isidro, R.R., Solana, R.R., D'Amore, F., Nuti, S. and Gonfiantini, R., (1993). Hydrology of the greater Tongonan Geothermal System, Philippines, as deduced from geochemical and isotopic data. *Geothermics*, 22: 435-449.
- Andres, G. and Egger, R., 1985. A new tritium interface method for determining the recharge rate of deep groundwater in the Bavarian Mollasse basin. *J. Hydrol.*, 82: 27-38.
- Andrews, J.N., 1985. The isotopic composition of radiogenic helium and its use to study groundwater movement in confined aquifers. *Chem. Geology*, 49: 339-351.
- Andrews, J.N., 1991. Noble gases and radioelements in groundwaters. In: R.A. Downing and W.B. Wilkinson (Editors), *Applied Groundwater Hydrology: A British Perspective*. Chapter 15, Clarendon Press, Oxford: 243-265.



## References

- Andrews, J.N., 1992. Mechanisms for noble gas dissolution by groundwaters. In: *Isotopes of Noble Gases as Tracers in Environmental Studies*, IAEA Vienna: 87-110.
- Andrews, J.N. and Fontes, J.C., 1992. Importance of the in situ production of  $^{36}\text{Cl}$ ,  $^{36}\text{Ar}$  and  $^{14}\text{C}$  in hydrology and hydrogeochemistry. In: *Isotope Techniques in Water Resources Development*, IAEA Vienna: 245-269.
- Andrews, J.N., Giles, I.S., Kay, R.L.F., Lee, D.J., Osmond, J.K., Cowart, J.B., Fritz, P., Barker, J.F. and Gale, J., 1982. Radioelements, radiogenic helium and age relationships of groundwaters from the granites at Stripa, Sweden. *Geochim. Cosmochim. Acta*, 46: 1533-1543.
- Andrews, J.N., Balderer, W., Bath, A.H., Clausen, H.B., Evans, G.V., Florkowski, T., Goldbrunner, J.E., Ivanovich, M., Loosli, H. and Zojer, H., 1984. Environmental isotope studies in two aquifer systems: A comparison of groundwater dating methods. In: *Isotope Hydrology 1983*, IAEA Vienna: 535-576.
- Andrews, J.N., Hussain, N. and Youngman, M.J., 1989. Atmospheric and radiogenic gases in groundwaters from the Stripa Granite. *Geochim. Cosmochim. Acta*, 53: 1831-1841.
- Aranyossy, J.F., Filly, A., Tandia, A.A., Ousmane, B., Louvat, D. and Fontes, J.C., 1991. Estimation du flux d'évaporation sous couvert sableux en climat hyper aride (erg de Bilma, Niger). In: *Isotope Techniques in Water Resources Development*, IAEA Vienna: 309-324.
- Aravena, R., Evans, M. L. and Cherry, J. A., 1996. Stable isotopes of oxygen and nitrogen in source identification of nitrate from septic systems. *Ground Water*, 31: 180-186.
- Aravena, R. and Wassenaar, L.I. , 1993. Dissolved organic carbon and methane in a regional confined aquifer: Evidence for associated subsurface sources. *Appl. Geochem.*, 8: 483-493.
- Balderer W. , 1993. Conclusions on the possible variations of chemical and isotopic composition of groundwater systems in response to changed hydrodynamic conditions. In: *Isotopic and geochemical precursors of earthquakes and volcanic eruptions*. IAEA-TECDOC-726, IAEA Vienna: 87-107.
- Balderer W. and Synal A. , 1995. Characterization of the groundwater circulation of tectonically active areas in western Turkey by the  $^{36}\text{Cl}$  method. In: *Isotopes in Water Resources Management Vol. 2*, IAEA Vienna: 164-167.
- Barnes, C.J. and Allison, G.B., 1983. The distribution of deuterium and oxygen-18 in dry soils: 1. Theory. *J. Hydrol.*, 60: 141-156.
- Barnes, C.J. and Allison, G.B., 1984. The distribution of deuterium and oxygen-18 in dry soils: 3. Theory for non-isothermal water movement. *J. Hydrol.*, 74: 119-135.

## References

- Barnes, C.J. and Allison, G.B., 1988. Tracing of water movement in the unsaturated zone using stable isotopes of hydrogen and oxygen. *J. Hydrol.* 100 (1-3): 143-176.
- Barnes, C.J. and Walker, G.B., 1989. The distribution of deuterium and oxygen-18 during unsteady evaporation. *J. Hydrol.* 112: 55-67.
- Barth, S., 1993. Boron isotope variations in nature: a synthesis. *Geol. Rundsch.* 82: 1177-1188.
- Bates, R.L. and Jackson, J.A. (Editors), 1980. *Glossary of Geology* (2<sup>nd</sup> edition), American Geological Institute, Falls Church, Virginia: 751 pp.
- Bath, A. H., Edmunds, W.M. and Andrews, J. N., 1979. Palaeoclimatic trends deduced from the hydrogeochemistry of a Triassic sandstone aquifer, United Kingdom. In: *Isotope Hydrology 1978*, Vol. II, IAEA Vienna: 545-567.
- Becker R.H. and Clayton R.N., 1976. Oxygen isotope study of a Precambrian banded iron formation. Hamersley Range, Western Australia. *Geochim. Cosmochim. Acta* 40: 1153-1165.
- Beekman, H.E., Gieske, A. and Selaolo, E.T., 1996. GRES – groundwater recharge studies in Botswana (1987 – 1996). *Botswana J. Earth Sci.* III: 1-17.
- Behrens, H., Moser, H., Oerter, H., Rauert, W., Stichler, W., Ambach, W. and Kirchlechner, P., 1979. Models for the runoff of a glaciated catchment area using measurements of environmental isotope contents. In: *Isotope Hydrology 1978*, Vol. II, IAEA Vienna: 829-845.
- Bendl, J., 1992. A study of  $^{87}\text{Sr}/^{86}\text{Sr}$  ratios in the exogene zone of the Krusne Hory Mts. (W. Bohemia). *Casopis pro mineralogii a geologii* 37: 339-347.
- Bentley, H.W., Phillips, F.M., Davis, S.N., Gifford, S., Elmore, D., Tubbs, L., and Gove, H.E., 1982. The thermonuclear  $^{36}\text{Cl}$  pulse in natural water. *Nature*, 300: 737-740.
- Bentley, H. W., Phillips, F. M. and Davis, S. N., 1986. Chlorine-36 in the terrestrial environment. In: P. Fritz and J. C. Fontes (Editors), *Handbook of Environmental Isotope Geochemistry* Vol. IIB, The Terrestrial Environment, Elsevier, Amsterdam New York: 427-480.
- Bertleff, B., Stichler, W., Stober, I. and Strayle, G., 1985. Geohydraulische und isotopenhydrologische Untersuchungen im Mündungsbereich zwischen Donau und Iller. *Abh. geol. Landesamt Baden-Württemberg* 11: 7-44.
- Bertleff, B., Watzel, R., Eichinger, L., Heidinger, M., Dehneider, K., Loosli, H.H. and Stichler, W., 1993. The use of isotope based modelling techniques for groundwater management in a Quaternary aquifer system. In: *Isotope Techniques in the Study of Environmental Change*, IAEA Vienna: 437-452.

## References

- Black, J.H., Kipp Jr. and K.L., 1983. Movement of tracers through dual porosity media - Experiments and modelling in the Cretaceous Chalk, England. *J. Hydrol.* 62: 287-312.
- Blattner P., 1985. Isotope shift data and the natural evolution of geothermal systems. *Chem. Geol.* 49: 187-203.
- Böttcher J, Strebel, O., Voerkelius, S. and Schmidt, H.L., 1990. Using isotope fractionation of nitrate nitrogen and nitrate oxygen for evaluation of nitrate in a sandy aquifer. *J. Hydrol.* 114: 413-424.
- Bottomley, D. J., Gascoyne, M. and Kamineni, D. C., 1990. The geochemistry, age and origin of groundwater in a mafic pluton, East Bull Lake, Ontario, Canada. *Geochim. Cosmochim. Acta* 54: 993-1008.
- Box W.T., D'Amore F. and Nuti S., 1987. Chemical and isotopic composition of fluids sampled during drilling at The Geysers (CA, USA). In: *Proc. Int. Symp. on Development and Exploitation of Geothermal Resources, CFE-CEE, Cuernavaca, Mexico: 172-177.*
- Burdon, D.J. , 1977. Flow of fossil groundwater. *Quarterly J. Eng. Geol.* 10: 97-124.
- Busenberg, E. and Plummer, L. N., 1992. The use of chlorofluorocarbons (CCl<sub>3</sub>F and CCl<sub>2</sub>F<sub>2</sub>) as hydrologic tracers and age-dating tools: the alluvium and terrace system of central Oklahoma. *Water Res. Res.* 28: 2257-2283.
- Butler, M. J. and Verhagen, B. T., 1997. Environmental isotopic tracing of water in the urban environment of Pretoria, South Africa. In: P. J. Chilton I(Editor), *Groundwater in the Urban Environment Vol. 1, Problems, Processes and Management*, Balkema, Rotterdam: 101-106.
- Buzek, F., Kadlecová, R. and Zák, K., 1998. Nitrate pollution of a karstic groundwater system. In: *Isotope Techniques in the Study of Environmental Change*, IAEA Vienna: 453-464.
- Calf, G.E. and Habermehl, M.A. , 1984. Isotope hydrology and hydrochemistry of the Great Artesian Basin, Australia. In: *Isotope Hydrology 1983*, IAEA Vienna: 397-414.
- Carmi, I. and Gat, J.R., 1992. Estimating the turnover time of groundwater reservoirs by the helium-3/tritium method in the era of declining atmospheric tritium levels: Opportunities and limitations in the time bracket 1990-2000. *Israel J. Earth Sci.* 43: 249-253.
- Chiba, H. and Sakai H., 1985. Oxygen isotope exchange rate between dissolved sulfate and water at hydrothermal temperatures. *Geochim. Cosmochim. Acta* 49: 993-1000.
- Clark, I.D., Bajjali, W.T. and Phipps, G. Ch., 1996. Constraining <sup>14</sup>C ages in sulphate reducing groundwaters: two case studies from arid regions. In: *Isotope in Water Resources Management*, IAEA Vienna: 43-56.
- Clark, I. D. and Fritz, P., 1997. *Environmental Isotopes in Hydrogeology*, Lewis Publishers, New York: 328 pp.

## References

- Clark, L., 1988. *The Field Guide to Water Wells and Boreholes*, Open University Press, Milton Keynes and Halsted Press, John Wiley and Sons, New York, Toronto: 155 pp.
- Claypool, G.E., Holser, W.T., Kaplan, I.R., Sakai, H. and Zak, I., 1980. The age curves of sulfur and oxygen isotopes in marine sulfate and their mutual interpretation. *Chem. Geology* 28: 199-260.
- Clayton, R.N. and Steiner, A.S., 1975. Oxygen isotope studies of the geothermal system at Wairakei, New Zealand. *Geochim. Cosmochim. Acta* 39: 1179-1186.
- Collon, P.A.E., Kutschera, W., Lehmann, B.E., Loosli, H.H., Purtschert, R., Love, A., Sampson, L., Davids, B., Fauerbach, M., Harkewicz, R., Morrissey, D., Sherrill, B., Steiner, M., Pardo, R. and Paul, M., 1999. Development of Accelerator Mass Spectrometry (AMS) for the detection of  $^{81}\text{Kr}$  and its first application to groundwater dating. In: *Int. Symp. on Isotope Techniques in Water Resources Development and Management*, IAEA Vienna, SM-361-18.
- Cook, P.G. and Solomon, D.K., 1997. Recent advances in dating young groundwater: chlorofluorocarbons,  $^3\text{H}/^3\text{He}$  and  $^{85}\text{Kr}$ . *J. Hydrol* 191: 245-265.
- Corbett, D.R., Burnett, W.C., Cable, P.H. and Clark, S.B., 1997. Radon tracing of groundwater input into Par Pond, Savannah River Site. *J. Hydrol.* 203: 209-227.
- D'Amore F. and Truesdell A.H. (1979). Models for steam chemistry at Larderello and The Geysers. In: *Proc. Fifth Stanford Geothermal Reservoir Engineering Workshop*: 283-297.
- D'Amore, F. and Truesdell, A.H., 1985. Calculation of geothermal reservoir temperatures and steam fraction from gas compositions. *Geotherm. Res. Coun. Trans.* 9: 305-310.
- D'Amore, F., Nuti, S. and Fancelli, R., 1988: Geochemistry and reinjection of waste waters in vapor dominated fields. In: *Proc. Int. Symp. on Geothermal Energy, Kumamoto and Beppu, Japan*: 244-248.
- Dansgaard, W., 1964. Stable isotopes in precipitation. *Tellus* 16: 436-468.
- Darling, W.G., Gizaw, B. and Arusei, M.K., 1996. Lake-groundwater relationships and fluid-rock interaction in the East African Rift Valley: an isotopic study. *J. African Earth Sci.* 22: 423-431.
- Datta, P.S., Goel, P.S., Rama, F.A. and Sangal, S.P., 1973. Groundwater recharge in western Uttar Pradesh. *Proc. Ind. Acad. Sci.*, Vol. LXXVIII (1A): 1-12.
- Davidson, G.R. and Bassett, R.L., 1993. Application of boron isotopes for identifying contaminants such as fly ash leachate in groundwater. *Environ. Sci. Techn.* 27: 172-176.
- Davis, S.N. and DeWiest, R.M., 1966. *Hydrogeology*, J. Wiley, New York, London, Sydney: 463 pp.

## References

- Deák, J., Stute, M., Rudolph, J. and Sonntag, C., 1987. Determination of the flow regime of Quaternary and Pleistocene layers in the Great Hungarian Plain (Hungary) by D,  $^{18}\text{O}$ ,  $^{14}\text{C}$  and noble gas measurements. In: *Isotope Techniques in Water Resources Development*, IAEA, Vienna: 335-350.
- Deák, J., Deseö, E., Böhlke, J.K. and Révész, R., 1995. Isotope hydrology studies in the Szigetköz region, northwest Hungary. In: *Isotopes in Water Resources Management Vol. I*, IAEA Vienna: 419-432.
- Degeldre, C., Pfeiffer, H.R., Alexander, W., Wehrli, B. and Breutsch, R., 1996. Colloid properties in granitic groundwater systems. I: Sampling and characterisation. *Appl. Geochem.*, 11: 677-695.
- Dincer, T., Al-Mugrin, W. and Zimmermann, V., 1974. Study of the infiltration and recharge through the sand dunes in arid zones with special reference to the stable isotopes and thermo-nuclear tritium. *J. Hydrol.*, 23: 79-109.
- Drever, J.I., 1997. *The Geochemistry of Natural Waters (3<sup>rd</sup> Edition)*, Prentice Hall, N.J., 436 pp.
- Dreybroth, W., 1988. *Processes in Karst Systems*, Springer, Heidelberg, 288 pp.
- Dürbaum, H.J., 1969. Der Durchlässigkeitsbeiwert von Lockergesteinen und seine Bestimmung. In: A. Bentz and H.J. Martini (Editors), *Lehrbuch der angewandten Geologie Vol. 2 (2)*, Ferdinand-Enke Verlag, Stuttgart: 1474-1513.
- Dymond, J., Cobler, R., Gordon, L., Biscaye, P. and Mathieu, G., 1983.  $^{226}\text{Ra}$  and  $^{226}\text{Rn}$  contents of Galapagos Rift hydrothermal waters - the importance of low-temperature interactions with crustal rocks. *Earth Planet. Sci. Letters*, 64: 417-429.
- Eastoe, C.J. and Guilbert, J.M., 1992. Stable chlorine isotopes in hydrothermal processes. *Geochim. Cosmochim. Acta*, 56: 4247-4255.
- Edmunds, W.M., Cook, J.M., Darling, W.G., Kinniburgh, D.G., Miles, D.L., Bath, A.H., Morgan-Jones, M. and Andrews, J.N., 1987. Baseline geochemical conditions in the Chalk aquifer, Berkshire, UK: a basis for groundwater quality management. *Appl. Geochem.*, 2: 251-274.
- Eggenkamp, H.G.M. and Coleman, M.L., 1998. Heterogeneity of formation waters within and between oil fields by halogen isotopes. In: G.B. Arehart and J.R. Hulston (Editors), *Water-Rock Interaction*, Balkema, Rotterdam: 309-312.
- Eggenkamp, H.G.M., 1994. The geochemistry of Chlorine isotopes. *Geologica Ultraiectina, Mededelingen van de Faculteit Aardwetenschappen, Rijksuniversiteit Utrecht*: 116 pp.
- Ekwurzel, B., Schlosser, P., Smethie, Jr., W.M., Plummer, L.N., Busenberg, E., Michel, R.L., Weppernig, R. and Stute, M., 1994. Dating of shallow groundwater: comparison of the transient tracers  $^3\text{He}/^3\text{H}$ , chlorofluorocarbons, and  $^{85}\text{Kr}$ . *Water Res. Res.*, 30: 1693-1708.

## References

- Elmore, D., Tubbs, L.E., Newman, D., Ma, X.Z., Finkel, R., Nishiizumi, K., Beer, J., Oeschger, H. and Andree, M., 1982.  $^{36}\text{Cl}$  bomb pulse measured in a shallow ice core from Dye 3, Greenland. *Nature*, 300: 735-737.
- Fabryka-Martin, J., Davis, S.N. and Elmore, D., 1987. Application of  $^{129}\text{I}$  and  $^{36}\text{Cl}$  in hydrology. *Nucl. Instr. Meth. Phys. Res. B*, 29: 361-371.
- Florkowski, T., Morawska, L. and Rozanski, K., 1988. Natural production of radionuclides in geological formations. *Nucl. Geophys*, 2: 1-14.
- Fontes, J.C., 1992. Chemical and isotopic constraints on  $^{14}\text{C}$  dating of groundwater. In: Taylor, R.E., Long, A. and Kra, R.S., (Editors). *Radiocarbon after Four Decades. An Interdisciplinary Perspective*, Springer, New York: 242-275.
- Fontes, J.-C., Yousfi, M. and Allison, G.B., 1986. Estimation of the long term, diffuse groundwater discharge in the Northern Sahara using stable isotope profiles in soil water. *J. Hydrol.*, 86: 315-327.
- Forster, M., Loosli, H. and Weise, S., 1992.  $^{39}\text{Ar}$ ,  $^{85}\text{Kr}$ ,  $^3\text{He}$  and  $^3\text{H}$  isotope dating of groundwater in the Bocholt and Segeberger Forest Aquifer Systems. In: G. Matthess et al. (Editors), *Progress in Hydrogeochemistry*, Springer, Berlin: 467-475.
- Foster, S.S.D. and Smith-Carrington, A., 1980. The interpretation of tritium in the chalk unsaturated zone. *J. Hydrol.*, 46: 343-364.
- Frape, S.K., Bryant, G., Blomquist, R. and Ruskeeniemi, T., 1995. Evidence from stable chlorine isotopes for multiple sources of chlorine in groundwaters from crystalline shield environments. In: *Isotopes in Water Resources Management Vol. I*, IAEA Vienna: 19-30.
- Frape, S.K., Bryant, G., Durance, P., Ropchan, J.C., Doupe, J., Blomquist, R., Nissinen, P., Kaija, J., 1998. The source of stable chlorine isotopic signatures in groundwaters from crystalline shielded rocks. In: G.B. Ahernt and J.R. Hulston (Editors) *Water-Rock Interaction*, Balkema, Rotterdam: 223-226.
- Freyer, H.D., 1978. Seasonal trends of  $\text{NH}_4^+$  and  $\text{NO}_3^-$  nitrogen isotopic composition in rain collected at Jülich, Germany. *Tellus*, 30: 83-92.
- Fritz, P., Cherry J.A., Weyer R.V. and Sklash M.G., 1976. Runoff analyses using environmental isotopes and major ions. In: *Interpretation of Environmental Isotope and Hydrochemical Data in Groundwater Hydrology*, IAEA Vienna: 111-130.
- Fritz, B., Clauer, N. and Sam, M., 1987. Strontium isotopic data and geochemical calculations as indicators of the origin of saline waters in crystalline rocks. In: P. Fritz and S.R. Frape (Editors) *Saline Water and Gases in Crystalline Rocks*, Special Paper 33, Geol. Assoc. of Canada: 121-126.
- Fritz, P., Frape, S.K., Drimmie, R.J., Appleyard, E.C. and Hattori K., 1994. Sulfate in brines in the crystalline rocks of the Canadian Shield. *Geochim. Cosmochim. Acta*, 58: 57-65.

## References

- Fröhlich, K. and Gellermann, R., 1986. On the potential use of uranium isotopes for groundwater dating. *Isot. Geosci. Sect.*, 65: 67-77.
- Galimov, E.M., 1973. *Carbon Isotopes in Petroleum Geology*, Nedra, Moscow.
- Gascoyne, M., 1981. A simple method of uranium extraction from carbonate groundwater and its application to  $^{234}\text{U}/^{238}\text{U}$  disequilibrium studies. *J. Geochem. Explor.*, 14: 199-207.
- Gat, J.R. and Carmi, I., 1970. Evolution of the isotopic composition of atmospheric waters in the Mediterranean Sea area. *J. Geophys. Res.*, 75: 3039-3048.
- Gat, J. and Gonfiantini, R. (Editors), 1981. *Stable Isotope Hydrology. Deuterium and Oxygen-18 in the Water Cycle*, Technical Reports Series No 210, IAEA Vienna: 337 pp.
- Geyer, S., Wolf, M., Wassenaar, L.I., Fritz, P., Buckau, G. and Kim, J.I., 1993. Isotope investigations on fractions of dissolved organic carbon from  $^{14}\text{C}$  dating. In: *Isotope Techniques in the Study of Past and Current Environmental Changes in the Hydrosphere and Atmosphere*, IAEA Vienna: 359-380.
- Geyh, M.A., 1972. Basic studies in hydrology and  $^{14}\text{C}$  and  $^3\text{H}$  measurements. In: *Proc. XXIV Int. Geol. Congr.*, 11: 227-234; Montreal.
- Geyh, M.A., 1992. The  $^{14}\text{C}$  time-scale of groundwater. Correction and linearity. In: *Isotope Techniques in Water Resources Development 1991*, IAEA Vienna: 167-177.
- Geyh, M.A., 1994. The paleohydrology of the eastern Mediterranean. In: O. Bar-Yosef and R.S. Kra (Editors) *Late Quaternary Chronology and Paleoclimates of the Eastern Mediterranean*, Radiocarbon, Tuscon.: 131-145.
- Geyh, M.A. and Backhaus, G., 1979. Hydrodynamic aspects of carbon-14 groundwater dating. In: *Isotope Hydrology 1978 Vol. II*, IAEA Vienna: 631-643.
- Geyh, M.A. and Kantor, W., 1998. Zusammenspiel zwischen Isotopenhydrologie und numerischer Strömungsmodellierung am Beispiel der Dübener Heide. In: *Proc. 4. GBL-Kolloquium*, 26.- 28. November 1997, Ergebnisse und Empfehlungen, Hannover, GBL-Heft, 5: 111-121.
- Geyh, M.A. and Künzl, R., 1981. Methane in groundwater and its effect on  $^{14}\text{C}$  groundwater dating. *J. Hydrol.*, 52: 355-358.
- Geyh, M.A. and Michel, G., 1981. Isotopen- und hydrochemische Betrachtungen über die Süßwasser/Salzwasser-Zone am Nordostrand des Münsterländer Beckens. *Z. dtsh. geol. Ges.*, 132: 597-611.
- Geyh, M.A. and Michel, G., 1982. Isotopical differentiation of groundwater of different hydrogeologic origin. *J. Hydrol.*, 59: 161-171.
- Geyh, M.A. and Schleicher, H., 1990. *Absolute Age Determination. Physical and Chemical Dating Methods and Their Application*, Springer, Berlin Heidelberg New York, 503 pp.

## References

- Geyh, M.A., Backhaus, G., Andres, G., Rudolph, R. and Rath, H.K., 1984. Isotope study on the Keuper sandstone aquifer with a leaky cover layer. In: *Isotope Hydrology 1983*, IAEA Vienna: 499-513.
- Geyh, M.A., Bender, H., Rajab, R. and Wagner, W., 1995. Application of  $^{14}\text{C}$ -groundwater dating to non-steady systems. In: Adar, E.M. and Leibundgut, Ch. (Editors) *Application of Tracers in Arid Zone Hydrology*, IAHS Press, Wallingford, Oxfordshire, IAHS Publ. No. 232: 225-234.
- Giggenbach, W.F., 1971. Isotopic composition of waters of the Broadlands geothermal field (New Zealand). *N.Z. J. Sci.*, 14: 959-970.
- Giggenbach, W.F., 1977. The isotopic composition of sulphur in sedimentary rocks bordering the Taupo Volcanic Zone. *Geochemistry 1977*. N.Z. DSM Bull., 218: 57-64.
- Giggenbach, W.F., 1978. The isotopic composition of waters from the El Tatio geothermal field, Northern Chile. *Geochim. Cosmochim. Acta*, 42: 979-988.
- Giggenbach, W.F., 1988. Geothermal solute equilibria. Derivation of Na-K-Mg-Ca geoindicators. *Geochim. Cosmochim. Acta*, 52: 2749-2765.
- Giggenbach, W.F., 1989. The chemical and isotopic position of Ohaaki field within the Taupo Volcanic Zone. *Proc. Eleventh N.Z. Geothermal Workshop*, Auckland: 81-88.
- Giggenbach, W., 1991. Isotopic composition of geothermal water and steam discharges. In: F. D'Amore (Editor), *Application of Geochemistry in Geothermal Reservoir*, UNITAR--UNDP: 119-144.
- Giggenbach, W., 1992. Isotopic shifts in water from geothermal and volcanic systems along convergent plate boundaries and their origin. *Earth Planet. Sci. Letters*, 113: 495-510.
- Giggenbach, W.F. and Lyon G.L., 1977. The chemical and isotopic composition of water and gas discharges from the Ngawha geothermal field, Northland. (Dept. Sci. Ind. Res., Chem. Div.) *Geotherm. Circ. CD 30/555/7-WFG*: 37 pp.
- Giggenbach, W.F. and Stewart M.K., 1982. Processes controlling the isotopic composition of steam and water discharges from steam vents and steam-heated pools in geothermal area. *Geothermics*, 11: 71-80.
- Gislason, S.R. and Eugster, H.P., 1987. Meteoric water-basalt interactions. II: A field study in N.E. Iceland. *Geochim. Cosmochim. Acta*, 51: 2841-2855.
- Grabczak, J., Zuber, A., Maloszewski, P., Rozanski, K., Weiss, W. and Sliwka, I., 1982. New mathematical models for the interpretation of environmental tracers in groundwaters and the combined use of tritium, C-14, Kr-85, He-3, and freon-11 for groundwater studies. *Beiträge zur Geologie der Schweiz – Hydrologie*, 28 II: 395-406.
- Grindrod, P., 1993. The impact of colloids on the migration and dispersal of radionuclides within fractured rock. *J. Contaminant Hydrol.*, 13: 167-181.



## References

- Gunter, B.D. and Musgrave, B.C., 1971. New evidence on the origin of methane in hydrothermal gases. *Geochim. Cosmochim. Acta*, 35: 113-118.
- Heaton, T.H.E., 1984. Sources of the nitrate in phreatic groundwater in the western Kalahari. *J. Hydrol.*, 67: 249-259.
- Heaton, T.H.E., 1986. Isotopic study of nitrogen pollution in the hydrosphere and atmosphere: a review. *Chem. Geology (Isot. Geosci. Sect.)*, 59: 87-102.
- Hedenquist, J.W., 1990. The thermal and geochemical structure of the Broadlands-Ohaaki geothermal system. *Geothermics*, 19:151-185.
- Henley R.W., Truesdell, A.H. and Barton, P.B., 1984. Fluid-mineral equilibria in hydrothermal systems. *Soc. of Econ. Geol., Reviews in Economic Geology*, 1: 267 pp.
- Hem, J. , 1985. Study and interpretation of Chemical Characteristics of Natural Water (3<sup>rd</sup> ed.), US Geol. Survey Water Supply, Paper, 2254: 263 pp.
- Herczeg, A.L., Love, A.J., Sampson, L., Cresswell, R.G. and Fifield, L.K., 1999. Flow velocities estimated from Cl-36 in the South-West Great Artesian basin, Australia.– Int. Symp. on Isotope Techniques in Water Resources Development and Management, IAEA Vienna: SM-361-34P.
- Hillaire-Marcel, C. and Ghaleb, B., 1997. Thermal ionization mass spectrometry measurements of <sup>226</sup>Ra and U isotopes in soils, surface and groundwaters. Analytical aspects and pore water–matrix interactions revisited. In: *Isotope Techniques in the Study of Past and Current Environmental Changes in the Hydrosphere and Atmosphere*, IAEA Vienna: 727-743.
- Hoehn, E., Willme, U., Hollerung, R., Schulte-Ebert, U. and Gunten, H.R., 1992. Application of the <sup>222</sup>Rn technique for estimating the residence times of artificially recharged groundwater. In: *Isotope in Water Resources Development*, IAEA Vienna: 712-714.
- Holser, W.T., Magaritz, M. and Wright, J., 1986. Chemical and isotopic variations in the world ocean during Phanerozoic time. In: O. Walliser (Editor), *Lecture Notes in Earth Sciences Vol. 8, Global Bio-Events*, Springer, Heidelberg: 63-74.
- Hübner, H., 1986. Chapter 9. Isotope effects of nitrogen in the soil and biosphere. In: P. Fritz and J. Ch. Fontes (Editors), *Handbook of Environmental Isotope Geochemistry Vol. II*, Elsevier, Amsterdam: 361-425.
- Hübner, H., Kowski, P., Hermichen, W.-D., Richter, W. and Schütze, H., 1979. Regional and temporal variations of deuterium in the precipitation and atmospheric moisture of Central Europe. In: *Isotope Hydrology 1978*, IAEA, Vienna, Vol. 1: 289-305.
- Hulston J.R., 1973. Estimation of underground temperature distribution in active hydrothermal systems using stable isotope equilibria. In: *Proc. 2<sup>nd</sup> Conf. Australian and New Zealand Society for Mass Spectrometry*, Melbourne.

## References

- IAEA (International Atomic Energy Agency), 1969, 1970, 1971, 1973, 1975, 1979, 1983, 1986, 1990, 1994. Environmental isotope data, Nos. 1 – 10: World Survey of Isotope Concentration in Precipitation. Tech. Rep. Ser. Nos. 96, 117, 129, 147, 169, 192, 226, 264, 311, 371. IAEA, Vienna.
- IAEA, 1983. Guidebook on Nuclear Techniques in Hydrology. Techn. Reports Series, 91: 456 pp.
- IAEA, 1987. Studies on Sulfur Isotope Variations in Nature: Chemistry, Geology and Raw Materials / Hydrology (Proc. Advisory Group Meeting), Vienna, 17 - 20 June, 1985: 124 pp..
- International Glossary of Hydrology, 1998. UNESCO, WMO, WMO/OMM/BMO, Geneva, No. 12: 343 pp.
- Johnston, C.D., 1988. Water and Solute Movement in Deeply Weathered Lateritic Soil Profiles Near Collie Western Australia. M. Sc. Thesis, Dept Soil Science and Plant Nutrition, Univ. Western Australia.
- Juraske, S., 1994. Diploma Thesis, University of Regensburg, Germany.
- Kattan, Z., 1996a. Chemical and environmental isotope study of precipitation in Syria.- Isotope Field Applications for Groundwater Studies in the Middle East. In: IAEA-TECDOC-890, IAEA Vienna: 185-202.
- Kattan, Z., 1996b. Environmental isotope study of the major karst springs in Damaskus limestone aquifer systems: case of the Fijeh and Barada springs. In: Isotope Field Applications for Groundwater Studies in the Middle East, IAEA-TECDOC-890: 127-150.
- Krause, H. R., 1987. Relationships between the sulphur and oxygen isotope composition of dissolved sulphate. In: Studies on Sulfur Isotope Variations in Nature. Panel Proc. Series, IAEA Vienna: 31-47.
- Krouse, H. R., 1980. Sulphur isotopes in our environment. In: P. Fritz and J.C. Fontes (Editors), Handbook of Environmental Isotope Geochemistry Vol. I, The Terrestrial Environment, Elsevier, Amsterdam: 435-471.
- Lehmann, B.E., Loosli, H.H., Rauber, D., Thonnard, N. and Willis, R.D. , 1991.  $^{81}\text{Kr}$  and  $^{85}\text{Kr}$  in groundwater, Milk River aquifer, Alberta, Canada. Applied Geochemistry, 6: 419-423.
- Lehmann, B.E., Purtschert, R., Loosli, H.H., Love, A., Sampson, L., Collon, P.A.E., Kutschera, W., Beyerle, U., Aechbach-Hertig, W. and Kipfer, R., 1999.  $^{81}\text{Kr}$ ,  $^{36}\text{Cl}$  and  $^4\text{He}$  dating in the Great Artesian basin, Australia. In: Isotope Techniques in Water Resources Development and Management, IAEA Vienna: SM-361-93P.
- Libby, W.F., 1946. Atmospheric helium three and radiocarbon from cosmic radiation. Phys. Rev., 69: 671-672.

## References

- Libby, W.F., 1953. The potential usefulness of natural tritium. *Proc. Nat. Acad. Sci.*, 39: 245-247.
- Lloyd, R.M. , 1968. Oxygen isotope behaviour in the sulfate-water system. *J. Geophys. Res.*, 73: 6099-6110.
- Loosli, H.H. , 1992. Applications of  $^{37}\text{Ar}$ ,  $^{39}\text{Ar}$  and  $^{85}\text{Kr}$  in hydrology, oceanography and atmospheric studies. In: *Isotopes of Noble Gases as Tracers in Environmental Studies*, IAEA Vienna: 73-85.
- Lyon, G.L. and Hulston, J.R., 1984. Carbon and hydrogen isotopic compositions of New Zealand geothermal gases. *Geochim. Cosmochim. Acta*, 48: 116-1171.
- Majoube, M., 1971. Fractionnement en oxygene-18 et en deuterium entre l'eau et sa vapeur. *J. Chim. Phys.*, 68: 1423-1436.
- Maloszewski, P. and Zuber, A., 1993. Principles and practice of calibration and validation of mathematical models for the interpretation of environmental tracer in aquifers. *Advances in Water Res.*, 16: 173-190.
- Maloszewski, P. and Zuber, A., 1996. Lumped parameter models for the interpretation of environmental tracer data. In: *Manual on Mathematical Models in Isotope Hydrology*, IAEA Vienna: 9-58.
- Maloszewski, P. and Zuber, A., 1998. Discussion: A general lumped parameter model for the interpretation of tracer data and transit time calculation in hydrologic systems (*Journal of Hydrology* 179 (1996) 1-21). *Comments. J. Hydrol.*, 204: 297-300.
- Mariotti, A. , 1984. Utilisation des variations naturelles d'abondance isotopique en  $^{15}\text{N}$  pour tracer l'origine des pollutions des aquiferes par les nitrates. In: *Isotope Hydrology 1983*, IAEA Vienna: 605-633.
- Mariotti, A., Landreau, A. and Simon, B., 1988.  $^{15}\text{N}$  isotope biogeochemistry and natural denitrification process in groundwater: Application to the chalk aquifer of northern France. *Geochim. Cosmochim. Acta*, 52: 1869-1878.
- Matsuhisa, Y., Goldsmith, J.R. and Clayton, R.N., 1979. Oxygen isotope fractionation in the system quartz-albite-anorthite-water. *Geochim. Cosmochim. Acta*, 43: 1131-1140.
- Mazor, E., 1991. *Applied Chemical and Isotopic Groundwater Hydrology*, John Wiley, New York: 274 pp.
- Mazor, E. , 1992. Reinterpretation of  $\text{Cl-36}$  data: physical processes, hydraulic interconnections, and age estimates in groundwater systems. *Appl. Geochem.*, 7: 351-360.
- McNutt, R.H. , 1987.  $\text{Sr}^{87}/\text{Sr}^{86}$  as indicators for water-rock interactions: applications to brines found in Precambrian age rocks from Canada.- In: P. Fritz and S.K. Frapè (Editors),

## References

- Saline Water and Gases in Crystalline Rocks, Geol. Assoc. of Canada, Special Paper 33: 81-88.
- Merlivat L., 1970. L'etude quantitative de bilans de lacs a l'aide des concentrations en deuterium et oxygene-18 dans l'eau. In: Isotope Hydrology, IAEA Vienna: 89-107.
- Merlivat, L. , 1978. Molecular diffusivities of  $H_2^{16}O$ , HDO and  $H_2^{18}O$  in gases. J. Chem. Phys., 69: 2864-2871.
- Merlivat L. and Jouzel J., 1979. Global climatic interpretation of the deuterium-oxygen 18 relationship for precipitation. J. Geophys. Res., 84: 5029-5033.
- Michel, G. and Struckmeier, W., 1985. The Cretaceous Basin of Münster – a regional groundwater system in response to multiple impacts (water supply, spas, deep mining). Mem. 18<sup>th</sup> IAH Congr., Cambridge: 150-159.
- Mizutani Y. and Rafter T.A. , 1969. Oxygen isotopic composition of sulphates, Part 3: - Oxygen isotopic fractionation in the bisulphate ion-water system. N.Z.J. Sci., 12: 54.
- Mook, W.G., 1970. Stable carbon and oxygen isotopes of natural waters in the Netherlands. In: Isotope Hydrology 1970, IAEA Vienna: 163-190.
- Mook, W. G., 1980. Carbon-14 in hydrogeological studies. In: P. Fritz and J. Ch. Fontes (Editors), Handbook of Environmental Isotope Geochemistry Vol. I, Elsevier, Amsterdam: 49-74.
- Mook, W.G., Groeneveld, D.J., Brouwn, A.E. and Van Ganswijk, A.J., 1974. Analysis of a run-off hydrograph by means of natural  $^{18}O$ . In: Isotope Techniques in Ground-Water Hydrology, IAEA Vienna: 145-153.
- Morgenstern, U., Taylor, C.B., Parrat, Y., Gäggeler, H.W. and Eichler, B., 1996.  $^{32}Si$  in precipitation: evaluation of temporal and spatial variation and as dating tool for glacial ice. Earth Planet. Sci. Letters, 144: 289-296.
- Moser, H. and Rauert, W. (Editors), 1980. Isotopenmethoden in der Hydrologie, Borntraeger, Berlin Stuttgart, 400 pp.
- Münnich, K.O., 1957. Messung des  $^{14}C$ -Gehaltes von hartem Grundwasser. Naturwiss., 34: 32-33.
- Münnich, K.O., 1968. Isotopen-Datierung von Grundwasser. Naturwiss., 55: 158-163.
- Münnich, K.O., 1983. Moisture movement in the unsaturated zone. In: Guidebook on Nuclear Techniques in Hydrology. Techn. Reports Series No. 91, IAEA Vienna: 109-118.
- Nuti S., Calore C. and Noto P., 1981. Use of environmental isotopes as natural tracers in a reinjection experiment at Larderello. In: Proc. 7<sup>th</sup> Stanford Geothermal Reservoir Engineering Workshop: 85-89.

## References

- Nuti S., Caprai A. and Noto P., 1985. Hypothesis on the origin of steam and on the deep temperatures of the fluids of Pozzuoli Solfatara (Campania, Italy). In: Proc. 9<sup>th</sup> Geothermal Energy Annual Meeting, Geothermal Resources Council Transactions.
- Oreskes, N., Shrader-Frechette, K. and Belitz, K., 1994. Verification, validation, and confirmation of numerical models in the earth sciences. *Science*, 263: 641-646.
- O'Neil, J.R., 1987. Preservation of H, C, and O isotopic ratios in the low temperature environment. In: T.K. Kyser (Editor), *Stable Isotope Geochemistry of Low Temperature Processes*. Mineral. Soc. Canada Short Course, 13: 85-128.
- Osmond, J.K., Cowart, J.B. and Ivanovich, M., 1983. Uranium isotopic disequilibrium in ground water as an indicator of anomalies. *Int. J. Appl. Radiat. Isot.*, 34: 283-308.
- Ousmane, B., Fontes, J.-C., Aranyossy, J.-F. and Joseph, A., 1983. Hydrologie isotopique et hydrochimie des aquifères discontinus de la bande sahélienne et de L'Air (Niger). In: *Isotope Hydrology 1983*, IAEA Vienna: 367-395.
- Paces, T., 1987. Hydrochemical evolution of saline waters from crystalline rocks of the Bohemian Massif (Czechoslovakia).- In: P. Fritz and S.K. Frapé (Editors), *Saline Water and Gases in Crystalline Rocks*, Geol. Assoc. of Canada, Special Paper, 33: 145-156.
- Paces T. (Editor) 1991. *Fluid Sampling for Geothermal Prospecting*, UNITAR/UNDP Centre on Small Energy Resources, Rome: 93 pp.
- Pang Zhonghe and Reed, M.H., 1998. Theoretical chemical geothermometry on geothermal waters: Problems and methods. *Geochim. Cosmochim. Acta*, 62: 1083-1091.
- Pang Zhonghe and Wang Jiyang, 1995. Application of isotope and geochemical techniques to geothermal exploration - the Zhangzhou Case. In: Proc. 1995 World Geothermal Congress, International Geothermal Association, Vol. 2: 1037-1042.
- Panichi, C., Nuti, S. and Noto P., 1979. Remarks on the use of isotopic geothermometers in the Larderello geothermal field. In: *Isotope Hydrology Vol. II*, IAEA Vienna: 613-630.
- Paul, M., Fink, D., Hollos, G., Kaufman, A., Kutschera, W. and Magaritz, M., 1987. Measurement of <sup>129</sup>I concentrations in the environment after the Chernobyl reactor accident. *Nucl. Instr. Meth. Phys. Rev. B*, 29: 341-345.
- Pauwels, H., Fouillac, C., Goff, F. and Vuataz, F.-D., 1997. The isotopic and chemical composition of CO<sub>2</sub>-rich thermal waters in the Mont-Dore region (Massif-Central, France). *Appl. Geochemistry*, 12: 411-427.
- Pearson, Jr. F.J. and Rightmire, C.T., 1980. Sulfur and oxygen isotopes in aqueous sulfur compounds. In: P. Fritz and J.Ch. Fontes (Editors), *Handbook of Environmental Isotope Geochemistry*, Elsevier, Amsterdam: 227-258.

## References

- Pearson, Jr., F.J., Noronha, C.J. and Andrews, R.W., 1983. Mathematical modeling of the distribution of natural  $^{14}\text{C}$ ,  $^{234}\text{U}$ , and  $^{238}\text{U}$  in a regional groundwater system. *Radiocarbon*, 25: 291-300.
- Petit, J.-C., Langevin, Y. and Dran, J.-C., 1985.  $^{234}\text{U}/^{238}\text{U}$  disequilibrium in nature. theoretical reassessment of the various proposed models. *Bull. Mineral.*, 108: 745-753.
- Phillips, F.M., Goff, F., Vuataz, F., Bentley, H.W., Elmore, D. and Gove, H.E., 1984a.  $^{36}\text{Cl}$  as a tracer in geothermal systems: example from Valles Caldera, New Mexico. *Geophys. Res. Letters*, 11 (12): 1227-1230.
- Phillips, F.M., Trotman, K.N., Bentley, H.W., Davis, S.N. and Elmore, D., 1984b. Chlorine-36 from atmospheric nuclear weapons testing as a hydrologic tracer in the zone of aeration in arid climates. In: *Proc. RIZA Symp*, Munnich: 47-56.
- Phillips, M., Bentley, H.W., Davis, S.N., Elmore, D. and Swanick, G.B., 1986. Chlorine-36 dating of very old groundwater 2. Milk River aquifer, Alberta, Canada. *Water Resour. Res.*, 22 (13): 2003-2016.
- Phillips, F.M., Tansey, M.K. and Peeters, L.A., 1989. An isotopic investigation of groundwater in the central San Juan Basin, New Mexico: carbon 14 dating as a basis from numerical flow modeling. *Water Res. Res.*, 25: 2259-2273.
- Plöthner, D. and Geyh, M.A., 1991.  $\delta^{18}\text{O}$  values as tracer of artificial groundwater recharge downstream of a reservoir. *Memoires XXII (Part 2)*, IAH, Lausanne: 533-539.
- Plummer, L.N., Prestemon, E.C. and Parkhurst, D.L., 1994. An interactive code (NETPATH) for modeling Net Geochemical Reactions along a Flow Path. Version 2.0. *Water-Resources Investigation Report*, 94-4169, U.S. Geol. Survey, Reston: 227 pp.
- Richet, P., Bottinga, Y. and Javoy, M., 1977. A review of hydrogen, carbon, nitrogen, oxygen, sulfur and chlorine stable isotope fractionation among gaseous molecules. *Ann. Reg. Earth Planet. Sci.*: 65-110.
- Richter, J., Szymczak, P., Abraham, T. and Jordan, H., 1993. Use of combinations of lumped parameter models to interpret groundwater isotopic data. *J. Contaminant Hydrol.*, 14: 1-13.
- Rogojin, V., Carmi, I. and Kronfeld, J., 1998.  $^{14}\text{C}$  and  $^{234}\text{U}$ -excess dating of groundwater in the Haifa Bay region, Israel. *Radiocarbon*, 40 (2): 945-951.
- Rozanski, K., 1985. Deuterium and Oxygen-18 in European groundwaters - links to atmospheric circulation in the past. *Chem. Geology (Isot. Geosci. Sect.)*, 52: 349-363.
- Rozanski, K. and Florkowski, T., 1979. Krypton-85 dating of groundwater. In: *Isotope Hydrology 1978 Vol.II*, IAEA Vienna: 949-959.
- Rye R.O. and Ohmoto H., 1974. Sulphur and carbon isotopes in ore genesis. *Econ. Geology*, 69: 910.

## References

- Sakai H. and Matsubaya O., 1977. Stable isotope studies of Japanese geothermal systems. *Geothermics*, 5: 97-124.
- Sakai, H., Gunnlaugsson, E., Tomasson, J. and Rouse, J.E., 1980. Sulphur isotope systematics in Icelandic geothermal systems and influence of seawater circulation at Reykianes. *Geochim. Cosmochim. Acta*, 44: 1223-1231.
- Salem, O., Visser, J.M., Deay, M. and Gonfiantini, R., 1980. Groundwater flow patterns in the western Lybian Arab Jamahitiya evaluated from isotope data. In: *Arid Zone Hydrology: Investigations with Isotope Techniques*, IAEA Vienna: 165-179.
- Salvamoser, J., 1986. Quantitative separation of admixed young groundwater and surface water with the  $^3\text{H}$ - $^{85}\text{Kr}$  method. In: *Conjunctive Water Use*, IAHS Publ. 156: 355-363.
- Saxena, R.K. and Dressie, Z., 1984. Estimation of groundwater recharge and moisture movement in sandy formations by tracing natural oxygen-18 and injected tritium profiles in the unsaturated zone. In: *Isotope Hydrology 1983*, IAEA Vienna: 139-150.
- Schaefer, R.W. and Usdowski, E., 1992. Application of stable carbon and sulfur isotope models to the development of groundwater in a limestone-dolomite-anhydrite-gypsum area. In: G. Matthes, G.F. Frimmel, P. Hirsch, H.D., Schulz, H.-E. and E. Usdowski (Editors) *Progress in Hydrogeochemistry*, Springer, Berlin: 157-163.
- Schlosser, P., Stute, M., Sonntag, C. and Münnich, K. O., 1989. Tritogenic  $^3\text{He}$  in shallow groundwater. *Earth Planet. Sci. Letters*, 94: 245-256.
- Seiler, K.P. and Rodriguez, C.O., 1980. Geological and hydraulic boundary conditions for the interpretation of isotope data. In: *Proc. Interamerican Symp. on Isotope Hydrology*, Fondo Colombiano de Investigaciones Cientificas y Proyectos Especiales, Bogota: 43-59.
- Smejkal V., 1978. Isotope geochemistry of the Cypris formation in the Cheb Basin, West Bohemia. I. Sulphur isotopes in sulphates and pyrites. *Vestnik Ustredniho ustava geologickeho*, 53: 3-18.
- Smejkal, V. and Jetel, J., 1990. Isotopic and geochemical indications of a drainless sulfate lake in the PermoCarboniferous of the Krkonose-piedmont basin. *Vestnik Ustredniho ustavu geologickeho*, 65: 339-352.
- Sonntag, C., Thoma, G., Münnich, K.O., Dincer, T. and Klitzsch E., 1980a. Environmental isotopes in North African groundwaters and the Dahna sand-dune study, Saudi Arabia. In: *Arid-Zone Hydrology: Investigations with Isotope Techniques*, IAEA Vienna: 77-84.
- Sonntag, C., Thorweihe, U., Rudolf, J., Löhnert, E.P., Junghans, C., Münnich, K.O., Klitzsch, E., El Shazly, E.M. and Swailem, F.M., 1980b. Paleoclimatic evidence in apparent  $^{14}\text{C}$  ages of Saharian groundwaters. *Radiocarbon*, 22 (III): 871-878.
- Sonntag, C., Christmann, D. and Münnich, K.O., 1985. Laboratory and field experiments on infiltration and evaporation of soil water by means of deuterium and oxygen-18. In:

## References

- Stable and Radioactive Isotopes in the Study of the Unsaturated Zone, IAEA-TECDOC-357, IAEA Vienna: 145-160.
- Stagg, K.A., Kleinert, U., Tellam, J.H. and Lloyd, J.W., 1997. Colloidal populations in urban and rural groundwaters, UK. In: P.J. Chilton (Editor), *Groundwater in the Urban Environment Vol. I, Problems, Processes and Management* Balkema, Rotterdam: 187-192.
- Stewart, M.K., 1975. Stable isotope fractionation due to evaporation and isotopic exchange of falling water drops: application to atmospheric processes and evaporation of lakes. *J. Geophys. Res.*, 80: 1133-1146.
- Stewart, M.K., 1978. Stable isotopes in waters from the Wairakei geothermal system, New Zealand. In: *Stable Isotopes in the Earth Sciences*, N.Z. DSIR Bull., 220: 113-119.
- Stichler, W. and Herrmann, A., 1983. Application of environmental isotope techniques in water balance studies of small basins. In: *New Approaches in Water Balance Computations*, IAHS, Hamburg, IAHS-148: 93-112.
- Stute, M. and Deak, M., 1989. Environmental isotopic study ( $^{14}\text{C}$ ,  $^{13}\text{C}$ ,  $^{18}\text{O}$ , D, noble gases) on deep groundwater circulation systems in Hungary with reference to paleoclimate. *Radiocarbon*, 31 (3): 902-918.
- Suckow, A. and Sonntag, C., 1993. The influence of salt on the noble gas geothermometer. In: *Isotopic Techniques in the Study of Past and Current Environmental Changes in the Hydrosphere and the Atmosphere*, IAEA Vienna: 307-318.
- Sukhija, B.S. and Shah, C.R., 1976. Conformity of groundwater recharge rate by tritium method and mathematical modelling. *J. Hydrol.*, 30: 167-78.
- Taran, Y.A., Pokrovsky B.G. and Esikov, A.D., 1988. Deuterium and oxygen-18 in fumarolic steam and amphiboles from some Kamchatka volcanoes. "Andesitic" waters. IAVCEI, Commission on the Chemistry of Volcanic Gases, Newsletter, 1: 15-18.
- Taylor H.P., 1974. The application of oxygen and hydrogen isotope studies to problems of hydrothermal alteration and ore deposition. *Econ. Geol.*, 69: 843-883.
- Taylor, H.P. jr., 1977. Water/rock interaction and the origin of  $\text{H}_2\text{O}$  in granitic batholiths. *J. Geol. Soc. London*, 133: 509-558.
- Taylor, B.E., Wheeler, M.C. and Nordstrom, D.K., 1984. Isotopic composition of sulfate in acid mine drainage as measure of bacterial oxidation. *Nature*, 308: 538-541.
- Thoma, G., Esser, N., Sonntag, C., Weiss, W. and Rudolph, J., 1979. New technique of in-situ soil-moisture sampling for environmental isotope analysis applied at Pilot sand dune near Bordeaux - HETP modelling of bomb tritium propagation in the unsaturated and saturated zones. *Isotope Hydrology 1978*, Vol. II, IAEA Vienna: 191-204.



## References

- Thorburn, P.J. and Walker, G.R., 1994. Variations in stream water uptake by *Eucalyptus camaldulensis* with differing access to stream water. *Oecologia*, 100: 293-301.
- Todd, D.K., 1959. *Groundwater Hydrology*, Wiley, New York: 336 pp.
- Toran, L. and Harris, R.F., 1989. Interpretation of sulphur and oxygen isotopes in biological and abiological sulfide oxidation. *Geochim. Cosmochim. Acta*, 53: 2341-2348.
- Torgersen, T. and Clarke, W.B., 1985. Helium accumulation in groundwater I: an evaluation of sources and the continental flux of crustal  $^4\text{He}$  in the Great Artesian Basin, Australia. *Geochim. Cosmochim. Acta*, 49: 1211-1218.
- Torgersen, T. and Clarke, W.B., 1987. Helium accumulation in groundwater. III. Limits on helium transfer across the mantle-crust boundary beneath Australia and the magnitude of mantle degassing. *Earth Planet. Sci. Letters*, 84: 345-355.
- Torgersen, T. and Ivey, G.N., 1985. Helium accumulation in groundwater. II: A model for the accumulation of the crystal  $^4\text{He}$  degassing flux. *Geochim. Cosmochim. Acta*, 49: 2445-2452.
- Tóth, J., 1963. A theoretical analysis of groundwater flow in small drainage basins. *J. Geophys. Res.*, 68: 4795-4812.
- Truesdell A.H. and Hulston J.R., 1980. Isotopic evidence on environments of geothermal systems. In: P. Fritz and J. Ch. Fontes (Editors), *Handbook of Environmental isotope Geochemistry Vol. I*: 179-226.
- Truesdell, A.H., Nathenson, M. and Rye, R.O., 1977. The effects of subsurface boiling and dilution on the isotopic composition of Yellowstone thermal waters. *J. Geophys. Res.*, 82: 3694-3704.
- Van Warmerdam, E.M., Frappe, S.K., Aravena, R., Drimmie, R.J., Flatt, H. and Cherry, J.A., 1995. Stable chlorine and carbon isotope measurements of selected organic solvents. *Appl. Geochem.*, 10: 547-552.
- Vengosh, A., Chivas, A.R., McCulloch, M.T., Starinsky, A. and Kolodny, Y., 1991. Borone-isotope geochemistry of Australian salt lakes. *Geochim. Cosmochim. Acta*, 55: 2591-2606.
- Vengosh, A., Heumann, K.G., Juraske, S. and Kasher, R., 1994. Boron isotope application for tracing sources of contamination on groundwater. *Environ. Sci. Technol.*, 28: 1968-1974.
- Vengosh, A., Kolodny, Y., and Spivack, A.J., 1998. Ground-water pollution determined by boron isotope systematics. In: *Application of Isotope Techniques to Investigate Groundwater Pollution*, IAEA-TECDOC-1046, IAEA, Vienna: 17-38.
- Verhagen, B.Th., Mazor, E. and Sellshop, J.P.F., 1974. Radiocarbon and tritium evidence for direct recharge to groundwaters in the Northern Kalahari. *Nature*, 249: 643-644.

## References

- Verhagen, B.Th., Geyh, M.A., Fröhlich, K. and Wirth, K., 1991. Isotope Hydrological Methods for the Quantitative Evaluation of Ground Water Resources in Arid and Semi-arid Areas. Development of a Methodology, Ministry of Economic Cooperation, Bonn: 164 pp.
- Vogel, J.C., 1970. Carbon-14 dating of groundwater. In: Isotope Hydrology 1970, IAEA Vienna: 225-240.
- Vogel, J.C., Ehhalt, D., 1963. The use of the carbon isotopes in groundwater studies. In: Radioisotopes in Hydrology, IAEA Vienna: 383-395.
- Wassenaar, L., Aravena, R., Hendry, J. and Fritz, P., 1991. Radiocarbon in dissolved organic carbon, a possible groundwater dating method: Case studies from western Canada. *Water Res. Res.*, 27: 1975-1986.
- Wakshal, E. and Yaron, F., 1974.  $^{234}\text{U}/^{238}\text{U}$  disequilibrium in waters of the Judea Group (Cenomanian-Turonian) aquifer in Galilee, northern Israel. In: Isotope Techniques in Groundwater Hydrology Vol. II, IAEA Vienna: 151-177.
- Walker, G.R., Hughes, M.W., Allison, G.B. and Barnes, C.J., 1988. The movement of isotopes of water during evaporation from a bare soil surface. *J. Hydrol.*, 97: 181-197.
- Weiss, W., Sittkus, A., Stockburger, H., Sartorius, H. and Münnich, K.O., 1983. Large-scale atmospheric mixing derived from meridional profiles of krypton-85. *J. Geophys. Res.*, 88 (C 13): 8574-8578.
- White, D.E., Barnes, I. and O'Neil, J.R., 1973. Thermal and mineral waters of nonmeteoric origin, California Coast Ranges. *Geol. Soc. Am. Bull.*, 84: 547-560.
- Wickman, T. and Jacks, G., 1992. Strontium isotopes in weathering budgeting. In: Y.K. Kharaka and A.S. Maest (Editors), *Water-Rock Interaction*: 611-614.
- Wigley, T.M.L., Plummer, L.N. and Pearson, F.J., Jr., 1978. Mass transfer and carbon isotope evolution in natural water systems. *Geochim. Cosmochim. Acta.*, 42: 1117-1139.
- Woods, P.H., 1990. Evaporative discharge of groundwater from the margin of the Great Artesian Basin near Lake Eyre, South Australia. Unpubl. PhD Thesis, Flinders University, South Australia
- Yechieli, Y., Ronen, D. and Kaufman, A., 1996. The source and age of groundwater brines in the Dead Sea area, as deduced from  $^{36}\text{Cl}$  and  $^{14}\text{C}$ . *Geochim. Cosmochim. Acta*, 60: 1909 - 1916.
- Yurtsever, Y. and Payne, B.R., 1979. Application of environmental isotopes to groundwater investigations in Qatar. *Isotope Hydrology 1978 Vol. II*, IAEA Vienna: 465-490.
- Zimmermann, U., Ehhalt, D. and Münnich, K.G., 1967. Soil water movement and evapotranspiration: changes in the isotopic composition of the water. In: *Isotopes in Hydrology*, IAEA Vienna: 567-584.

## References

- Zuber, A., 1986. Chapter 1. Mathematical models for the interpretation of environmental radioisotopes in groundwater systems. In: P. Fritz and J. Ch. Fontes (Editors), *Handbook of Environmental Isotope Geochemistry* Vol. 2, Elsevier, Amsterdam: 1-59.

# LITERATURE

- |  |  |  |
|--|--|--|
| <b>H.Moser</b><br><b>W.Rauert</b>        | <b>Isotopenmethoden in der Hydrologie</b> (1980)<br>(in German language) ISBN 3-443-01012-1  | Gebr. Borntraeger<br>Berlin, Stuttgart   |
| <b>P.Fritz</b><br><b>J.Ch.Fontes</b>     | <b>Handbook of Environmental Isotope<br/>Geochemistry</b> ISBN 0-444-41781-8<br><br>Vol.1. The Terrestrial Environment A (1980)<br>Vol.2. The Terrestrial Environment B (1986)<br>Vol.3. The Marine Environment A (1989) | Elsevier Science Publ.<br>Amsterdam, Oxford<br>New York, Tokyo<br>ISBN 0-444-41780-X<br>ISBN 0-444-42225-0<br>ISBN 0-444-42764-3 |
| <b>F.J.Pearson</b><br><b>e.a.</b>        | <b>Applied Isotope Hydrogeology</b> , a case study<br>in Northern Switzerland (1991)<br>ISBN 0-444-88983-3   | Elsevier Science Publ.<br>Amsterdam, Oxford,<br>New York, Tokyo  |
| <b>I.Clark</b><br><b>P.Fritz</b>         | <b>Environmental Isotopes in Hydrogeology</b><br>(1997)<br>ISBN 1-56670-249-6  | Lewis Publishers<br>Boca Raton,<br>New York  |
| <b>F.Gasse</b><br><b>Ch.Causse</b>       | <b>Hydrology and Isotope Geochemistry</b><br>ISBN 2-7099-1377-1  | Editions de l'Orstom<br>Paris  |
| <b>W.Kaess</b>                           | <b>Tracing in Hydrogeology</b> (1998)<br>ISBN 3-443-01013-X  | Balkema, Rotterdam   |
| <b>C.Kendall</b><br><b>J.J.McDonnell</b> | <b>Isotopes in Catchment Hydrology</b> (1998)<br>ISBN 0-444-50155-X  | Elsevier/North<br>Holland Publ.Comp.<br>Amsterdam  |

Literature

- |   |  |                    |
|---|--|--------------------|
| <b>E.Mazor</b>  | <b>Chemical and Isotopic Groundwater<br/>Hydrology – The applied approach (1998)</b><br>ISBN 0-8247-9803-1 | Marcel Dekker Inc. |
| <b>P.G.Cook</b><br><b>A.L.Herczeg</b><br><b>(ed.)</b> | <b>Environmental Tracers in Subsurface<br/>Hydrology (2000)</b><br>ISBN 0-7923-7707-9                      | Kluwer Acad. Publ. |

# IAEA PUBLICATIONS

## IAEA CONFERENCE PROCEEDINGS

- 1963 **Radioisotopes in Hydrology**, Tokyo, 5-9 March 1963, IAEA, Vienna, 459 pp. (STI/PUB/71) (out of print).
- 1967 **Isotopes in Hydrology**, Vienna, 14-18 November 1966, IAEA, Vienna, (in co-operation with IUGG), 740 pp. (STI/PUB/141) (out of print).
- 1970 **Isotope Hydrology**, Vienna, 6-13 March 1970, IAEA, Vienna, (in co-operation with UNESCO), 918 pp. (STI/PUB/255) (out of print).
- 1974 **Isotope Techniques in Groundwater Hydrology**, Vienna, 11-15 March 1974, IAEA, Vienna, 2 volumes: 504 and 500 pp. (STI/PUB/373) (out of print).
- 1979 **Isotope Hydrology** (in 2 volumes), Neuherberg, Germany, 19-23 June 1978, IAEA, Vienna, (in co-operation with UNESCO), 2 volumes of 984 pp. (STI/PUB/493) ISBN 92-0-040079-5 and ISBN 92-0-040179-1.
- 1983 **Isotope Hydrology**, Vienna, 12-16 September 1983, IAEA, Vienna, (in co-operation with UNESCO), 873 pp. (STI/PUB/650) ISBN 92-0-040084-1.
- 1987 **Isotope Techniques in Water Resources Development**, Vienna, 30 March-3 April 1987, IAEA, Vienna, (in co-operation with UNESCO), 815 pp. (STI/PUB/757) ISBN 92-0-040087-6.
- 1992 **Isotope Techniques in Water Resources Development**, Vienna, 11-15 March 1991, IAEA, Vienna, (in co-operation with UNESCO), 790 pp. (STI/PUB/875) ISBN 92-0-000192-0.
- 1993 **Isotope Techniques in the Study of Past and Current Environmental Changes in the Hydrosphere and the Atmosphere**, Vienna, 19-23 April 1993, IAEA, Vienna, 624 pp. (STI/PUB/908) ISBN 92-0-103293-5.
- 1995 **Isotopes in Water Resources Management** (in 2 volumes), IAEA, Vienna, 20-24 March 1995, IAEA, Vienna, 2 volumes: 530 and 463 pp. (STI/PUB/970) ISBN 92-0-105595-1 and 92-0-100796-5.
- 1998 **Isotope Techniques in the Study of Environmental Change**, Vienna, 14-18 April 1997, IAEA, Vienna, 932 pp. (STI/PUB/1024) ISBN 92-0-100598-9.
- 1999 **Isotope Techniques in Water Resources Development and Management**, 10-14 May 1999, IAEA, Vienna, CD Rom (IAEA-CSP-2C) ISSN 1562-4153.

## **SPECIAL IAEA SYMPOSIA**

- 1967 **Radioactive Dating and Methods in Low-Level Counting**, Monaco, 2-10 March 1967, IAEA, Vienna, 744 pp. (STI/PUB/152) (out of print).
- 1979 **Behaviour of Tritium in the Environment**, San Francisco, USA, 16-20 October 1978, 711 pp. (STI/PUB/498) ISBN 92-0-020079-6.
- 1981 **Methods of Low-Level Counting and Spectrometry**, Berlin, Germany, 6-10 April 1981, IAEA, Vienna, 558 pp. (STI/PUB/592) (out of print).

## **IAEA REPORTS AND TECHNICAL DOCUMENTS (TECDOCS)**

- Environmental Isotope Data no.1 – no.10: World Survey of Isotope Concentration in Precipitation**, Data from network of IAEA and WMO over period 1953-1991, published 1969-1994.
- Interpretation of Environmental Isotope and Hydrochemical Data in Groundwater Hydrology**, Proc. Adv. Group Meeting, Vienna, 27-31 January 1975, IAEA, Vienna, 1976, 230 pp. (STI/PUB/429) ISBN 92-0-141076-X.
- Isotopes in Lake Studies**, Proc. Adv. Group Meeting, Vienna, 29 August-2 September 1977, IAEA, Vienna, 1979, 290 pp. ISBN 92-0-141179-0 (out of print).
- Arid Zone Hydrology: Investigations with Isotope Techniques**, Proc. Adv. Group Meeting, Vienna, 6-9 November 1978, IAEA, Vienna, 1980, 265 pp. (STI/PUB/547) ISBN 92-0-141180-4.
- Stable Isotope Standards and Intercalibration on Hydrology and Geochemistry**, (R. Gonfiantini ed.), Report on Consultants' Meeting, Vienna, 8-10 September 1976, IAEA, Vienna, 1977.
- Stable Isotope Hydrology Deuterium and Oxygen-18 in the Water Cycle**, (J.R. Gat and R. Gonfiantini eds.), Monograph by Working Group, IAEA, Vienna, 1981, 340 pp. (STI/DOC/10/210).
- Palaeoclimates and Palaeowaters: A Collection of Environmental Isotope Studies**, Proc. Adv. Group Meeting, Vienna, 25-28 November 1980, IAEA, Vienna, 1981, 207 pp. (STI/PUB/621) ISBN 92-0-141083-2.

- Guidebook on Nuclear Techniques in Hydrology**, by Working Group IAEA, Vienna, 1983, 439 pp. (STI/DOC/10/91/2)
- Stable Isotope Reference Samples for Geochemical and Hydrological Investigations**, (R. Gonfiantini ed.), Report by Advisory Group's Meeting, Vienna, 19-21 September 1983, IAEA, Vienna, 1984.
- Stable and Radioactive Isotopes in the Study of the Unsaturated Soil Zone**, Proc. Meeting on IAEA/GSF Progr., Vienna, 10-14 September 1984, IAEA, Vienna, 1985, 184 pp. (TECDOC-357)
- Isotope Techniques in the Study of the Hydrology of Fractured and Fissured Rocks**, Proc. Adv. Group Meeting, Vienna, 17-21 November 1986, IAEA, Vienna, 1989, 306 pp. (STI/PUB/790)
- Stable Isotope Reference Samples for Geochemical and Hydrological Investigations**, Report on Consultants' Meeting, Vienna, 16-18 September 1985, edited by G. Hut, IAEA, Vienna, 1987.
- Use of Artificial Tracers in Hydrology**, Proc. Adv. Group Meeting, Vienna, 19-22 March 1990, IAEA, Vienna, 1990, 230 pp. (TECDOC-601)
- C-14 Reference Materials for Radiocarbon Laboratories**, (K. Rozanski, ed), Report on Consultants' Meeting, Vienna, 18-20 February 1981, IAEA, Vienna 1991.
- Guidelines for Isotope Hydrology**, Manuel for Operation of an Isotope Hydrology Laboratory IAEA, Vienna, 1999 (in prep.)
- Isotopes of Noble Gases as Tracers in Environmental Studies**, Report by Consultants' Meeting, Vienna, 29 May-2 June, 1989, IAEA, Vienna, 305 pp. (STU/PUB/859) (out of print) ISBN 92-0-100592-X
- Statistical Treatment of Data on Environmental Isotopes in Precipitation**, IAEA, Vienna, 1992, 781 pp. (STI/DOC/10/331)
- Isotope and Geochemical Techniques applied to Geothermal Investigations**, Proc. Res. Coord. Meeting, Vienna, 12-15 October 1993, IAEA, Vienna, 1995, 258 pp. (TECDOC-788)
- Reference and Intercomparison Materials for Stable Isotopes of Light Elements**, Proc. Cons. Meeting, Vienna, 1-3 December 1993, IAEA, Vienna, 1995. (TECDOC-825)
- Manual on Mathematical Models in Hydrogeology**, IAEA, Vienna, 1996, 107 pp. (TECDOC-910)



# CONSTANTS

a	year = $3.1558 \times 10^7$ s
amu	atomic mass unit = $1.660\ 54 \times 10^{-27}$ kg
c	velocity of light (in vacuum) = $2.997\ 925 \times 10^8$ m·s <sup>-1</sup>
cal	calorie = 4.184 J
e	elementary/electron/proton charge = $1.602\ 18 \times 10^{-19}$ C
eV	electronvolt = $1.602\ 18 \times 10^{-19}$ J
g	acceleration of free fall = $9.806\ 65$ m·s <sup>-2</sup>
h	Planck constant = $6.626\ 08 \times 10^{-34}$ J·s
J	Joule = 0.2390 cal
k	Boltzmann constant = $1.380\ 54 \times 10^{-23}$ J/K
m <sub>e</sub>	electron mass = $9.109\ 39 \times 10^{-31}$ kg
m <sub>n</sub>	neutron mass = $1.674\ 93 \times 10^{-27}$ kg
m <sub>p</sub>	proton mass = $1.672\ 62 \times 10^{-27}$ kg
M/E eq.	mass/energy equivalence: 1 amu ≈ 931.5 MeV
N <sub>A</sub>	Avogadro constant = $6.022\ 14 \times 10^{23}$ mol <sup>-1</sup>
π	= 3.141 592 6535
R	gas constant = $8.314\ 51$ J·K <sup>-1</sup> ·mol <sup>-1</sup>
T	thermodynamic temperature = t (°C) + 273.15 K
V <sub>m</sub>	molar volume (= 22.41 L·mole <sup>-1</sup> at STP)

# GLOSSARY

The following text books were used for the glossary: Glossary of Geology (1980) and International Glossary of Hydrology (1998), IHP/OHP-Reports, Koblenz, 243 pp.

**Age:** → *Water age*

**Apparent age:** Age determined by any method without consideration of all necessary corrections and conventions.

**Applied hydrology:** Branch of hydrology which applies to its application to the field connected with water-resources development and management.

**Aquiclude:** A body of relatively impermeable rock that is capable of absorbing water slowly but functions as an upper or lower boundary of an aquifer and does not transmit groundwater rapidly enough to supply a well or spring.

**Aquifer:** A body of rock that contains sufficient saturated permeable material to conduct groundwater and to yield economically significant quantities of groundwater to wells and springs (→ *permeability, Sect. 1.1*).

**Aquitard:** A confining bed that retards but does not prevent the flow of water from an adjacent aquifer (leaky confining bed). It does not readily yield water to wells or springs, but may serve as a storage unit for groundwater (→ Sect. 1.1).

**Artesian aquifer:** A confined aquifer containing groundwater under pressure, high enough to cause outflow in a well or spring.

**Artesian spring:** A spring discharging confined water from an underlying aquifer through a fissure or other opening in the confining bed that overlies the aquifer (→ Sect. 3.1.4.1).

**Artesian water:** In the traditional sense groundwater with a piezometric pressure high enough to cause outflow from a well or spring (→ *confined groundwater*).

**Artesian well:** A well tapping a confined or artesian aquifer in which the static water level stands above the surface of the ground or at least of the level of the shallow groundwater (→ confined aquifer).

**Artesian recharge:** Recharge of groundwater at a rate greater than natural, resulting from the activities of man, by means of dug basins, drilled wells, or spreading of water across the land surface.

- Base flow:** The part of the discharge, which enters a stream channel from groundwater. This is the runoff observed during long periods when no precipitation or snowmelt occurs.
- Boundary conditions:** Set of conditions to be satisfied by the solution of a differential equation at the boundary (including fluid boundary) of the region in which the solution is sought.
- Brackish water:** Groundwater with a total salt concentration of 1000 to 10 000 mg/L.
- Capillary fringe:** The zone immediately above the water table, where water is drawn upward by capillary attraction.
- Catchment area:** The entire area between the recharge and the discharge area
- Coefficient of filtration:** → *hydraulic conductivity* (Sect.3.1.1)
- Cone of depression:** → *Pumping cone*. Depression, in the shape of a cone with convex upwards limits, of the piezometric surface which defines the area of influence of a well.
- Conceptual hydrological model:** Simplified mathematical representation of some or all of the processes in the hydrological cycle by a set of hydrological concepts expressed in mathematical notations and linked together in a time and space sequence corresponding to that occurring in nature. Hydrological conceptual models are used for simulation of the behaviour of a basin (Sect.3.1.2 and 3.1.3; Volume VI).
- Confined aquifer:** An aquifer bounded above and below by impermeable beds or by beds of distinctly lower permeability than that of the aquifer itself, an aquifer containing confined groundwater.
- Confined groundwater:** Groundwater under a pressure significantly greater than that of the atmosphere. If tapped by a borehole, the water level in the borehole rises so that it corresponds to the pressure height at the point where it was tapped.
- Confined groundwater surface:** The upper surface of the groundwater body is under a pressure higher than that of the atmosphere. Identical with the upper surface of a confined aquifer. If tapped by a borehole, groundwater rises to the piezometric surface.
- Confining bed:** The formation overlying or underlying a much more permeable aquifer. → *aquiclude, aquitard*
- Connate water:** Water entrapped in the interstices of a sedimentary rock at the time of its deposition that has been out of contact with the atmosphere for at least an appreciable part of a geologic period.
- Darcy law:** → Sect.3.1.1
- Diffusion:** Process of spreading of a solute as a result of the thermal movement of the molecules of this solute. → Sect.3.1.2

**Direct runoff:** Flow of water entering stream channels promptly. It includes surface flows and interflow and is used where interflow cannot be separated in hydrological analysis. This part of surface runoff which reaches the catchment outlet shortly after the rain starts. Its volume is equal to rainfall excess. Some procedures for its derivation include prompt subsurface runoff but all exclude base flow.

**Distance velocity:** (syn. tracer velocity) – Velocity of a tracer defined by the quotient of distance and time. → *filter velocity* (Sect.3.1.1).

**Drawdown:** The distance by which the water level in a well is lowered by the withdrawal of water.

**Effective porosity:** The percentage of the total volume of a given mass of soil or rock that consists of interconnecting interstices through which water or other fluids can travel. → Sect.1.3.1

**Field capacity:** amount of water held in a soil after gravitational water has drained away. → Sect.1.3.2

**Filter velocity:** mass transport velocity in volume unit per time and area units calculated by the Darcy law. → Sect.3.1.1

**Fossil water:** Water recharged in an ancient geological period and not participating in the contemporary hydrological cycle.

**Free water table:** The unconfined groundwater level at which the pressure is equal to the atmospheric pressure.

**Freshwater:** Naturally occurring water having a concentration of salt < 1000 mg/L.

**Gravitational water:** (syn. mobile water) – Water in the unsaturated zone which moves under the influence of gravity. → Sect.1.3.1

**Groundwater:** (a) Subsurface water that is in the zone of saturation. It includes underground streams. (b) Loosely all subsurface water (excluding internal water) as distinct from surface water.

**Groundwater dating:** Determination of the time between the recharge of the groundwater and its sampling. → Sect.5.2.2

**Groundwater divide:** Line on a water table or piezometric surface on either side of which the groundwater flow diverges.

**Groundwater level:** (syn. groundwater table) – The elevation, at a certain location and time, of the phreatic or piezometric surface of an aquifer.

**Groundwater level:** Elevation, at a certain location and time, of the water table or piezometric surface of an aquifer.

**Groundwater mining:** Withdrawal from an aquifer containing fossil groundwater (Sect.3.2.1).

**Groundwater overexploitation:** Withdrawal of a groundwater reservoir in excess of the average rate of replenishment.

**Groundwater recharge** → *Recharge*

**Groundwater table:** (syn. groundwater level, phreatic surface) – The surface within the zone of saturation of an unconfined aquifer along which the pressure is atmospheric.

**Head, total:** The sum of the elevation head, the pressure head, and the velocity head at a given point in an aquifer.

**Histogram:** Univariate frequency diagram with rectangles proportional to the area to the class frequency, erected on a horizontal axis with width equal to the class interval.

**Hydraulic conductivity (K):** (syn. permeability coefficient) – A coefficient of proportionality describing the rate at which water can move through a permeable medium. The density and kinematic viscosity must be considered in determining the hydraulic conductivity. It has a dimension of velocity. → Sect.1.3.3

**Hydrological cycle:** Succession of stages through which water passes from the atmosphere to the earth and returns to the atmosphere: evaporation from the land or sea or inland water, condensation to form clouds, precipitation, accumulation in the soil or in bodies of water, and re-evaporation. → Volume I

**Hydrological regime:** Variations in the state and characteristics of a water body which are regularly repeated in time and space and which pass through phases, e.g. seasonal. → Sect.1.4.2

**Hydrosphere:** That part of the earth covered by water and ice. → Volume I

**Intermediate zone:** That part of the unsaturated zone below the root zone and above the capillary fringe. → Sect.5.1

**Infiltration coefficient:** Ratio of infiltration to rainfall.

**Interflow:** That portion of the precipitation which has not passed down to the water table, but is discharged from the unsaturated zone by lateral movement during and immediately after a precipitation event. The water moving as interflow discharges directly into a stream channel or lake.

**Intermittent spring:** Spring, which discharge occurs only during certain periods and ceases at other periods. → Sect.3.1.4.1

**Juvenile water:** A term applied to water that is known to have been derived directly from magma and that is thought to have come to the Earth's surface for the first time.

**Karst:** Limestone and dolomite areas that possess a topography peculiar to and dependent upon underground solution and the diversion of surface waters to underground routes. → Sect.1.4.2.4

**Leaky aquifer:** Aquifer overlain and/or underlain by a relatively thin semi-pervious layer, through which flow into or out of the aquifer can take place.

**Magmatic water:** Water brought to the earth's surface from great depths by the upwards movement of intrusive igneous rocks. → Chapter 6

**Modern water:** The groundwater directly recharged after 1963/64 labeled by higher activities of nuclear-bomb-produced tritium and radiocarbon. → Sect.5.2.2.1 and 5.2.2.2

**Moisture content or soil humidity:** The *weighted moisture content* is expressed by the ratio of the mass of water  $M_w$  to the total mass or to the mass of the solid  $M_t$ . The *volumetric humidity* or *volumetric water content* is the ratio of the volume of water  $V_w$  to the total volume of the sample  $V_t$ . → Sect.5.1.1

**Observation well:** Well used for measuring the static head of groundwater, and specially to observe the frequency and magnitude of changes in head or another physical or chemical parameter. → Sect.3.1.4.2

**Perched groundwater:** Unsaturated groundwater separated from an underlying main body of groundwater by an unsaturated zone (Sect.5.1).

**Permeability:** The property or capacity of a porous rock, sediment, or soil for transmitting a fluid; it is a measure of the relative ease of fluid flow under unequal pressure. The expressions “permeable” and “impermeable” have a relative meaning. An intercalation of the same permeability between layers of lesser permeability can act as an aquifer while between more permeable layers; it can act as an aquiclude. → Sect.1.3.3

**Phreatic surface:** The surface between the zone of saturation and the zone of aeration at which the pressure is equal to that of the atmosphere.

**Phreatic water:** A term that originally was applied only to water that occurs in the upper part of the zone of saturation under water-table conditions, but has come to be applied to all water in the zone of saturation, thus making it an exact synonym of groundwater.

**Piezometer:** A pipe sealed along its length, open to water flow at the bottom and open to the atmosphere at the top, that is used to measure the piezometric head at the point of an aquifer to which it reaches.

**Piezometric head:** (a) The elevation to which water of a given aquifer will rise in a piezometer. (b) The sum of the elevation and the pressure head in a liquid expressed in units of height.

**Piezometric surface:** (syn. potentiometric surface) – The surface to which water would rise in piezometers reaching into the same aquifer. In general, the piezometric surface is not

horizontal and plane but curved and it reflects the distribution of the hydraulic potential; i.e. of the mechanical energy of water within the aquifer at the depth reached by the piezometers. → Sect.1.3.4

**Playa:** Lake bed found in arid or desert regions in the lower part of a enclosed valley whose drainage is centripetal or inward. The lake is usually dry, except after heavy rains storms, when it may be covered by a thin sheet of water which quickly disappears through evaporation and/or infiltration.

**Porosity:** The *total porosity* is defined by the ratio of the total volume of water  $V_w$  and gas  $V_g$  available for water to the total volume of the sample  $V_t$ . This parameter may vary in case of refraction or expansion of the solid matrix (clays, gypsum). The *effective porosity* is defined by  $V_w / V_t$ . → Sect.1.3.1

**Potential evaporation:** Quantity of water valour which could be emitted by a surface of pure water in the existing conditions.

**Potentiometric surface:** → *Piezometric surface*

**Pumping cone:** The area around a discharging well where the hydraulic head in the aquifer has been lowered by pumping. → *cone of depression*

**Pumping test:** (syn. aquifer test) – A test made by pumping a well for a period of time and observing the change in hydraulic head in the aquifer. A pumping test may be used to determine the capacity of the well and the hydraulic characteristics of the aquifer.

**Recharge:** *Direct recharge* is related to the seepage of rainwater through the unsaturated zone into the aquifer. *Indirect recharge* is the recharge via rivers, lakes and other superficial water resources. *Artificial recharge* is the seepage of e.g. river water into a superficial sand bed where it recharge an exploited aquifer.

**Residence time:** Period during which water or a substance remains in a component part of the hydrological cycle. → Sect.3.1.2

**Return flow:** Any flow returns to a stream channel or to the groundwater after use.

**Root zone:** The zone from the land surface to the depth penetrated by plant roots. The root zone may contain part or all of the unsaturated zone, depending upon the depth of the roots and the thickness of the unsaturated zone (Sect.5.1).

**Runoff:** The total amount of water flowing in a stream. It includes overland flow, return flow, interflow and base flow.

**Safe yield:** Amount of water (in general, the long-term average amount) which can be withdrawn from a groundwater basin or surface water system without causing undesirable results.

**Salt water:** Water of which salt concentration exceeds 10 g/L.

**Saturated zone:** → *Zone of saturation*.

**Secondary porosity:** The porosity developed in a rock after its deposition or emplacement, through such processes as solution or fracturing.

**Storage coefficient:** (syn. storativity) – Volume of water an aquifer releases from or takes into storage per unit surface area of the aquifer per unit change of head.

**Subsurface water:** (syn. subterranean water, underground water, groundwater) – Water in the lithosphere in solid, liquid, or gaseous form. It includes all water beneath the land surface and beneath the bodies of surface water.

**Time series:** Set of observations, in order, taken at successive points of time, commonly at a fixed interval.

**Tracer velocity:** → *Distance velocity*, Sect. 3.1.1

**Transmissivity:** The rate at which water of prevailing density and viscosity is transmitted through a unit width of an aquifer or confining bed under a unit hydraulic gradient. It is a function of properties of the liquid, the porous media, and the thickness of the porous media. → Sect.1.3.3

**Turnover rate:** Ratio of the annual average groundwater recharge, expressed in volume, to the average groundwater storage of an aquifer. → Sect.3.1.2

**Turnover time:** Time required for supplying a volume equal to the total water reserve in a surface or groundwater reservoir, at the average rate of natural inflow or replenishment. → Sect.3.1.2

**Unconfined aquifer:** An aquifer containing unconfined groundwater. → *phreatic water*

**Unconfined groundwater:** Groundwater that has a free water table, i.e. water not confined under pressure beneath impermeable rocks. → *phreatic water*

**Unconfined groundwater level:** The groundwater level at which the pressure is equal to the atmospheric pressure, i.e. the surface of groundwater in an unconfined aquifer. → *phreatic water*

**Unsaturated zone:** The zone between the land surface and the water table. It includes the root zone, intermediate zone, and capillary fringe. The pore spaces contain water at less than atmospheric pressure, as well as air and other gases. Saturated bodies, such as perched groundwater, may exist in the unsaturated zone. Also called zone of aeration and vadose zone. → *zone of aeration*, Sect.5.1

**Vadose water:** any water that occurs in the unsaturated zone. → Sect.5.1

**Velocity:** → *Distance velocity*

**Zone of aeration:** (syn. unsaturated zone) – A subsurface zone containing water under pressure less than that of the atmosphere. It bears water held by capillary forces and air or



gases generally under atmospheric pressure. This zone is limited above by the land surface and below by the surface of the zone of saturation, i.e. the water table. The zone is subdivided into the belt of soil water, the intermediate belt and the capillary fringe. → Sect. 5.1

**Zone of saturation:** A subsurface zone in which all the interstices are filled with water under pressure greater than that of the atmosphere. → Sect. 5.2.

# SYMBOLS

c	solute concentration in water	$\varepsilon$	enrichment or depletion = $\alpha - 1$
d	thickness	$\lambda$	radioactive decay constant
d	deuterium excess	$\rho$	density of liquid or vapour
f	residence-time distribution function	$\sigma$	standard deviation
g	acceleration due to gravity	$\tau_0$	tortuosity
h	height	$\Delta$	difference
k	distribution coefficient	??	volumetric water content, humidity, field capacity
m	thickness	$\Sigma$	sum
q	deposition rate		
r	residual fraction		
s	slope		
t	age, time		
$\bar{t}$	mean residence time		
v	velocity		
x	proportion for mixing; x coordinate		
y	horizontal axis, y coordinate		
z	length, distance; z coordinate		
A	area; amplitude; specific activity = disintegrations/s		
D	diffusion or dispersion coefficient		
H	relative humidity; enthalpy		
J	flux of solute		
K	hydraulic conductivity		
M	mass		
$N_{\text{Sat}}$	saturated water vapour density		
MIX	mixed sample		
Q	discharge, recharge, evaporation rate		
R	atomic ratio between a rare and the abundant isotope of an element		
S	storage coefficient or degree of saturation		
T	temperature		
$T_{1/2}$	half-life		
V	volume		
X	end-member of mixing		
Y	mixed sample		
$\alpha$	equilibrium fractionation factor		
$\alpha_{\text{kin}}$	kinetic fractionation factor		
$\beta$	compressibility of the rock, water		
$\delta$	relative deviation of an isotope ratio from that of a standard		

## SUBSCRIPTS

aqu	aquifer
atm	atmospheric
avg	average
bnr	bound
cap	capillary
char	characteristic
diff	diffusion
dis	discharge
disp	dispersion
ef	evaporation front
eff	effective
equ	equilibrium
eva	evaporation
gas	gas
in	input
init	initial
isot	isotope species
kin	kinetic
liq	liquid
mob	mobile
out	output
por	pores
rec	recharge
res	feed soil water
rock	rock
sol	solid
spl	sample
std	standard
tot	total
trac	tracer

# SUBJECT INDEX

$^2\text{H}$  66  
 $^3\text{H}$  96  
 $^3\text{He}$  96  
 $^4\text{He}$  22, 113  
 $^{11}\text{B}$  89  
 $^{13}\text{C}$  72  
 $^{14}\text{C}$  18, 100  
 $^{14}\text{N}$  18, 75  
 $^{16}\text{O}$  66  
 $^{32}\text{Si}$  107  
 $^{34}\text{S}$  18, 79  
 $^{36}\text{Cl}$  107  
 $^{39}\text{Ar}$  109  
 $^{81}\text{Kr}$  110  
 $^{85}\text{Kr}$  111  
 $^{86}\text{Sr}$  17, 48, 92  
 $^{129}\text{I}$  112  
 $^{222}\text{Ra}$  114  
 $^{226}\text{Ra}$  114  
 $^{234}\text{U}$  115  
 $^{234}\text{U}/^{238}\text{U}$  115

## a

---

absorption 42  
accelerator mass spectrometry  $\Rightarrow$  AMS  
Ad Rhuma springs 106  
admixture  
    seawater 46  
    surface water 71  
adsorption 42  
advection 51  
age  
    absolute 74, 101, 116, 153, 182  
    apparent 19, 177, 182  
    conventional 107, 182  
    determination 95  
    groundwater 95  
    model 182  
    relative 153, 182  
    retention 2  
alluvial plain 12, 14  
altitude effect 69, 71  
amount effect 68

AMS 101  
anion exclusion 42, 51, 97  
anthropogenic disturbance 37  
Antilebanon mountains 151  
aquiclude 177  
aquifer 177  
    artesian 11  
    confined 4, 13, 25, 178  
    leaky 31, 180  
    perched 180  
    open 25  
    phreatic 4, 31, 180  
    unconfined 25, 182  
aquitard 177  
argon-39 109  
arid regions 7  
Azraq springs 38

## b

---

base flow 8, 177  
Berlin geothermal field, Salvador 140  
Black Triangle, Czech Republic 94  
black-box model 30  
Bohemian Massiv 47  
boron isotopes 89  
boundary conditions 177  
Botswana 59, 157  
brackish water 177  
by-pass flow 53

## c

---

capillary fringe 177  
carbon dioxide  
    biogenic 74  
    magmatic 74  
carbon isotopes  
    stable 72  
    radioactive 18, 100  
carbonate- $\text{CO}_2$  system 43, 103  
catchment area 178  
CFC  $\Rightarrow$  chlorofluorocarbon  
Cheb, Czech Republic 86, 87  
chemical reactions

carbonate 43, 74  
 organic matter 44  
 sulfur compounds 46  
 chlorine isotopes  
   stable 89  
   radioactive 107  
 chlorine-36 107  
 chlorofluorocarbon 22, 100, 111, 187  
 coefficient  
   filtration 178  
   infiltration 179  
   storage 4, 181  
 colloids 21, 46  
 conceptual model 178  
 conductivity, hydraulic 5, 26, 27, 177  
 confined  
   aquifer 178  
   bed 178  
   groundwater 178  
 connate water 178  
 continental effect 69, 72  
 convection 51  
 correction of  $^{14}\text{C}$  groundwater age  
   Gonfiantini model 74, 103  
   geochemical modelling 44, 107  
   Oeschger model 44, 106  
 Cyprus 71, 73

## d

Dahna dune field, Saudi Arabia 56  
 Darcy  
   law 26  
   velocity 27  
 dating 95  
 DCT  $\Rightarrow$  Diablo Canyon Iron Meteorite  
 (standard) 79  
 decay constant 31  
 dehydration 41, 50  
 delta value 17  
 denitrification 41  
 desulfurification 41  
 deuterium 66  
 deuterium excess 66, 188  
 Diablo Canyon Iron Meteorite (standard) 79  
 DIC 18, 102  
 diffusion 17  
 discharge 32, 64  
 dispersion 25, 51  
 dissolved inorganic carbon  $\Rightarrow$  DIC  
 DOC 102  
 Dortmund, Germany 114  
 drawdown 178  
 dual-pathway flow 9, 32, 53

dug well 98, 153

## e

effective porosity 178, 181  
 El Tatio geothermal field 161  
 evaporation rate 59  
 exchange;  
   ion 43  
   isotopic 41, 123

## f

FA (fulvic acids) 102, 189  
 fallout 58, 189  
 fertiliser 77  
 field capacity 4, 178  
 Fijeh springs, Syria 151  
 filtration velocity 27  
 flow  
   direction 6, 36, 108  
   laminar 25  
   line 6  
   macropore 53  
   modelling 25, 32  
   net, arid regions 5, 7  
   net, humid regions 7  
   velocity 26  
 fluid  
   geothermal 109, 119  
   history 130  
   origin 130  
 formation water 82, 130, 159  
 fossil groundwater 179  
 fractionation factor, isotopic 76, 119, 138  
 freshwater 179  
 fulvic acid 101, 189

## g

Galapagos geothermal field 115, 159  
 gases, noble 22  
 geohydraulics 25  
   unsaturated zone 50  
 geothermal oxygene-isotope shift 189  
 geothermometry, isotopic 120, 125  
   carbon dioxide – methane 126  
   sulphate-water geothermometer 129  
   water-hydrogen geothermometer 128  
 Geyser geothermal field 139  
 Gonfiantini correction model 74, 103  
 grain size 4  
 Great Artesian Basin 12, 65, 70, 90, 108, 111,

114  
 groundwater 179  
 abstraction 179  
 age 18  
 artesian 177  
 confined 178  
 connate 178  
 dating 18, 179  
 discharge 32  
 divide 179  
 head 79  
 level 179  
 mining 35, 37, 39  
 old 19  
 origin 65  
 overexploitation 37, 179  
 phreatic 180  
 oxidation of organic matter 44, 105  
 shallow 11, 49  
 recharge regime 10  
 table 179  
 unconfined 182  
 groundwater regime 10, 35

## h

---

half-life 18  
 Hamad region 37  
 Harz mountains 83  
 heat loss 134, 141  
 helium isotopes 113  
 high temperature systems 119  
 histogram 179  
 Hörter 75  
 humid regions 7  
 humidity, soil 180  
 hydraulic conductivity 6, 178  
 hydraulic gradient 5  
 hydrogen isotopes  
 stable 66  
 radioactive 96  
 hydrogeology 8  
 hydrograph 33, 68  
 hydroisochron 5  
 hydrological cycle 179  
 regime 179  
 hydrosphere 179

## i

---

IAEA  
 global network ([www.iaea.or.at](http://www.iaea.or.at)) 97  
 incongruent precipitation 96

infiltration coefficient 179  
 initial <sup>14</sup>C activity 16, 103  
 initial specific activity 18  
 input function 16, 20  
 interflow 32, 179  
 iodine-129 112  
 ion exchange 43  
 irrigation return flow 181  
 isotope fractionation factor 76, 138  
 isotope production ⇒ production

## j

---

juvenile water 180

## k

---

karst system 9, 12, 113  
 kinematic dispersion 52  
 krypton-81 110  
 krypton-85 111

## l

---

Larderello geothermal field 143, 146, 166  
 latitude effect 190  
 leaching of salt 72  
 leaky aquifer 31, 110, 153  
 liquid-vapour separation 137  
 low-temperature systems 49

## m

---

macropore flow 53  
 magmatic water 180  
 Massif Central 93, 166  
 matrix diffusion 105, 191  
 mean residence time 8  
 Mediterranean  
 Meteoric Water Line 66, 191  
 slope 63, 67  
 Meteoric Water Line 66  
 methane  
 genesis 44  
 isotopic geothermometer 127  
 microbial processes 41, 82  
 Milk River aquifer 109, 164, 166  
 mixing line 20, 71, 76, 84, 93, 130  
 model  
 age 102, 191  
 black-box 30  
 compartmental 31

conceptional 31, 177  
 dispersion 30  
 exponential 25, 29  
 flow 32  
 hydrochemical 74  
 lump-parameter 30, 97  
 piston-flow 25, 28  
 two-component 20, 28, 71, 82, 93, 131  
 three-component 21, 28, 42, 71  
 moisture content 180  
 MRT  $\Rightarrow$  mean residence time  
 multi-isotope study 151  
 multi-stage steam separation 135  
 MWL  $\Rightarrow$  meteoric water line

## n

NETPATH 43, 74  
 Ngawha geothermal field 123, 124, 162  
 nitrification 41, 75  
 nitrogen isotopes 18, 75  
   mineralisation of organic nitrogen 75  
   biological fixation 77  
 noble gases 22  
 non-steady state  
   recharge-discharge 13, 36, 104  
   anthropogenic disturbance 37  
   palaeoclimatic change 36  
 northern India 58  
 Nubian Sandstone Basin 12  
 nuclear-weapon test 16

## o

observation well 180  
 Oeschger correction 106  
 origin of groundwater 65  
 oxidising zone 115, 117  
 oxygen isotopes 66  
   geothermal  $\delta^{18}\text{O}$ -shift 121, 131

## p

palaeoclimate effect 36, 69  
 palaeohydrology 37  
 palaeogroundwater 36  
   Holocene 70  
   Pleistocene 70  
 Palinpinon geothermal field 146  
 Pelat 57  
 percent modern carbon  $\Rightarrow$  pMC  
 perched aquifer 34, 180

permeability 5, 180  
 phreatic aquifer 180, 182  
 piezometer 180  
 piezometric surface 180  
 piston-flow model 25, 28  
 planning isotope studies 152  
 plant water extraction 54, 65  
 platform sediments 12  
 playa 180  
 Pleistocene palaeowater 70  
 pluvial period 36, 38  
 pMC 101  
 pollution studies 90  
 pore water 53  
 porosity 2  
   effective 178, 181  
   total 181  
   secondary 181  
 potential evaporation 181  
 potentiometric surface 180  
 production, isotopic  
   cosmogenic 102  
   subsurface 19, 96, 107, 108, 111  
 production well 34  
 pumping  
   cone 178, 181  
   test 5, 71, 181

## r

radioactive decay 18  
 radiocarbon 18, 100  
 radium/radon 114  
 radon 114  
 reactions, chemical  
   carbonate 43  
   organic matter 44  
   sulfur compounds 46  
 recharge  
   area 69, 103  
   artesian 177  
   artificial 181  
   direct 181  
   indirect 181  
   temperature 22, 23  
 recharge rate  
   mass balance method 54, 58  
   temperature 22  
   tracer-peak displacement method 55  
    $^3\text{H}$ -interface method 99  
 reducing zone of aquifers 115  
 regime, hydrological 10, 179  
 regional flow systems 192  
 re-injecting thermal waste water 141

- reservoir correction 19, 103, 105  
 reservoir effect 102  
 retention, specific 3  
 return flow 181  
 rocks  
   consolidated sedimentary 9  
   crystalline 11  
   igneous 8  
   karstified 12  
   metamorphic 9  
   sedimentary 11  
   unconsolidated 10  
   volcanic 11  
 root zone 181  
 runoff, direct 32, 178
- S**
- 
- safe yield 181  
 Sahara desert 64, 70, 160  
 salination processes 72, 109  
 saline water 181  
 sampling 35, 151  
 saturated zone 65  
 seasonal isotope variation 68  
 sedimentary rocks 11  
 separated vapour 123, 137  
 sewage 76, 90, 92  
 Showashinzan Volcano, Japan 134  
 silicon-32 107  
 SMOW  $\Rightarrow$   
   Vienna Standard Mean Ocean Water  
 solute transport 51, 53  
 specific yield 2, 4  
 spring  
   artesian 34, 177  
   barrier 34  
   descending 34  
   intermittent 33, 180  
   perennial 33  
   periodic 33  
 steady-state condition 36, 50  
 steam  
   loss 134  
   separation, single-step 135  
   separation, continuous 137, 145  
   separation, multi-stages 136  
 storage coefficient 4, 181  
 storativity 181  
 Stripa mine 48, 89, 94  
 strontium isotopes 17, 48, 92  
 sulphur isotopes 18, 79  
   atmospheric sulphate 81  
   marine sulphate 81  
   mixing 84  
   oxidation of sulphides 82  
   sulphate reduction 44, 46, 81  
   terrestrial sulphate 82  
 surface  
   equipotential 5  
   piezometric 4, 180  
   potentiometric 181  
   runoff 178
- t**
- 
- temperature effect 66  
 The Geysers geothermal field 147  
 time series 98, 181  
 Tongonan geothermal field 132  
 tracer 15  
   balance method 53  
   bomb 15  
   chemical 20  
   colloids 21  
   conservative 20, 66  
   environmental 15  
   historical 15  
   noble gases 22  
   non-conservative 17  
   radioactive isotopes 18  
   stable isotopes 17  
   peak displacement 51, 53, 55, 58, 73  
 tracer velocity 178  
 transmissivity 182  
 tritium  
   peak 55, 96  
   ingrowth technique 101  
   input function 16, 99  
   time-series 98  
   unit 97  
 tritium/helium method 100  
 true water age 103  
 TU 97  
 turnover  
   time 97, 182  
   rate 182
- u**
- 
- U/He method 113  
 unconfined aquifer 182  
 unsaturated zone 49, 182  
 uranium isotope ratio 115  
 uranium/helium 114

**V**


---

vadose water 182  
 velocity  
   actual 26  
   apparent 38  
   Darcy 27  
   distance 178  
   filtration 27, 179  
   tracer 26, 178  
 Vienna Standard Mean  
   Ocean Water (standard) 66  
 volumetric humidity 3, 180  
 volumetric water content 3, 180  
 V-SMOW (standard) ⇒  
   Vienna Standard Mean Ocean Water

**W**


---

Wairakai geothermal field, Phillipines 139  
 water  
   andesitic 121, 131, 135  
   basaltic water 131  
   brackish 177  
   connate 178  
   constitutive 50  
   formation 82, 130, 159  
   fossil 179  
   gravitational 179  
   juvenile 121, 180  
   magmatic 121, 180  
   meteoric 121  
   modern 180

  mineral 73  
   mobile 49, 179  
   retentative 50  
   saline 181  
   subsurface 181  
   table, free 179  
   vadose 182  
   waste 76, 90, 141  
 water-rock interaction 41, 123  
 weathering studies 94  
 well  
   artesian 34, 177  
   construction 35  
   drilled 34  
   dug 34, 98  
   observation 36, 180  
   production 34

**y**


---

Yellowstone field 128, 135, 169

**Z**


---

Zhangzhou geothermal field 129, 166  
 zone  
   aeration 182  
   intermediate 179  
   root 181  
   saturated 65, 181, 182  
   transition 133  
   unsaturated 49, 182